LINKING LAND USE, CLIMATE, AND COASTAL ECOSYSTEMS: A WATERSHED PERSPECTIVE FOR A CHANGING SOUTH CAROLINA COAST

A thesis submitted in partial fulfillment of the requirements for the degree

MASTER OF SCIENCE

in

ENVIRONMENTAL AND SUSTAINABILITY STUDIES

by

KEVIN LLOYD HILL
DECEMBER 2020

at

THE GRADUATE SCHOOL OF THE UNIVERSITY OF CHARLESTON, SOUTH CAROLINA AT THE COLLEGE OF CHARLESTON

Approved by:

Dr. Andrew Tweel, Thesis Advisor

Sharleen Johnson

Dr. Barbara Beckingham

Dr. Timothy Callahan

Dr. Godfrey Gibbison, Dean of the Graduate School

ABSTRACT

LINKING LAND USE, CLIMATE, AND COASTAL ECOSYSTEMS: A WATERSHED PERSPECTIVE FOR A CHANGING SOUTH CAROLINA COAST

A thesis submitted in partial fulfillment of the requirements for the degree

MASTER OF SCIENCE

in

ENVIRONMENTAL AND SUSTAINABILITY STUDIES

by

KEVIN LLOYD HILL
DECEMBER 2020

at

THE GRADUATE SCHOOL OF THE UNIVERSITY OF CHARLESTON, SOUTH CAROLINA AT THE COLLEGE OF CHARLESTON

South Carolina's growing population has resulted in widespread changes in land use. Urbanized watersheds lead to increases in stormwater runoff and the transport of contaminants to downstream aquatic ecosystems. This data synthesis project explored long-term and large-scale environmental datasets to construct a history of habitat quality in South Carolina's estuaries over the last 20 years. Previous studies in coastal South Carolina have demonstrated connections between developed watersheds and degraded, downstream aquatic habitats. Data on water quality, sediment contamination, and biological communities (macroinvertebrate infauna and nekton) were analyzed in relation to upstream watershed characteristics such as impervious surface cover along a gradient of development intensities. These relationships were further explored within the larger context of a changing climate. By linking spatially explicit temperature, precipitation, and landcover data with measures of habitat quality from 1999-2018, this project used past associations among these factors to predict impacts of projected changes in climate and development on coastal ecosystems. Understanding this climate-watershed connection will aid coastal managers in planning for future changes to coastal ecosystems and communities.

ACKNOWLEDGEMENTS

First and foremost, I would like to thank my academic advisor, Dr. Andrew Tweel, for providing me the opportunity to work on this project. Over the course of two years, he has both challenged and supported me through a difficult and rewarding process – a true mentor. I was lucky to have such a great committee. My researcher advisors, Sharleen Johnson, Dr. Beckingham, and Dr. Callahan, each brought a valuable and unique perspective to this project and challenged me to ask new questions. I would also like to thank the members of the Environmental Research Section at DNR for their constant support and guidance. Additionally, I want to thank my friends and family who were there for me throughout my grad school journey.

I would also like to acknowledge the financial support I received from the Masters of Environmental Studies Student Association, the Graduate School at the College of Charleston, and South Carolina Department of Natural Resources to attend and present at conferences which gave me the opportunity to grow as a scientist. Lastly, this project would not have been possible without funding from the South Carolina Sea Grant Consortium.

TABLE OF CONTENTS

LIST OF FIGURES

LIST OF TABLES

CHAPTER 1: INTRODUCTION

South Carolina's coastal landscape is defined by its tidal wetlands and estuaries. Nearly 140,000 hectares of salt marsh line the South Carolina coast – more than any other state on the Atlantic (SCDNR, 2012). Formed at the intersection of fresh and saltwater systems, estuaries are some of the most productive ecosystems on the planet. Estuaries, and their associated tidal wetlands, provide a wealth of ecosystem services for coastal South Carolina. For example, salt marshes provide the first line of defense against coastal erosion, rising sea levels, and storm surges (Shepard et al., 2011). Inland coastal waters also provide critical nursery habitat for several commercially and recreationally important fishery species such as shrimp, blue crab, flounder, and redfish (Wiegert and Freeman, 1990). Additionally, the social and aesthetic qualities of South Carolina's coastal landscape serve as the cultural backdrop of the "Lowcountry." However, a growing coastal population threatens these important ecosystems.

Coastal counties contribute less than 10% of the United States' land area but are home to 40% of the nation's population (NOAA, 2013). As the United States' population grows, population density in the coastal zone will continue to increase. South Carolina, a state with vast coastal resources, is no exception to this trend. From 2000 to 2018, South Carolina's population grew from 4.01 to 5.08 million people (a 26% increase) making it the 11th fastest growing state in the nation (US Census Bureau, 2018). This growth is

especially prominent along the coast; for instance, the City of Charleston is growing at a rate three times the national average (CRDA, 2018).

Coastal South Carolina has undergone widespread changes in land use and landcover to accommodate this influx of new residents. New infrastructures such as homes, roads, parking lots, golf courses, and shopping centers have spread across the landscape in a process known as urban sprawl. This change in landcover has many impacts including habitat loss and an increase in contaminants entering downstream aquatic systems via nonpoint source pollution. According to NOAA's Coastal Change and Analysis Program, Charleston County gained 4,530 ha of developed landcover between 1996 and 2010 which resulted in a 20% increase in impervious surface coverage (NOAA C-CAP). These impervious surfaces represent a significant threat to South Carolina's estuarine systems.

Impervious surfaces, such as pavement or rooftops, impact the water cycle at the watershed scale. In an undeveloped watershed, rainfall is intercepted by vegetation, slowed down, and allowed to percolate into the soil; however, rainfall on impervious surfaces is rapidly converted into surface runoff. "SWARM", standing for stormwater runoff modeling system, was adapted from the USDA Natural Resources Conservation Services' TR-55 model and calibrated for the shallow water table conditions of coastal South Carolina (Blair et al., 2014). According to this model, 67% of rainfall is converted into runoff in urban watersheds compared to 27% in forested watersheds. In addition to increasing the risk of flooding, stormwater runoff transports pollutants into the aquatic environment and has been identified by the EPA as the leading cause of nonpoint source

pollution (US EPA, 2016). In coastal South Carolina, tidal creeks and estuaries bear the burden of draining an increasingly urbanized landscape.

Holland and others (2004) used impervious cover as an indicator of environmental quality in 23 tidal creeks across coastal South Carolina. Their results demonstrated a correlation between a watershed's impervious cover and physical, chemical, and biological changes in tidal creeks such as altered salinity and sediment dynamics, increased pollutants, and elevated levels of fecal coliform bacteria. When the impervious cover of watersheds exceeded 20%, data on the health of biological communities in tidal creeks showed negative impacts. These biological impacts included a reduction in stress-sensitive benthic organisms and lower shrimp abundances. This study supports the link between watershed development and decreased water quality and, most notably, demonstrates the biological impact of these changes. Holland and others' (2004) paper is one of many in a growing body of research exploring the connection between urbanized watersheds and degraded estuarine environments in South Carolina (Parker, 2018; Sanger et al., 1999a; Sanger et al., 1999b; Sanger et al., 2015; Van Dolah et al., 2008).

Since these earlier studies, development has not slowed down in the region and coastal South Carolina's population continues to grow. Sustainable development requires finding the balance between population growth and protecting the coastal environment. Reassessing the relationship between urbanization and estuarine habitat quality can aid resource managers, municipalities, developers, and other stakeholders in finding this balance. This project built upon previous studies by expanding the geographical range,

utilizing more contemporary datasets, exploring a broader range of environmental parameters, and incorporating an additional theme of climate change.

Anthropogenic climate change is arguably the greatest environmental issue of our time. While threats of sea-level rise and hurricanes garner considerable attention from coastal communities, research into the effects of climate change on changing temperature and precipitation regimes on coastal ecosystems is less common. The Fourth National Climate Assessment (NCA) report highlights some of the anticipated impacts of climate change for the Southeast such as warming temperatures, increasing precipitation, and more frequent extreme precipitation and extreme heat events (USGCRP, 2017).

In the Southeast, the 2010's were the warmest decade on record (Vose et al., 2017). Under their most conservative climate change scenario, the NCA predicts annual average temperature in the Southeast will increase 1.89 ºC by 2065 and 2.46 ºC by the end of the 21st Century (Vose et al., 2017). Warming temperatures could have important implications for estuarine ecosystems. For example, changes in temperature can impact the structure of tidal wetland plant communities as seen in the conversion of marshes to mangroves (Gabler et al., 2017). Additionally, warmer water temperatures correspond with low dissolved oxygen levels and can increase stress on aquatic organisms such as fish and crustaceans (Wetz et al., 2013). From a human health perspective, increased water temperatures can also facilitate the growth of harmful algal blooms and pathogenic bacteria and viruses (O'Neil et al., 2012; Paerl and Huisman, 2008). In addition to increasing temperatures, climate change is also expected to cause changes in precipitation patterns in the Southeast.

According to the NCA, the United States experienced a 4% increase in annual precipitation between 1901 and 2015 (Easterling et al., 2017). While this trend is likely to continue under a changing climate, changes in precipitation will vary considerably region to region. In the Southeast, annual precipitation totals are expected to increase 5-10% by 2065 (Easterling et al., 2017). The nature of precipitation is also expected to change in the Southeast. Both the number of days between precipitation events and the frequency of extreme precipitation events are expected to increase due to climate change (Easterling et al., 2017). This means the Southeast may become a climate punctuated by periods of drought and extreme precipitation events. Heavy precipitation could intensify stormwater runoff and increase the volume of pollutants entering the estuarine environment. On the other extreme, periods of drought could be detrimental to South Carolina's coastal ecosystems. Drought has been implicated as a leading cause of salt marsh dieback along the Gulf of Mexico (McKee et al., 2004). Drought can also reduce freshwater inflows to estuaries leading to changes in salinity and water quality, thus altering the spatial distribution and abundance of biological communities (Palmer and Montagna, 2015).

South Carolina's estuaries are defined by change. Twice a day, tidal exchanges of up to three meters result in rapid changes to water depth, salinity, and temperature. Organisms that reside within these dynamic environments are well adapted to these fluctuations, but climate change could amplify these stressors and impact biological communities in the water column and in the sediment. At the same time, population growth and urbanization are changing the physical landscape of the South Carolina coast. The purpose of this project is to examine the intersection of these two forces of change and their compounded effects on South Carolina's estuarine systems. While the

connections between urbanization and estuarine environmental quality have been established in prior studies, few have explored this relationship within the context of a changing climate. This project utilized a novel data synthesis approach to answer these questions.

Data synthesis is the use of secondary data pulled from a variety of sources to test hypotheses. A study design based upon data synthesis can utilize a wealth of datasets to answer big-picture questions spanning large geographical areas and long timeframes – questions that may otherwise be inaccessible to researchers relying on primary data. This study compiled datasets on landcover and land use, weather and climate, and environmental quality to describe the condition of South Carolina's coastal landscape over a 20-year period from 1999 to 2018. This diverse assemblage of data was linked across space and time to create a synthesized database capable of testing hypotheses relating landcover, climate, and coastal ecosystems. After establishing past relationships among these factors, this project used linear modeling to predict the future of the estuarine environment in a changing South Carolina coast. Understanding this climate-watershed connection will aid coastal managers in planning for future changes to coastal ecosystems and communities.

CHAPTER 2. METHODS

2.1. Data Collection

As a data synthesis project, this study relied on existing datasets to test its hypotheses. Extensive data on landcover, land use, weather, climate, and the estuarine environment were gathered and organized from multiple sources to characterize the status of South Carolina's coast during the 20-year study period (1999-2018). These data were organized into three categories – physiographic, weather and climate, and environmental data.

2.1.1. Physiographic Data

Physiographic data describe the physical landscape of South Carolina's coast and include data on land use, landcover, soil types, stormwater infrastructure, and human population. The National Land Cover Dataset (NLCD) is a landcover product available online through the Multi-Resolution Land Characteristics Consortium (MRLC) (Yang et al., 2018). The NLCD provides a detailed dataset of landcover for the United States using Landsat imagery to categorize the landscape into 16 landcover classes (see Table 1) at a

30x30 m resolution. NLCD landcover data were downloaded for South Carolina, North Carolina, and Georgia for years 2001, 2004, 2006, 2008, 2011, 2013, and 2016.

In addition to these landcover classes, the NLCD also produces a dataset of urban impervious cover for the United States (Yang et al., 2018). This dataset, derived from Landsat imagery, assigns each 30x30 m pixel a value from 0 to 100 based on a calibrated model. This value represents the percentage of impervious cover with 100 indicating complete imperviousness. Impervious cover data were downloaded for South Carolina, North Carolina, and Georgia for years 2001, 2006, 2011, and 2016.

Hydrologic soil groups, established by the United States Department of Agriculture (USDA), describe soil drainage and are commonly included in stormwater runoff models such as the Natural Resource Conservation Service's (NRCS) TR-55 method (USDA, 1986). Hydrologic soil group data were downloaded for the state of South Carolina using the NRCS web soil survey tool (NRCS, 2019) and are summarized in Appendix A.

Stormwater retention ponds are a common method of stormwater management across the urban-suburban landscape. In 2015, the South Carolina Department of Natural Resources (SCDNR) compiled a database of over 20,000 artificial ponds across coastal South Carolina's eight coastal counties (Cotti-Rausch et al., 2018). Ponds from this database are divided into seven classes (rural, forest, mining, residential, golf, commercial, and mixed), but only five classes specific to stormwater infrastructure were used for this study (rural, residential, golf, commercial, and mixed).

South Carolina population totals were downloaded from the United States Census Bureau at census block and county levels (US Census Bureau, 2018). Census blocks offer

the finest spatial resolution but are limited to official census years, with 2010 being the most recent at the time of this study. Annual population estimates are available, but only at the county-level.

2.1.2. Weather and Climate Data

This study utilized a combination of short-term weather and long-term climate data to explore the effects of temperature and precipitation on South Carolina's estuarine environment. These data were collected from a variety of sources to cover the 20-year study period (1999-2018) and large study area. Daily air temperature averages and precipitation totals were downloaded using the National Oceanic and Atmospheric Administration's (NOAA) Climate Data Online tool (NOAA NCEI). These weather data were compiled for the entire study period (1999-2018) from all available weather stations in coastal South Carolina counties as well as bordering coastal counties in North Carolina and Georgia. Given this project's extensive study area and time period, data coverage from many individual weather stations were either incomplete or inconsistent. To fill in potential coverage gaps, interpolated weather datasets were also downloaded. This study used Oak Ridge National Laboratories' (ORNL) DAYMET gridded weather data product to supplement daily weather observations (Thornton et al., 2018). DAYMET offers a 1x1 km grid of daily weather estimates (*e.g.*, temperature and precipitation) for all of North America from 1980 to present.

In addition to daily weather data, NOAA's Climate Data Online service also provides climate normals (*i.e.*, 30-year temperature and precipitation averages) for select

weather stations (NOAA NCEI). The most recent climate normals data were derived from 1980-2010 and are summarized by month, season, and year. The definition of seasons used throughout this study follow NOAA's climate normals and are referenced in Appendix B. Normals were downloaded for three weather stations that represent the northern, central, and southern regions of the South Carolina coast – Brookgreen Gardens, Charleston International Airport, and Savannah International Airport, respectively (see Figure 1). Climate normal values are summarized in Table 2. These three stations were selected because they represent some of the longest-running weather datasets along the SC coast.

Several indices have been developed to describe drought. While most of these indices have origins in agriculture, their inclusion in this study offers insight into long-term precipitation patterns along South Carolina's coast. Monthly drought index values are available from NOAA's National Climate Data Center's Drought Atlas (NOAA NCDC). Drought index data were downloaded from the NCDC Drought Atlas for South Carolina's coastal climate divisions (see Figure 2) from January 1999 to December 2018. The drought indices selected for this study are summarized in Appendix C.

Climate teleconnections describe global climatic patterns that can sometimes be linked to local weather impacts. The El Niño-Southern Oscillation (ENSO) is perhaps the most well-known of these climate teleconnections. Other climate teleconnections incorporated in this study are the Atlantic Multidecadal Oscillation (AMO), North Atlantic Oscillation (NAO), and the Arctic Oscillation (AO). These teleconnections are summarized by index values representing their positive-negative or warm-cool phases. These indices were downloaded by month for the entire study period using R's 'rsoi'

package (Albers, 2019; R Core Team, 2019). More information on the effect of these teleconnections on South Carolina's climate can be found in Appendix D.

2.1.3. Environmental Data

South Carolina's Estuarine and Coastal Assessment Program (SCECAP) is a multi-agency environmental monitoring program run by SCDNR with cooperation from the South Carolina Department of Health and Environmental Control (SCDHEC), NOAA, the Environmental Protection Agency (EPA), and the US Fish and Wildlife Service (USFWS). SCECAP's mission is to monitor the environmental health of South Carolina's estuaries and provide detailed, periodic reports to resource managers and the public (Sanger et al, 2016). Launched in 1999, SCECAP has produced 20 years of environmental data on South Carolina's estuarine environment. During this time, over 800 sites have been sampled spanning the full range of South Carolina's estuarine habitats from small tidal creeks to large estuaries (see Figure 3). From 1999 to 2006, 60 SCECAP sites were sampled per year, and from 2007 onward, 30 sites are sampled per year. Sites are randomly selected from all South Carolina estuarine waters and are split evenly into two habitat categories – open water and tidal creek. Tidal creeks are estuarine habitats with channel widths less than 100 m and open water sites have channel widths greater than 100 m. SCECAP data collection primarily occurs during July and August (although in some earlier SCECAP years sampling began in June) and is conducted within three hours of low tide.

SCECAP collects a wide range of data to assess water quality, sediment quality, and biological quality (see Appendix E). At each sampling location, several water and sediment samples are collected from the water column and channel bottom, respectively. These samples are then analyzed for water quality and contaminant data. A separate set of sediment samples are further processed to identify and quantify benthic invertebrate infauna. Bottom trawls are conducted at each SCECAP site to evaluate the site's nekton community. These trawls capture fish and large invertebrates which are identified to species, measured, and released. More information on SCECAP and its sampling protocol can be found in SCDNR's most recent report (Sanger et al., 2016).

2.2. Data Processing

This diverse assortment of data required extensive processing before incorporation into the study. Microsoft Excel, Microsoft Access, ArcMap, and R were the key instruments used in processing, organizing, and storing these data. Examples of data processing include identifying gaps in data coverage, detecting erroneous values, analyzing spatial data in GIS, and converting environmental data into useable formats.

2.2.1. Physiographic Data

ArcMap GIS software was the primary tool to process physiographic data (ESRI, 2018). Physiographic data were summarized by spatial units (*e.g.*, watersheds) to link estuarine habitat quality and the surrounding landscape. Hydrologic Unit Code

watersheds (HUCs) were the primary units of analysis in this study. HUCs are standardized, USGS-delineated watersheds that range in size from large river basins to small headwater watersheds. HUCs spanning the full reach of coastal South Carolina were downloaded from the USGS' Watershed Boundary Dataset (WBD, 2013). Watershed size is indicated by the number of HUC digits; 8-digit HUCs were the largest and 14-digit HUCs were the smallest used in this study. Figure 4 displays the extent of these watersheds. While HUC watersheds offer a standardized and hydrologically-derived spatial grouping system, alternative spatial units such as grids and buffers were explored to better understand spatial relationships among the data.

To create gridded spatial units, ArcMap's fishnet grid tool was used to overlay a square grid across South Carolina's coast. The resulting grid contained four cell sizes (25, 100, 400, 1600 km^2) arranged to simulate HUC watersheds' nested organization (see Figure 5). These gridded spatial groupings allow for more randomized spatial analyses with uniformly sized and spaced units. In addition to watersheds and gridded spatial units, buffers were established around environmental data points to summarize nearby physiographic data. ArcMap's multiple ring buffer tool was used to draw circular buffers around each SCECAP sampling station with radii of 1, 2, and 3 km. The benefit of buffers is their ability to capture physiographic data at a more localized scale than the HUC watersheds or grid cells (see Figure 6).

After establishing spatial units, physiographic data were summarized using ArcMap's spatial analysis toolbox. NLCD landcover data were summarized by spatial unit using the tabulate area tool for each year of data. This tool totaled the area (m^2) each landcover category contributed to each spatial unit (*i.e.*, watershed or grid cell). In

instances where spatial units overlapped (*i.e.*, buffers), the tabulate intersection tool was used instead. The tabulate intersection tool handles overlapping polygons better than the tabulate area tool, but required additional processing in R to produce compatible outputs. After organizing these outputs into a data table, landcover categories were translated into percent total upland area. Upland area was defined as non-water and non-marsh landcover categories. Landcover data classes were also condensed into broader landcover categories (see Table 1).

Landcover data were further processed to capture changes within each landcover category during the study period (*e.g.*, hectares of forest converted to development). ArcMap's reclassify tool converted NLCD landcover categories into numeric variables for years 2001 and 2016. The raster calculator tool was then used to overlay and multiply the reclassified NLCD pixels and resulted in a new layer representing landcover change between 2001 and 2016. Numeric values were converted back into landcover categories to display the change in landcover between 2001 and 2016. The tabulate area tool was used to summarize landcover change at the county level (see Figures 7-9).

Unlike categorical NLCD landcover data, urban impervious cover is a continuous variable and requires a different set of spatial tools. Impervious cover data were processed using ArcMap's zonal statistics tool for each year of available data. To focus on upland impervious cover, spatial units were modified to represent upland area before running the zonal statistics tool. Upland landcover categories (*i.e.*, not open water or marsh) were combined and intersected with each spatial unit to create upland watersheds, grid cells, and buffers. The zonal statistics tool calculated the mean pixel value across the upland spatial unit (*i.e.*, watershed, grid cell, or buffer). The final result were data tables

of mean upland urban impervious cover (%) for each spatial unit and year of available data.

Hydrologic soil groups were summarized by spatial unit using the tabulate area tool which totaled the area (m^2) each soil group contributed to the upland spatial unit (*i.e.*, watershed or grid cell). Outputs were summarized into a data table where hydrologic soil groups were translated into percent upland area. Additionally, soil group data were simplified into poorly- and well-drained categories (see Appendix F).

NLCD landcover, urban imperviousness, and hydrologic soil group data are all examples of raster datasets; however, stormwater pond and census data are vector datasets and required different processing methods. Stormwater pond count and area (m^2) were calculated for each spatial unit using the tabulate intersection tool. In cases where ponds spanned multiple spatial units, only ponds with more than 50% of their area within that unit were included in the total count. Outputs were organized into a data table where density (ponds/ha) and percent total area were calculated.

Population totals for each spatial unit were estimated using the tabulate intersection tool. When census blocks did not align with the spatial unit, population was prorated based on the proportion of the block within the watershed. This method provided a good estimate of population but assumed an even distribution throughout the census block. Population totals were then divided by area to estimate population density (persons/ha) for each spatial unit.

2.2.2. Weather and Climate Data

Daily weather observations from NOAA were summarized by calculating multi-day, running averages of daily temperature and totals of precipitation for 1 to 7-day periods. Temperature and precipitation data from the three primary weather stations were summarized by month, season, and year. These data were subtracted from their corresponding 30-year climate normals to calculate deviation from normal. Deviations from normal offered insight into long-term climatic patterns and were used to classify South Carolina's climate history into cool and dry, cool and wet, warm and dry, and warm and wet periods (see Figures 10-11).

DAYMET's daily temperature and precipitation estimates were downloaded using the 'daymetr' R package (Hufkens et al., 2018). Each DAYMET pixel was matched with each SCECAP site's sampling date and geographical coordinates. DAYMET data were then processed in R to calculate rolling averages and totals of temperature and precipitation for 1, 2, 3, 5, 7, 10, 14, 30, 45, 60, and 90-day intervals.

Weather data were used to identify extreme weather events during the study period. This study classified extreme weather events as maximum daily temperature and 24-hour precipitation totals in excess of the 95th percentile of all observations compiled for 1999 to 2018. The 95th percentile values were calculated for each of the three primary weather stations and summarized in Table 2. Extreme temperature and precipitation were summarized by year and weather station by tallying the number of days per year in which temperature and precipitation exceeded the 95th percentile threshold.

2.2.3. Environmental Data

The majority of SCECAP environmental data had already been processed by SCDNR staff before its incorporation into this study. For example, sediment contamination effects range median quotients (ERMQ) were calculated from raw concentration data for each of the sediment contaminant categories studied. ERMQ uses the biological impacts of multiple contaminants to create a standardized score for each category of contaminant (*e.g.*, PAHs, PCBs, metals) (Long et al., 1995; Hyland et al., 1999). Measurements of water quality were taken with YSI Model 6920 multiprobes deployed at each site. Water quality parameters (*e.g.*, dissolved oxygen, temperature, salinity) used in this study are averages from the duration of data logger deployment (25-hours to capture full tidal and diurnal cycles). Channel width was estimated for each SCECAP site using ArcMap's measure distance tool and satellite imagery to measure the distance between channel banks.

Estuarine biological conditions at SCECAP sites were described with measures of abundance (*i.e.*, number of individuals per site) and species richness (*i.e.*, number of unique species per site) for the nekton and benthic communities. Nekton and benthic community data were derived from trawls and benthic grabs, respectively. Per SCECAP protocol, trawls at open water sites are towed for 1,000 m whereas trawls at tidal creek sites are towed for 500 m. Abundance data were standardized by dividing the number of individuals captured by area (m^2) trawled. Trawl area was calculated by multiplying distance towed by the width of the trawl net's opening (2.76 m). With this formula, open water sites had a trawl area of 2,760 m^2 and tidal creek sites had a trawl area of 1,380 m^2.

Benthic abundance was similarly converted to abundance per unit area by dividing the number of individuals by area sampled. Each benthic grab sampled an area of 0.044 m^2 which was doubled to 0.088 m^2 because two grabs were performed at each site. While total abundance was standardized by area, the relationship between species richness and sample area is more complex (Connor and McCoy, 1979). Consequently, species richness was not standardized by area and nekton species richness data were analyzed separately by habitat type. Benthic species richness, on the other hand, was analyzed across both habitat types because sampling protocol did not differ between tidal creek and open water sites.

Community data were further summarized by SCDNR staff into indices that represent the biological integrity of each site. The two benthic indices used in this study are the Benthic Index of Biological Integrity (BIBI) and the Multivariate AZTI's Marine Benthic Index (MAMBI) (Muxika, 2007; Van Dolah, 1999). BIBI and MAMBI values describe the benthic community structure in relation to environmental stressors. Higher BIBI and MAMBI values indicate benthic communities with greater relative abundance of pollution-sensitive species, and lower BIBI and MAMBI values indicate benthic communities with greater relative abundance of pollution-tolerant species. The BIBI has the benefit of being locally calibrated to represent taxa in the Carolinian province. MAMBI, on the other hand, was originally developed for European waters and many taxa collected at SCECAP sites were not represented in AZTI's database (although the AZTI database has since been supplemented with more United States specific taxa). To account for these unassigned taxa, MAMBI values were omitted from analyses in sites where

>20% of the benthic sample were not assigned to an ecological group (~28% of SCECAP sites).

2.3. Data Integration

The data integration phase of this project linked all physiographic, weather, and environmental data across space and time to create an analysis-ready database. SCECAP sites were linked to their respective spatial unit (*e.g.*, watershed, grid cell) using ArcMap's spatial join tool. When physiographic data had a time component (*e.g.*, NLCD year), SCECAP sites were linked to the most recent year of data that would have been available at the time of sampling. For example, a SCECAP site sampled in 2015 would be linked to 2013, not 2016, NLCD data.

Weather, particularly sub-tropical summer thunderstorm activity, is highly localized; therefore, this study matched environmental sampling sites to the nearest weather station. ArcMap's point distance tool provided distances between each SCECAP site and every weather station. Due to inconsistent data coverage of weather stations (*i.e.*, missing dates), these linkages were processed in R so that each SCECAP site was matched with the closest weather station that also had overlapping temporal coverage. To link environmental data with long-term weather trends, ArcMap's near tool was used to pair each SCECAP station with the closest primary weather station (*i.e.*, Brookgreen Gardens, Charleston International Airport, or Savannah International Airport). For drought data, the spatial join tool was used to match SCECAP sites to their respective climate division. After establishing these spatial relationships, environmental and

weather-climate data were linked across time based on the SCECAP sampling date. The final product of the data integration phase was a Microsoft Access database capable of storing and indexing large amounts of data for easy querying. Access's relational features allowed for the creation of large, analysis-ready data tables linking weather, physiographic, and environmental data.

2.4. Data Analysis

The data analysis process was divided into exploratory and confirmatory phases. Exploratory data analysis helped establish general trends in the data. *t*-tests explored variations in environmental data between broad categories of data (*e.g.*, open water vs. tidal creek) and hot spot and time series analyses explored spatiotemporal trends in the data. These exploratory data analyses were instrumental in developing a better understanding of the dataset while informing and improving the project's hypotheses. While exploratory data analysis contributes to hypothesis building, confirmatory data analysis was best suited for hypothesis testing. In this project, linear regression models were the primary instrument in confirmatory data analysis.

2.4.1. t-tests

Welch's *t*-test was used to compare means of environmental parameters between broad categories of data. Welch's *t*-test is an adaptation of Student's *t*-test and was selected for its ability to compare means between two unpaired populations of unequal

variance and different sample size. Normally distributed data is one assumption of the *t*-test and many variables in this study do not follow a normal distribution; however, the study's large sample size (N=865) allows for this assumption to be relaxed. Furthermore, non-parametric alternatives to the *t*-test such as the Wilcoxon-Mann-Whitney test also carry assumptions not fully met by these data (*e.g.*, populations of equal variance).

SCECAP environmental data were categorized into groups based upon habitat type, watershed development, and time period. For habitat type, data were split into open water and tidal creek sites per SCECAP sampling methodology. Watershed development was based upon mean upland impervious cover within coastal South Carolina's 14-digit HUCs. Watersheds were binned into two categories (developed and undeveloped) using the median value of impervious cover (18.9%) from the study dataset. 14-digit HUCs with mean upland impervious cover >18.9% were classified as developed and 14-digit HUCs with <18.9% mean upland impervious cover were classified as undeveloped. SCECAP data were classified into early and late time periods by splitting the sampling years into the first and last ten years of data – 1999-2008 and 2009-2018.

After grouping SCECAP data into these categories, Welch's *t*-tests were performed for each environmental parameter to compare population means between groups. Tests were run before and after splitting SCECAP sites into open water and tidal creek sites. *t*-tests operate on a null hypothesis of no significant difference between means in two populations. This null hypothesis was rejected when the *t*-test produced a *p*-value of ≤0.05. R's 'broom' package was used to automate *t*-tests and store their results into data tables (Robinson and Hayes, 2020) (see Tables 3-9). Differences between

environmental parameters within the various groupings are visually summarized with boxplots (see Figures 12-26).

2.4.2. Time Series Analysis

Generalized least squares (GLS) regression was used to evaluate trends in environmental and weather data over the course of the study period. In time series analysis, GLS regression provides a cursory glance as to whether variables are increasing or decreasing over time (*i.e.*, slope $\neq 0$). To prepare the data for GLS regression, environmental and weather data were averaged by year. Environmental data were summarized across all habitat types as well as split into open water and tidal creek categories. Weather data were summarized by year and by each of the three major weather stations (Brookgreen Gardens, Charleston International Airport, and Savannah International Airport). These weather data were also summarized across all three stations to represent coastal South Carolina weather as a whole. While Charleston International Airport and Savannah International Airport weather stations had complete data coverage during the study period, there were several gaps in data coverage from the Brookgreen Gardens station. Seasons and years with more than 20% of missing days were excluded from analysis.

After preparing the data, R's 'nlme' package was used to run GLS regression models with year as the independent variable (Bates et al., 2019). To account for temporal autocorrelation (*i.e.*, lack of independence between years), a first-order autoregressive correlation structure was included in the models (corAR1=~Year). The

null hypothesis (slope=0) was rejected in models with *p*-values ≥0.05. Figures 27-40 display the results of these GLS regression models. Model outputs were summarized into tables using R's 'stargazer' package and can be seen in Tables 10-15 (Hlavac, 2018).

2.4.3. Hot Spot Analysis

While time series analyses offered insight into temporal variability within the data, hot spot analyses were used to capture spatial variability. ArcMap's optimized hot spot analysis tool was used to identify hot and cold spots for environmental parameters along South Carolina's coast. This tool applied the Getis-Ord Gi* statistic to identify spatial units with significantly greater (hot spot) or lesser (cold spot) values than the surrounding units (Getis and Ord, 2010). The optimized hot spot analysis tool was run for select SCECAP environmental parameters aggregated by 14-digit HUC watersheds, and results are displayed as maps in Figures 41-52.

2.4.4. Multiple Linear Regression

While *t*-tests, time-series analysis, and hot spot analysis were great tools for exploratory data analyses, linear modeling was best suited for the confirmatory data analysis phase of this project. Specifically, multiple linear regression was used to examine relationships among the full suite of independent and dependent variables accumulated during this study. Multiple linear regression was selected over other statistical methods for its ability to incorporate multiple predictors, interpretability, and

predictive capabilities. Multiple linear regression uses the following formula to test the combined effects of multiple predictors on one response variable by fitting a least squares line of best fit:

$$y_i = \beta_0 + \beta_1 x_1 + \beta_2 x_2 + \cdots \beta_i x_i + \varepsilon_i$$

Where:

y_i = dependent variable

β_0 = intercept

β_i = regression coefficient

x_i = independent variables

ε_i = error term

The volume of data in this project presented many challenges in modeling. Exploring every possible combination of predictor variable across multiple temporal and spatial scales proved impractical; therefore, stepwise regression was used to narrow down the number of variables and select the most significant predictors for each response variable. Stepwise regression is an automated model selection tool that works by adding and subtracting predictor variables in a multiple linear regression formula and selecting the combination of variables that produces the best model. Several criteria can be used to determine the best model such as the Akaike Information Criterion (AIC) or Bayesian Information Criterion (BIC). BIC was selected for this project because it penalizes the addition of new variables. By favoring simplicity, BIC avoids overfitted models which is

a concern when dealing with such a large suite of variables. Using JMP statistical software, Stepwise BIC regression was run for each response variable (see Appendix E) with all explanatory variables (see Appendices B, F, G) as input parameters (SAS, 2019). To better understand the spatial relationships between physiographic data and environmental responses, stepwise regressions were run separately for each spatial unit (*e.g.*, 12-digit HUC, 1 km buffer, 400 km^2 grid). Automated model outputs were further refined by removing outliers in the dataset and, when appropriate, removing redundant or conflicting explanatory variables. These final models were recreated in R where the 'broom' package was used to organize model outputs into one dataset (Robinson and Hayes, 2020).

2.4.5. Model Meta-Analysis

After organizing all model outputs into a single dataset, meta-analyses were performed on the linear model results. Meta-analyses help reveal overarching trends in the data. For example, model performance (*i.e.*, R^2) was compared among different spatial groupings to determine the extent to which landcover variables influence environmental responses. Meta-analysis results related to model R^2 are summarized in Table 16. Additionally, explanatory variables were tallied up across all models to identify the most prevalent parameters in the dataset. Parameter frequency was then calculated by dividing the number of occurrences by the total number of models. Parameters with higher frequencies might indicate variables with greater explanatory power. Parameter frequency can also reveal temporal patterns within the data. For example, weather

patterns in winter may be more prevalent predictors than other seasons or 10-day rainfall totals may be more frequent predictors than 3-day rainfall totals. Meta-analysis results related to model parameters are summarized in Tables 17-20.

2.4.6. Linear Model Selection and Refinement

While stepwise regression was suitable for processing the large number of potential models, a more supervised approach was followed to create a robust set of "final" linear models for making predictions. For each response variable, the model with the highest adjusted R^2 was chosen as the "best" model for further refinement. The number of response variables was also reduced during this stage. In sediment quality models, measurements of ERMQs were chosen over raw concentration data because they produced models with higher R^2 values. Similarly, MAMBI was chosen over BIBI to represent benthic community structure.

Once selected, these "best" models were tested to see if they violated any of the underlying assumptions of linear modeling. Residual plots were visually inspected for homoscedasticity. When appropriate, outliers were removed to improve the dispersion of residuals. Response variables were also log transformed and model results were compared side-by-side with the untransformed model results. Transformed response variables were selected if model performance significantly improved or residuals became more heteroscedastic.

Another assumption of linear models is absence of multicollinearity. This assumption proved difficult to maintain because the explanatory variables of this project

represent complex phenomena such as climate. To mitigate this concern, interaction effects among each independent variable were tested in every model. If significant, these interaction terms were included in the final model. Detailed model outputs from this final selection are summarized in Tables 21-24.

2.4.7. Predictive Modeling

One goal of this project is to extrapolate trends from historical environmental conditions into the future under different population growth and climate change scenarios. Linear models developed during this project offered a statistically valid tool to make such predictions. Population growth and climate change scenarios were established from the literature. Estimated future population data were downloaded from Hauer's (2019) online dataset. Hauer calculated county-level population projections at 5-year intervals from 2015-2100 for the entire US under different growth scenarios, known as shared socioeconomic pathways (SSPs). To capture both low and high ends of these population projections, data were downloaded for two SSPs. These were the sustainable growth pathway (SSP1) and fossil-fueled development pathway (SSP5). Population totals from these two SSPs were downloaded for the year 2065 and summed up across all eight coastal South Carolina counties. The year 2065 was chosen because it matched available climate change scenario data for the mid-21st century. 2010 US Census population numbers were then totaled across South Carolina's coastal counties and compared to the 2065 projections to calculate percent change.

Climate change scenarios for this project were informed by the Fourth National Climate Assessment's (NCA) Climate Science Special Report (USGCRP, 2017). This report integrates multiple climate change studies to deliver a comprehensive assessment of climate change, and its many effects, for the United States. The NCA report was particularly helpful for this project because of its region-specific projections of precipitation and temperature changes under different climate change scenarios, known as Representative Concentration Pathways (RCPs). This project used mid-21st century (2065) temperature and precipitation projections for the Southeastern US under low emissions (RCP 4.5) and high emissions (RCP 8.5) climate change scenarios. These values were taken from data tables and figures in chapters 6 and 7 of the NCA report (Easterling et al., 2017; Vose et al., 2017). While precipitation projections were already available as percent change, temperature projections were only available as °F increase. These data were compared to 30-year climate normals data averaged across the project's three primary weather stations to calculate percent change. Summaries of these projections for coastal South Carolina can be found in Table 25.

After establishing these predictions, scenarios were created for each combination of population growth, precipitation change, and temperature change under low and high projections. Scenario definitions are summarized in Table 26. Prediction datasets were then created for each scenario to feed into previously developed linear models. To create these prediction datasets, all independent variables were averaged across the entire SCECAP dataset with habitat types (*i.e.*, tidal creek, open water) averaged separately and together. Independent variables influenced by population growth or climate change were modified according to the scenario's projections. For example, population, developed

landcover types, and impervious surfaces were increased by the scenario's population percent change (assuming a 1:1 relationship between population growth and development).

Climate variables were altered to represent the different climate change scenarios. Observed daily temperature averages and precipitation totals were increased by the scenario's respective percent change values. Seasonal and annual weather data were calculated as differences from 30-year climate normals, thus could not be simply modified by multiplying percent change. Instead, these data were increased by the scenario's predicted changes in °C or cm.

Baseline conditions (scenario 0) were estimated using SCECAP-wide averages of population, developed landcover, impervious cover, and weather observations. Since seasonal and annual weather variables were calculated as difference from normal, these values were changed to zero in the baseline scenario to reflect 30-year climate normal data. Results from these scenarios were organized into a final prediction dataset mirroring the dataset used in model creation.

The finalized selection of linear models were rerun with the prediction dataset for each scenario and response variable using R's 'predict.lm' function. This function produced predicted responses (*e.g.*, ERMQ metals, enterococci) with accompanying 95th percentile upper and lower confidence intervals. Model prediction results for each response variable and scenario were organized into one dataset for further analysis. At this stage, response variables that had been transformed during modeling were untransformed for easier interpretation. Predicted responses were also compared to baseline responses to calculate percent change. Scenario prediction outputs for each

response variable are available as data tables (see Tables 27-38) and graphs (see Figures 53-65).

CHAPTER 3. RESULTS

3.1. Data Collection and Processing

3.1.1. Physiographic Data

Despite a rapidly growing population, coastal South Carolina remains a largely natural landscape. The composition of coastal South Carolina's landcover, and how it compares to the rest of the state, is showcased in Table 1. Results were from the most recent NLCD product (2016) and were reported as coastal (*i.e.*, eight coastal counties) and statewide totals. County-level NLCD landcover data were further summarized and plotted over time as seen in Figure 66. These results show that coastal South Carolina is a predominantly forested landscape (66%). Woody wetlands (34%) and evergreen forest (23%) were the two most common forest types in coastal South Carolina. Developed landcover represents the second most common landcover type for coastal South Carolina. The majority of developed landcover comes from low intensity development categories. The third most prominent landcover category in coastal South Carolina is marshland (*i.e.*, emergent herbaceous wetlands) which comprise 10% of total coastal landcover. These tidally influenced wetlands define South Carolina's coastal landscape and range from freshwater to saltwater. In saltwater and brackish conditions, these systems are dominated

by a single species – smooth cordgrass (*Spartina alterniflora*). As marshlands transition to freshwater, smooth cordgrass is replaced with other graminoid species such as black needlerush (*Juncus roemerianus*). Agriculture and open water are the fourth and fifth most prominent landcover categories, respectively.

These landcover data showcase South Carolina's diverse coastal landscape. Results from the landcover change analysis, visualized in Figure 7, help create a more complete picture of a changing landscape. Figure 7 displays the hectares of each county that remained the same or changed between 2001 and 2016. The majority (96%) of coastal counties' areas did not experience change in landcover during the study period. Figure 8 breaks down the area of coastal counties that did experience changes in landcover by category. Low intensity development, high intensity development, and water were the only three landcover categories that experienced a net increase with low intensity development showing the largest gain (+15,194 ha). Forested uplands, forested wetlands, marsh, and agriculture all experienced a net decrease with forested uplands losing the most area (-12,749 ha). These changes were further analyzed at the county level in Figure 9. Rural counties such as Colleton experienced very little change whereas counties with rapidly rising populations (*e.g.*, Horry county) experienced the greatest change in landcover. To explore which landcover categories were converted to which, these data were visualized using a Sankey diagram (Figure 67). Forested uplands and forested wetlands were the two landcover types with the largest areas lost to development. There was no loss of high intensity developed landcover and all lost low intensity developed landcover was converted into high intensity development, suggesting an irreversible pattern of development. Agricultural land experienced a decline in area

during the study period, primarily due to conversion into forested uplands. Another noteworthy pattern of landcover change occurred between forested wetlands and marshes. These two landcover types showed significant gains and losses between each other which suggests a dynamic boundary between forested wetlands and marsh habitats.

In terms of impervious cover, more populated counties such as Charleston, Beaufort, and Horry exhibit a significantly larger urban footprint than rural counties such as Colleton, Georgetown, and Jasper (Figure 68). Beaufort, Charleston, and Horry counties also demonstrated higher levels of impervious surface cover than the statewide average. Across South Carolina, impervious surface cover has been steadily increasing with the sharpest increase occurring between 2001 and 2006.

Census estimates, available by year and county, were used to summarize population growth in coastal South Carolina. Beaufort, Charleston, Dorchester, and Horry all have higher population densities than the statewide average (Figure 69). These counties also demonstrate a faster rate of population growth than the more rural counties of Colleton, Georgetown, and Jasper. Table 39 provides a more detailed summary of population changes between 2000 and 2018. The state of South Carolina grew from 4.02 million in 2000 to 5.08 million people in 2018. When data were combined for all coastal counties, an increase from 0.99 million in 2000 to 1.45 million people in 2018 was observed. Comparing these data in the form of percent change indicate that coastal populations increased at a rate of 47% – nearly double the state's growth rate of 26%. While Charleston County held the largest number of residents, its growth rate (31%) was lower than the coastal average and only slightly higher than the state average. Horry County demonstrated the highest percent change of 74% followed by Dorchester (66%),

Beaufort (53%), and Berkeley (53%). Colleton was the only coastal county to experience a decrease in population during the study period (-2%).

Physiographic data were processed beyond the county level using a variety of spatial units such as HUC watersheds, grids, and buffers. Table 40 provides basic statistics on the HUC watersheds analyzed in this study. 8-digit HUCs were the largest watersheds studied with an average size of 262,213 ha and 14-digit HUCs were the smallest with an average size of 205 ha. Data were processed for a total of 19 8-digit, 60 10-digit, 264 12-digit, and 205 14-digit HUC watersheds. Figure 70 provides an example of physiographic data processing outputs for a 14-digit HUC watershed in Charleston, SC.

3.1.2. Weather and Climate Data

Daily weather data were compiled from a total of 401 weather stations spanning South Carolina's coastal counties and neighboring Brunswick County, North Carolina and Chatham County, Georgia. These data were collected from January 1st, 1999 to December 31st, 2018 for a total of 7,305 days. Daily weather observation data were compiled into a single database resulting in a total of 588,092 precipitation records and 176,260 temperature records.

30-year climate normal data from the three primary weather stations are summarized in Table 2. The southernmost station (Savannah International Airport, GA) had the warmest and driest climate, the northernmost station (Brookgreen Gardens, SC) had the coolest and wettest climate, and climate at the Charleston International Airport

station was in the middle of the two other stations. Table 2 also defines extreme temperature and extreme precipitation events for these three weather stations. Extreme temperature events are days with a maximum temperature greater than 33.3, 34.3, and 35.0 °C at Brookgreen Gardens, Charleston International Airport, and Savannah International Airport stations, respectively. Extreme precipitation events are days with rainfall totals greater than 2.34, 2.26, and 2.11 cm at Brookgreen Gardens, Charleston International Airport, and Savannah International Airport stations, respectively.

Observed weather data were compared to climate normal data to calculate seasonal and annual temperature and precipitation deviations from normal. These results were averaged across all three primary weather stations and reported in Figures 10 and 11. Figure 10 displays the yearly deviations from normal with temperature on the y-axis and precipitation on the x-axis. This type of scatterplot allows for an assessment of warm and wet, warm and dry, cool and wet, and cool and dry years or seasons. Out of the last ten years of data (2008-2018), seven years were warmer, and eight years were drier than average. Climate data are then broken down into seasons and displayed in Figure 11. Seasonal data follow a similar pattern to annual data with more recent years found in the warm and dry quadrant. Figure 11 also serves as a visualization tool for assessing variation in the data. Data points for spring and summer are more tightly clustered than fall and winter data points meaning that more climate variability occurs in fall and winter than spring and summer. Information can also be gathered from the shape of these data point clusters in Figure 11. For example, winter variability is greater along the temperature axis and fall variability is greater along the precipitation axis.

The PDSI, PMDI, and PHDI all respond similarly during the study period; however, the Palmer Z-Index (ZNDX) stands out from other drought indices with pronounced, short-term fluctuations which demonstrates its ability to explain drought on shorter time frames (Figure 71). When comparing data between the two climate divisions, both regions of the South Carolina coast experience drought similarly. This suggests that drought occurs at a more regional scale than local weather observations. Standard precipitation indices (SPI) for the two climate divisions are broken down by the number of months included in the drought calculation; for example, SP01 describes a 1-month SPI value and SP24 describes a 24-month SPI value (Figure 72). Spikes in the SPI value become less pronounced as the months increase with SP12 and SP24 describing long term drought conditions across the landscape. As with the Palmer indices, SPI values differ little between the two climate divisions. These graphs can be used to identify drought years within the study period. Both Palmer and SPI drought indices show periods of drought in 2003, 2008, and 2012 with the most extreme drought occurring around 2003.

Monthly climate teleconnection indices include the North Atlantic Oscillation (NAO), Arctic Oscillation (AO), Atlantic Multidecadal Oscillation (AMO), and the Oceanic Niño Index (ONI) (Figure 73). The NAO and AO demonstrate significant variability throughout the study period, whereas the AMO maintains a smooth upward (*i.e.*, warming) trend. The ONI can be used to identify El Niño and La Niña years within the study period. El Niño is determined when the ONI is greater than 0.5, La Niña is determined when the ONI is less than -0.5, and values between -0.5 and 0.5 are deemed neutral phases. Pronounced El Niño events are seen in 2002-2003, 2009-2010, and 2015-

2016, with the latter being the most intense. La Niña events in the study period have occurred in 1999-2000, 2007-2008, and 2010-2011. Years of La Niña and El Niño were identified in Figures 10 and 11. For example, the winter of 2010 was a strong La Niña year and had a noticeably cooler and wetter climate than other years of data.

3.1.3. Environmental Data

Environmental data were compiled from a total of 811 SCECAP sites spanning South Carolina's coast from 1999 to 2018. Four hundred-and-eight of these sites were classified as open water (channel width ≥100 m) and 403 were classified as tidal creek sites (channel width ≤100 m). Figure 3 displays the distribution of SCECAP sites along the South Carolina coast. A greater number of sites were sampled in the southern half of the state due to the region's larger estuarine habitat. Sampling protocol changed in 2007, transitioning to 30 sites visited per year in contrast to the previous 50 to 60 sites. During the course of the study period, new environmental parameters have been added to SCECAP's sampling protocol. For example, testing for PBDEs in sediment samples began in 2003 and testing for enterococci in the water column began in 2007. Channel width ranged in size from 11 m to over 11 km with an average width of 823 m. Station depth ranged from 0.3 to 17.6 m with an average depth of 3.7 m. Salinity ranged from 0 to 41 ppt with an average of 28 ppt. pH ranged from 4.9 to 8.5 with an average of 7.5. These differences in habitat characteristics demonstrate the diversity of South Carolina's estuaries.

3.2. Data Analysis

3.2.1. t-Tests

Results from *t*-tests were compiled into Tables 3-9 and visualized as boxplots in Figures 12-26. Data were grouped by habitat type (open water vs. tidal creek), time period (1999-2008 vs. 2009-2018), and watershed development (developed vs. undeveloped). Tests between time periods and watershed development were run for all sites as well as split by habitat type. Environmental data were grouped into three categories – water quality, sediment quality, and biological quality. Statistical significance between group means were signified by asterisks in boxplots and bold text in tables.

Compared to open water sites, tidal creek sites displayed higher water temperatures, lower dissolved oxygen, lower pH, and higher levels of bacteria. Tidal creek sites also showed higher levels of sediment contamination. Looking at raw concentration data, metals, PAHs, and DDT were higher in sediments from tidal creeks than open water sites. When looking at ERMQ scores, metals, DDT, and the combined ERMQ were also on average higher in tidal creek sites than open water sites. Data on biological quality showed significant differences between these two habitat types. Despite being towed for half the distance of open water sites, trawls in tidal creeks exhibited higher species richness. Benthic species richness and abundance were higher in open water sites than tidal creek sites. Both benthic indices (*i.e.*, BIBI and MAMBI) indicated healthier, less-stressed benthic communities in open water sites when compared

to tidal creek sites. These findings suggest that tidal creeks are in general more polluted and stressed habitats compared to open water sites. When comparing biological data between these two habitat types, nekton biodiversity is higher in tidal creeks and benthic biodiversity is higher in open water habitats. This could be the result of the gear used during SCECAP sampling as their trawl nets more effectively capture smaller fish and invertebrates which are more likely to be found in tidal creek habits.

Results from *t*-tests comparing environmental data between time periods (*i.e.*, 1999-2008 vs. 2009-2018) are displayed as boxplots (Figures 15-20) and data tables (Tables 4-6). Water temperature and enterococci concentrations were on average higher in 2009-2018 data and pH was on average lower in 2009-2018 data (see Figure 15). When broken down by habitat type, there were no significant differences between water quality parameter means across time periods in open water habitats (see Figure 17). In tidal creeks, water temperature and enterococci concentrations were on average higher in later years. When looking at sediment quality between time periods, PAH, DDT, and PBDE concentrations were on average higher in the second half of the study period (see Figure 17). In both tidal creeks and open water sites, DDT and PBDE concentrations were higher in later time periods (see Figure 18). PAH concentrations were higher in later time periods in tidal creeks but no difference was detected between time periods in open water sites. All biological quality variables showed significant differences in means between time periods (Figure 19). Nekton abundance and species richness, benthic abundance and species richness, and both benthic indices (BIBI and MAMBI) were on average lower in the later time period suggesting a decrease in biodiversity during the course of the study period. When broken down by habitat type, nekton abundance, nekton

species richness, and benthic species richness were lower in later years in both habitat types (see Figure 20). Benthic abundance was only significantly lower in later years in open water sites, and MAMBI was only significantly lower in later years in tidal creek sites.

Results from *t*-tests comparing environmental data between watershed development categories (*i.e.*, developed vs. undeveloped) are displayed as boxplots (Figures 21-26) and data tables (Tables 7-9). Water temperature and fecal coliform concentrations were on average higher in developed watersheds, and dissolved oxygen and pH were on average higher in undeveloped watersheds (Figure 21). Open water sites in developed watersheds had higher pH, higher fecal coliform concentrations, and lower water temperature than open water sites in undeveloped watersheds. (Figure 22). Tidal creek sites in developed watersheds had on average higher dissolved oxygen and higher pH than tidal creek sites in undeveloped watersheds. Concentrations of metals, PAHs, PCBs, PBDEs, DDT were all on average higher in sediments from developed watersheds than sediments from undeveloped watersheds (Figure 23). When sediment quality data were broken down by habitat type, only open water sites showed significant differences in sediment contamination between developed and undeveloped watersheds (Figure 24). Nekton abundance was the only biological metric with significant differences between developed and undeveloped watersheds; sites from undeveloped watersheds had greater average nekton abundances than sites in developed watersheds, and this trend was significant in both open water and tidal creek sites (Figures 25 and 26).

3.2.2. Time Series Analysis

Results from time series analysis of weather and environment data are displayed as line plots in Figures 27-40. These figures are also accompanied by model outputs summarized in Tables 10-15. While water quality and sediment quality data experienced variation during study period, time series analysis did not reveal significant trendlines in these data (Figures 27-30). However, time series analysis on biological quality data produced significant trendlines. When all sites were analyzed together, nekton species richness, nekton abundance, benthic species richness, and MAMBI experienced a significant decline during the study period (Figure 31). When open water sites were analyzed separately, only nekton species richness and benthic species richness showed a significant decrease (Figure 32). In tidal creeks, significant negative trendlines were only observed in nekton species richness, nekton abundance, and MAMBI data (Figure 32).

Trends in weather data were also analyzed using time series regression; the results of which are represented by line plots (Figures 33-40) and model output tables (Tables 14-15). Figures 33 and 34 display annual trends in temperature and precipitation. Annual average temperature in coastal South Carolina showed a significant increase during the study period (Figure 33). When weather data were averaged across all three stations, time series analysis on total annual precipitation did not produce a significant trendline (Figure 33). When broken down into individual weather stations, only Charleston International Airport and Savannah International Airport stations demonstrated a significant increase in average annual temperature (Figure 34). Additionally, annual precipitation showed a significant, increasing trend at the Charleston International Airport station (Figure 34).

In addition to annual weather data, time series analyses were run on seasonal weather patterns. Time series analysis did not produce significant trendlines when seasonal temperature data were analyzed by averaging all three weather stations (Figure 35). However, Charleston International Airport and Savannah International Airport stations experienced significant increases in summer and fall temperatures during the study period (Figure 36). Additionally, time series analysis showed increasing spring temperature at the Savannah International Airport station but not at the other two stations. Time series analyses did not reveal significant trends in seasonal precipitation data averaged across all three weather stations (Figure 37). When seasonal precipitation data were analyzed by station, winter precipitation appeared to be increasing at the Savannah International Airport station (Figure 38). Changes in frequency of extreme temperature and precipitation events are shown in Figures 39 and 40. Time series analysis of the number of extreme temperature events over the study period did not produce a significant trendline; however, the number of extreme precipitation events per year experienced a significant increase over the course of the study period (Figure 39). Extreme weather data were also analyzed at the station level; however, only the Charleston International Airport station experienced a significant increase in extreme precipitation during the study period (Figure 40).

3.2.3. Hot Spot Analysis

Hot spot analyses were performed for a subset of SCECAP environmental parameters summarized by 14-digit HUC watersheds and are displayed as maps in

Figures 41-52. Hot and cold spots are signified by the degree of confidence that a watershed is significantly different than its neighborhood (determined by the G_i* statistic) (Getis and Ord, 2010). In the case of sediment contaminants, hot spots represent watersheds with high levels of estuarine sediment contamination and cold spots represent watersheds with relatively unpolluted estuarine sediments. For biological data, hot spots are watersheds with greater biodiversity and benthic integrity within their estuaries and cold spots represent watersheds with degraded, estuarine biological communities.

Hot spot analyses helped reveal spatial patterns in the environmental dataset. For example, sediment contaminant and fecal coliform hot spots were more prominent in the central region of the South Carolina coast suggesting a correlation between the urbanization of the Charleston region and water and sediment contamination (Figures 42-46). Spatial patterns among biological data were harder to discern. Data on benthic communities appeared to follow a latitudinal trend with benthic biodiversity increasing from north to south (Figures 49-52). Spatial trends in nekton community data, on the other hand, were less pronounced than benthic data (Figures 47-48). Hot spots of nekton richness appeared in the coastal region between Charleston and Beaufort (Figure 47). For nekton abundance data, only two watersheds along the southern coast were identified as hot spots (Figure 48).

3.2.4. Multiple Linear Regression

A total of 209 multiple linear regression models were created during the stepwise regression modeling phase. Model inputs included 19 response variables and 106

explanatory variables, all analyzed at 11 different spatial scales. The full list of these inputs can be found in Appendices B, E, F, and G. Each multiple linear regression formula represented an environmental response variable (*e.g.*, fecal coliform) with a list of explanatory variables (*e.g.*, impervious cover), and was modelled by spatial unit of interest (*e.g.*, 12-digit HUC watershed). The number of predictive terms (excluding intercepts) in these models ranged from 3 to 8 with an average of 5.4. This large set of stepwise-generated models served as the source for more detailed linear models and provided a dataset for meaningful meta-analyses.

3.2.5. Model Meta-Analysis

Meta-analyses were performed on all stepwise regression outputs to reveal overarching trends in the data. Table 16 displays the R^2 values averaged by response variable category and spatial unit of analysis. R^2 values represent the proportion of variance explained by a model and were the chosen statistic to reflect goodness of fit. The average R^2 among all 209 models was 0.30. The response variable category with the highest average R^2 was sediment quality (R^2=0.36), whereas biological quality models had the lowest average R^2 (R^2=0.22). On average, HUC watersheds produced the best models (R^2=0.33), grids produced the worst models (R^2=0.28), and buffers were somewhere in between (R^2=0.31). Within each spatial grouping system, 3 km buffers, 1600 km^2 grids, and 10-digit HUCs resulted in the highest R^2 values. Each response variable category had a different spatial unit of analysis that produced the highest R^2 values. Buffers with 2 km radii were best at explaining water quality models (R^2=0.36),

10-digit HUCs were best at explaining sediment quality models (R^2=0.40), and 12-digit HUCs were best at explaining biological quality models (R^2=0.23).

While Table 16 summarizes general model performance, Tables 17-20 detail the frequencies and coefficient estimates of the independent parameters within the models. Across all models, variables representing physical habitat (*e.g.*, salinity, channel size) appeared most frequently. Silt and clay content, for example, occurred in 61% of all models. Impervious cover was the most frequent landcover variable, followed by marsh and population density. Winter temperature and precipitation were selected as model variables more frequently than any other weather or climate variables. These meta-analysis were also used to reveal temporal trends in the weather data. Water quality data were most often correlated with 2-day precipitation totals, biological quality data were most often correlated with temperature and precipitation values at 30- and 45-day intervals, and sediment quality data were most often correlated with seasonal weather patterns (*e.g.*, winter precipitation). While this type of meta-analysis can help identify the most prevalent predictors, information can also be gathered from parameters that were featured infrequently or not at all. For example, hydrologic soil data and stormwater pond data appeared only sporadically throughout the modeling process. Additionally, some variables such as the Oceanic Niño Index (ONI) or Palmer Z-Index (ZNDX) did not appear at all.

Tables 17-20 also provide mean coefficient estimates. Mean coefficient estimates were calculated by averaging coefficient estimates for each parameter across all models and were used to reveal generalized correlations among the data. For example, channel width, depth, and salinity were all negatively correlated with water quality response

variables suggesting smaller and less saline estuaries experienced higher levels of water quality impairment (*e.g.*, bacterial contamination). Marshes, on average, were negatively correlated with measures of pollution and positively correlated with measures of biological integrity. This suggests the presence of marshes were correlated with better environmental condition. On the other hand, development-related explanatory variables were positively associated with measures of pollution and negatively associated with measures of biological integrity.

3.2.6. Final Model Selection and Refinement

Out of the 209 models produced through stepwise regression, 13 were chosen for further refinement. Each of the 13 final models represented a different response variable selected by the spatial scale with the highest adjusted R^2. Some response variables were excluded altogether during this stage. For example, contaminants measured by their ERMQs produced models with higher R^2 values than their raw concentration counterparts; as a result, only the ERMQ sediment contamination data were included in the final set of models. Models of PBDE contamination were excluded altogether from the final set of models because no ERMQ scores were available for this contaminant. Although the BIBI was specifically calibrated for estuaries in the Southeastern United States, MAMBI was ultimately selected as the preferred benthic index for the final modeling stage because of its better modeling performance (*i.e.*, higher R^2 values).

Tables 21-24 provide detailed model diagnostics and summaries of these final models. Table 21 displays model outputs for ERMQ scores for four categories of

contaminants (DDT, metals, PAHs, PCBs) as well as a combined ERMQ score for all contaminants. These variables were all modelled at the 10-digit HUC watershed scale. Adjusted R^2 values for these models ranged from 0.17 (DDT) to 0.82 (metals). Sediment composition was strongly correlated with levels of sediment contamination, and higher TOC and silt-clay content in samples were associated with higher levels of sediment contamination. Winter and spring precipitation were positively correlated with contaminant levels in sediments collected during the summer months, and winter temperature and fall precipitation were negatively correlated with contaminant levels. In some models, significant interaction effects were observed. For example, the interaction between winter precipitation and winter temperature was negatively correlated with PAHs, and the interaction between spring precipitation and winter temperature was negatively correlated with PCBs. These interactions suggest that wet winters and wet springs are positively correlated with sediment contamination unless these conditions cooccur with warm winters. Measures of human activity in the watershed, such as impervious cover or population density, were positively correlated with sediment contamination.

Table 22 displays the results of bacterial contamination modelled using 2 km buffers. The fecal coliform response variable created a much better model (R^2=0.46) than enterococci levels (R^2=0.24); different sample sizes between these variables could be one explanation for different model performance since enterococci data only go back to 2007. Lower salinity systems with smaller channel sizes were correlated with higher levels of bacteria. Percent of impervious surface cover was also positively correlated with bacteria levels. Forty-eight-hour precipitation totals from the nearest weather station proved to be

the most significant weather-related predictor variable, indicating that peak bacteria levels are found two days following a rain event.

Trawl nekton data were analyzed at the 12-digit HUC level and are summarized in Table 23. Nekton abundance had the highest R^2 of these models (R^2=0.18) and tidal creek nekton species richness had the lowest (R^2=0.15). Parameters of watershed development were notably absent from nekton models, with the exception of the nekton abundance model in which impervious cover was negatively correlated with abundance. The North Atlantic Oscillation (NAO) index was significantly correlated with nekton abundance and nekton species richness; the only instance of a climate teleconnection making it into the final models. Channel width was negatively correlated with all three nekton models suggesting higher nekton biodiversity in smaller-channel estuarine habitats. Annual temperature averages were negatively correlated with species richness in both tidal creek and open water habitats. In tidal creeks, annual average temperature from the preceding year was most significant, and in open water sites, annual average temperature from the current year was most significant.

Model results for benthic data are displayed in Table 24. Physiographic data in benthic abundance and benthic species richness models were analyzed by 12-digit HUC; however, landcover in the MAMBI model were analyzed by 400 km^2 grid cells. Overall, benthic models performed better than nekton models. R^2 values for benthic abundance, species richness, and MAMBI models were R^2=0.19, R^2=0.42, and R^2=0.47, respectively. Benthic models were the only cases of development being associated with better environmental outcomes. Low intensity development and developed open spaces were both positively correlated with benthic species richness and MAMBI. However, high

intensity development was negatively correlated with MAMBI values. According to these models, benthic community data are best explained by 45-day precipitation and 90-day temperature patterns. At these time scales, warmer and drier conditions were correlated with lowered measures of benthic biodiversity. Benthic models were also strongly tied to physical habitat characteristics, with larger channels and more saline conditions producing higher measures of benthic health.

3.2.7. Predictive Modeling

A total of 15 scenarios were created for predictive modeling. These scenarios represent different combinations of precipitation change, temperature change, and population growth under high and low projections (Table 26). Table 25 summarizes the predictions used to define these scenarios. The population of South Carolina's coastal counties is expected to increase 2.8 million by 2065 under a sustainable growth scenario (SSP1) and 3.4 million under a fossil-fueled growth scenario (SSP5) (Hauer, 2019). When compared to the 1.2 million people counted in 2010 Census, SSP1 and SSP5 growth scenarios would account for an increase of 130% and 180%, respectively. Assuming a 1:1 relationship with population, developed landcover and impervious surfaces were also increased by 130% and 180% in these scenarios. In reality, population growth and landcover changes may not be exhibit a perfect 1:1 linear relationship; however, slopes of increasing population and developed landcover were roughly parallel over the course of the study period which helped justify this assumption (Figures 68 and 69). According to 2011 NLCD data, impervious surfaces covered 2.59% and developed

landcover covered 9.89% of coastal South Carolina counties. Under the higher population projection (+180%), these values are predicted to increase to 7.26% impervious cover and 27.69% developed landcover by 2065.

Temperature and precipitation predictions were based on climate change projections from the Fourth National Climate Assessment (NCA) report (USGCRP, 2017). According to this report's projections for the mid-21st century (2065), average temperature in the Southeast is expected to increase by 1.9 °C under the low emission scenario (RCP4.5) and 2.4 °C under the high emission scenario (RCP8.5). When this change was applied to 30-year climate normals for coastal South Carolina, the annual average temperature (19.0 °C) increased by 5% (20.9 °C) in the low projection and by 6.5% (21.4 °C) in the high projection. The NCA report also predicts an increase in precipitation by 5-10% for the Southeast by 2065. According to the 30-year climate normal data, average annual precipitation for coastal South Carolina is 129.7 cm. This value would increase to 136.4 and 142.8 cm at the low (+5%) and high (+10%) end of NCA's projections, respectively. Although changes in precipitation will likely exhibit seasonal variation, projected increases in annual precipitation totals were evenly distributed across seasons in these scenarios.

Predicted outcomes from these scenarios were entered as parameters into the final set of linear models, and the resulting model outputs were summarized into Tables 27-38. On average, response variables from open water sites experienced greater changes than those from tidal creeks under these scenarios. Additionally, water quality values (*i.e.*, bacterial contamination) experienced the greatest increase under these scenarios. Levels of sediment contamination and bacteria concentrations increased under change scenarios,

whereas measures of biological quality decreased. Together, these predictions point to a decline in the overall quality of the estuarine environment under climate change and population growth. Changes to temperature, precipitation, and population were modelled individually in some scenarios to isolate their potential effects. On average, changes to precipitation resulted in the lowest amount of observed change in response variable predictions and changes to temperature resulted in the highest amount of observed change in response variable predictions. The scenario resulting in the greatest amount of change within response variable predictions was Scenario 14 which included population growth, temperature change, and precipitation changes under the highest projections.

Figures 53-65 display the predicted outcomes of each response variable under these different change scenarios. These figures helped visualize predictions and their confidence intervals alongside baseline conditions. Confidence intervals were extrapolated from error terms within the original linear models and varied from response to response. Interpretations of scenario outcomes should be made with caution in cases where confidence intervals of a prediction overlap the confidence intervals of the baseline.

Although enterococci and fecal coliform levels both increased within change scenarios, each responded differently to change (Figures 53 and 54). Temperature change was the primary driver for increased enterococci whereas population growth was responsible for increases in fecal coliform bacteria. Each bacteria model included precipitation as a predictor; however, projected increases in precipitation were not adequate to significantly increase bacteria levels above the baseline.

Scenario predictions of sediment contamination are displayed in Figures 55-59. In these sediment models, population had the greatest influence on the predicted response. With the exception of DDT, population growth resulted in levels of sediment contamination significantly higher than the baseline. Increases to temperature resulted in lowered predictions of sediment contamination. Temperature-driven changes in PAHs, PCBs, and combined ERMQ scores were significantly lower than the baseline value. Although precipitation was included in these sediment models, changes to precipitation did not result in significant differences from baseline conditions. Changes to precipitation alone might not result in significantly higher levels of sediment contamination, but it may interact with population growth and result in more contaminated estuarine sediments.

Biological responses to change scenarios were more variable than water quality and sediment quality models (Figures 60-65). Nekton abundance was less than baseline in all predicted scenarios; however, only scenarios which included temperature change resulted in nekton abundance predictions with confidence intervals outside the baseline. Nekton species richness, in both habitat types, decreased from baseline conditions in all scenarios, although precipitation and population changes resulted in species richness predictions with confidence intervals overlapping baseline values. Benthic abundance predictions increased under all scenarios; however, due to the high level of uncertainty in the benthic model, none of the predictions were significantly above baseline. Benthic species richness predictions were significantly higher than baseline conditions in population growth scenarios except scenarios included temperature change. Temperature increases, with or without changes to precipitation, resulted in benthic species richness predictions significantly lower than baseline. MAMBI responses to scenarios were

similar to benthic species richness models except all scenarios which included population growth resulted in significantly higher-than-baseline MAMBI predictions. Both high intensity development and developed open spaces were included as explanatory variables in the MAMBI model. In the MAMBI model, developed open space landcover was positively correlated and high intensity developed landcover negatively correlated with MAMBI values. According to these predictions, the positive effect of developed open space landcover on MAMBI values outweighed the negative correlation between high intensity developed landcover and MAMBI values. Increases to temperature, with or without precipitation change, resulted in significantly lower MAMBI predictions.

CHAPTER 4. DISCUSSION

4.1. A Changing South Carolina Coast

Landcover and population data collected and analyzed for this project demonstrated significant changes to South Carolina's coastal landscape during the study period. Between 2000 and 2018, the population of coastal South Carolina has grown by nearly half a million – a 46% increase (Table 39). This growth rate outpaced the nationwide increase of 16% during the same time period (US Census Bureau, 2018). NLCD data show that measures of development (*e.g.*, impervious surface cover) have risen in tandem with this population growth (Figures 68 and 69). A closer look at Figure 68 shows that the sharpest increase in impervious surface cover occurred between 2001 and 2006. This could suggest that conversion of landcover precedes population growth, and perhaps that the rate of urbanization will plateau as more people move into the region. Nevertheless, impervious cover continued to climb during the later years of data, albeit at a slower rate. Results from this project were compared with previous studies which have explored the issue of population growth and landcover change in coastal South Carolina.

In 2003, Allen and Lu recognized a rapidly growing coastal population and created a GIS model of urban growth for the Charleston Tri-County area (Berkeley,

Charleston, and Dorchester counties). Allen and Lu predicted a population of 795,879 in the Tri-County region by the year 2030. In 2018, more than ten years ahead of their predictions, this area already had an estimated population of 787,643 (Table 39). In their paper, Allen and Lu also modelled urban expansion in the Tri-County area and predicted the urban zone would expand from 75,887 ha in 2000 to 170,680 ha by 2020. The authors used a different set of spatial data and tools from this project; therefore, direct comparisons were not made between their predictions and this project's NLCD-derived data. However, it may still be worthwhile to compare percent changes between similar time periods. Allen and Lu's projection resulted in a 125% increase of urban area between 2000 and 2020. In comparison, NLCD developed landcover for the Tri-County area increased from 70,823 to 80,450 ha, or 14%, between 2001 and 2016. While the current population of the Charleston metropolitan area has surpassed their predictions, Allen and Lu may have overestimated the rate of urban sprawl.

Exploring non-development landcover types proved to be a worthwhile exercise and helped create a more holistic picture of coastal change in South Carolina. Despite rapidly growing urban areas such as Charleston or Horry counties, much of coastal South Carolina remains a largely natural landscape with two-thirds of coastal area covered in forest (Table 1). Overall, these landcover analyses revealed a patchwork of urban, rural, and natural landscapes across coastal South Carolina. This gradient of development intensity served as an important foundation for subsequent data analysis relating urbanization and estuarine environmental condition.

The only non-development landcover type that experienced a net increase during the study period was open water. Sea-level rise and other forms of coastal erosion may

very well be responsible for this increase. To some extent, rising sea levels will be met with inland marsh migration (Feagin et al., 2010). However, the ongoing urban conversion of land within the coastal zone can impede this natural transition as infrastructure could prevent inland marsh migration in a process referred to as the "coastal squeeze" (Torio and Chmura, 2013). Open water experienced a net increase of 5,562 ha, while marshes experienced a net decrease of 3,987 ha (Figure 8). As development continues along the marsh's edge, this boundary between water and wetlands will prove critical under a changing climate. To account for sea level rise and marsh migration, future growth should consider wider buffers of forest between marsh and development or designating green space and conservation areas to allow for future migration pathways.

While sea level rise is and will continue to be a serious challenge for coastal communities, this study was more focused on understanding climate change's impacts on weather, particularly changes to temperature and precipitation. Data gathered on temperature and precipitation over the study period revealed broad patterns of change across South Carolina's coast consistent with climate predictions (Mizzell et al., 2014). By focusing on three long-term weather stations (Brookgreen Gardens, Charleston International Airport, and Savannah International Airport), this project was able to explore climate change trends specific to coastal South Carolina. Time series analyses proved to be a useful tool in demonstrating changes in weather during the study period. From 1895 to 2016, annual average temperature in the contiguous United States has increased by 0.7-1.0 ºC (Vose et al., 2017). However, changes in temperature were not uniform across the United States, and out of all the regions, the Southeast experienced the

smallest annual average increase in temperature (0.26 ºC) (Vose et al., 2017). Time series analyses aligned with these studies and indicated a significant increasing trend in annual average temperature during 1999-2018 for coastal South Carolina (0.03-0.07 ºC/year, Table 14). When broken down by station, all but the Brookgreen Gardens station experienced this significant increase. The urban heat island effect may be one explanation for these differences in trends. While Charleston International Airport and Savannah International Airport stations are situated within metropolitan areas, the area surrounding the Brookgreen Gardens station is much less urbanized. Changes in average temperatures by season were less consistent. When all three stations were analyzed together, no significant changes in seasonal temperatures were observed (Figure 35). But when analyzed separately, both Charleston International Airport and Savannah International Airport stations experienced increasing summer and fall temperatures. While annual average temperature may be rising, seasonal warming trends appear to be more variable.

Annual precipitation increased by approximately 4% in the United States between 1901 and 2015; however, changes in precipitation varied considerably region to region and season to season (Easterling et al., 2017). Although precipitation is expected to increase by 5-10% in the Southeast by the mid-21st century, time series analyses of past weather data did not indicate significant changes in precipitation during the study period. The one exception was a significant trend of increasing winter precipitation observed at the Savannah International Airport station (Figure 38). Out of all the seasons, the NCA projects greater increases in precipitation in the Southeast during winter months (Easterling et al., 2017). The significant increase in winter precipitation observed at the Savannah International Airport station may be one indication of this seasonal pattern.

As coastal South Carolina becomes warmer and wetter, the frequency of extreme weather events is also expected to increase due to climate change. This project defined extreme weather as daily temperature maximums and 24-hour precipitation totals above the 95th percentile of observations from the 1999-2018 weather dataset (Table 2). Time series analyses were run on the number of extreme weather events per year to explore changes in extreme weather during the study period. Although the NCA predicts heat waves will increase in intensity and frequency due to climate change, no significant trends in extreme temperature events were observed in this project's dataset (Figures 39 and 40) (Vose et al., 2017).

In addition to extreme temperature, the frequency and intensity of extreme precipitation events are also expected to increase due to climate change. The Southeast alone may see up to a 21% increase in extreme precipitation events (Easterling et al., 2017). Time series analysis aligned with this projection and revealed a significant increasing trend in extreme precipitation across coastal South Carolina during the study period (Figure 39). The trendline from this analysis indicated that the frequency of extreme precipitation events has increased by one day every four years over the course of the study period (Figure 39, Table 15).

The purpose of analyzing historic weather data was to explore local weather patterns in the context of regional climate models and investigate how these trends may influence local environmental quality. Nonetheless, results from time series analysis corroborated trends established in the literature. Coastal South Carolina is becoming warmer, and while trends in precipitation may be subtle, the observed increase in extreme precipitation has important implications for the coastal environment.

4.2. Exploratory Data Analysis

The results from the *t*-tests demonstrated that environmental quality in South Carolina estuaries vary spatially (Tables 7-9) and temporally (Tables 4-6). Table 7 shows that estuarine sediments from developed watersheds had significantly higher DDT, metal, PAH, and PCB concentrations than samples from undeveloped watersheds. In 1995, Sanger and others (1999a, 1999b) tested sediments for the same set of contaminants in 28 tidal creeks along South Carolina's coast and found higher concentrations of contaminants in samples from urban watersheds than those collected in forested watersheds. With over 800 sample sites and 20 years of data, this project has shown that the link between urban watersheds and contaminated estuarine sediments persists at a much larger scale than Sanger and others' (1999a, 1999b) original findings. Sanger and others (1999a, 1999b) focused on headwater portions of tidal creeks as the primary link between uplands and coastal systems; however, these results indicate that open water sites are just as vulnerable to contamination from developed watersheds – a relationship also noted by Van Dolah and others (2008).

In addition to sediment contamination, higher levels of fecal coliform bacteria were detected in the water column of estuaries draining developed watersheds than those draining undeveloped watersheds (Table 7). This pattern of bacterial contamination in South Carolina's urbanized estuaries has been previously established in the literature (Kelsey et al., 2004; Holland et al., 2004; Van Dolah et al., 2008). *Enterococcus* bacteria were also sampled, but no significant difference was detected between concentrations in developed versus undeveloped watersheds. As enterococci data were only available post

2007, differing sample sizes between enterococci (*N*=337) and fecal coliform data (*N*=799) could be responsible for the differences in results between these two indicator bacteria.

A key finding in Holland others' 2004 study was in the biological response to watershed development. They found lower abundances of stress- and pollution-sensitive benthic invertebrates and lower abundances of Penaeoid species (*i.e.*, shrimp) in tidal creeks draining more developed watersheds. However, *t*-tests in this study compared measures of biodiversity between developed and undeveloped watersheds did not identify significant differences (Figures 25 and 26). Summarizing biological data at the scale of overall species richness and abundance may have been too coarse to reflect the estuarine ecosystem. Benthic indices (*e.g.*, BIBI), which have been proven to be useful indicators of watershed development on estuarine health, were also not significantly different between developed and undeveloped watersheds in these *t*-test analyses (Hale et al., 2004). Although this study's *t*-test analyses did not reveal significant differences in biodiversity between developed and undeveloped watersheds, significant temporal patterns were observed in the biological data.

t-tests between earlier and later halves of SCECAP data (1999-2008 versus 2009-2018) revealed significant declines in biological condition in South Carolina's estuaries (Tables 4-6). Species richness and abundance in both nekton and benthic communities were significantly lower in later years. The BIBI and MAMBI, which measure the biological integrity of benthic communities, also declined in the latter half of this study period. This observed decline in biodiversity in South Carolina's estuaries was followed up with time series analyses to better evaluate changes in the data over time.

Time series GLS regression of nekton species richness, nekton abundance, benthic species richness, and MAMBI data produced significant, negative trendlines over the study period (Figure 31). The fact that benthic species richness declined while abundance remained stable may signify changes within the benthic community structure. For example, generalist species may be filling in the gaps left behind by specialist species displaced by a rapidly changing habitat. This "functional homogenization" has been observed in ecosystems around the globe as a result of climate change and habitat disturbances (Clavel et al., 2011). Time series analysis results varied when biodiversity data were analyzed by habitat type (Figure 32). Open water sites only experienced a decline in nekton and benthic species richness, and tidal creek sites only experienced a decline in nekton species richness, nekton abundance, and MAMBI. Habitat differences between tidal creek and open water sites are likely responsible for these different responses. Additional data analyses included physical habitat parameters (*e.g.*, channel size, salinity) to better explain changes in the biological data across all habitat types. Estuarine and marine ecosystems around the globe are experiencing a decline in biodiversity (Lotze et al., 2006; Worm et al., 2006). This observed trend of declining biodiversity within South Carolina's estuaries should alarm researchers and natural resource managers alike and certainly warrants further investigation. However, SCECAP early data suggests higher than average trawl catches and benthic invertebrate counts in 2019.

In addition to *t*-tests and time series analyses, hot spot analysis proved to be another important exploratory tool to identify trends in the environmental data. Figures 42-52 offer quick, visual tools to assess the environmental condition of South Carolina's

coast based on a subset of parameters. To help explain geographic patterns within the environmental data, coastal South Carolina was divided into three regions – the Grand Strand (Horry and Georgetown counties), the Tri-County (Berkeley, Charleston, and Dorchester counties), and the Lowcountry (Beaufort, Colleton, and Jasper counties). In measures of sediment contamination (ERMQ), hot spots were often located in the Tri-County whereas cold spots were often located in the Lowcountry (Figures 42-46). Although comparable in area, 54% of South Carolina's coastal population live within the Tri-County whereas only 18% reside in the Lowcountry (Table 39). Differences in population are a likely explanation for the observed distribution of hot and cold spots in sediment contaminant data. While areas like Myrtle Beach are highly developed, the Grand Strand does not stand out as either a cold or hot spot in most of these analyses. Tidal amplitudes in South Carolina, as well as resulting estuarine area, increase from north to south; as a result, fewer SCECAP sites are located in the northern part of the coast. More limited data may be one explanation for the lack of sediment contaminant hot spots in the Grand Strand. Estuaries along the Grand Strand are also in closer proximity to the open ocean and beaches, and these contaminants may be dispersing and diluting in the swash zone (Jackson et al., 2017).

Hot spot analysis results from biological data were less predictable. Hot and cold spots of nekton species richness and abundance data were sporadically distributed along the coast (Figures 47 and 48). Benthic data, on the other hand, seemed to follow a latitudinal gradient. Cold spots of benthic species richness and MAMBI were found in watersheds in the northern region of the coast, while Lowcountry watersheds reliably produced hot spots (Figures 49 and 52). Although trends in benthic abundance and BIBI

hot spots were less discernable, benthic biodiversity appeared to increase southward along South Carolina's coast (Figures 50 and 51). This could be the result of a larger, more diverse estuarine habitat and a smaller anthropogenic footprint in Lowcountry watersheds.

Hot spot analysis, time series regression, and *t*-tests represented the first steps in analyzing the environmental dataset. Generally, measures of pollution (*e.g.*, ERMQs, fecal coliform) varied spatially and reflected patterns of urbanization, whereas measures of biodiversity (*e.g.*, nekton species richness, MAMBI) varied temporally and signaled an ecosystem in decline. As population growth and climate change pose compounding threats for the state's coastal ecosystems, these trends have important implications for South Carolina. By modeling historic environmental data with landcover and climate, this project delved deeper into the data to uncover the underlying mechanisms behind these observed trends.

4.3. Stepwise Regression and Model Meta-Analysis

Stepwise linear regression proved to be an invaluable tool to reduce the total variable pool and identify key variables. Care was taken to not rely too heavily on automated models and to ensure that selected variables were meaningful and interpretable. Freedman's Paradox states that when modeling with a large enough set of predictor variables, significance may appear randomly during the variable selection process (Lukacs et al., 2010). Recognizing these potential pitfalls, this project used a combination of automated and supervised linear modeling approaches. Stepwise

regression was used to handle the bulk of data, while a select set of models were fine-tuned by hand to best characterize the estuarine environmental response to landcover and climate.

One benefit of stepwise regression was the potential for meta-analyses on a large dataset of linear model outputs. Meta-analyses helped answer some important research questions such as the effect of spatial scales on model results. Multiple spatial units (*i.e.*, HUC watersheds, grid cells, and buffers) at multiple sizes (*e.g.*, 12-digit, 400 km^2, 3 km) were used to explain the effects of land use and landcover on environmental response variables. With R^2 as the chosen statistic to represent model performance, models across each category of response variable and spatial unit of analysis were summarized in Table 16. Overall, HUC watersheds produced the best models. Grid cells, on the other hand, produced the worst models. Grid cells were generated in ArcMap to mimic HUC watersheds in size while offering a uniform, pixelized system of analyzing landcover data. The fact that grid cells produced models with lower R^2 values than HUC watersheds provides further evidence for the hydrologic connection between uplands and downstream estuarine environment. On average, R^2 values from models using circular buffers were in between R^2 values of models using HUC watersheds and grid cells. However, when broken down by response variable category, buffers outperformed other spatial units in explaining water quality models.

The purpose of including buffers in this study was to explore the localized effect of landcover on environmental responses. In fecal coliform and enterococci models, impervious cover within a 1-3 km radius (314-2,287 ha) was more influential than impervious cover analyzed at the watershed scale. There could be many explanations for

this pattern. These indicator bacteria, carried by stormwater, may be dying off as they travel downstream, and as a result can only be detected in close proximity to their source (Anderson et al., 2005). Sediment contaminants, on the other hand, are more persistent in the estuarine environment (Farmer, 1991). Ten-digit HUC watersheds produced the best sediment quality models, which on average delineate an area of 51,632 ha in coastal South Carolina. While bacteria levels responded to landcover within the immediate surroundings, sediment contamination responded to landcover at large spatial scales. These models suggest organic and nonorganic pollutants from upland development travel long distances throughout the region's estuaries before settling out in the sediment. The effects of spatial scale were less clear for the biological quality models. 12-digit HUC watersheds seemed to produce the best biological models, but a few models of benthic data were best explained by landcover analyzed by 400 km^2 grid cells. Differences between nekton and benthic responses were expected as nekton can move in response to environmental stressors whereas benthic invertebrates are relatively sessile.

Additional meta-analyses summarized the frequency of independent variables within the stepwise-produced models (Tables 17-20). The three most frequent independent variables were silt-clay content, salinity, and channel width – all measures of physical habitat. While these variables are unlikely to change with population growth or climate change, they were essential in environmental modeling to control for the large variation in habitat across the study area. For example, silt-clay content figured prominently in the sediment quality models. Due to clay's high cation exchange capacity and greater surface area, sediments with higher silt and clay content are more likely to

attract metal and, to some extent, organic pollutants (Kowalska et al., 1994; Uddin, 2017).

The two most frequent landcover variables were upland impervious cover and marsh. The fact that impervious cover was more prevalent than other measures of development provides further evidence for stormwater runoff being responsible for the observed declines in estuarine habitat quality. While population density was a significant variable in some models, on average, impervious cover was a better predictor in these models. Measures of natural landcover types also proved to be important in these models. For example, presence of marshes were positively correlated with measures of biodiversity and negatively correlated with presence of contaminants. This observation may indicate the role marshes play in maintaining water quality and buffering pollution. Salt marshes have been shown to intercept excess nutrients from entering coastal waters (Brin et al., 2010). Marshlands provide many other ecosystem services for coastal residents such as protection from storm surge and coastal erosion. These models demonstrated a correlation between marsh landcover and better estuarine habitat quality, thus providing additional justification for protecting and preserving marshland habitats. Artificial stormwater infrastructure (*i.e.*, stormwater ponds), on the other hand, were absent as predictor variables during the modeling process raising questions about their efficacy.

4.4. Water Quality Models

The final set of bacteria models included landcover analyzed at 2 km buffers. This scale was used because it provided the best predictive capacity among the 1 km, 3 km, and various HUC and grids tested (Table 22). Out of the 1- to 90-day precipitation totals included in the model selection process, 2-day precipitation totals were the most significant predictors in both enterococci and fecal coliform models. Interestingly, this 2-day precipitation signal matched earlier studies. Kelsey and others (2004) modelled fecal coliform concentrations in Murrells Inlet (an estuary in South Carolina) with 1- to 14-day precipitation totals and found 2-day precipitation totals to be the best predictor of bacteria. The Palmer Drought Severity Index (PDSI) was also a significant predictor in the fecal coliform model. In this model, the PDSI was negatively correlated with bacteria concentrations meaning higher levels of bacteria were observed during drought conditions. Although this may seem inconsistent with the effect of 2-day precipitation totals, heavy precipitation events during dry conditions may lead to runoff carrying a greater load of accumulated contaminants from upland sources. This "first flush" effect has been studied in urban watersheds where the highest levels of fecal coliform bacteria were observed in stormwater at the onset of rain events (Hathaway and Hunt, 2011).

Fecal bacteria in waterways can have many sources including failing septic tanks, pet waste, surface runoff, livestock, or wildlife. Webster and others (2004) sampled *E. coli* bacteria from South Carolina's estuaries and tested for antibiotic resistance to differentiate between human and non-human sources. Although non-human sources of bacteria were identified in some rural watersheds, bacteria sampled from urban

watersheds were more significantly tied to human sources (Webster et al., 2004). Without these molecular tools, it is not be possible to identify the sources of bacteria measured in this project without relying on correlative analysis. In both bacteria models, upland impervious cover was positively correlated with bacteria concentration suggesting an anthropogenic source of contamination. However, mixed forest landcover was also positively correlated with fecal coliform concentration which may indicate a wildlife signal.

4.5. Sediment Quality Models

Population density and impervious surface cover were significant predictors in sediment quality models, and both were positively correlated with sediment contamination. This positive correlation provides further evidence linking urbanized watersheds and polluted estuaries. Van Dolah and others (2008) modelled this same suite of contaminants in estuarine sediments across South Carolina and identified similar connections. In their study, the authors analyzed data on landcover and sediment contamination by 14-digit HUC watersheds and found higher levels of sediment contamination in estuaries draining urban-suburban watersheds. Van Dolah and others (2008) shared some of the same data as this project including 180 SCECAP stations sampled from 1999-2002. This project expanded this dataset to include over 800 SCECAP stations sampled from 1999-2018 and found the relationships observed by Van Dolah and others (2008) continuing into the present. Additionally, this project analyzed landcover variables at multiple spatial scales and found 10-digit HUC watersheds to be

the most effective unit of analysis. This suggests the effects of urbanization are farther reaching than Van Dolah and others (2008) had originally proposed.

The silt-clay content of sediment samples featured prominently in these models (Table 21) because samples with finer grain size tend to sorb pollutants more readily than coarser grained samples (Ackerman et al., 1983; Kowalska et al., 1994; Uddin, 2017). Although silt-clay content was responsible for much of the variation within the sediment quality models, by controlling for this factor, other relationships were able to be quantified. This includes explaining the overall variation of habitats when modeling effects of landcover and climate on sediment response variables.

Several variables of weather and climate were also featured in the sediment quality models. Winter precipitation, in particular, was positively correlated with three out of the five ERMQ models. The prevalence of winter precipitation as a predictor was one of the more interesting findings in this project. Winter precipitation occurred as a significant predictor in 32% of all models making it the most frequent weather or climate independent variable (Table 20). If runoff is the mechanism by which contaminants move from developed upland areas to downstream estuarine sediments, then there are several possible explanations for this correlation between wet winters and higher ERMQ values. As deciduous vegetation cover decreases in winter months, more rainfall is converted into runoff due to less interception in the canopy (Xiao et al., 2000). However, the majority of forest type in coastal South Carolina is evergreen and heavy rainfall events are more typical of summer thunderstorms than winter precipitation.

Another possible explanation for this association between wet winters and higher ERMQ values may be biological. Constructed wetlands have been successfully used in

wastewater treatment because microbial communities within the rhizosphere are particularly adept at breaking down and assimilating excess nutrients and organic pollutants (Stottmeister et al., 2003; Vymazal, 2007). These biological processes become less active during cold months which could explain this seasonal pattern (Zou et al., 2016). With this explanation, surface runoff could be transporting contaminants into estuaries year-round, but in warm months, contaminants are broken down by an active biological community before settling in the sediment. However, the compounds studied in this project were selected in part due to their persistence in the environment and biological degradation may not be significant enough to explain these seasonal patterns.

The prevalence of winter precipitation as a predictor in these sediment contaminant models may also be a reflection of seasonality in the distribution of these compounds. PAHs, for example, have been found in higher concentrations during winter months as a result of increased energy consumption (*e.g.*, home heating) and lowered rates of photodegradation (Bandowe et al., 2014). These compounds can also be stored on plant tissue and may become remobilized during the winter season as plants senesce (Simonich and Hites, 1994). Thus, precipitation may have a greater potential to mobilize these contaminants into the estuarine environment during the winter.

The use of the insecticide DDT was banned in the United States in 1972; however, it was included in the final set of sediment quality models because of its status as a legacy contaminant. Nearly 50 years after it was banned, DDT and its metabolites are still being detected in South Carolina's estuarine sediments. Both agricultural and impervious surface cover were positively correlated with DDT ERMQ scores suggesting

that human alteration of watersheds, both agricultural and urban, can have lasting impacts on the environment.

4.6. Biological Quality Models

Overall model performance of biological data lagged behind sediment and water quality models, perhaps because of the greater complexity, mobility, and variability in biota. Additionally, landcover data representing urbanization were less prominent in these models. While impervious cover and high intensity development were negatively correlated with nekton abundance and MAMBI values, other measures of human land use (*e.g.*, agriculture, low intensity development) were positively associated with nekton and benthic species richness (Tables 23 and 24). Earlier studies have demonstrated a connection between urban watersheds and degraded biological communities, particularly in tidal creek headwaters (Holland et al., 2004; Parker, 2018). Thus, the positive correlation between low intensity development and biodiversity observed in these models was unexpected. One explanation could be that high-intensity and low-intensity types of development are mutually exclusive as watersheds characterized by low-intensity development may be less likely to be heavily urbanized.

The inconsistent role of landcover within this project's biodiversity models could also be explained by how biological communities were defined and analyzed. Both Holland and others (2004) and Parker (2018) targeted a particular component of the biological community to test their hypotheses. For example, Holland and others (2004) only found a significant nekton response to development when looking at Penaeoid

species, and Parker (2018) studied abundances of pollution indicative benthic invertebrates in response to coastal development. By studying nekton and benthic communities as a whole, this project's approach to biodiversity may have been too general to identify specific changes within community structure. It's also possible that effects of landcover on biodiversity were too subtle to detect at the 12-digit HUC watershed scale; however, model performance also decreased when these data were modelled with buffers. There was a gap in this project's spatial analysis between the largest 3 km buffers (2,827 ha) and smallest 14-digit HUC watersheds (8,937 ha). Future studies may find better connections between landcover and biodiversity by looking at smaller, more localized watersheds between this range.

Several weather and climate variables were also significant predictors in biological quality models. While water quality was most impacted by recent weather patterns and sediment quality by seasonal weather patterns, biological models responded best to 30- to 90-day temperature and precipitation patterns. Benthic biodiversity was positively correlated with 45-day precipitation totals and negatively correlated with 90-day temperature averages. Hot and dry summers may result in stressed benthic communities and lowered biodiversity. However, drought conditions have been shown to increase benthic invertebrate diversity in some estuaries by increasing salinities (Palmer and Montagna, 2015).

Annual average temperature of both the study year and preceding year were significant predictors of nekton species richness. While nekton species richness in open water sites was negatively correlated with annual temperature from the current year, species richness in tidal creeks were negatively correlated with temperature averages

from the previous year. This relationship between temperature and biodiversity is worth investigating further as climate change will result in warmer air and water temperatures. Higher water temperatures may increase the likelihood and severity of hypoxic conditions which pose a threat to estuarine biological communities (Altieri and Gedan, 2015). There may also be ecological significance in the timing of annual temperature increases within these models. Species richness in tidal creeks responded to annual temperature from the preceding year which could support the importance of tidal creeks as nursery habitats. Climate-driven hypoxia in estuaries has been shown to negatively impact survival of fish in early life stages (Nicholson et al., 2008). Thus, higher temperatures during the previous year may cause reduced nekton recruitment in tidal creeks and result in lower species richness in the following year's trawls.

Climate teleconnection indices only appeared as a predictor of nekton abundance and tidal creek nekton species; the North Atlantic Oscillation (NAO), which has been shown to impact fisheries, was positively correlated with both of these measures. An inverse relationship between NAO and abundance of cod and haddock has been observed in the eastern North Atlantic (Fromentin and Planque, 1996; Solow, 2002). Interestingly, the opposite effect was observed in these models where positive NAO values were correlated with greater nekton abundance. NAO in the positive phase is associated with warmer and wetter winters in the Southeast (Appendix D). These milder winters have been correlated with higher levels of shrimp abundance in South Carolina's ACE Basin; however, winter weather data were included in the modeling process and were not identified as significant predictors in these nekton models (DeLancey et al., 2008).

4.7. Predictive Modeling

The purpose of predictive modeling was to use linear regression formulas produced in this project to envision a future of coastal South Carolina's estuarine environment shaped by climate change and population growth. Predictive models can be used to answer questions regarding the impacts of increased development and changing weather patterns on local water quality and explore potential interactions among these variable sets.

In most of the defined scenarios, bacteria levels were predicted to be significantly higher than the current baseline. Enterococci, but not fecal coliform, levels were not predicted to rise significantly under population growth scenarios (Figure 53). Conversely, predictions of fecal coliform were significantly higher under warmer and wetter predictions, but enterococci levels did not respond to climate change scenarios (Figure 54). These two bacteria, while both important indicators of water quality, have different public health roles. Concentrations of *Enterococcus* bacteria are used to issue swim advisories in coastal areas, whereas high levels of fecal coliform are responsible for closing shellfish grounds. Presence of either bacteria can negatively affect the quality of life for coastal residents. Regardless of increased development, fecal coliform levels were predicted to increase due to climate change which could mean more frequent shellfish harvest closures. Alternatively, enterococci concentrations remained stable in response to increases in precipitation and temperature but were more sensitive to changes in landcover. Thus, a growing population may be met with more frequent coastal swim advisories.

Increases in sediment contamination may not have as visible of an impact for coastal residents as shellfish harvest advisories or beach closures; however, contaminants modelled in this project have potential human health impacts. Many PAHs, for example, are known carcinogens and pose significant health risks (ATSDR, 1995). Sanders (1995) sampled oyster tissue from estuaries in Murrells Inlet, SC and found significantly higher levels of PAHs in tissues from oysters in urbanized versus forested watersheds. These contaminants are not only confined to sediments at the bottom of estuaries, rather they are present within the biological community and pose human health risks.

All sediment quality models contained variables linked to watershed development. With the exception of the DDT model, changes in population alone were enough to significantly increase the concentration of contaminants above baseline values (Figures 55-59). As a growing population leads to more urbanized watersheds, more contaminants are expected to make their way into the region's estuarine systems. However, sediment contamination predictions varied when population growth was combined with temperature and precipitation changes.

Both temperature and precipitation were included in sediment quality predictive models. As coastal South Carolina transitions into a warmer and wetter climate, these models can help predict potential changes to sediment quality. Excess runoff from increased precipitation may lead to higher concentrations of contaminants; however, precipitation increases alone were insufficient to raise sediment contaminants above baseline values. The NCA predicts the most substantial increases in precipitation will occur during winter months in the Southeast (Easterling et al., 2017). Interestingly, winter precipitation was the most significant weather variable for many of these sediment

quality models. Changes in precipitation totals in climate change scenarios were evenly distributed across seasons. Perhaps if these scenarios were season-specific, more significant changes to sediment contamination would have been predicted.

Measures of temperature were negatively correlated with most sediment contaminant concentrations. As temperature increased in the change scenarios, predictions of PAHs and PCBs were significantly lower than baseline values. Since runoff is the likely mechanism by which these contaminants enter estuaries, the effect of temperature is somewhat difficult to interpret. Temperature and precipitation are interconnected weather phenomena, and in the case of these models, it's possible that cool winters tend to coincide with wet winters. However, the PAH model included an interaction effect between winter temperature and precipitation and still predicted lower values under temperature increases. While there may be many explanations, these results suggest warmer temperatures may buffer the effects of population and precipitation on increased sediment contamination.

Overall, models of biological quality had poorer predictive power than sediment quality and water quality models; therefore, predictions of biodiversity under change scenarios were more variable. Under many of these scenarios, benthic biodiversity was predicted to improve and nekton biodiversity was predicted to worsen (Figures 60-65). Increases in temperature resulted in the most changes to nekton abundance and species richness predictions; however, changes to precipitation and population were less significant. While changes to precipitation or population may not be significant on their own, they may still influence the outcomes of predictions when combined with increased temperatures.

Many of the nekton species captured by SCECAP trawls are economically important fishery species such as blue crab and shrimp. While warmer winters have been correlated with increased shrimp abundance, overall increases in temperature appear to have a negative effect on nekton abundance in these predictions (DeLancey et al., 2008). Predictions of both open water and tidal creek species richness decreased under temperature change scenarios, but only changes in tidal creek richness were significantly lower than baseline (Figures 61 and 62). Tidal creeks have been described as "sentinel habitats" meaning that tidal creek ecosystems are the first to experience declines in habitat quality and may signal large-scale degradation of the estuarine environment (Sanger et al., 2015). This observed difference in species richness predictions between the two habitat types may support the sentinel habitat hypothesis. To explore this hypothesis further, average percent changes of different scenarios were calculated from all predictive model results (Tables 28-39). On average, predictions were 7.0% different than baseline in open water sites but only 4.9% different than baseline in tidal creek sites. This suggests environmental variables in open water sites are more susceptible to change than tidal creek sites. While this runs counter to the sentinel habitat hypothesis, it could be the result of open water sites having relatively undisturbed baselines.

Although predictions of benthic abundance were not significantly different than baseline values, benthic species richness and MAMBI demonstrated significant changes from baseline values. These predictive models included measures of low-intensity developed landcover that were positively correlated with benthic species richness and MAMBI. In these instances, scenarios with population growth resulted in improved benthic invertebrate communities. This finding contradicted the expectation that estuaries

will experience declining benthic health in response to watershed development. Low-intensity development may be a positive predictor in benthic models because it represents the absence of high-intensity development. It's also possible that watersheds with sparser and lower-intensity development are located in regions that exhibit more diverse benthic communities. Hot spot analyses revealed hot spots of both MAMBI and benthic species richness in Lowcountry watersheds where development is less dense than the Tri-County and Grand Strand areas (Figures 49 and 52). The positive correlation between low-intensity development and benthic biodiversity could also be evidence for the intermediate disturbance hypothesis which claims biodiversity is at its highest when the ecosystem is subjected to recurring, low-level disturbances (Connell, 1978).

4.8. Next Steps and Future Studies

This project successfully used linear regression to explore relationships among a large suite of independent and dependent variables relating climate, land use, and environmental quality. Linear regression also provided statistically vetted formulas to make predictions of environmental responses under different population growth and climate change scenarios. However, linear regression modeling may have its shortcomings in explaining more complex relationships among the data. Early on in the modeling process, Generalized Additive Models (GAMs) were explored as an alternative to standard linear modeling. GAMs are a versatile tool that use smoothing terms to establish non-linear relationships between response and explanatory variables. GAMs were ultimately thrown out in favor of multiple linear regression formulas because they

produced marginally higher R^2 values at the expense of models that were more difficult to interpret and apply. Now that this project has developed specific models and narrowed down the number of variables, GAMs could prove useful in exploring the structure of these relationships in greater detail or identifying thresholds in some of these relationships.

Another statistical tool considered during this project was Geographically Weighted Regression (GWR) which integrates linear regression and spatial data. Physiographic data were an essential part of this project, and GWR could be a powerful tool in developing more spatially explicit models. For example, GWR could better explain the effects of landcover on environmental data by creating watershed-specific regression formulas. This type of analysis could help remedy some of the unintended effects of spatial autocorrelation within the data. Further, GWR may also reveal which watersheds are more vulnerable to changes in landcover and which are more resilient.

Time series analysis and linear regression models revealed interesting patterns in both benthic and nekton biodiversity. For the sake of simplicity, this project had only analyzed biodiversity at the coarsest resolution – abundance and species richness. Future studies could look into these biological communities with greater detail by focusing on specific taxa such as pollution indicative benthic invertebrates or commercially important fishery species. The complexity of estuarine ecosystems over such a large study area presented many challenges in measuring biodiversity. Future studies could learn a lot by exploring the structure of these diverse biological communities and their responses to environmental change.

This project reaffirmed the value of long-term environmental monitoring while demonstrating the efficacy of data synthesis methodology. This data-rich world presents many more opportunities to explore other long-term environmental datasets. At the start of this study, environmental datasets other than SCECAP (*e.g.*, EPA's STORET database) were considered for this project. Future studies could easily build upon this project by incorporating other environmental datasets into it the steps and procedures that have been outlined. These additional datasets may include more response variables (*e.g.*, nutrients) as well as cover gaps in seasonal coverage as SCECAP data were only collected during the summer.

CHAPTER 5. CONCLUSION

Regional shifts in land use and landcover have altered the physical characteristics of South Carolina's coastal watersheds. These watersheds represent an important link between upland habitats and downstream estuarine ecosystems. As a growing population continues to put pressure on coastal ecosystems, understanding this watershed connection will become ever more pertinent. It is also worthwhile to evaluate the estuarine environmental response to physical changes in the watershed within the context of a changing climate. Coastal South Carolina's climate is becoming warmer and wetter. Higher temperatures may put added stress on biological communities while increases in heavy precipitation events could exacerbate the impacts of stormwater runoff. The compounded effects of urbanization and climate change present an uncertain future for South Carolina's important estuarine ecosystems. Results from this project provide insight into some of these concerns and represent first steps towards addressing these challenges.

Bacteria concentration and sediment contaminant models showed negative correlations between urbanization and environmental quality. Overall, urbanized watersheds had more indications of impaired environmental quality than undeveloped watersheds, and this was seen across the region's estuaries. Although the effects of changing landcover on biological quality were more subtle in linear models, this project's

time series analyses documented an alarming trend of declining biodiversity in both nekton and benthic communities. In addition to landcover, variables of weather and climate figured prominently into this project's models. In sediment and water quality models, measures of precipitation were positively correlated with levels of contamination implicating runoff as the primary mechanism by which surface contaminants enter the estuarine environment. Timing of precipitation also appeared to be an important factor. While bacteria levels were most influenced by 2-day precipitation totals, measures of sediment contamination were more influenced by seasonal precipitation patterns. Interestingly, winter precipitation proved to be an important predictor in most sediment quality models which raised many questions for future research. The influence of temperature was more variable across different models; however, in most biological quality models, temperature was negatively correlated with measures of benthic and nekton biodiversity.

These past relationships were then extrapolated into future scenarios defined by population growth and climate change. Based on these models, increases in population will be met with higher levels of sediment contamination and fecal coliform bacteria in coastal South Carolina's estuaries. These models were also used to predict the potential effects of climate change on the estuarine environment. Increases in precipitation resulted in predictions of bacterial and sediment contamination only slightly above baseline conditions. However, the effects of increased temperature were more noticeable and resulted in predictions of nekton and benthic biodiversity significantly lower than baseline conditions.

Whether observing trends in historic data or forecasting future responses, this project provides examples of how a changing landscape and climate can negatively impact the estuarine environment of South Carolina. The purpose of this project was not to add another voice to a growing chorus of environmental alarmism, but rather to inform potential policies and solutions that protect and preserve South Carolina's coastal ecosystems. A guiding principle of sustainable development is finding a balance between economic growth and environmental health. As increasing stormwater runoff has the potential to further degrade South Carolina's important estuarine systems, effective and ecologically informed stormwater management is critical in finding this balance.

The prevailing method of stormwater management in coastal South Carolina is the stormwater retention pond. Stormwater ponds are designed to intercept and store excess water and are a common feature of coastal South Carolina's urban and suburban landscape. As ubiquitous as stormwater ponds may be, questions have been raised about their efficacy, maintenance costs, lifespan, and ecology (Beckingham et al., 2019; Cotti-Rausch et al., 2018). Fortunately, there are alternatives. Low Impact Development (LID) is a relatively new approach to stormwater management that prioritizes ecological design and function (Dietz, 2007).

Ellis and others (2014) created a LID planning and design guide tailored for coastal South Carolina. This guide offers a full suite of LID design ideas including bioretention (*e.g.*, bioswales and constructed wetlands), permeable pavement, green roofs, and rainwater harvesting. LID stormwater designs offer many environmental and economic benefits (Dietz, 2007, US EPA 2007). If adopted at the watershed scale, LID could help mitigate the negative impacts of stormwater runoff on South Carolina's

estuarine systems. Solutions to stormwater runoff occur at the local level; however, addressing climate change will require global reductions in carbon emissions. While LID stormwater management may not mitigate climate change, the widespread adoption of green infrastructure is a climate adaptation that can help create a resilient South Carolina coast.

LITERATURE CITED

Ackermann, F., H. Bergmann, and U. Schleichert. "Monitoring of heavy metals in coastal and estuarine sediments-a question of grain-size:<20 μm versus <60 μm." *Environmental Technology* 4.7 (1983): 317-328.

Agency for Toxic Substances and Disease Registry (ATSDR). 1995. Toxicological profile for polycyclic aromatic hydrocarbons (PAHs). Atlanta, GA: U.S. Department of Health and Human Services, Public Health Service.

Albers, Sam (2019). rsoi: import various northern and southern hemisphere climate indices. R package version 0.5.0. https://CRAN.R-project.org/package=rsoi.

Allen, Jeffery, and Kang Lu. "Modeling and prediction of future urban growth in the Charleston region of South Carolina: a GIS-based integrated approach." *Conservation Ecology* 8.2 (2003).

Altieri, Andrew H., and Keryn B. Gedan. "Climate change and dead zones." *Global Change Biology* 21.4 (2015): 1395-1406.

Anderson, Kimberly L., John E. Whitlock, and Valerie J. Harwood. "Persistence and differential survival of fecal indicator bacteria in subtropical waters and sediments." *Applied and Environmental Microbiology* 71.6 (2005): 3041-3048.

Bandowe, Benjamin A. Musa, et al. "$PM_{2.5}$-bound oxygenated PAHs, nitro-PAHs and parent-PAHs from the atmosphere of a Chinese megacity: seasonal variation, sources and cancer risk assessment." *Science of the Total Environment* 473 (2014): 77-87.

Beckingham, Barbara, Timothy Callahan, and Vijay M. Vulava. "Stormwater ponds in the southeastern US coastal plain: hydrogeology, contaminant fate, and the need for a social-ecological framework." *Frontiers in Environmental Science* 7 (2019): 117.

Blair, A., et al. "Quantifying and simulating stormwater runoff in watersheds." *Hydrological Processes* 28.3 (2014): 559-569.

Brin, Lindsay D., et al. "Nitrogen interception and export by experimental salt marsh plots exposed to chronic nutrient addition." *Marine Ecology Progress Series* 400 (2010): 3-17.

Charleston Regional Development Alliance (CRDA). “Population & demographics.” Population and Demographics in Charleston, SC Metro Region, 2018, www.crda.org/localdata/population-demographics/.

Clavel, Joanne, Romain Julliard, and Vincent Devictor. "Worldwide decline of specialist species: toward a global functional homogenization?." *Frontiers in Ecology and the Environment* 9.4 (2011): 222-228.

Conley, Daniel J., et al. "Ecosystem thresholds with hypoxia." *Eutrophication in Coastal Ecosystems*. Springer, Dordrecht, 2009. 21-29.

Connell, Joseph H. "Diversity in tropical rain forests and coral reefs." *Science* 199.4335 (1978): 1302-1310.

Connor, Edward F., and Earl D. McCoy. "The statistics and biology of the species-area relationship." *The American Naturalist* 113.6 (1979): 791-833.

Cotti-Rausch, B.E., Majidzadeh, H., and DeVoe, M.R., eds. (2018), Executive summary of: stormwater ponds in coastal South Carolina-2018 state of knowledge report. S.C. Sea Grant Consortium, Charleston, S.C.

Curtis, Scott. "The Atlantic multidecadal oscillation and extreme daily precipitation over the US and Mexico during the hurricane season." *Climate Dynamics* 30.4 (2008): 343-351.

Dietz, Michael E. "Low impact development practices: a review of current research and recommendations for future directions." *Water, Air, and Soil Pollution* 186.1-4 (2007): 351-363.

DeLancey, Lawrence, Elizabeth Wenner, and James Jenkins. "Long-term trawl monitoring of white shrimp, *Litopenaeus setiferus* (Linnaeus), stocks within the ACE Basin National Estuarine Research Reserve, South Carolina." *Journal of Coastal Research* 55 (2008): 193-199.

Easterling, D.R., K.E. Kunkel, J.R. Arnold, T. Knutson, A.N. LeGrande, L.R. Leung, R.S. Vose, D.E. Waliser, and M.F. Wehner, 2017: Precipitation change in the United States. In: *Climate Science Special Report: Fourth National Climate Assessment, Volume I* [Wuebbles, D.J., D.W. Fahey, K.A. Hibbard, D.J. Dokken, B.C. Stewart, and T.K. Maycock (eds.)]. U.S. Global Change Research Program, Washington, DC, USA, pp. 207-230, doi: 10.7930/J0H993CC.

Ellis, K., C. Berg, D. Caraco, S. Drescher, G. Hoffmann, B. Keppler, M. LaRocco, and A.Turner. 2014. Low impact development in coastal South Carolina: a planning and design guide. ACE Basin and North Inlet – Winyah Bay National Estuarine Research Reserves, 462 pp.

ESRI 2018. ArcMap 10.6. Redlands, CA: Environmental Systems Research Institute.

Farmer, John G. "The perturbation of historical pollution records in aquatic sediments." *Environmental Geochemistry and Health* 13.2 (1991): 76-83.

Feagin, Rusty A., et al. "Salt marsh zonal migration and ecosystem service change in response to global sea level rise: a case study from an urban region." *Ecology and Society* 15.4 (2010).

Federal standards and procedures for the National Watershed Boundary Dataset (WBD); 2013; TM; 11-A3; Section A: Federal Standards in Book 11 Collection and Delineation of Spatial Data; U.S. Geological Survey; U.S. Department of Agriculture; Natural Resources Conservation Service.

Fromentin, Jean-Marc, and Benjamin Planque. "Calanus and environment in the eastern North Atlantic. II. Influence of the North Atlantic Oscillation on *C. finmarchicus* and *C. helgolandicus*." *Marine Ecology Progress Series* 134 (1996): 111-118.

Gabler, Christopher A., et al. "Macroclimatic change expected to transform coastal wetland ecosystems this century." Nature Climate Change 7.2 (2017): 142.

Getis, Arthur, and J. Keith Ord. "The analysis of spatial association by use of distance statistics." *Perspectives on Spatial Data Analysis*. Springer, Berlin, Heidelberg, 2010. 127-145.

Hale, Stephen S., John F. Paul, and James F. Heltshe. "Watershed landscape indicators of estuarine benthic condition." *Estuaries* 27.2 (2004): 283-295.

Hathaway, Jon M., and William F. Hunt. "Evaluation of first flush for indicator bacteria and total suspended solids in urban stormwater runoff." *Water, Air, & Soil Pollution* 217.1-4 (2011): 135-147.

Hauer, Mathew E. "Population projections for US counties by age, sex, and race controlled to shared socioeconomic pathway." *Scientific Data* 6 (2019): 190005.

Hlavac, Marek (2018). stargazer: well-formatted regression and summary statistics tables. R package version 5.2.1. https://CRAN.R-project.org/package=stargazer.

Holland, A. Frederick, et al. "Linkages between tidal creek ecosystems and the landscape and demographic attributes of their watersheds." *Journal of Experimental Marine Biology and Ecology* 298.2 (2004): 151-178.

Hufkens et al. (2018). An integrated phenology modelling framework in R: modelling vegetation phenology with phenor. Methods in Ecology & Evolution, 9(2), 1-10.

Hyland, Jeffrey L., Robert F. Van Dolah, and Timothy R. Snoots. "Predicting stress in benthic communities of southeastern US estuaries in relation to chemical contamination of sediments." *Environmental Toxicology and Chemistry: An International Journal* 18.11 (1999): 2557-2564.

Jackson, Nancy L., Karl F. Nordstrom, and Eugene J. Farrell. "Longshore sediment transport and foreshore change in the swash zone of an estuarine beach." *Marine Geology* 386 (2017): 88-97.

JMP®, Version 14.3. SAS Institute Inc., Cary, NC, 1989-2019.

Kelsey, H., et al. "Using geographic information systems and regression analysis to evaluate relationships between land use and fecal coliform bacterial pollution." *Journal of Experimental Marine Biology and Ecology* 298.2 (2004): 197-209.

Kowalska, Maria, Hülya Güler, and David L. Cocke. "Interactions of clay minerals with organic pollutants." *Science of the Total Environment* 141.1-3 (1994): 223-240.

Long, Edward R., et al. "Incidence of adverse biological effects within ranges of chemical concentrations in marine and estuarine sediments." *Environmental Management* 19.1 (1995): 81-97.

Lotze, Heike K., et al. "Depletion, degradation, and recovery potential of estuaries and coastal seas." *Science* 312.5781 (2006): 1806-1809.

Lukacs, Paul M., Kenneth P. Burnham, and David R. Anderson. "Model selection bias and Freedman's paradox." *Annals of the Institute of Statistical Mathematics* 62.1 (2010): 117.

Mizzell, Hope, Mark Malsick, and Ivetta Abramyan. "South Carolina's climate report card: understanding South Carolina's climate trends and variability." *Journal of South Carolina Water Resources* 1.1 (2014): 1.

Mizzell, Hope, and Jennifer Simmons. "South Carolina's climate report card: the influence of the El Niño Southern Oscillation cold warm event cycles on South Carolina's seasonal precipitation." *Journal of South Carolina Water Resources* 2.1 (2015): 6.

Mizzell, Hope, Mark Malsick, and Wes Tyler. "The historic South Carolina rainfall and major floods of October 1-5, 2015." *Journal of South Carolina Water Resources* 3.1 (2016): 2.

Muxika, Inigo, Angel Borja, and Juan Bald. "Using historical data, expert judgement and multivariate analysis in assessing reference conditions and benthic ecological status, according to the European Water Framework Directive." *Marine Pollution Bulletin* 55.1-6 (2007): 16-29.

NCSU North Carolina Climate Office. Global Patterns: Arctic & North Atlantic Oscillations. https://climate.ncsu.edu/climate/patterns/nao.

Nicholson, Geoff, et al. "Physical environmental conditions, spawning and early-life stages of an estuarine fish: climate change implications for recruitment in intermittently open estuaries." *Marine and Freshwater Research* 59.8 (2008): 735-749.

NOAA Coastal Change Analysis Program (C-CAP) Regional Land Cover Database. Data collected 1995-present. Charleston, SC: National Oceanic and Atmospheric Administration (NOAA) Office for Coastal Management. Data accessed at coast.noaa.gov/landcover.

NOAA National Climate Data Center. Climate Data Online. Drought Atlas. https://www7.ncdc.noaa.gov/CDO/CDODivisionalSelect.jsp#.

NOAA National Centers for Environmental Information. Climate Data Online. Retrieved from https://www.ncdc.noaa.gov/cdo-web/.

NOAA. "National coastal population report: population trends from 1970 to 2020." *NOAA State of the Coast Report Series* (2013).

O'Neil, J. M., et al. "The rise of harmful cyanobacteria blooms: the potential roles of eutrophication and climate change." *Harmful Algae* 14 (2012): 313-334.

Paerl, Hans W., and Jef Huisman. "Blooms like it hot." *Science* 320.5872 (2008): 57-58.

Palmer, Terence A., and Paul A. Montagna. "Impacts of droughts and low flows on estuarine water quality and benthic fauna." *Hydrobiologia* 753.1 (2015): 111-129.

Parker, Catherine E. "An assessment of southeast United States headwater tidal creek sediment contamination and the macrobenthic community over a twenty-year period in relation to coastal development." MS Thesis. College of Charleston, 2018.

Pinheiro J, Bates D, DebRoy S, Sarkar D, R Core Team (2019). nlme: Linear and Nonlinear Mixed Effects Models_. R package version 3.1-140, <URL: https://CRAN.R-project.org/package=nlme>.

R Core Team (2019). R: A language and environment for statistical computing. R Foundation for Statistical Computing, Vienna, Austria. URL https://www.R-project.org/.

Robinson, David and Hayes, Alex (2020). broom: convert statistical analysis objects into tidy tibbles. R package version 0.5.5. https://CRAN.R-project.org/package=broom.

Sanders, M. "Distribution of polycyclic aromatic hydrocarbons in oyster (*Crassostrea virginica*) and surface sediment from two estuaries in South Carolina." *Archives of Environmental Contamination and Toxicology* 28.4 (1995): 397-405.

Sanger, D. M., A. F. Holland, and G. I. Scott. "Tidal creek and salt marsh sediments in South Carolina coastal estuaries: I. Distribution of trace metals." *Archives of Environmental Contamination and Toxicology* 37.4 (1999): 445-457.

Sanger, D. M., A. F. Holland, and G. I. Scott. "Tidal creek and salt marsh sediments in South Carolina coastal estuaries: II. Distribution of organic contaminants." *Archives of Environmental Contamination and Toxicology* 37.4 (1999): 458-471.

Sanger, D., et al. "Impacts of coastal development on the ecology of tidal creek ecosystems of the US Southeast including consequences to humans." *Estuaries and Coasts* 38.1 (2015): 49-66.

Sanger, D.M., S.P. Johnson, M.V. Levisen, S.E. Crowe, D.E. Chestnut, B. Rabon, M.H. Fulton, and E.F. Wirth. 2016. The condition of South Carolina's estuarine and coastal habitats during 2011-2014: technical report. Charleston, SC: South Carolina Marine Resources Division. Technical Report No. 108. 58p.

SCDNR. (2012). Marine salt marsh habitat. Retrieved from http://dnr.sc.gov/marine/habitat/saltmarsh.html.

Shepard, Christine C., Caitlin M. Crain, and Michael W. Beck. "The protective role of coastal marshes: a systematic review and meta-analysis." *PloS One* 6.11 (2011): e27374.

Simonich, Staci L., and Ronald A. Hites. "Importance of vegetation in removing polycyclic aromatic hydrocarbons from the atmosphere." *Nature* 370.6484 (1994): 49-51.

Soil Survey Staff, Natural Resources Conservation Service, United States Department of Agriculture. Web Soil Survey. Available online at https://websoilsurvey.nrcs.usda.gov/.

Solow, Andrew R. "Fisheries recruitment and the North Atlantic Oscillation." *Fisheries Research* 54.2 (2002): 295-297.

Stottmeister, U., et al. "Effects of plants and microorganisms in constructed wetlands for wastewater treatment." *Biotechnology Advances* 22.1-2 (2003): 93-117.

Thornton, P.E., M.M. Thornton, B.W. Mayer, Y. Wei, R. Devarakonda, R.S. Vose, and R.B. Cook. 2018. Daymet: daily surface weather data on a 1-km grid for North America, Version 3. ORNL DAAC, Oak Ridge, Tennessee, USA. https://doi.org/10.3334/ORNLDAAC/1328.

Torio, Dante D., and Gail L. Chmura. "Assessing coastal squeeze of tidal wetlands." *Journal of Coastal Research* 29.5 (2013): 1049-1061.

Uddin, Mohammad Kashif. "A review on the adsorption of heavy metals by clay minerals, with special focus on the past decade." *Chemical Engineering Journal* 308 (2017): 438-462.

US Census Bureau. "State population totals: 2010 - 2017." U.S. Census Data, 4 Sept. 2018, www.census.gov/data/datasets/2017/demo/popest/statetotal.html#par_textimage_500989927.

U.S. Department of Agriculture, Soil Conservation Service (USDA SCS). 1986. Urban hydrology for small watersheds, Second Edition, Technical Release 55 (TR 55). Conservation Engineering Division.

US EPA. "Reducing stormwater costs through low impact development (LID) strategies and practices." 2007. https://www.epa.gov/sites/production/files/2015-10/documents/2008_01_02_nps_lid_costs07uments_reducingstormwatercosts-2.pdf.

US EPA. "National nonpoint source program – a catalyst for water quality improvements." 2016. https://www.epa.gov/sites/production/files/2016-10/documents/nps_program_highlights_report-508.pdf.

USGCRP, 2017: *Climate Science Special Report: Fourth National Climate Assessment, Volume I* [Wuebbles, D.J., D.W. Fahey, K.A. Hibbard, D.J. Dokken, B.C. Stewart, and T.K. Maycock (eds.)]. U.S. Global Change Research Program, Washington, DC, USA, 470 pp., doi: 10.7930/J0J964J6.

Van Dolah, R. F., et al. "A benthic index of biological integrity for assessing habitat quality in estuaries of the southeastern USA." *Marine Environmental Research* 48.4-5 (1999): 269-283.

Van Dolah, Robert F., et al. "Estuarine habitat quality reflects urbanization at large spatial scales in South Carolina's coastal zone." *Science of the Total Environment* 390.1 (2008): 142-154.

Vose, R.S., D.R. Easterling, K.E. Kunkel, A.N. LeGrande, and M.F. Wehner, 2017: Temperature changes in the United States. In: *Climate Science Special Report: Fourth National Climate Assessment, Volume I* [Wuebbles, D.J., D.W. Fahey, K.A. Hibbard, D.J. Dokken, B.C. Stewart, and T.K. Maycock (eds.)]. U.S. Global Change Research Program, Washington, DC, USA, p. 185-206, doi: 10.7930/J0N29V45.

Vymazal, Jan. "Removal of nutrients in various types of constructed wetlands." *Science of the Total Environment* 380.1-3 (2007): 48-65.

Webster, Laura F., et al. "Identification of sources of *Escherichia coli* in South Carolina estuaries using antibiotic resistance analysis." *Journal of Experimental Marine Biology and Ecology* 298.2 (2004): 179-195.

Wetz, Michael S., and David W. Yoskowitz. "An 'extreme' future for estuaries? Effects of extreme climatic events on estuarine water quality and ecology." *Marine Pollution Bulletin* 69.1-2 (2013): 7-18.

Wiegert, Richard G., and B. J. Freeman. *Tidal salt marshes of the southeast Atlantic coast: a community profile*. Vol. 85. No. 7. US Department of the Interior, Fish and Wildlife Service, 1990.

Worm, Boris, et al. "Impacts of biodiversity loss on ocean ecosystem services." *Science* 314.5800 (2006): 787-790.

Xiao, Qingfu, et al. "Winter rainfall interception by two mature open-grown trees in Davis, California." *Hydrological Processes* 14.4 (2000): 763-784.

Yang, Limin, Jin, Suming, Danielson, Patrick, Homer, Collin G., Gass, L., Bender, S.M., Case, Adam, Costello, C., Dewitz, Jon A., Fry, Joyce A., Funk, M., Granneman, Brian J., Liknes, G.C., Rigge, Matthew B., Xian, George, A new generation of the United States National Land Cover Database—Requirements, research priorities, design, and implementation strategies: ISPRS Journal of Photogrammetry and Remote Sensing, v. 146, p. 108–123, at https://doi.org/10.1016/j.isprsjprs.2018.09.006.

Zou, Xiangxu, et al. "Decreasing but still significant facilitation effect of cold-season macrophytes on wetlands purification function during cold winter." *Scientific Reports* 6.1 (2016): 1-9.

FIGURES

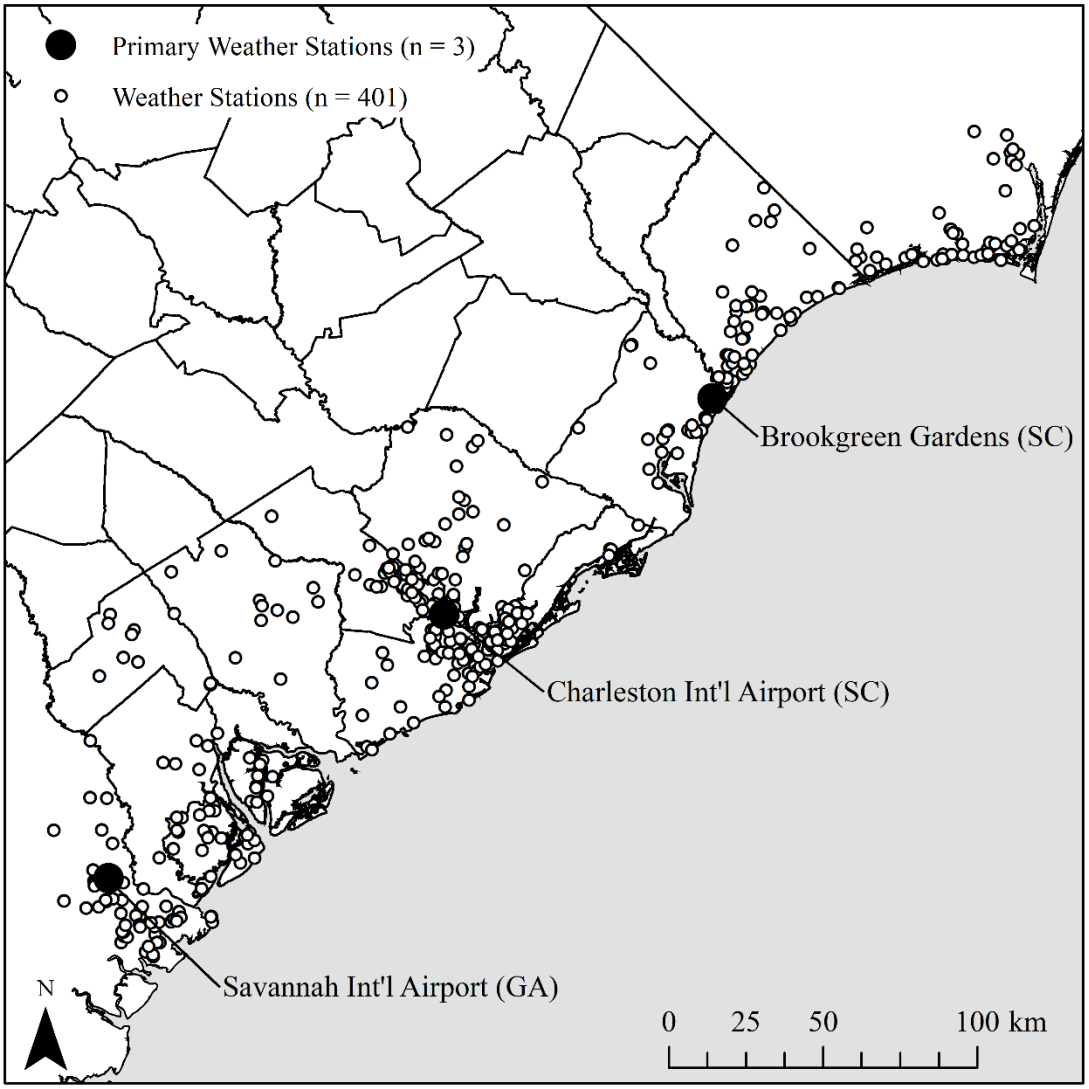

Figure 1. Map of weather stations of South Carolina's coast

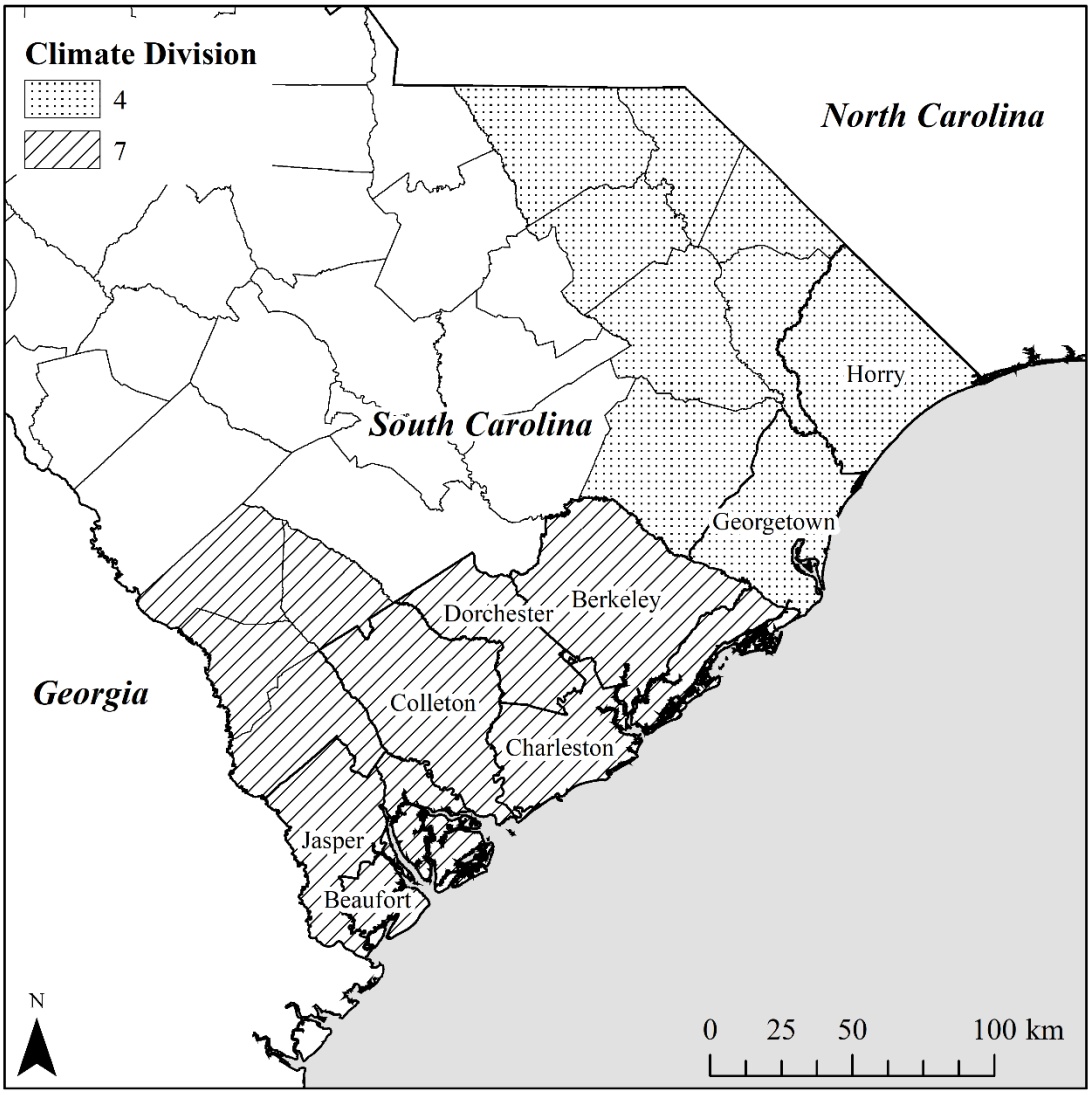

Figure 2. Map of coastal South Carolina's counties and climate divisions. Climate divisions (4 and 7) defined by NOAA National Climate Data Center (NOAA NCDC).

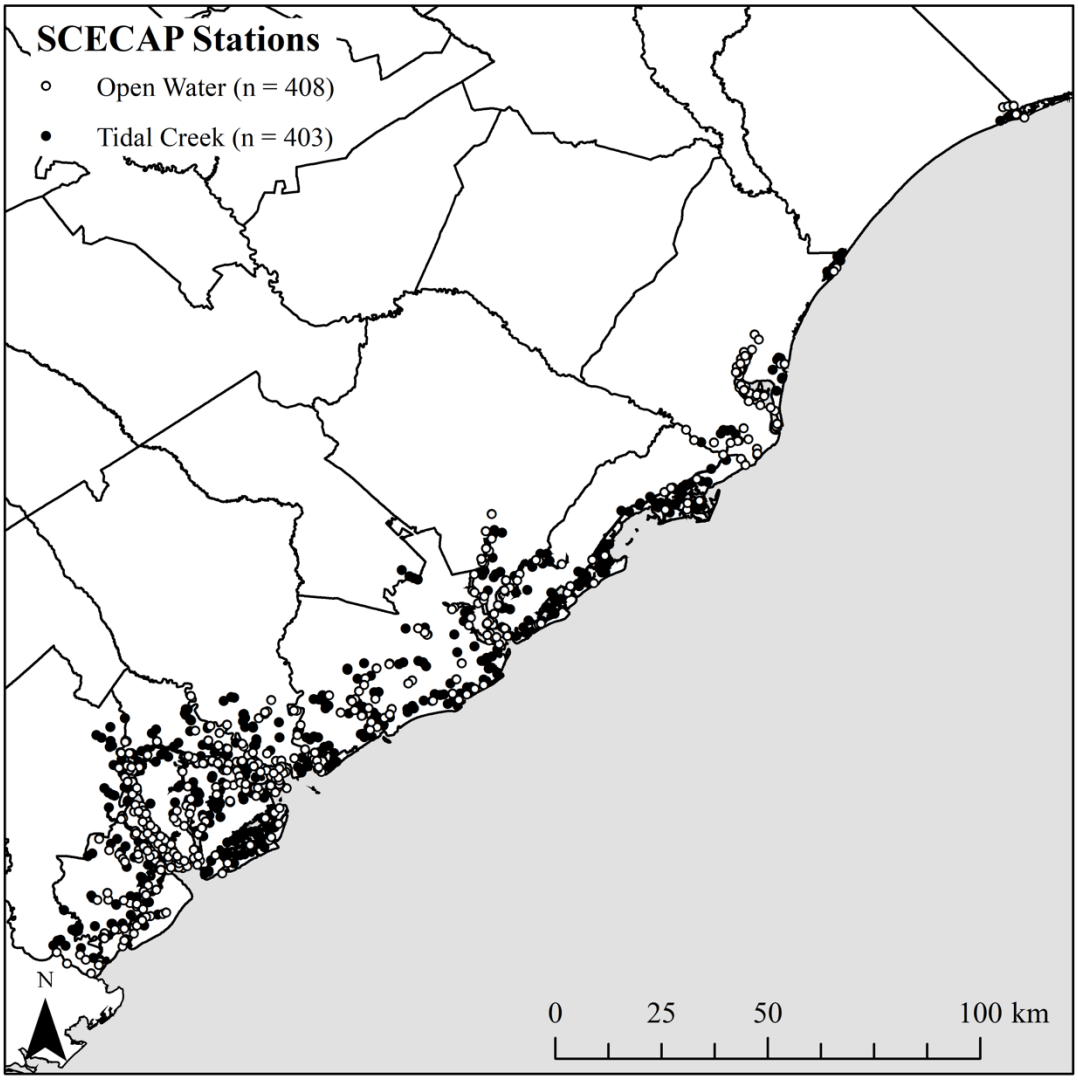

Figure 3. Map of SCECAP stations (1999-2018)

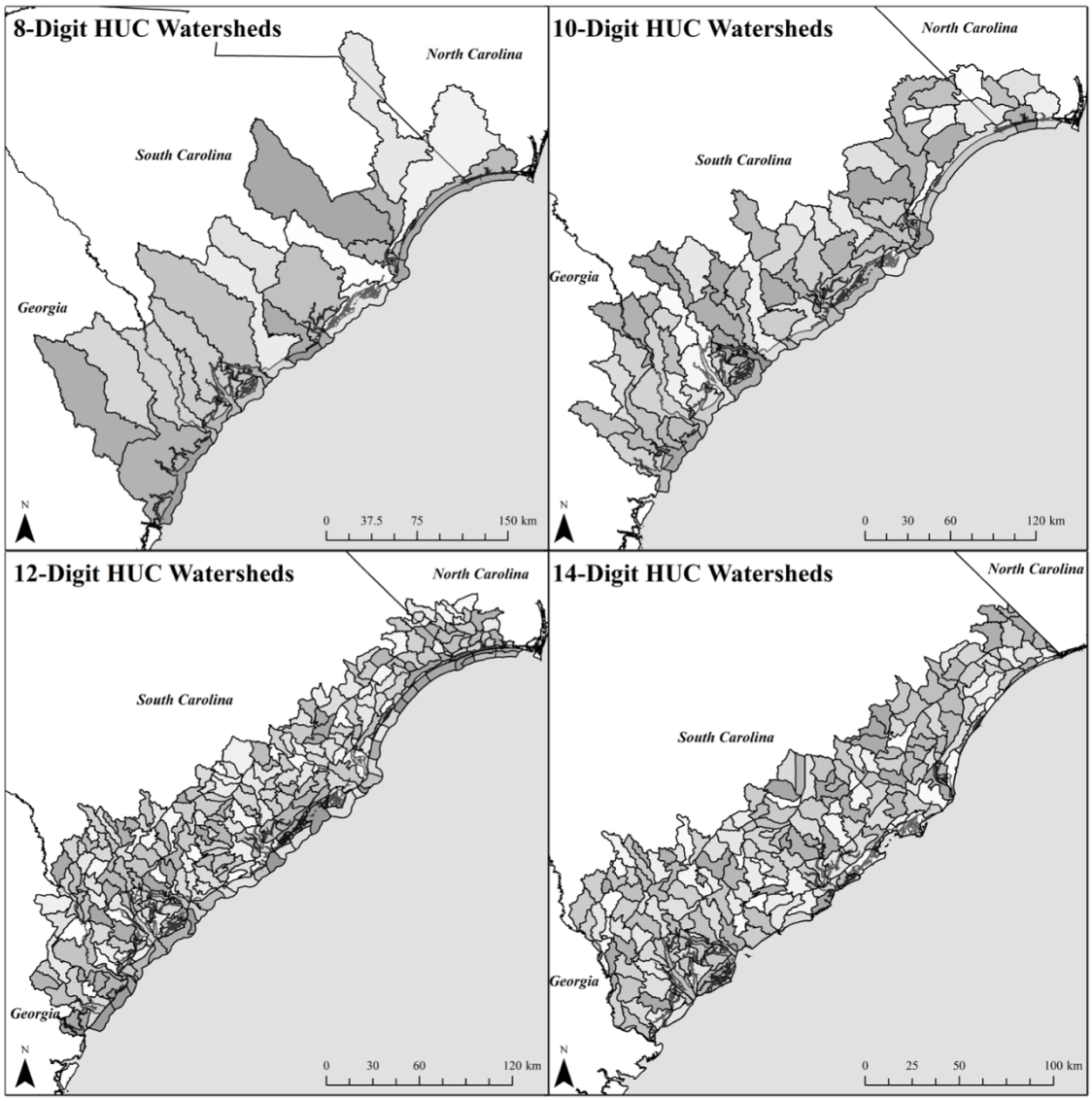

Figure 4. Map of 8, 10, 12, and 14-digit HUC watersheds along South Carolina's coast

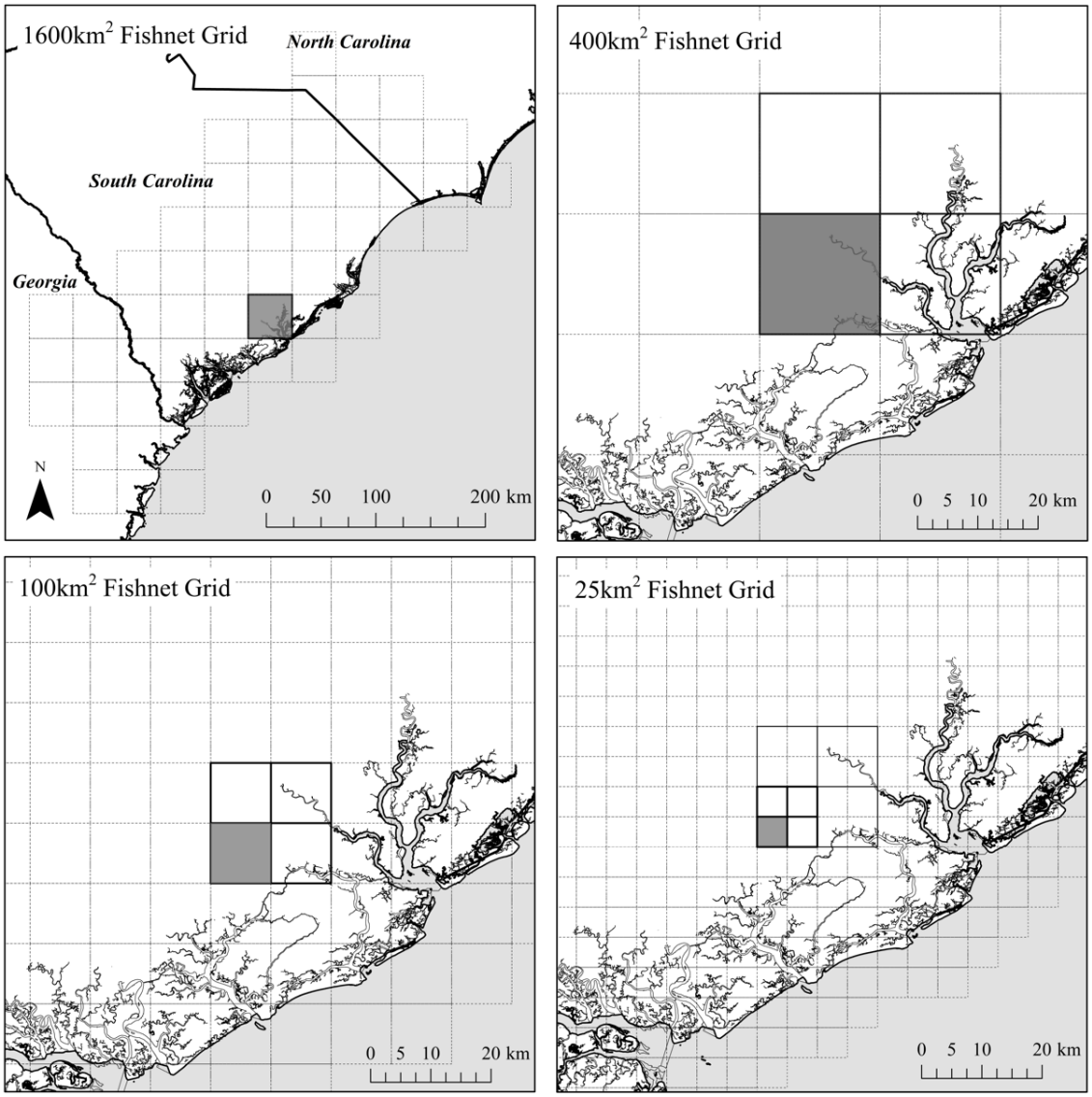

Figure 5. Examples of nested fishnet grid cells over coastal South Carolina

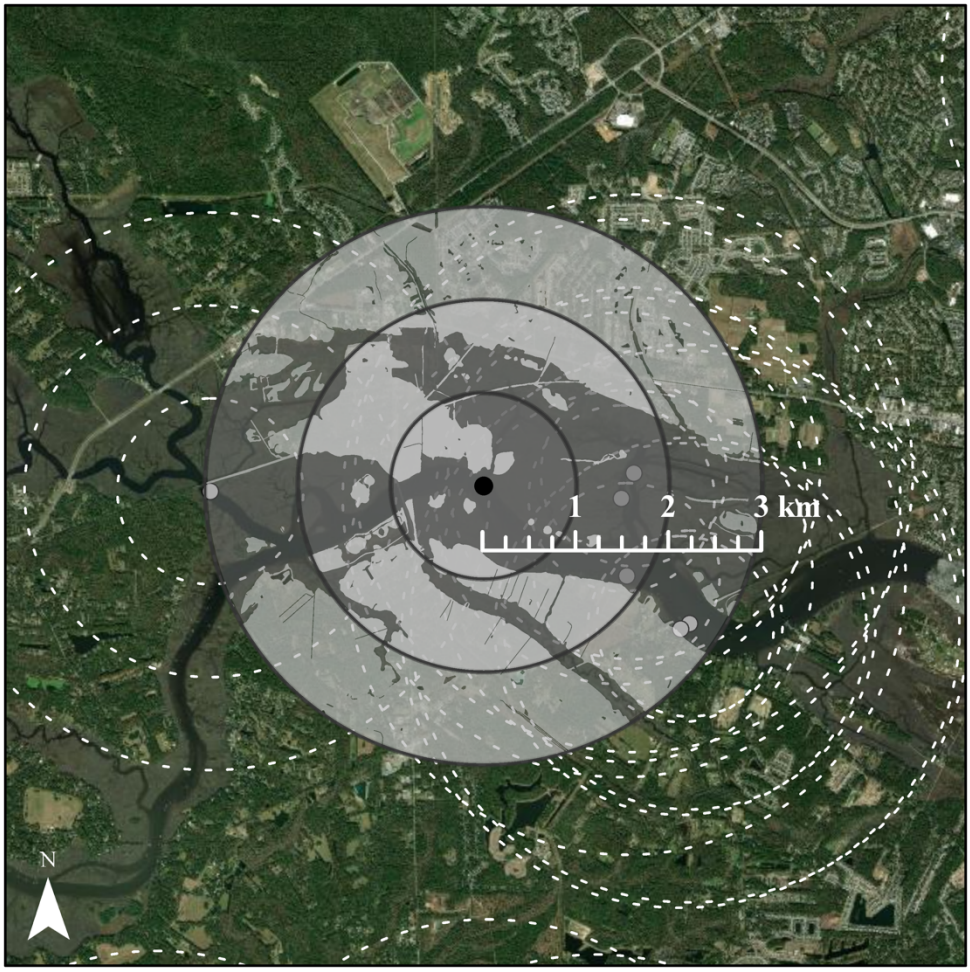

Figure 6. Examples of 1, 2, and 3 km buffers for spatial analysis. Center points of buffers are SCECAP stations.

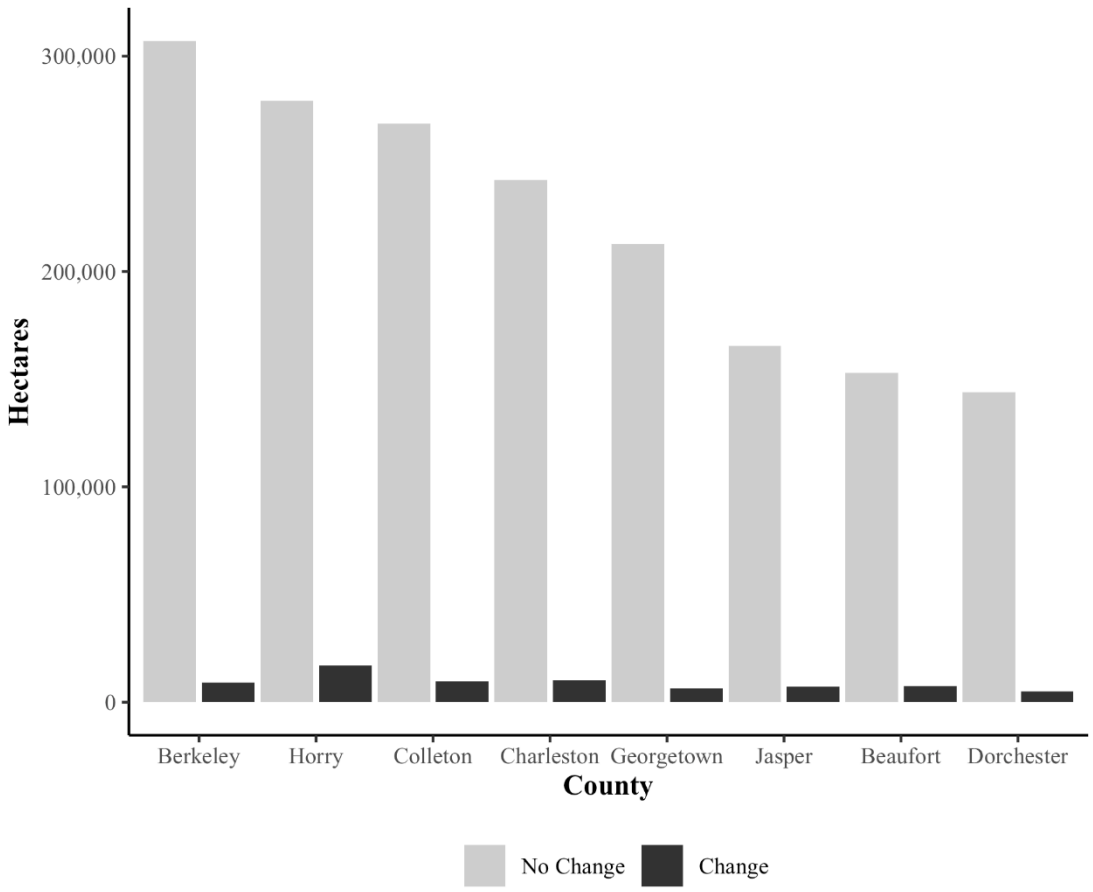

Figure 7. Hectares of coastal South Carolina counties that experienced changes in landcover between 2001 and 2016. Supplementary data from landcover change analysis available in Appendices H and I.

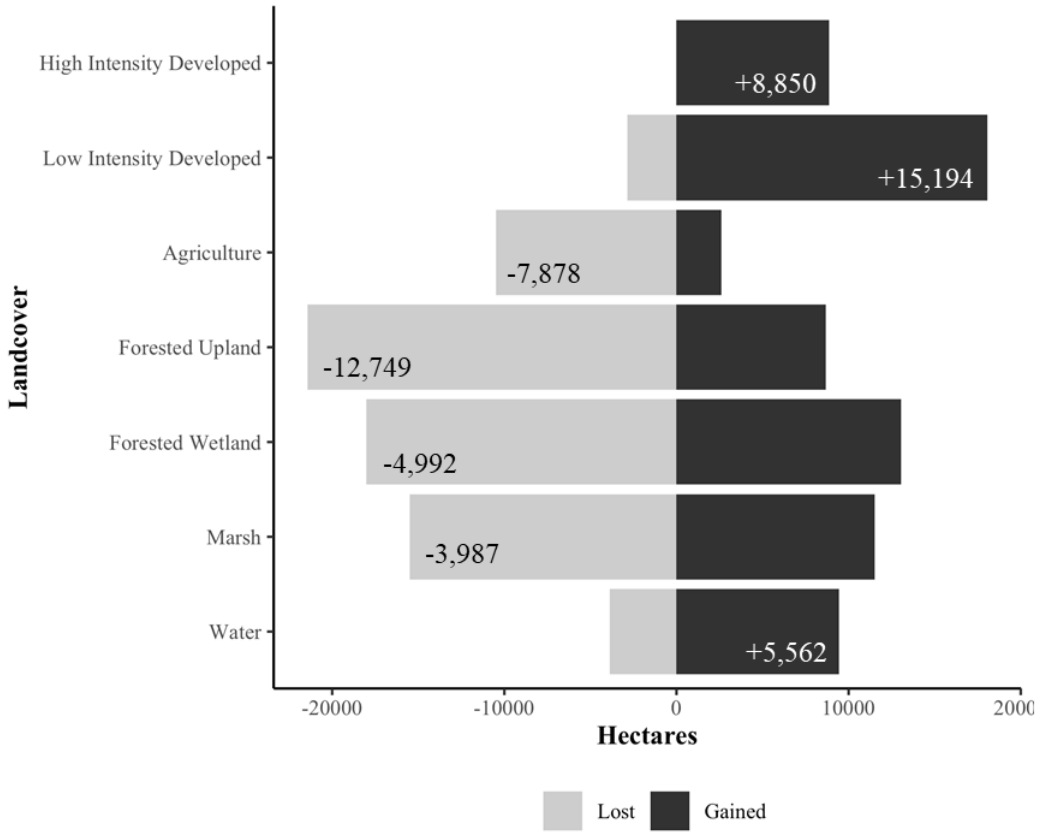

Figure 8. Hectares of landcover classes lost and gained in coastal South Carolina between 2001 and 2016. Numbers within bars represent net change in hectares for that category. Supplementary data from landcover change analysis available in Appendices H and I.

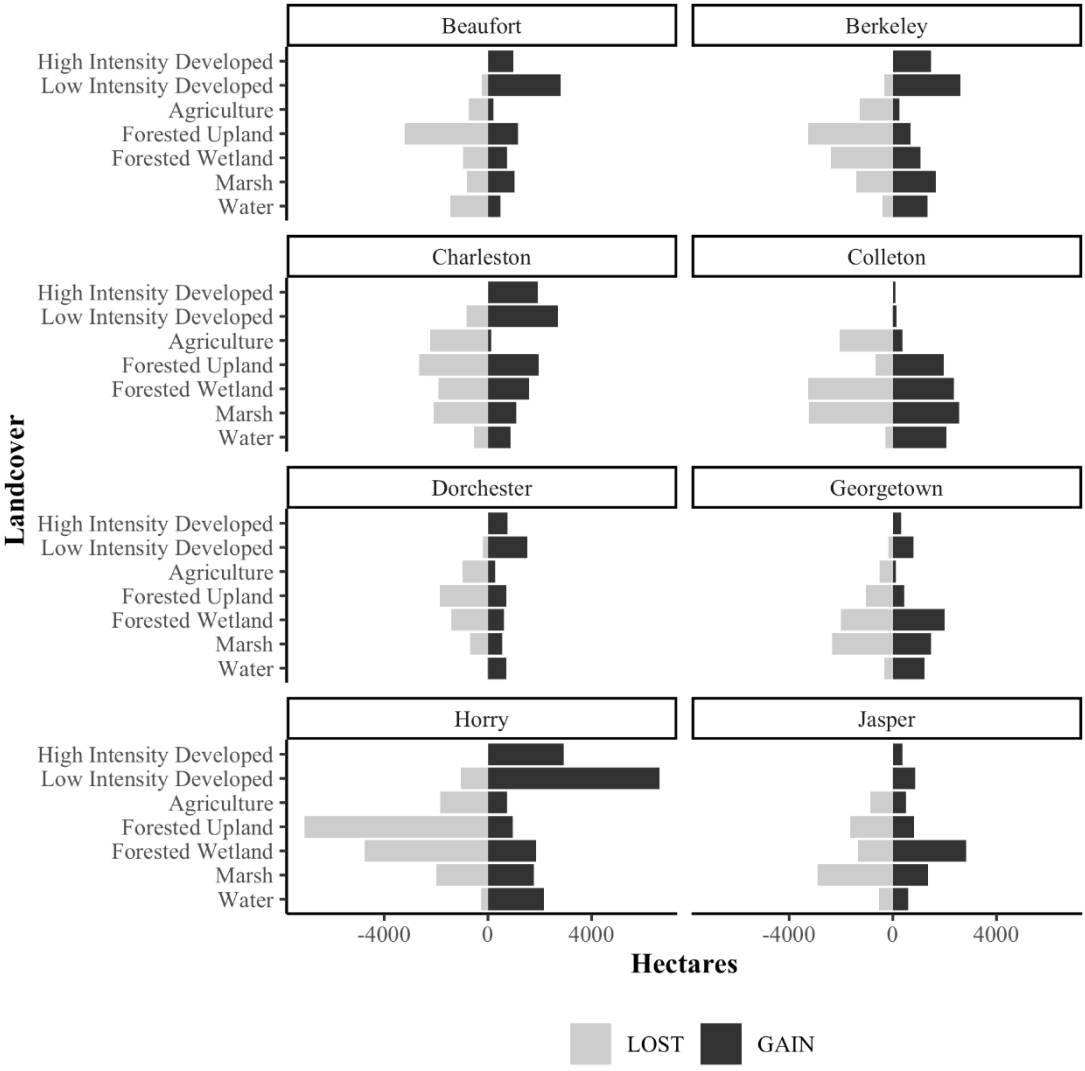

Figure 9. Hectares of landcover classes lost and gained in coastal South Carolina counties between 2001 and 2016. Supplementary data from landcover change analysis available in Appendices H and I.

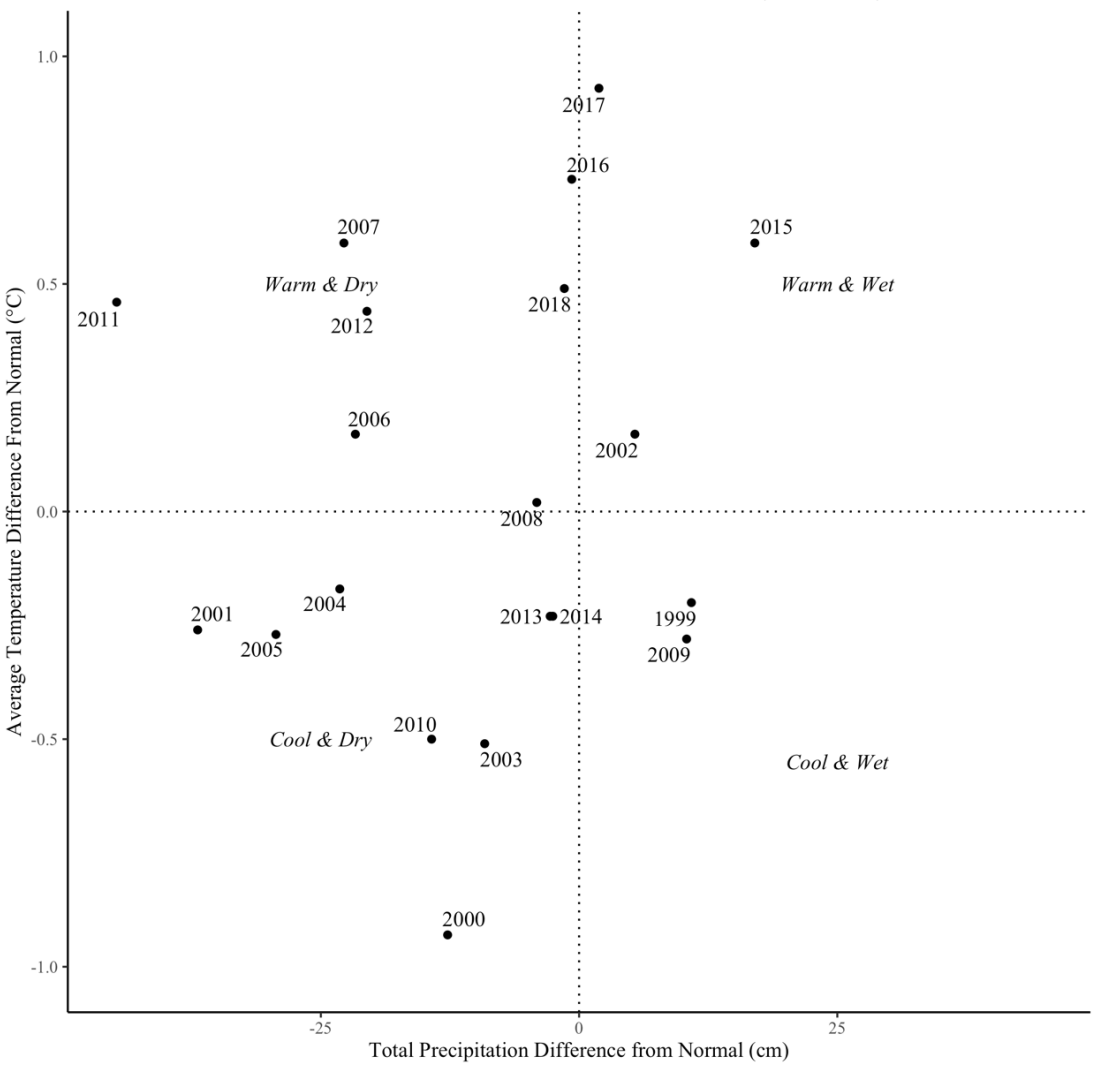

Figure 10. Observed annual climate from 1999 to 2018 in coastal South Carolina compared to 30-year climate normals. It should be noted that 2015 was an anomaly for South Carolina as most of the year was in a drought leading up to historic rainfall totals caused by Hurricane Joaquin from October 1-5 (Mizzell et al., 2016).

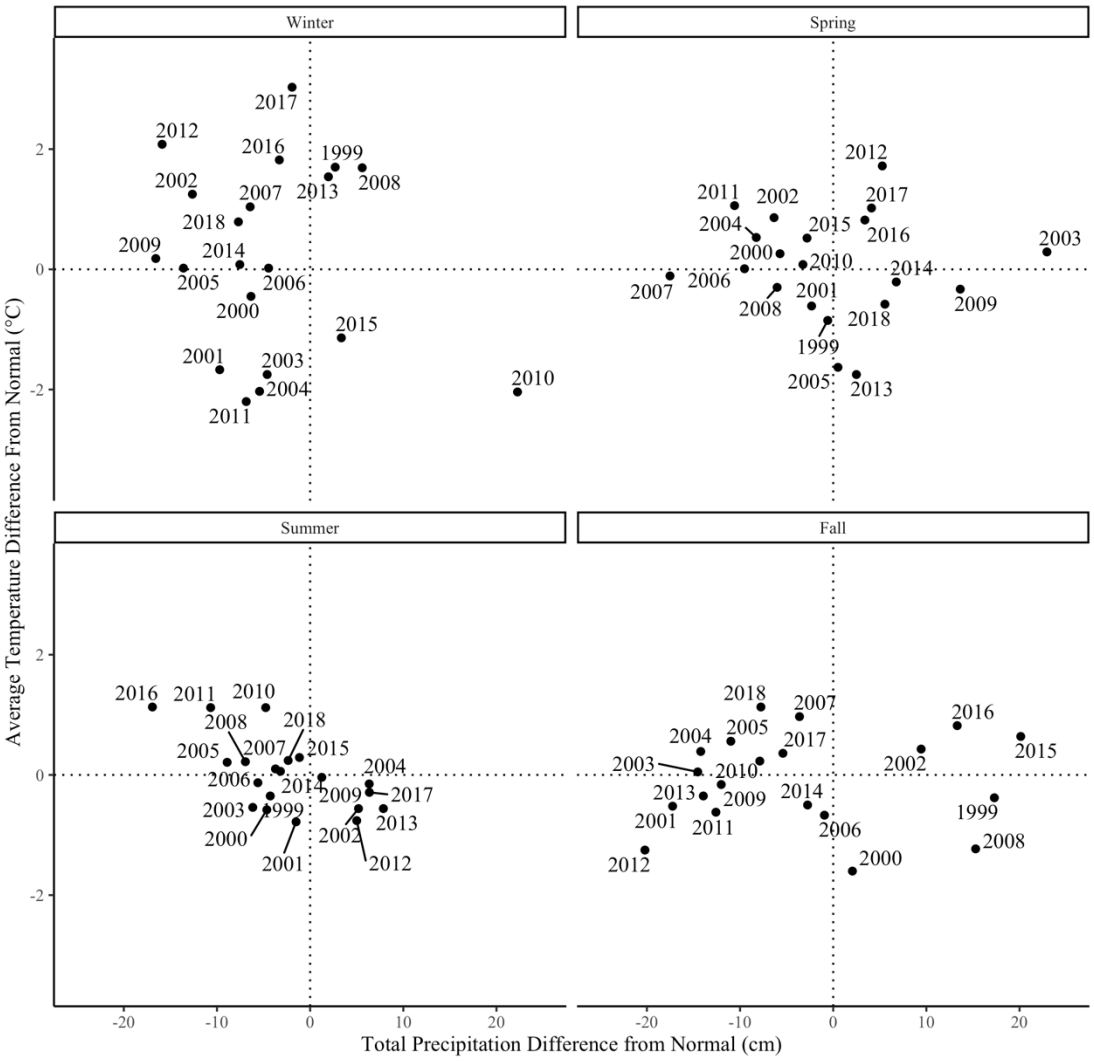

Figure 11. Observed seasonal climate from 1999 to 2018 in coastal South Carolina compared to 30-year climate normals. Seasons broken down as follows: Winter (Dec., Jan., Feb.), Spring (Mar., Apr., May), Summer (Jun., Jul., Aug.), and Fall (Sep., Oct., Nov.).

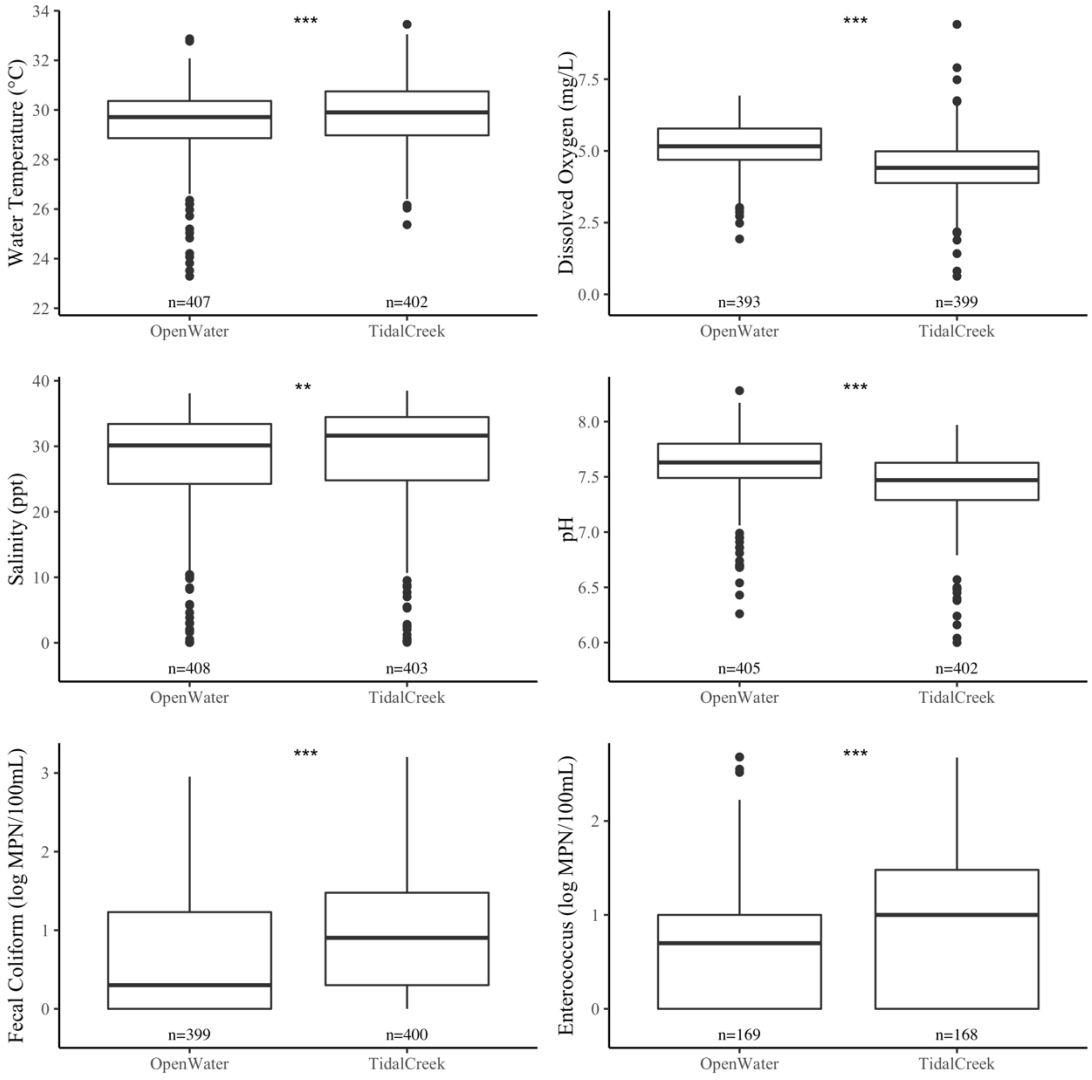

Figure 12. Comparisons of SCECAP water quality data by habitat type. Asterisks signify *p*-values from *t*-tests ($^{***}p \leq 0.01$, $^{**}p \leq 0.05$, $^{*}p \leq 0.10$). For supplemental results, see Table 3.

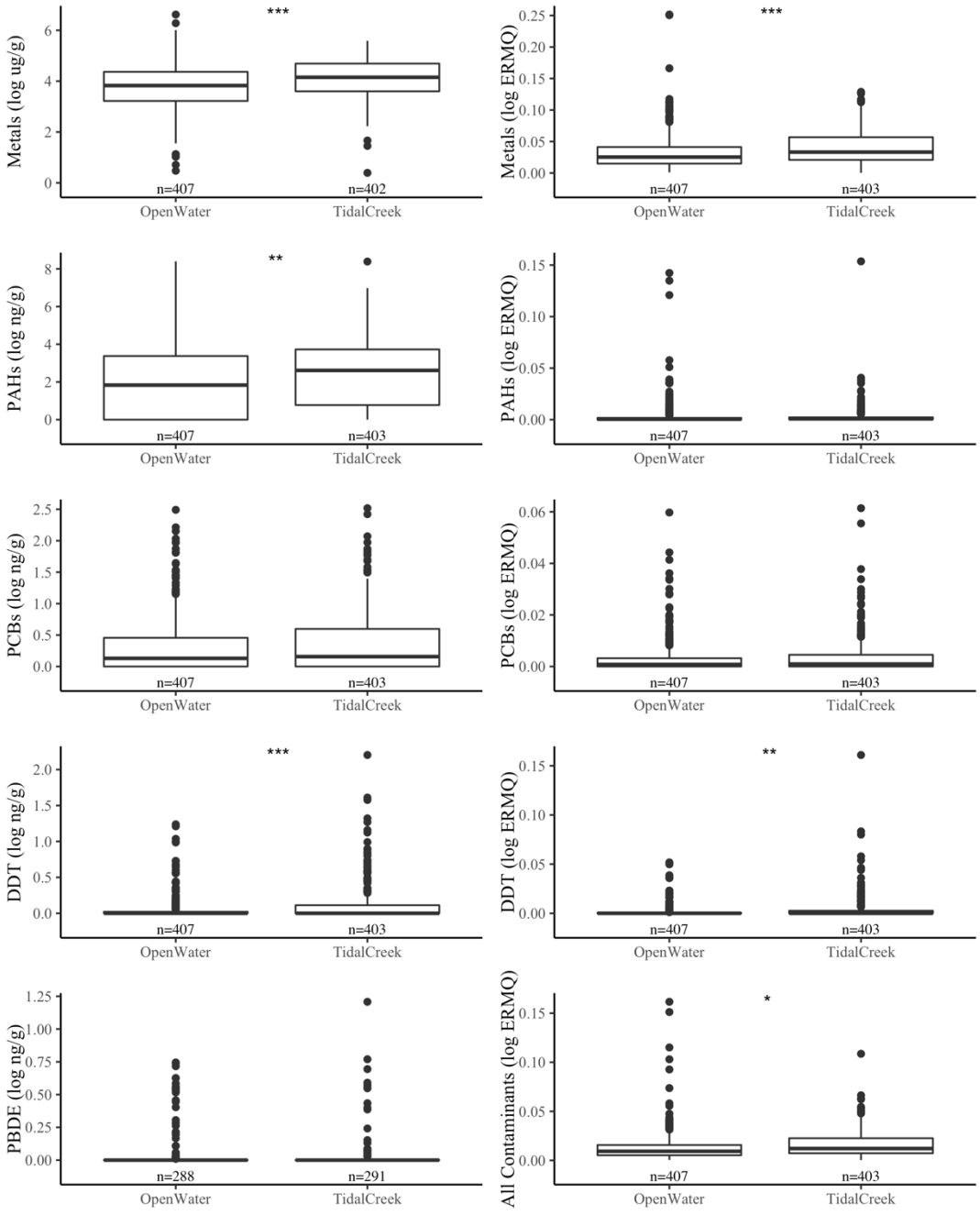

Figure 13. Comparisons of SCECAP sediment quality data by habitat type. Asterisks signify *p*-values from *t*-tests ($^{***}p \leq 0.01$, $^{**}p \leq 0.05$, $^{*}p \leq 0.10$). For supplemental results, see Table 3.

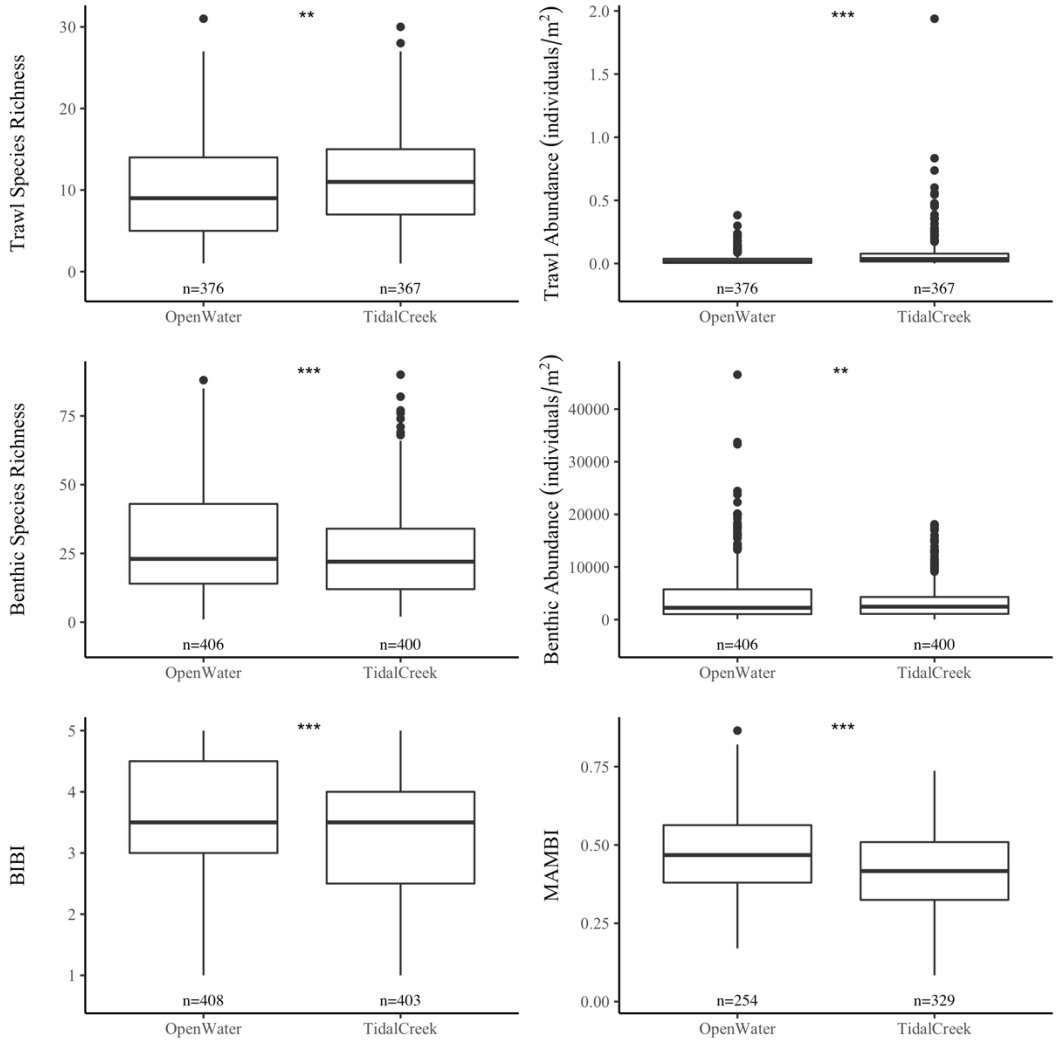

Figure 14. Comparisons of SCECAP biological quality data by habitat type. Asterisks signify *p*-values from *t*-tests ($^{***}p \leq 0.01$, $^{**}p \leq 0.05$, $^{*}p \leq 0.10$). For supplemental results, see Table 3.

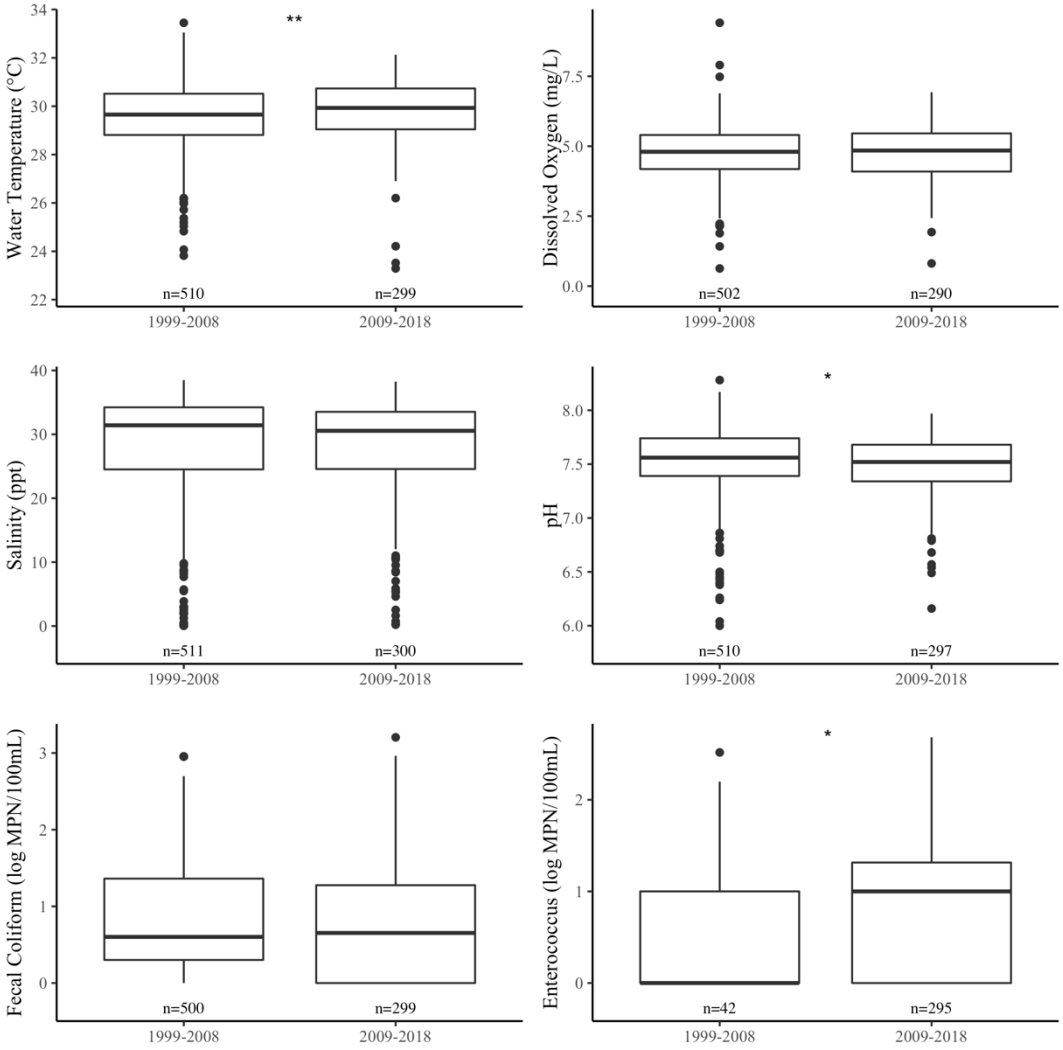

Figure 15. Comparisons of SCECAP water quality data by time period (all sites). Asterisks signify *p*-values from *t*-tests ($^{***}p \leq 0.01$, $^{**}p \leq 0.05$, $^{*}p \leq 0.10$). For supplemental results, see Table 4.

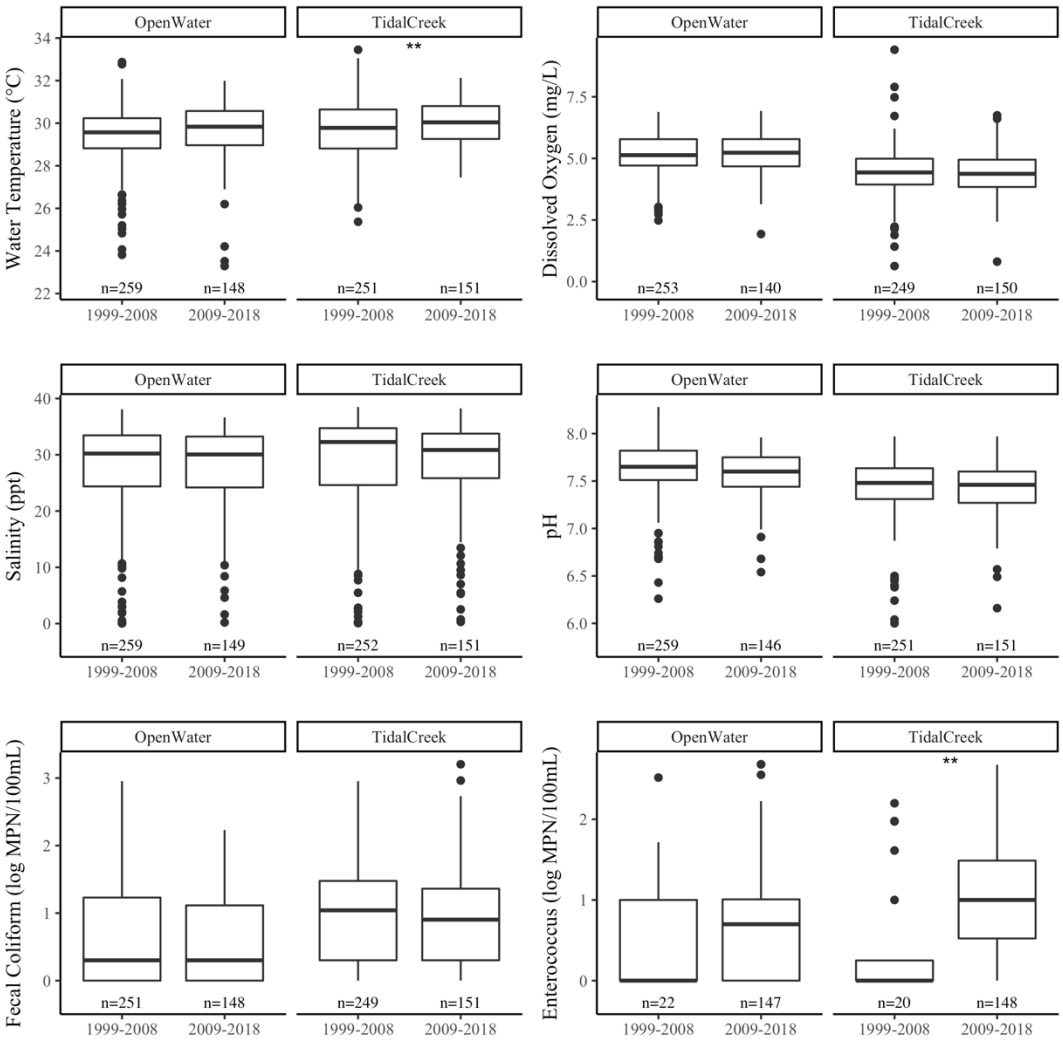

Figure 16. Comparisons of SCECAP water quality data by time period (open water vs. tidal creek sites). Asterisks signify *p*-values from *t*-tests ($^{***}p \leq 0.01$, $^{**}p \leq 0.05$, $^{*}p \leq 0.10$). For supplemental results, see Tables 5 and 6.

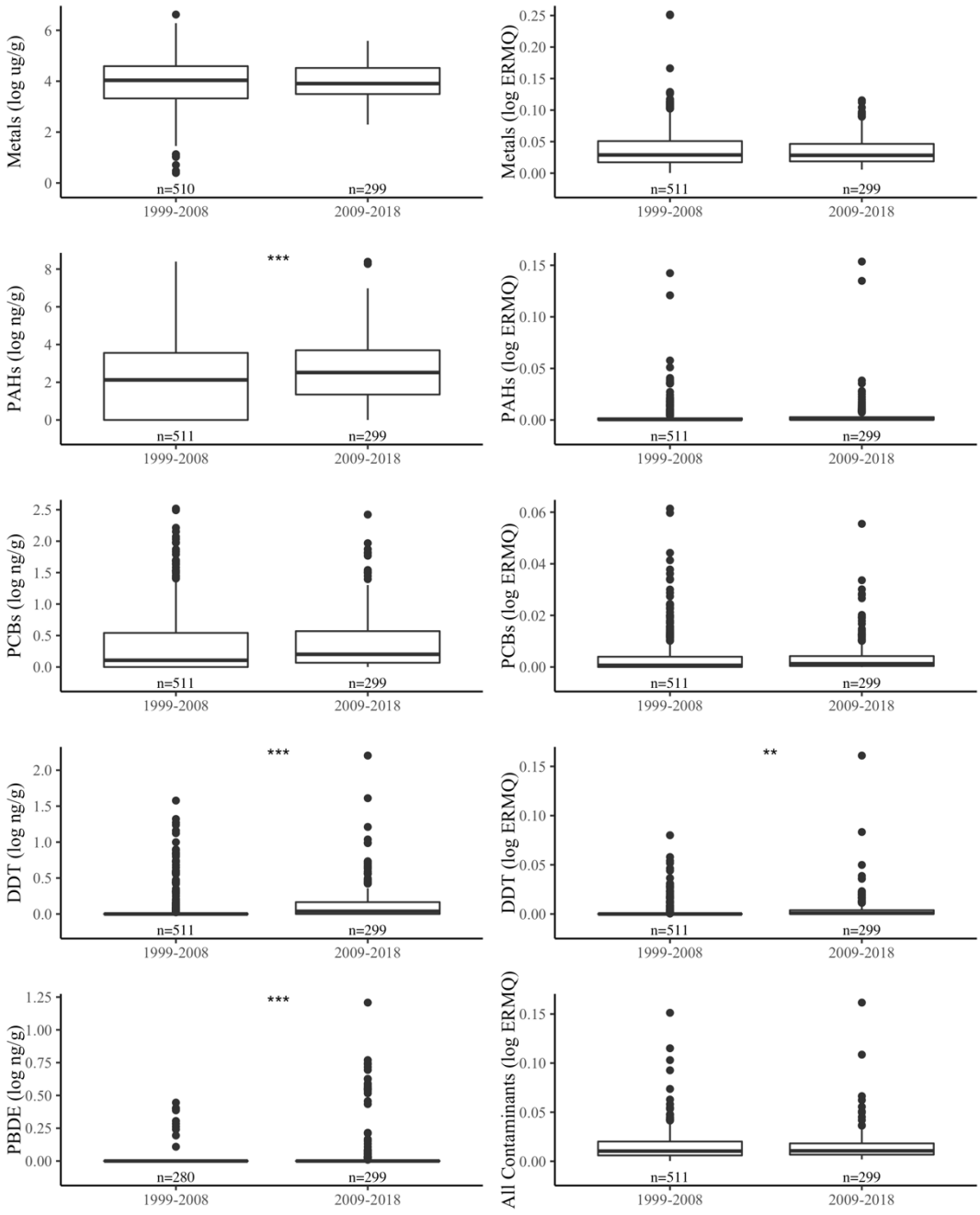

Figure 17. Comparisons of SCECAP sediment quality data by time period (all sites). Asterisks signify *p*-values from *t*-tests ($^{***}p \leq 0.01$, $^{**}p \leq 0.05$, $^{*}p \leq 0.10$). For supplemental results, see Table 4.

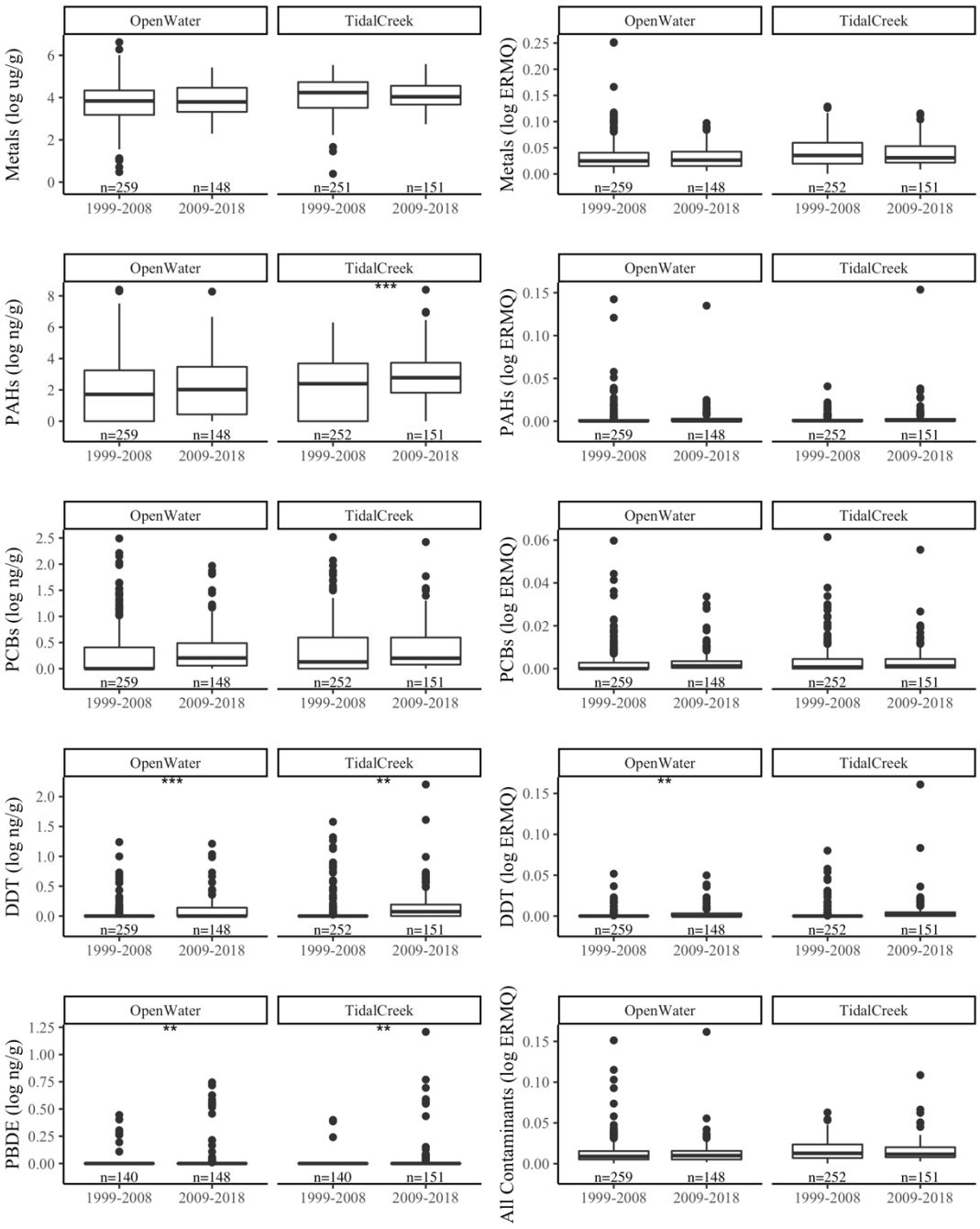

Figure 18. Comparisons of SCECAP sediment quality data by time period (open water vs. tidal creek sites). Asterisks signify *p*-values from *t*-tests ($^{***}p \leq 0.01$, $^{**}p \leq 0.05$, $^{*}p \leq 0.10$). For supplemental results, see Table 5 and 6.

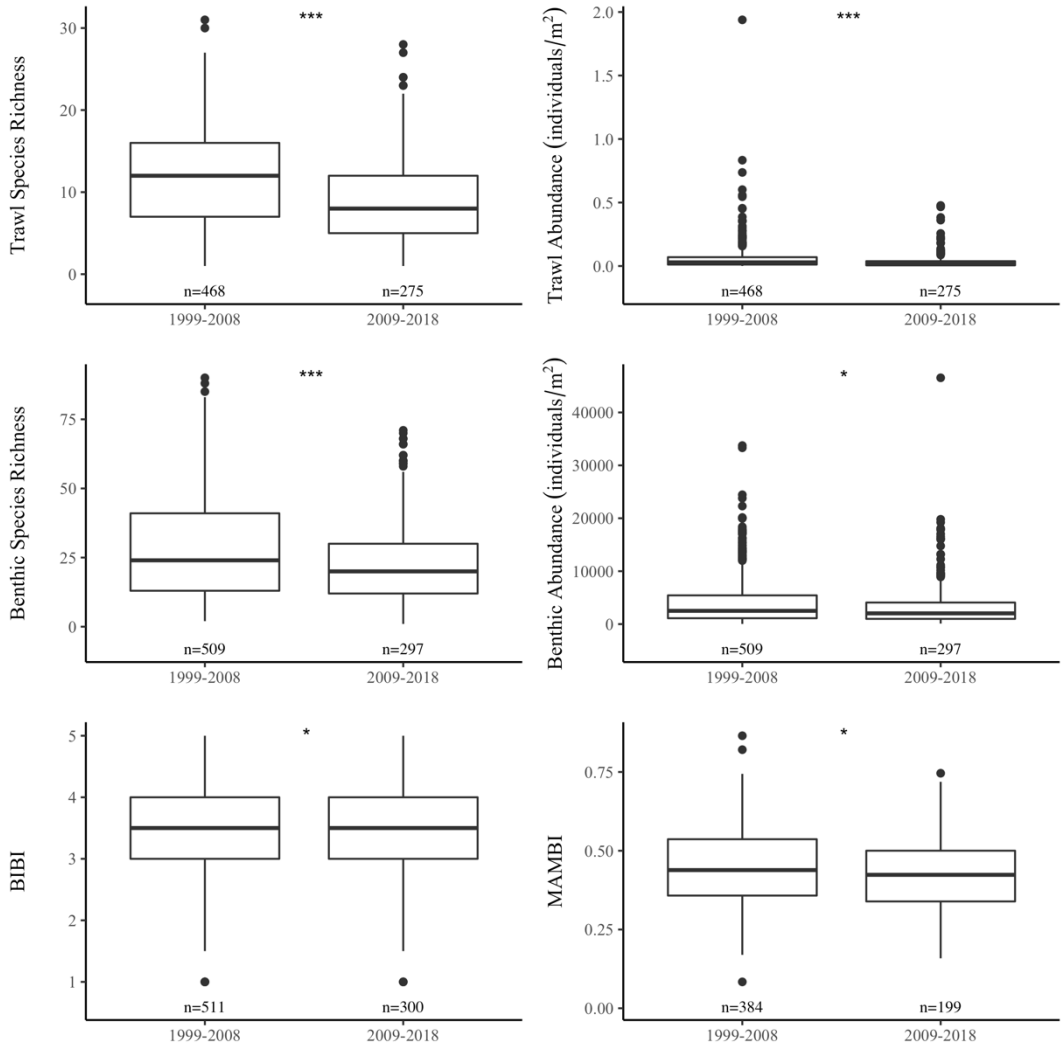

Figure 19. Comparisons of SCECAP biological quality data by time period (all sites). Asterisks signify *p*-values from *t*-tests ($^{***}p \leq 0.01$, $^{**}p \leq 0.05$, $^{*}p \leq 0.10$). For supplemental results, see Table 4.

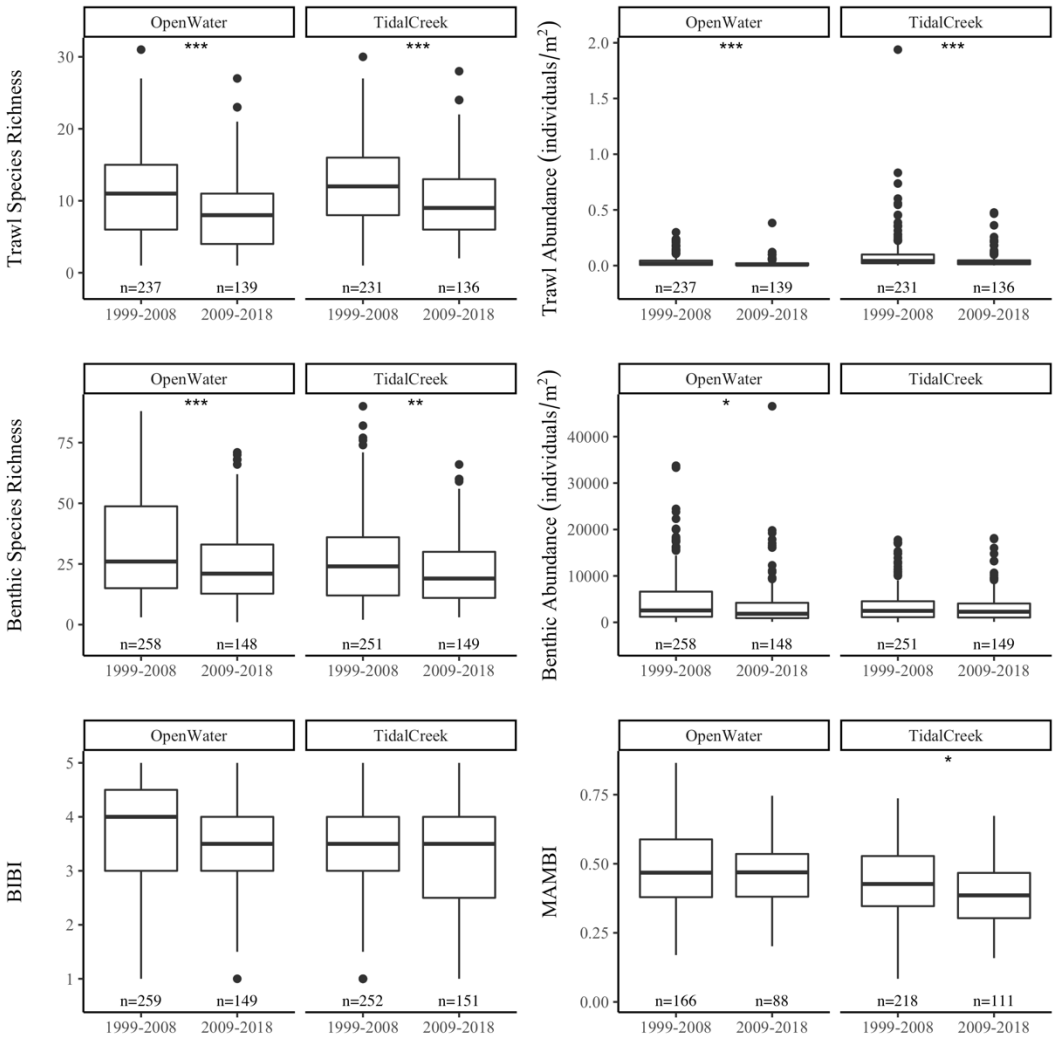

Figure 20. Comparisons of SCECAP biological quality data by time period (open water vs. tidal creek sites). Asterisks signify *p*-values from *t*-tests ($^{***}p \leq 0.01$, $^{**}p \leq 0.05$, $^{*}p \leq 0.10$). For supplemental results, see Table 5 and 6.

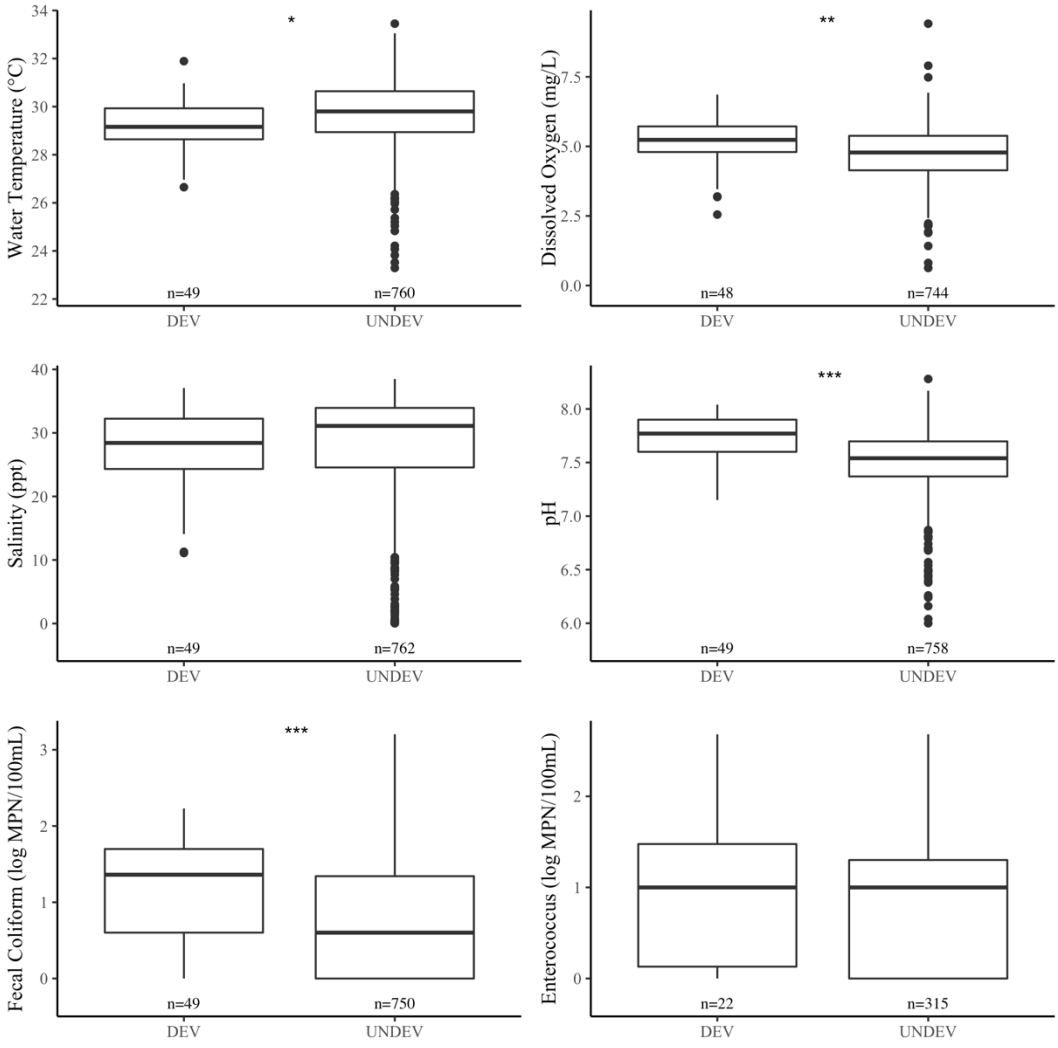

Figure 21. Comparisons of SCECAP water quality data by watershed development (all sites). Asterisks signify *p*-values from *t*-tests ($^{***}p \leq 0.01$, $^{**}p \leq 0.05$, $^{*}p \leq 0.10$). For supplemental results, see Table 7.

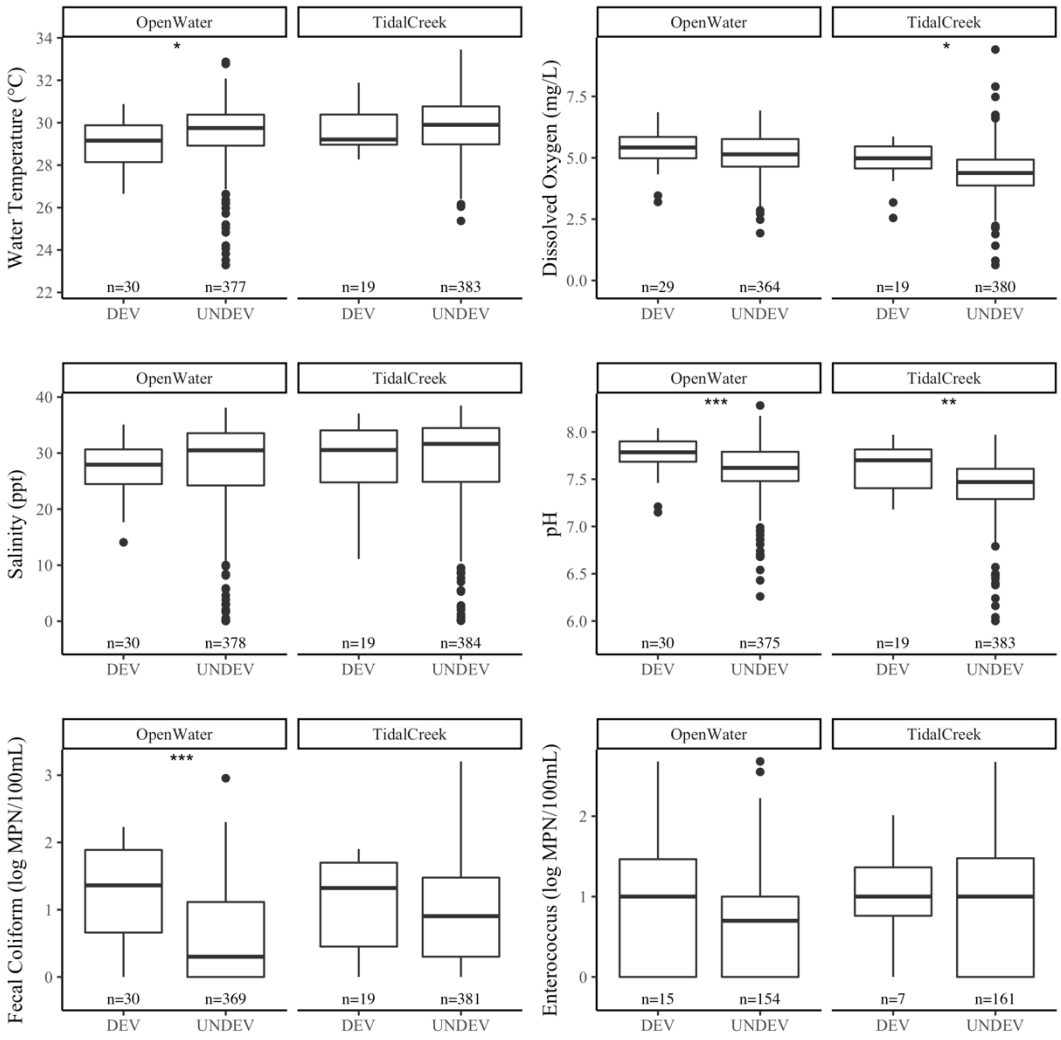

Figure 22. Comparisons of SCECAP water quality data by watershed development (open water vs. tidal creek sites). Asterisks signify *p*-values from *t*-tests ($^{***}p \leq 0.01$, $^{**}p \leq 0.05$, $^{*}p \leq 0.10$). For supplemental results, see Table 8 and 9.

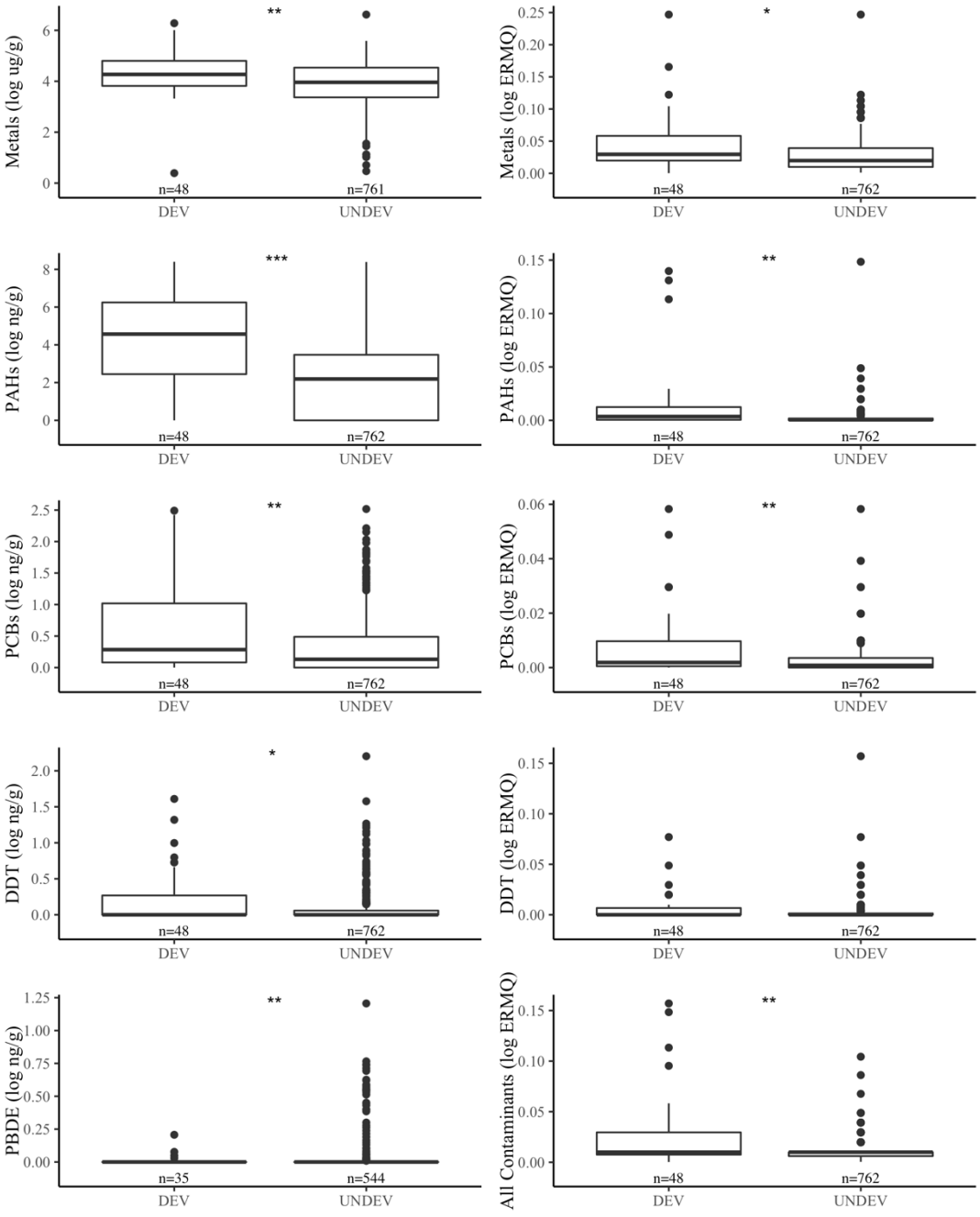

Figure 23. Comparisons of SCECAP sediment quality data by watershed development (all sites). Asterisks signify *p*-values from *t*-tests ($^{***}p \leq 0.01$, $^{**}p \leq 0.05$, $^{*}p \leq 0.10$). For supplemental results, see Table 7.

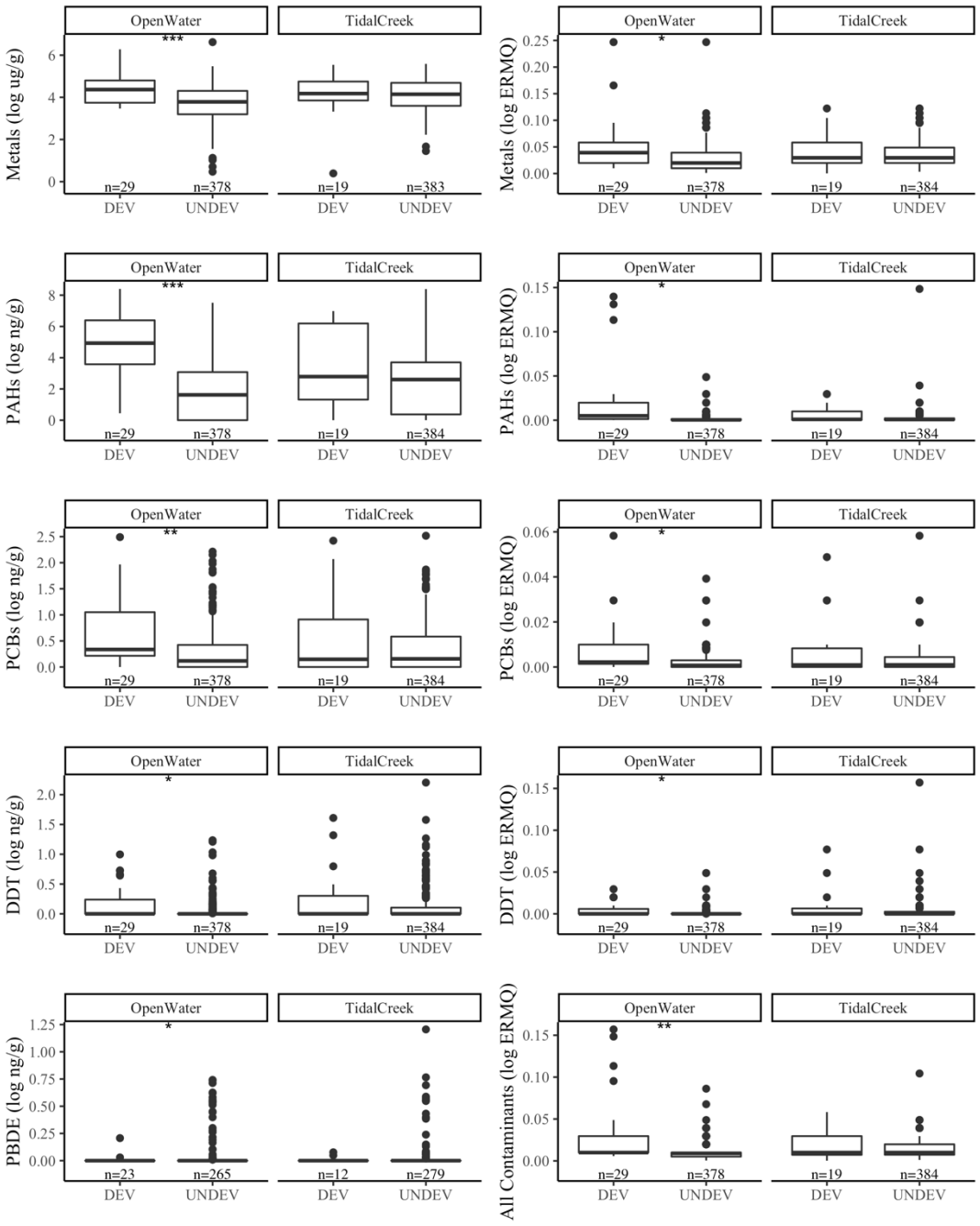

Figure 24. Comparisons of SCECAP sediment quality data by watershed development (open water vs. tidal creek sites). Asterisks signify *p*-values from *t*-tests ($^{***}p \leq 0.01$, $^{**}p \leq 0.05$, $^{*}p \leq 0.10$). For supplemental results, see Table 8 and 9.

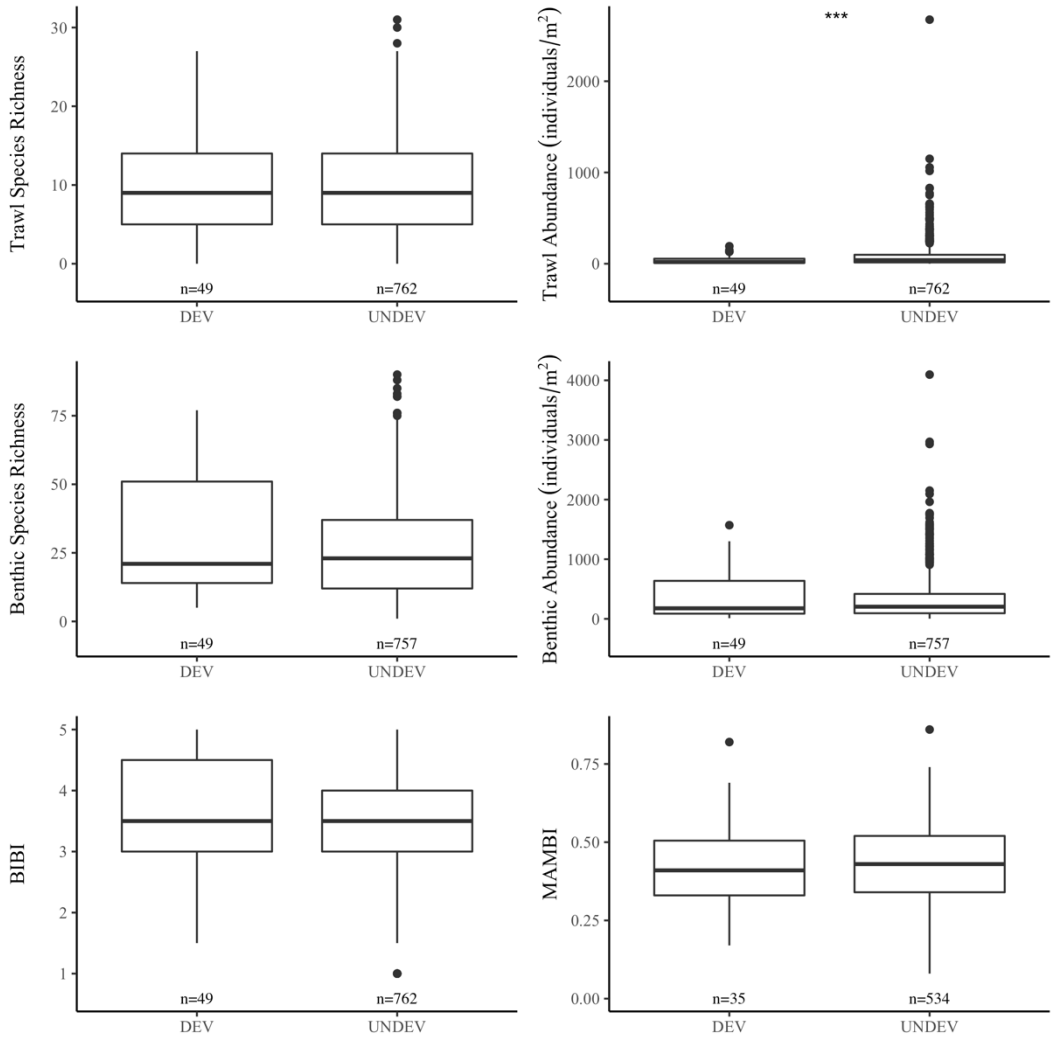

Figure 25. Comparisons of SCECAP biological quality data by watershed development (all sites). Asterisks signify *p*-values from *t*-tests ($^{***}p \leq 0.01$, $^{**}p \leq 0.05$, $^{*}p \leq 0.10$). For supplemental results, see Table 7.

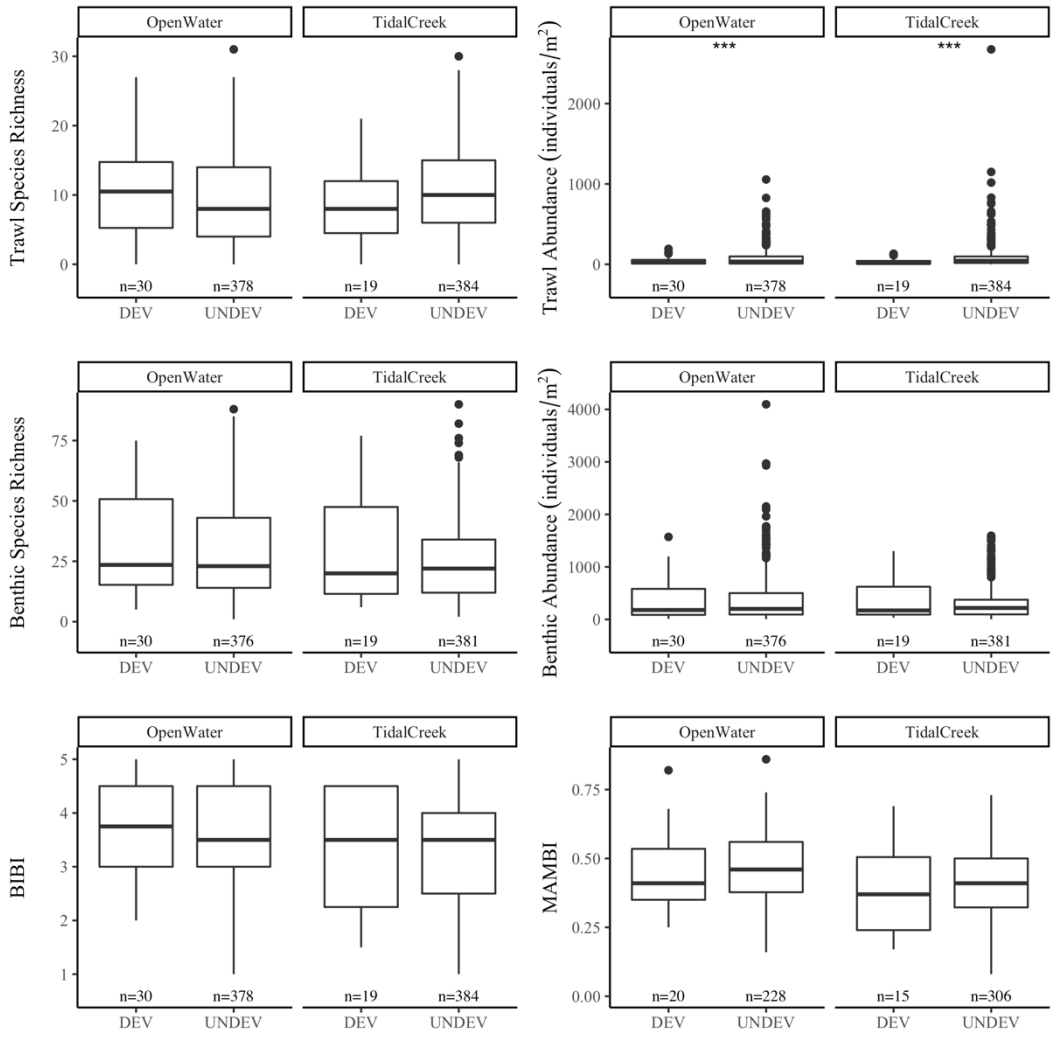

Figure 26. Comparisons of SCECAP biological quality data by watershed development (open water vs. tidal creek sites). Asterisks signify *p*-values from *t*-tests ($^{***}p \leq 0.01$, $^{**}p \leq 0.05$, $^{*}p \leq 0.10$). For supplemental results, see Table 8 and 9.

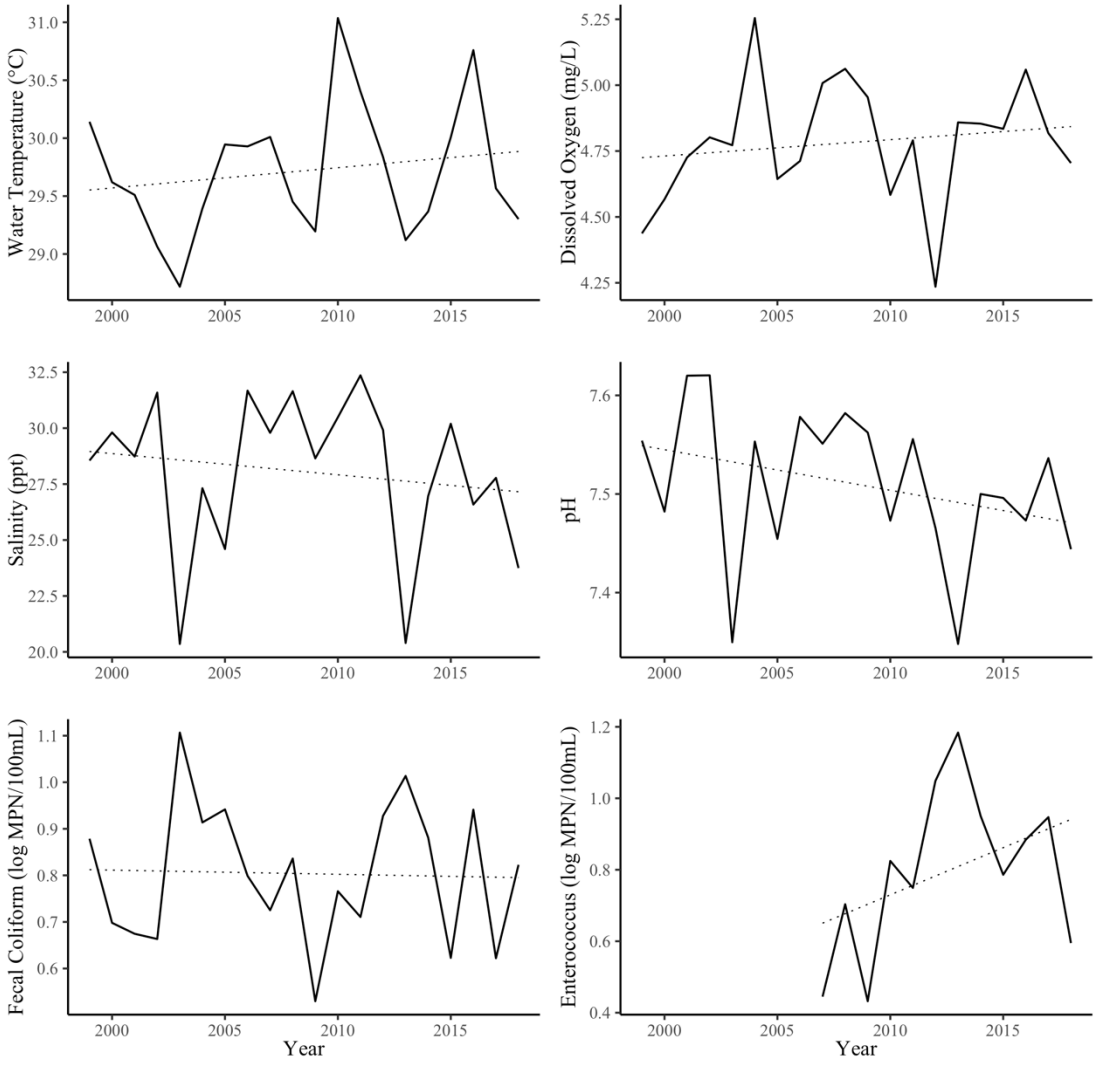

Figure 27. Time series analysis of SCECAP water quality annual averages from 1999-2018 (all sites). Dotted lines represent GLS regression trendlines not significantly different than zero (p-value>0.05). Gaps in line graph indicate missing data. For supplemental results, see Table 10.

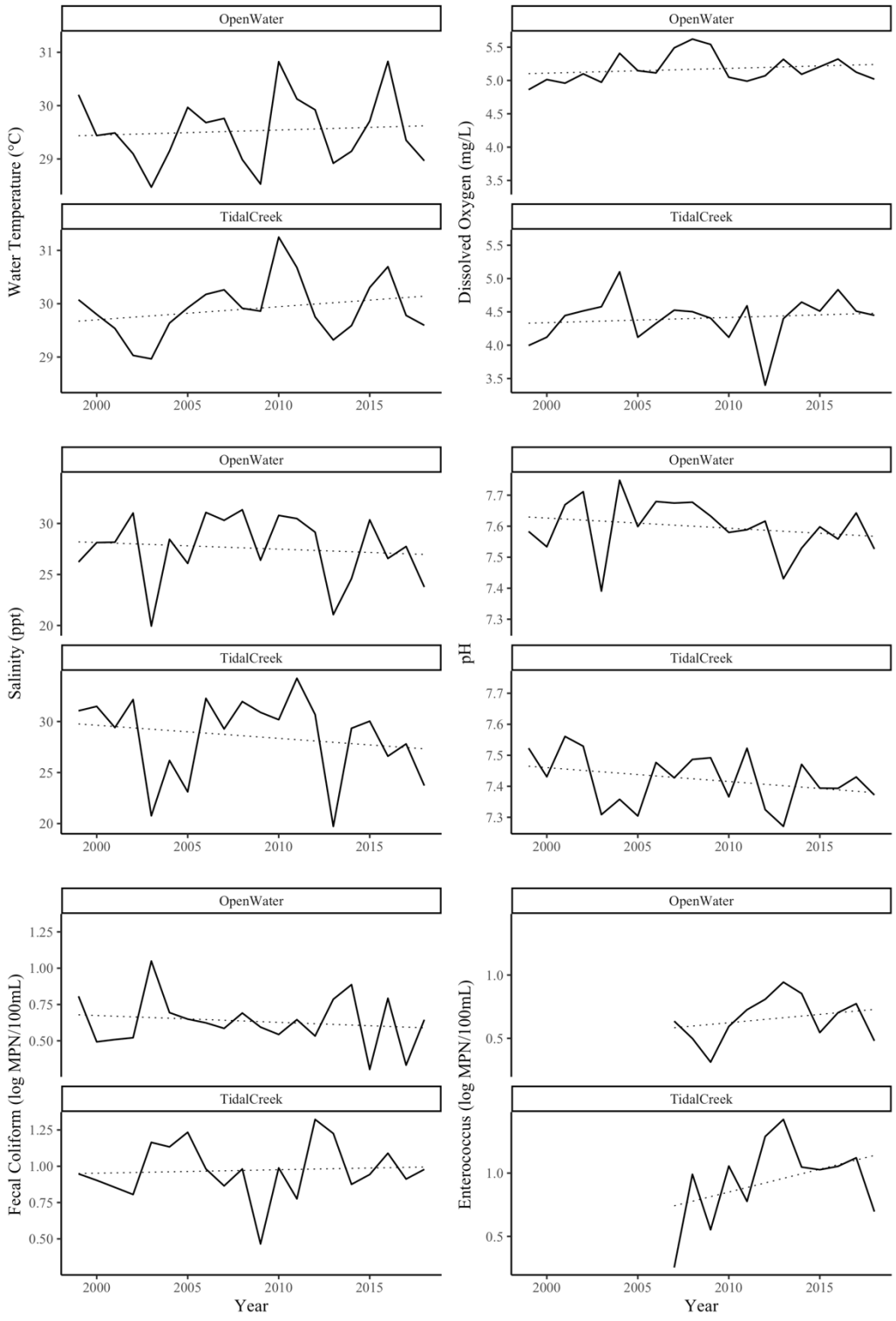

Figure 28. Time series analysis of SCECAP water quality annual averages from 1999-2018 (open water vs. tidal creek sites). Dotted lines represent GLS regression trendlines not significantly different than zero (p-value>0.05). Gaps in line graph indicate missing data. For supplemental results, see Table 10.

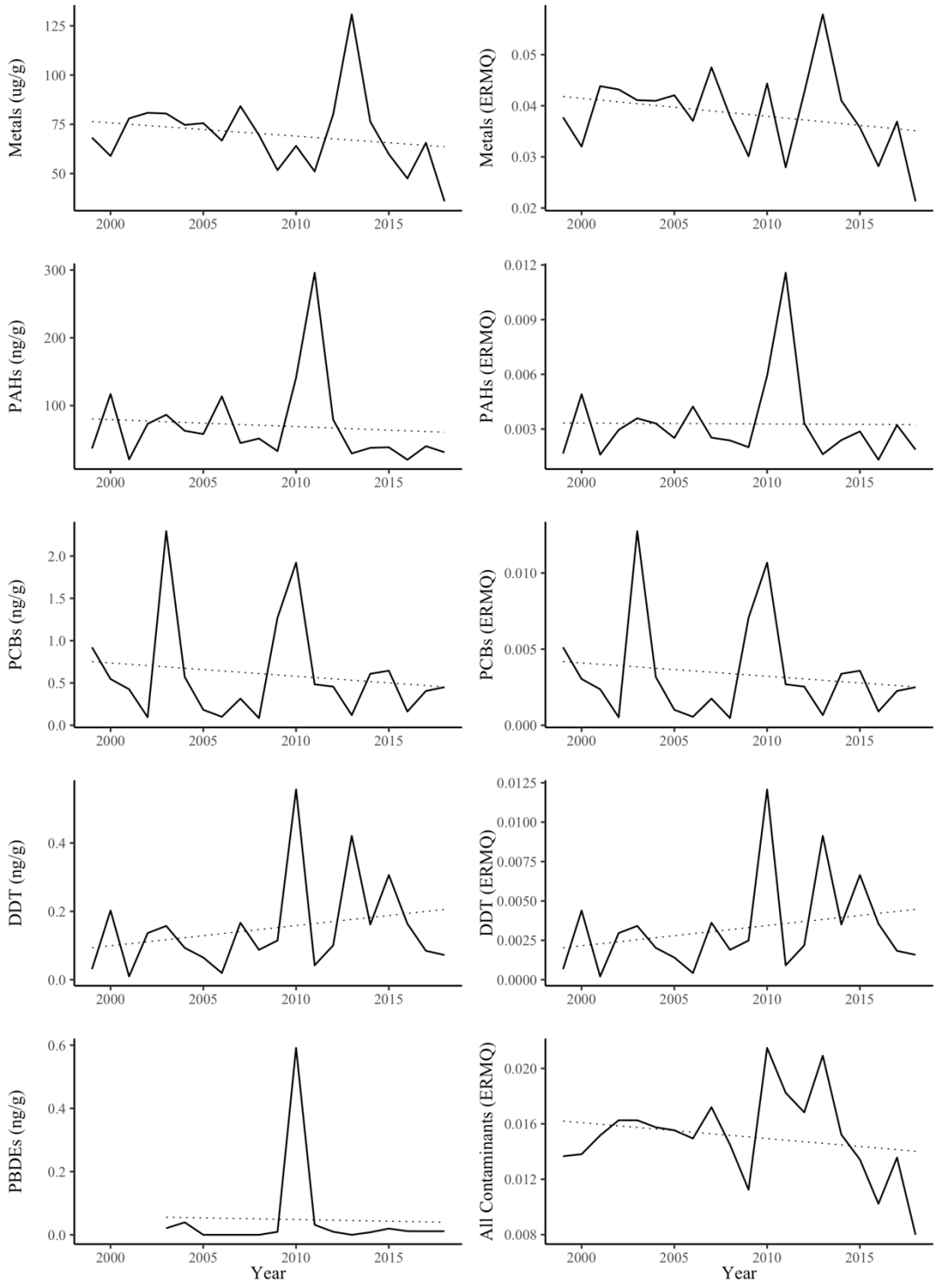

Figure 29. Time series analysis of SCECAP sediment quality annual averages from 1999-2018 (all sites). Dotted lines represent GLS regression trendlines not significantly different than zero (p-value>0.05). Gaps in line graph indicate missing data. For supplemental results, see Tables 11 and 12.

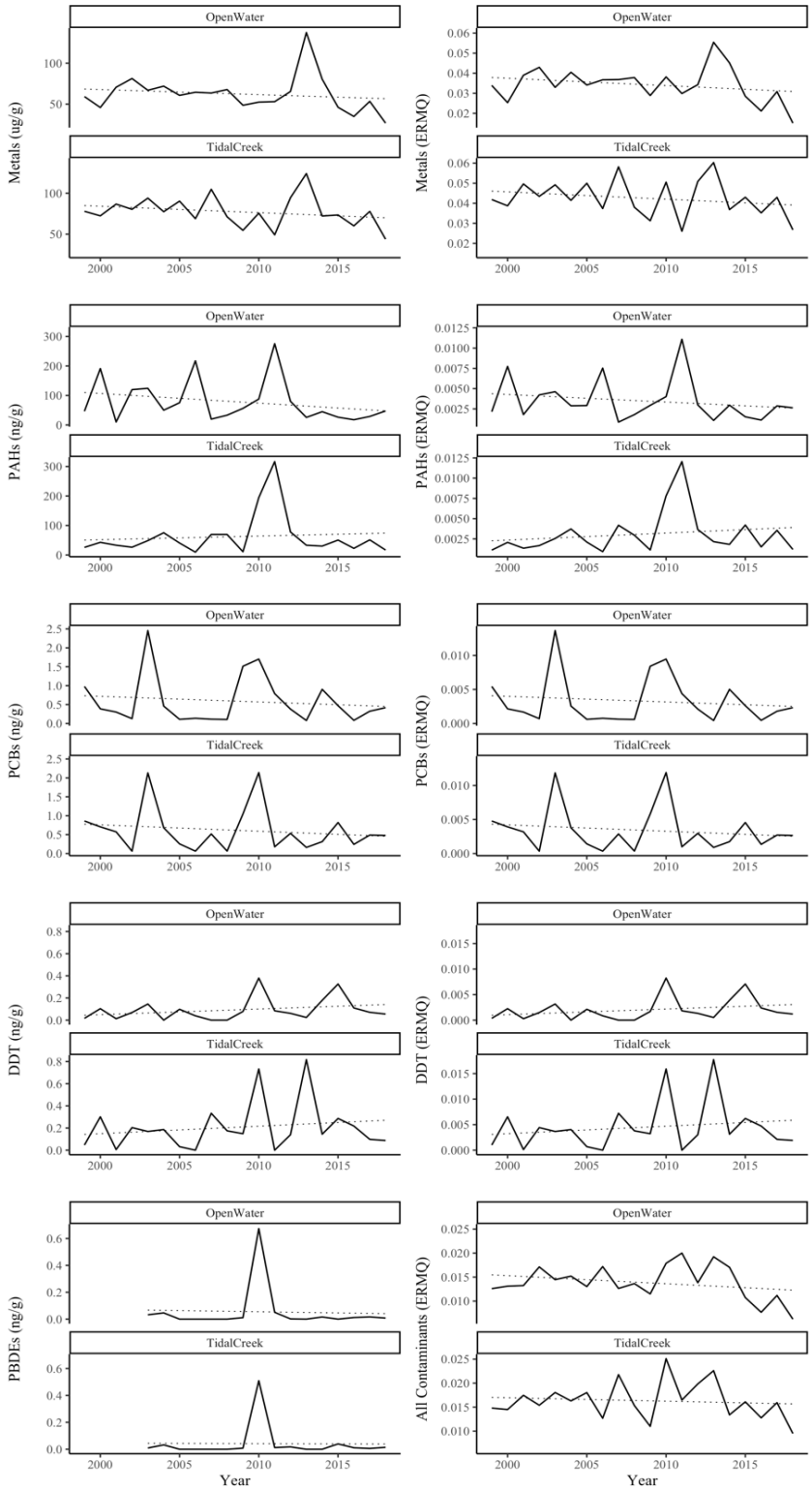

Figure 30. Time series analysis of SCECAP sediment quality annual averages from 1999-2018 (open water vs. tidal creek sites). Dotted lines represent GLS regression trendlines not significantly different than zero (p-value>0.05). Gaps in line graph indicate missing data. For supplemental results, see Tables 11 and 12.

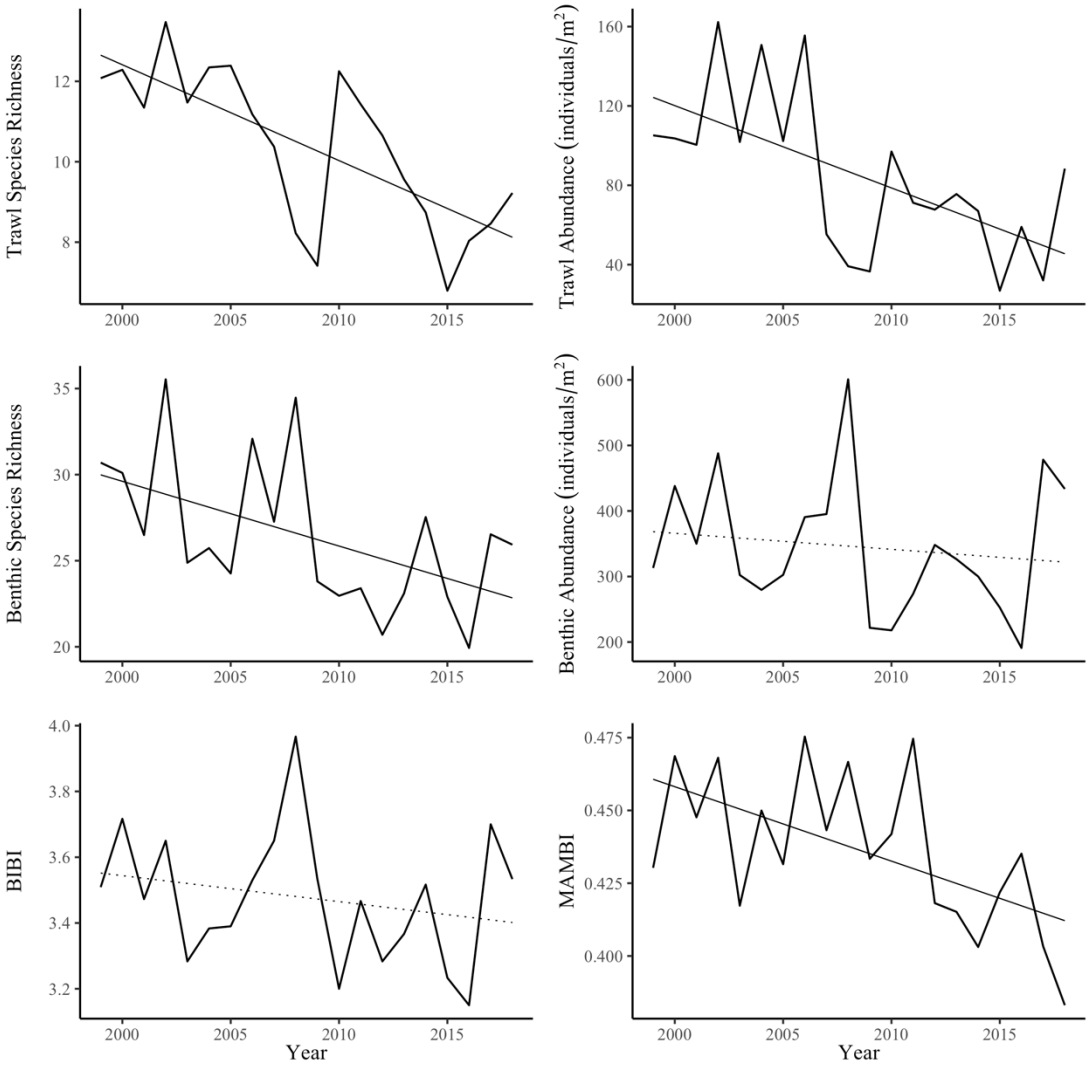

Figure 31. Time series analysis of SCECAP biological quality annual averages from 1999-2018 (all sites). Solid lines represent GLS regression trendlines with slopes significantly different from zero (p-value≤0.05); dotted lines not statistically significant (p-value>0.05). For supplemental results, see Table 13.

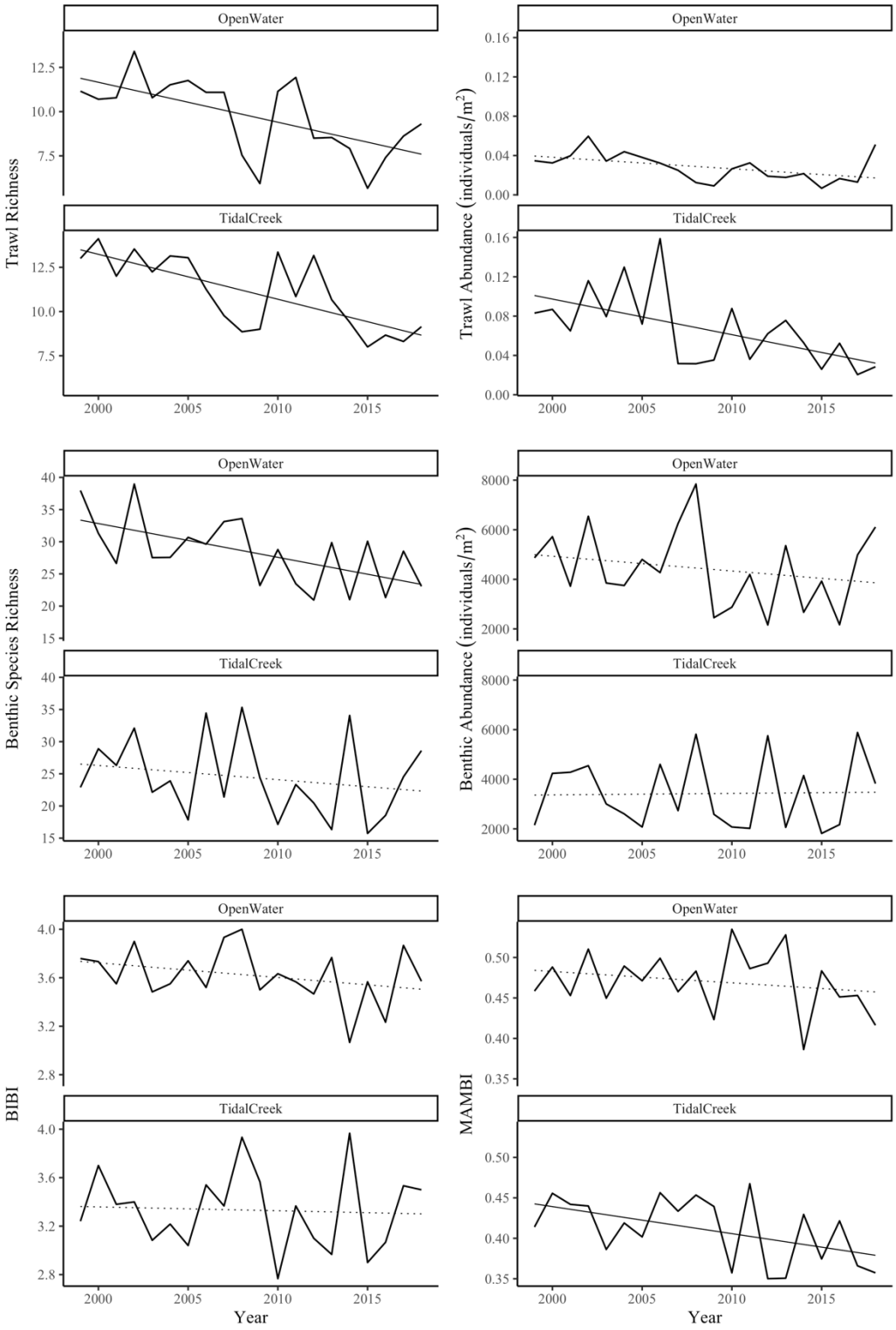

Figure 32. Time series analysis of SCECAP biological quality annual averages from 1999-2018 (open water vs. tidal creek sites). Solid lines represent GLS regression trendlines with slopes significantly different from zero (p-value≤0.05); dotted lines not statistically significant (p-value>0.05). For supplemental results, see Table 13.

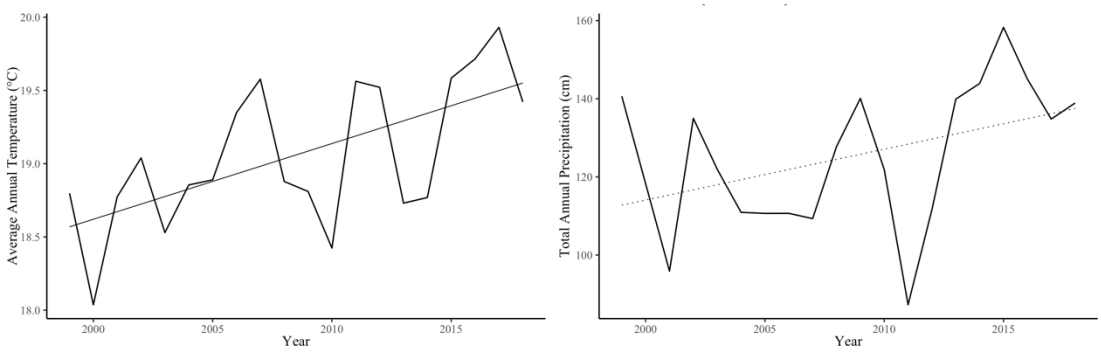

Figure 33. Time series analysis of annual climate in coastal South Carolina from 1999-2018 (average of 3 primary weather stations). Solid lines represent GLS regression trendlines with slopes significantly different from zero (p-value≤0.05); dotted lines not statistically significant (p-value>0.05). For supplemental results, see Tables 14 and 15.

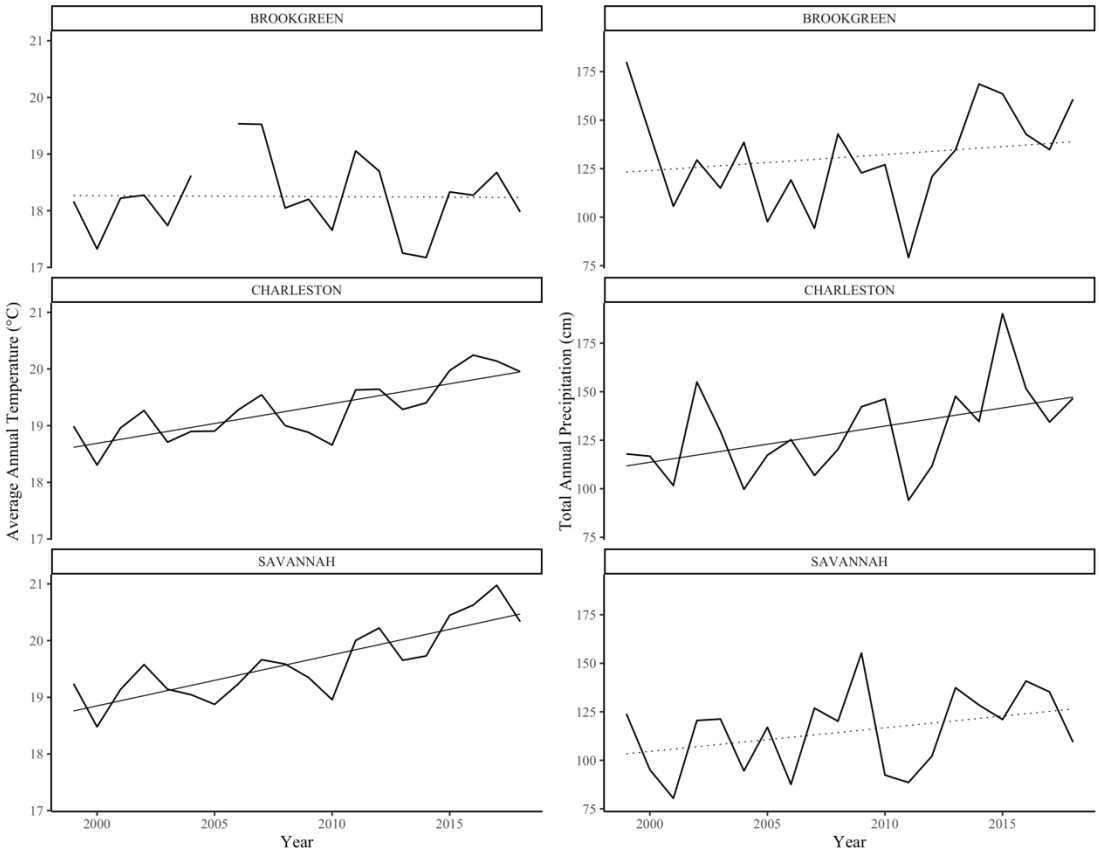

Figure 34. Time series analysis of annual climate in coastal South Carolina from 1999-2018 (by 3 primary weather stations). Solid lines represent GLS regression trendlines with slopes significantly different from zero (p-value≤0.05); dotted lines not statistically significant (p-value>0.05). Gaps in line graph indicate missing data. For supplemental results, see Tables 14 and 15.

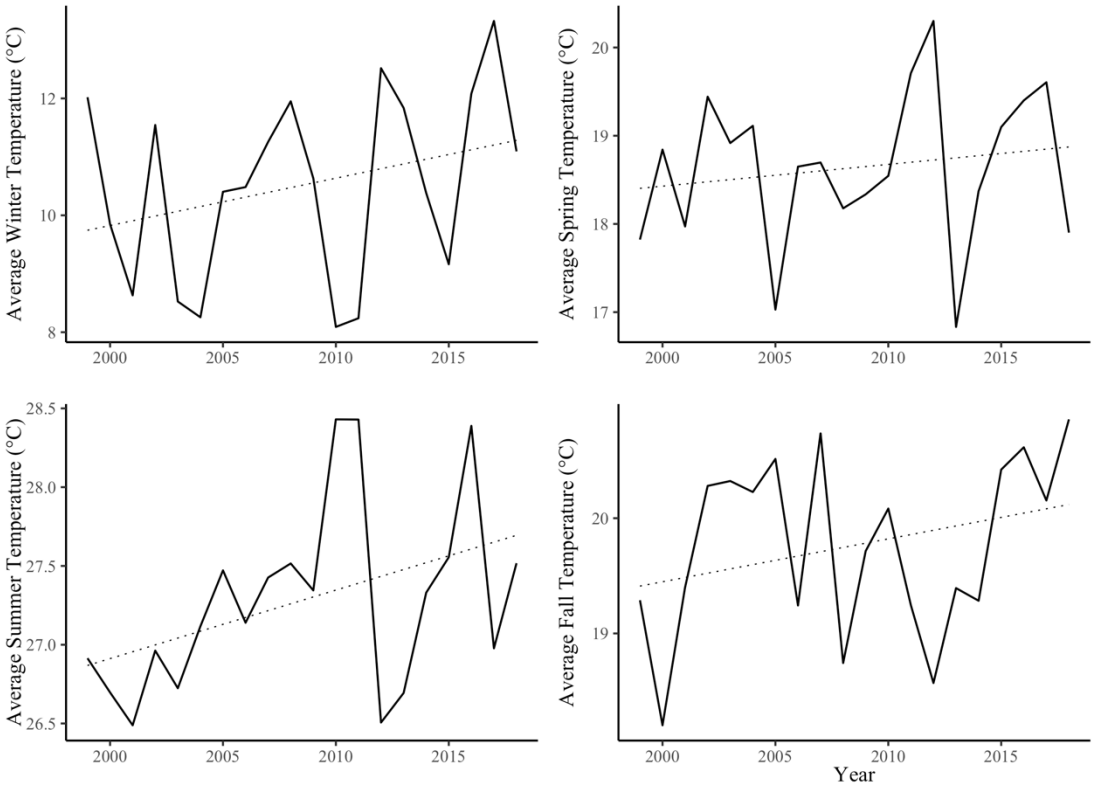

Figure 35. Time series analysis of seasonal temperature in coastal South Carolina from 1999-2018 (average of 3 primary weather stations). Dotted lines represent GLS regression trendlines not significantly different than zero (p-value>0.05). For supplemental results, see Tables 14 and 15.

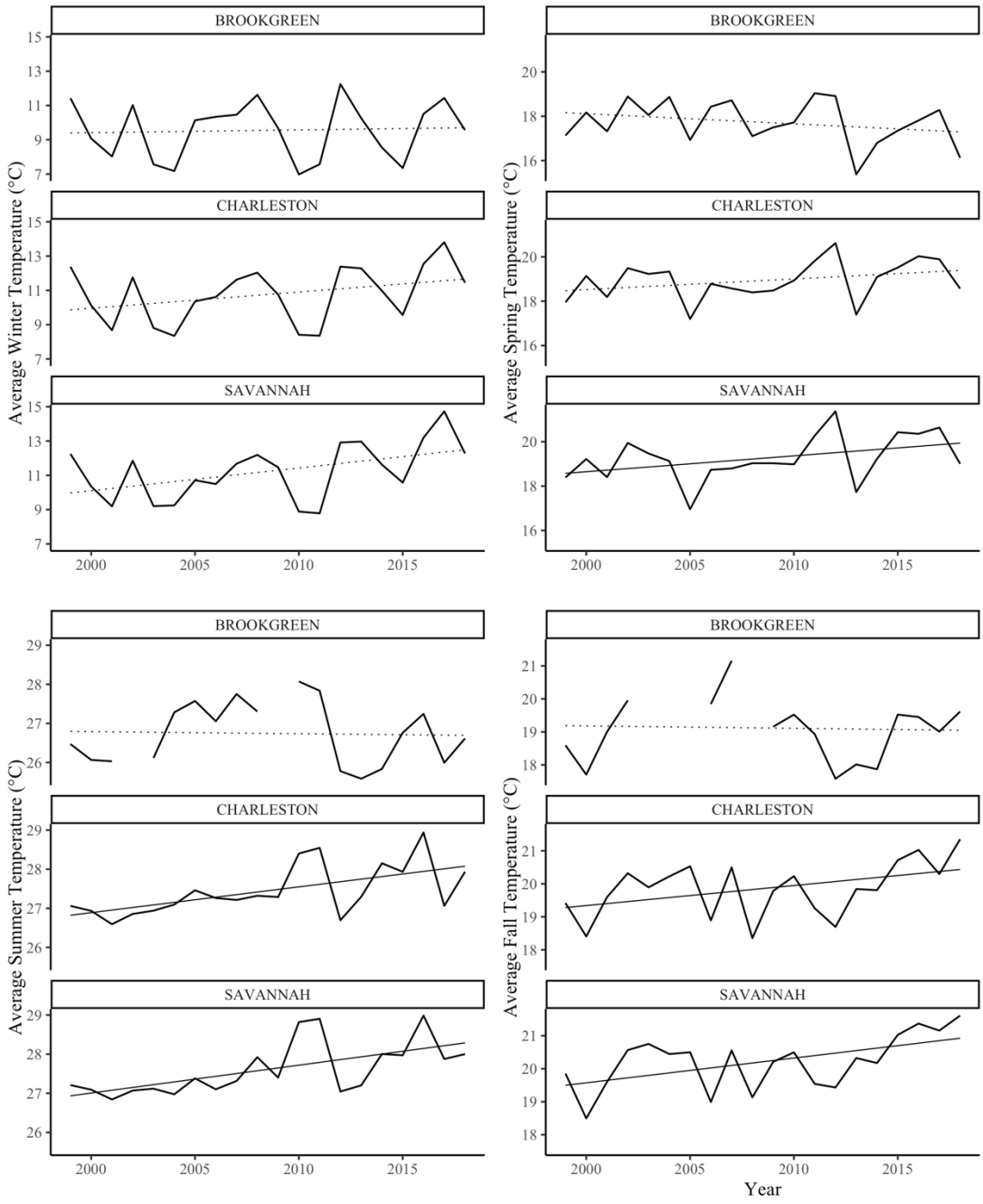

Figure 36. Time series analysis of seasonal temperature in coastal South Carolina from 1999-2018 (by 3 primary weather stations). Solid lines represent GLS regression trendlines with slopes significantly different from zero (p-value≤0.05); dotted lines not statistically significant (p-value>0.05). Gaps in line graph indicate missing data. For supplemental results, see Tables 14 and 15.

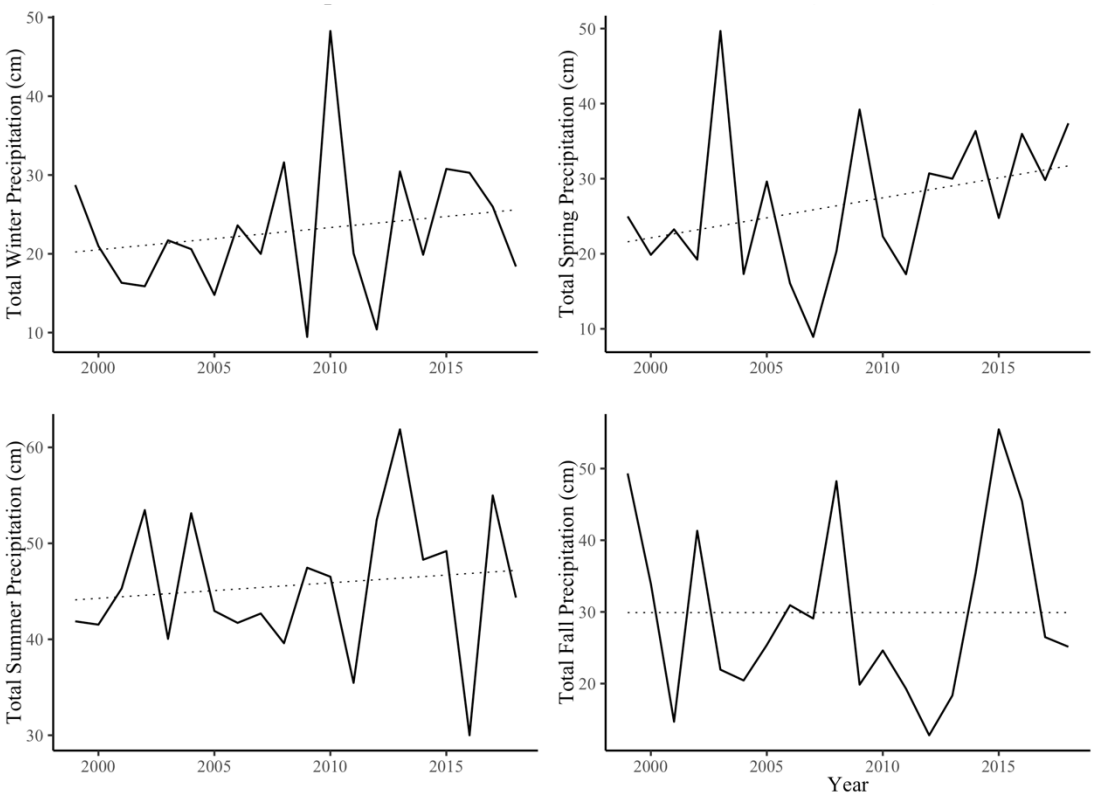

Figure 37. Time series analysis of seasonal precipitation in coastal South Carolina from 1999-2018 (average of 3 primary weather stations). Dotted lines represent GLS regression trendlines not significantly different than zero (p-value>0.05). For supplemental results, see Tables 14 and 15.

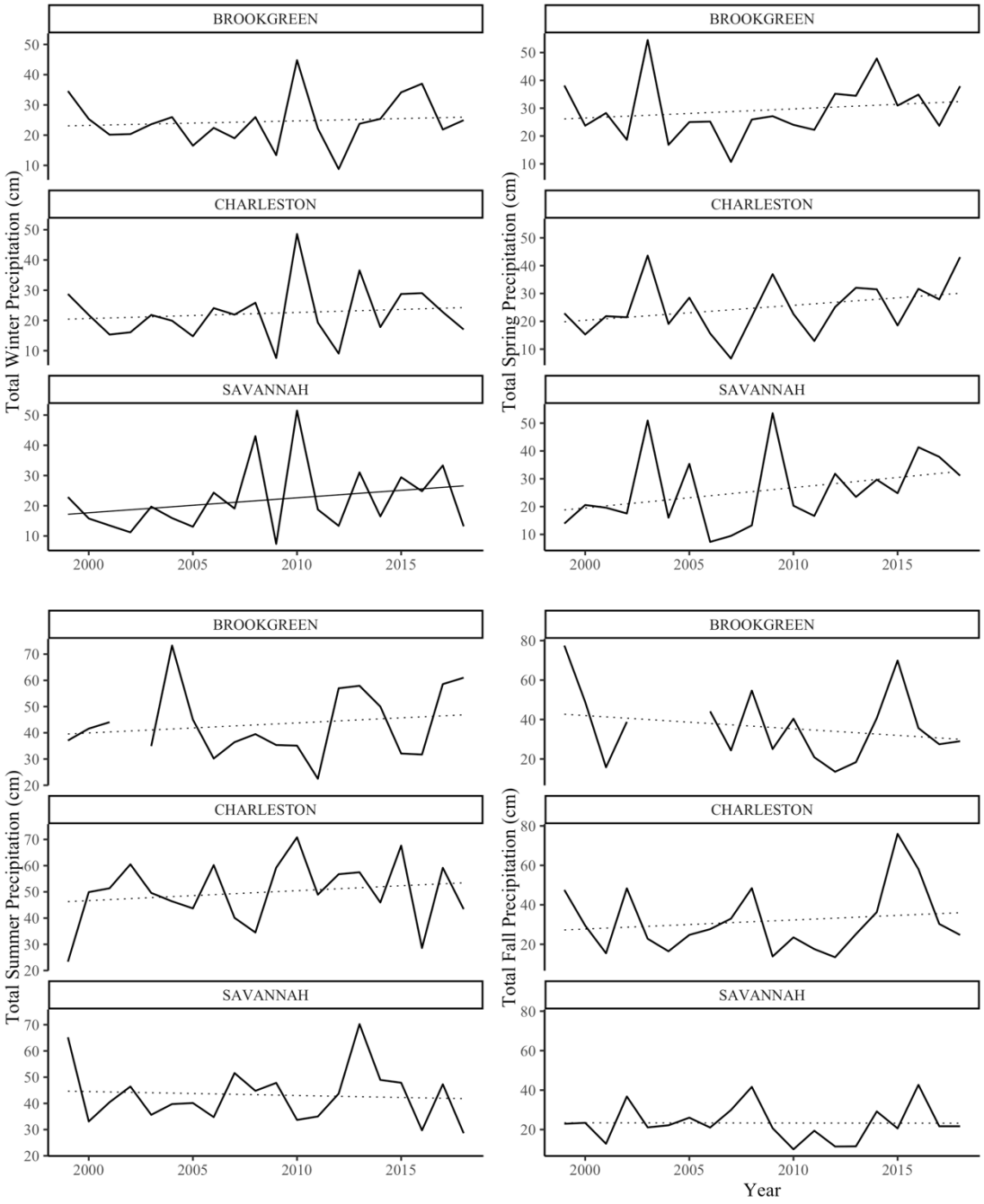

Figure 38. Time series analysis of seasonal precipitation in coastal South Carolina from 1999-2018 (by 3 primary weather stations). Solid lines represent GLS regression trendlines with slopes significantly different from zero (p-value≤0.05); dotted lines not statistically significant (p-value>0.05). Gaps in line graph indicate missing data. For supplemental results, see Tables 14 and 15.

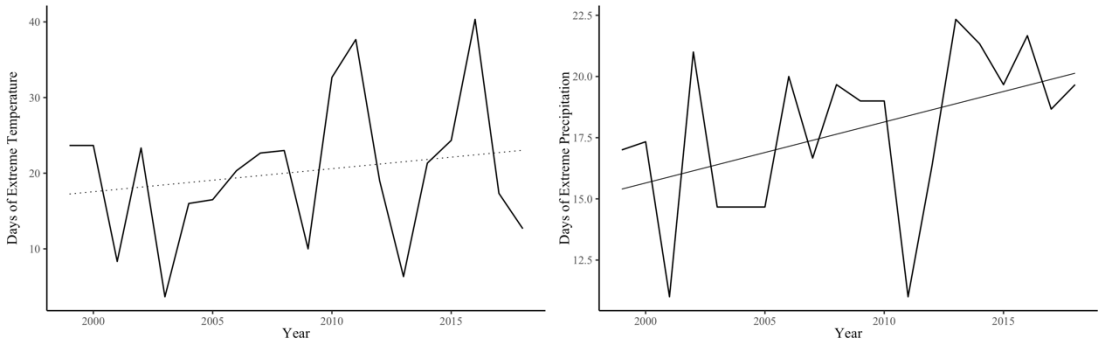

Figure 39. Time series analysis of extreme weather occurrences in coastal South Carolina from 1999-2018 (average of 3 primary weather stations). Solid lines represent GLS regression trendlines with slopes significantly different from zero (p-value≤0.05); dotted lines not statistically significant (p-value>0.05). For supplemental results, see Tables 14 and 15.

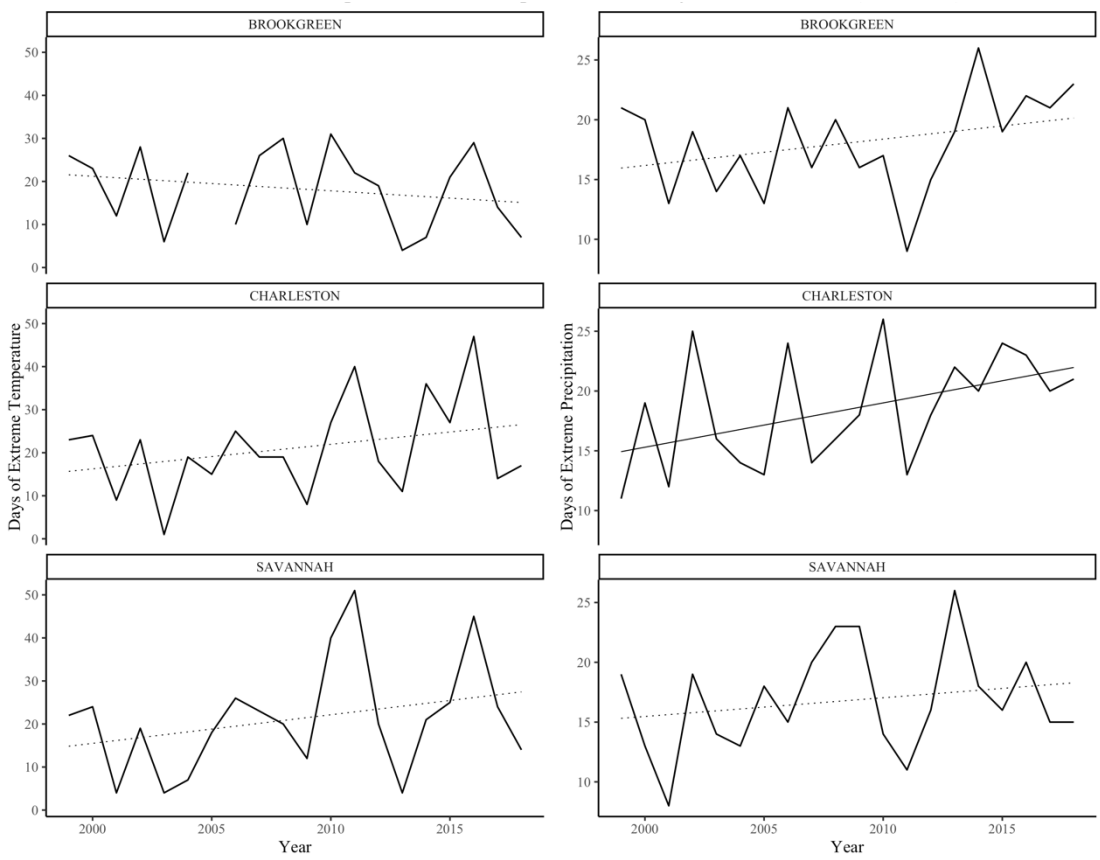

Figure 40. Time series analysis of extreme weather occurrences in coastal South Carolina from 1999-2018 (by 3 primary weather stations). Solid lines represent GLS regression trendlines with slopes significantly different from zero (p-value≤0.05); dotted lines not statistically significant (p-value>0.05). Gaps in line graph indicate missing data. For supplemental results, see Tables 14 and 15.

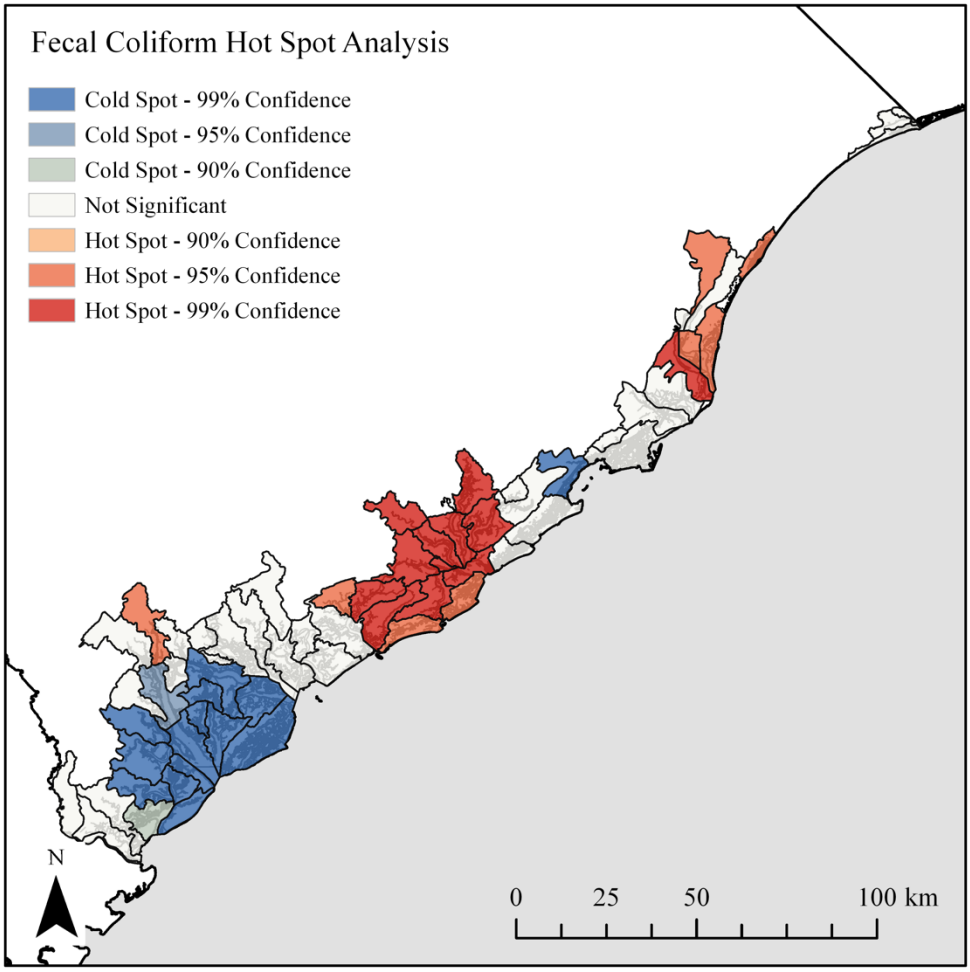

Figure 41. Map of fecal coliform hot spots in coastal South Carolina by 14-digit HUC watershed

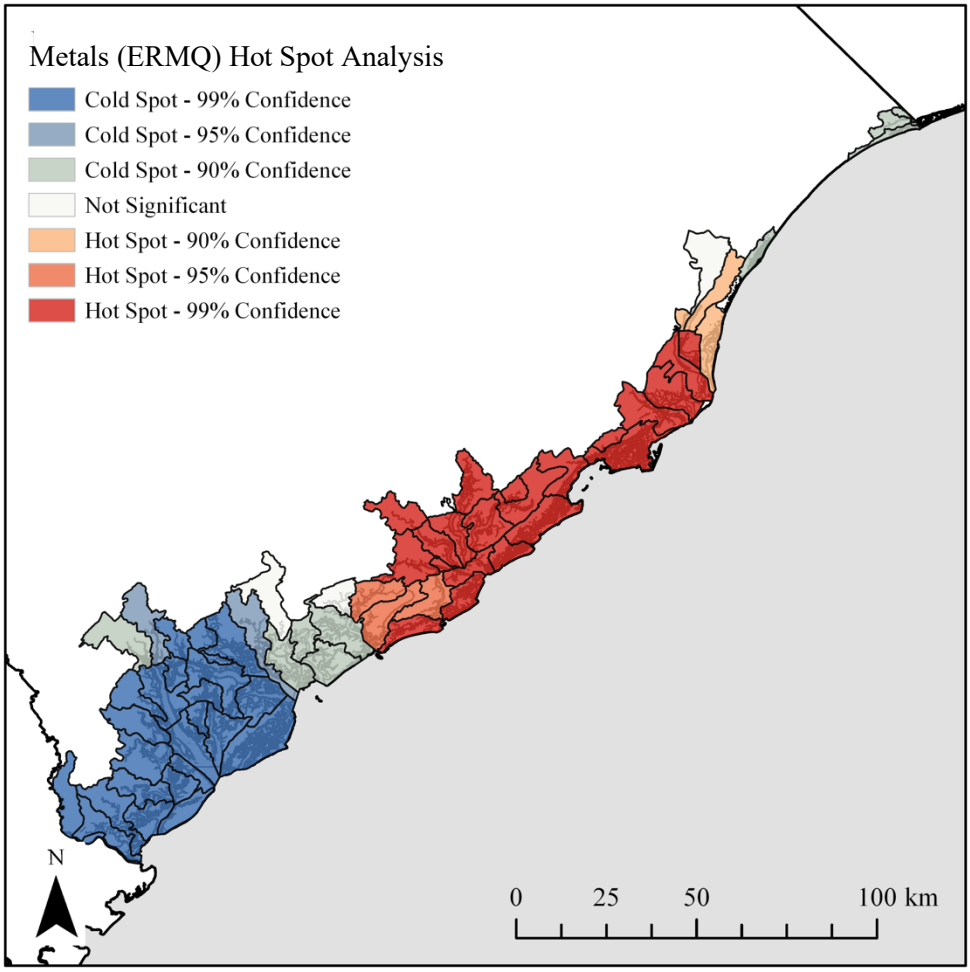

Figure 42. Map of metal (ERMQ) sediment contamination hot spots in coastal South Carolina by 14-digit HUC watershed

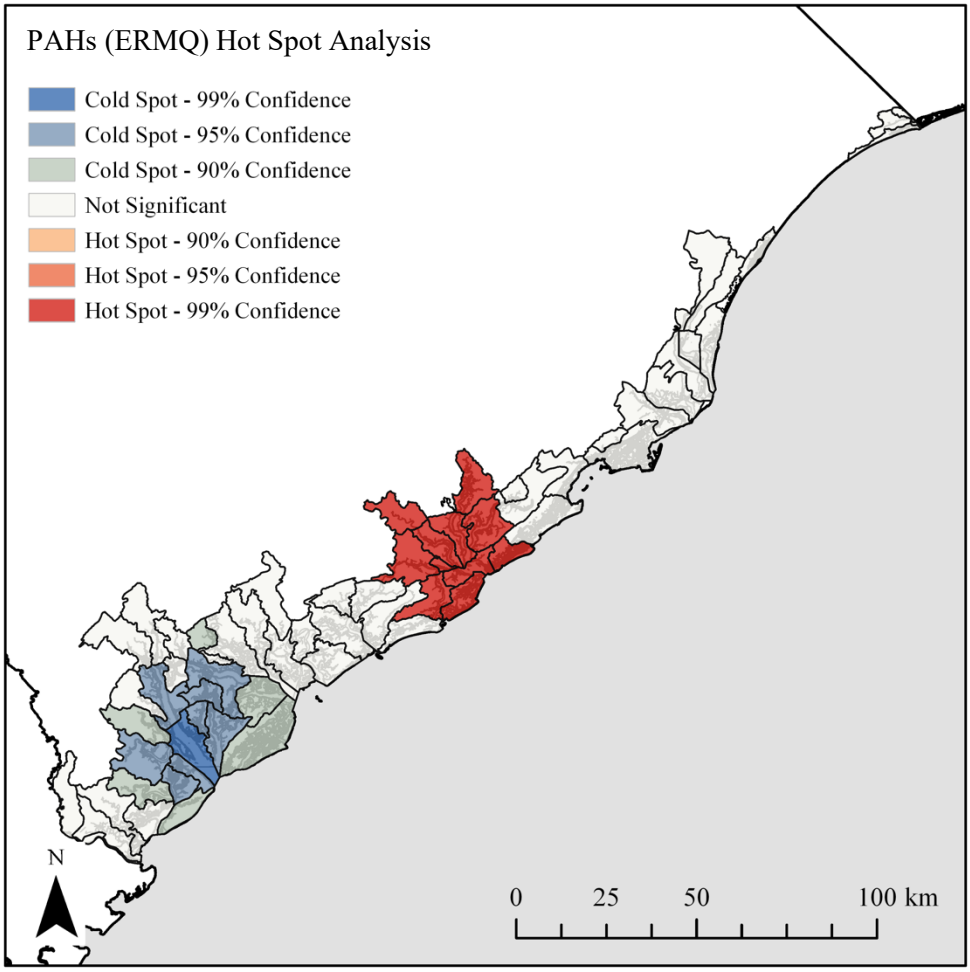

Figure 43. Map of PAH (ERMQ) sediment contamination hot spots in coastal South Carolina by 14-digit HUC watershed

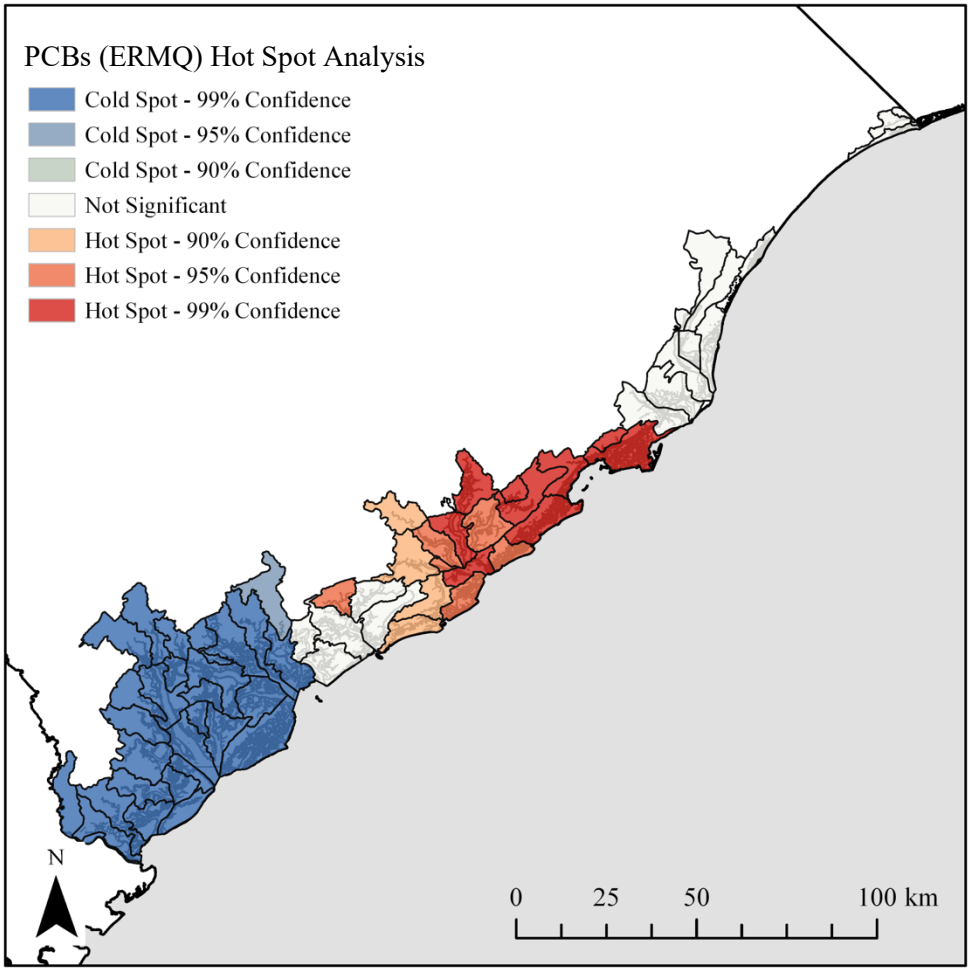

Figure 44. Map of PCB (ERMQ) sediment contamination hot spots in coastal South Carolina by 14-digit HUC watershed

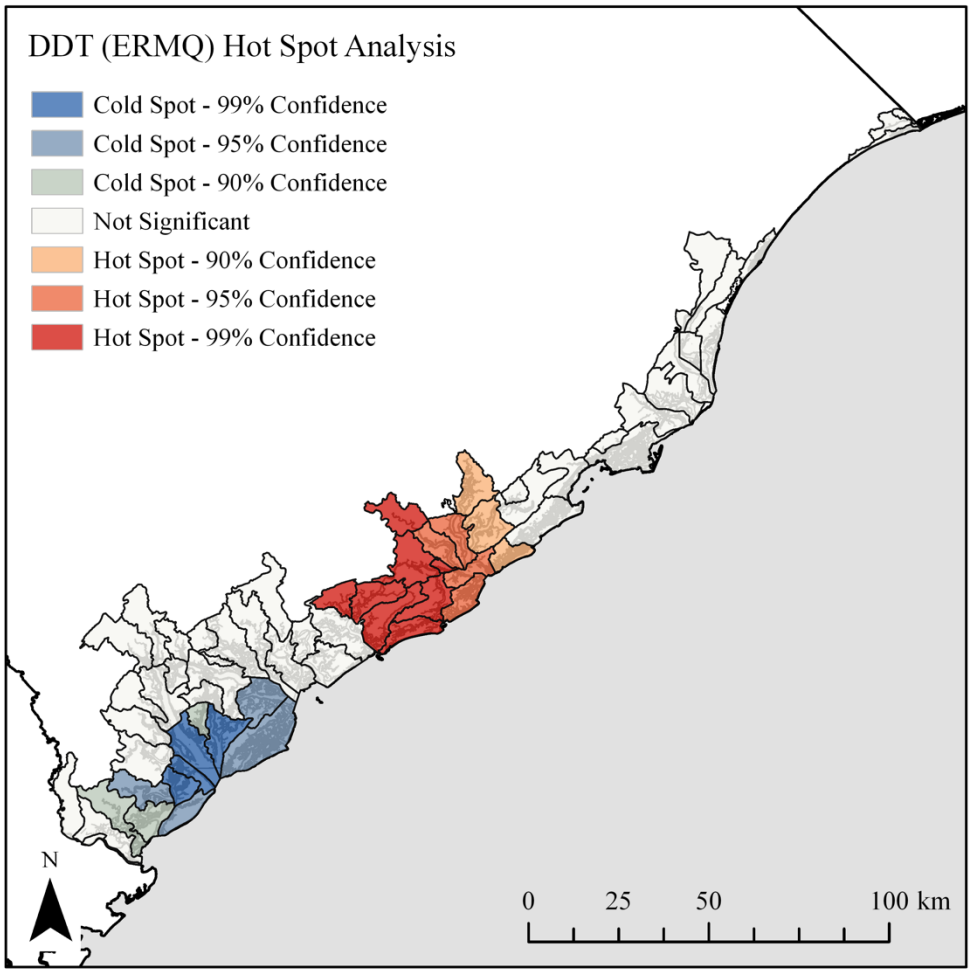

Figure 45. Map of DDT (ERMQ) sediment contamination hot spots in coastal South Carolina by 14-digit HUC watershed

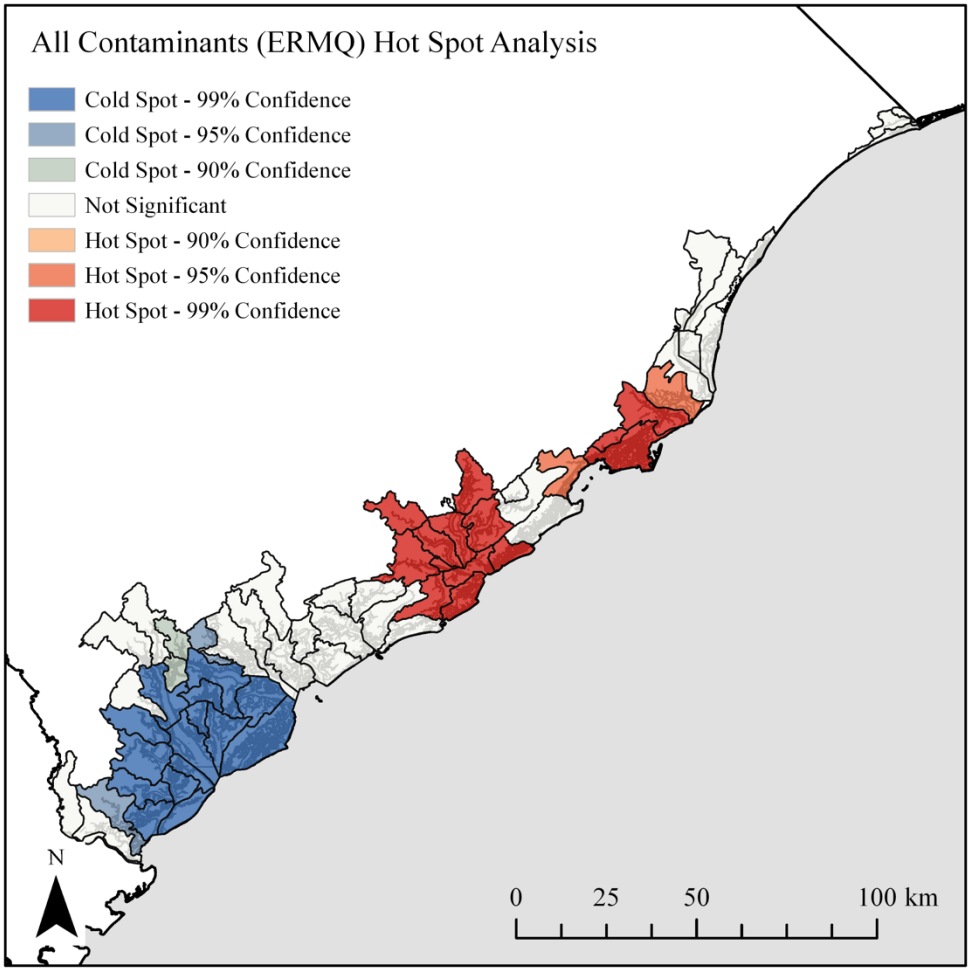

Figure 46. Map of total ERMQ sediment contamination hot spots in coastal South Carolina by 14-digit HUC watershed

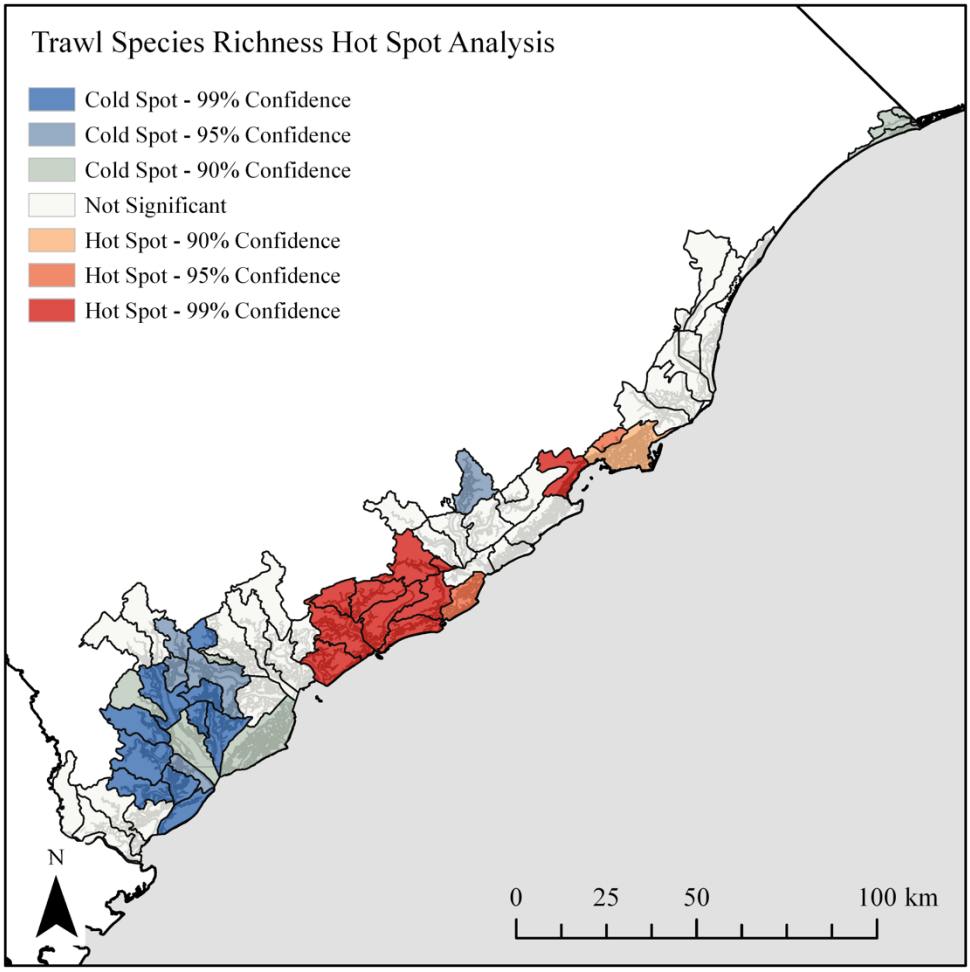

Figure 47. Map of trawl species richness hot spots in coastal South Carolina by 14-digit HUC watershed

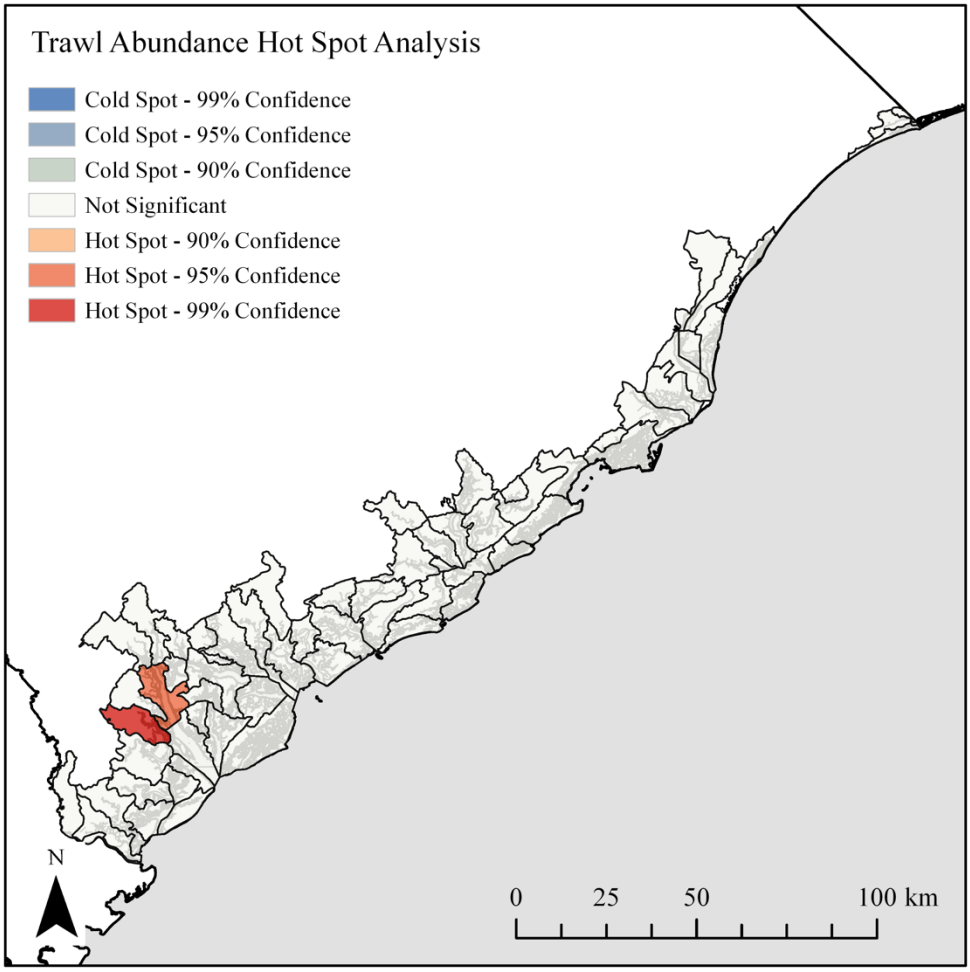

Figure 48. Map of trawl abundance hot spots in coastal South Carolina by 14-digit HUC watershed

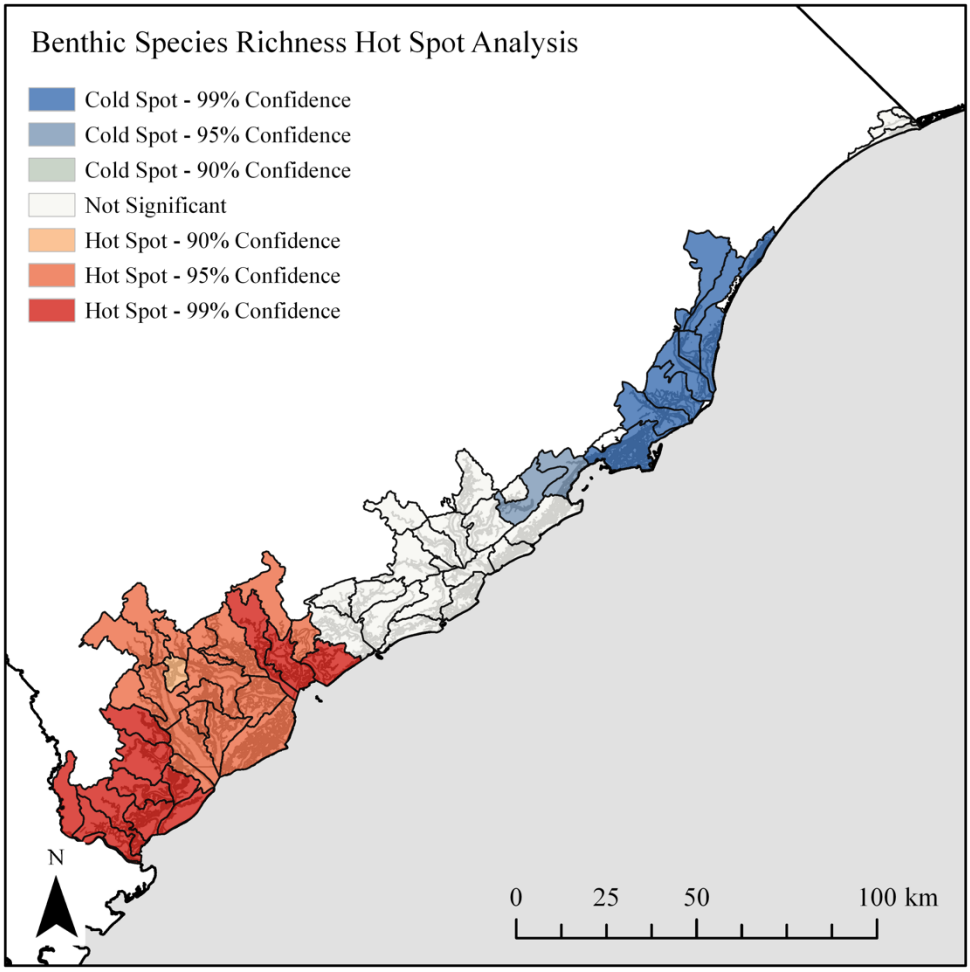

Figure 49. Map of benthic species richness hot spots in coastal South Carolina by 14-digit HUC watershed

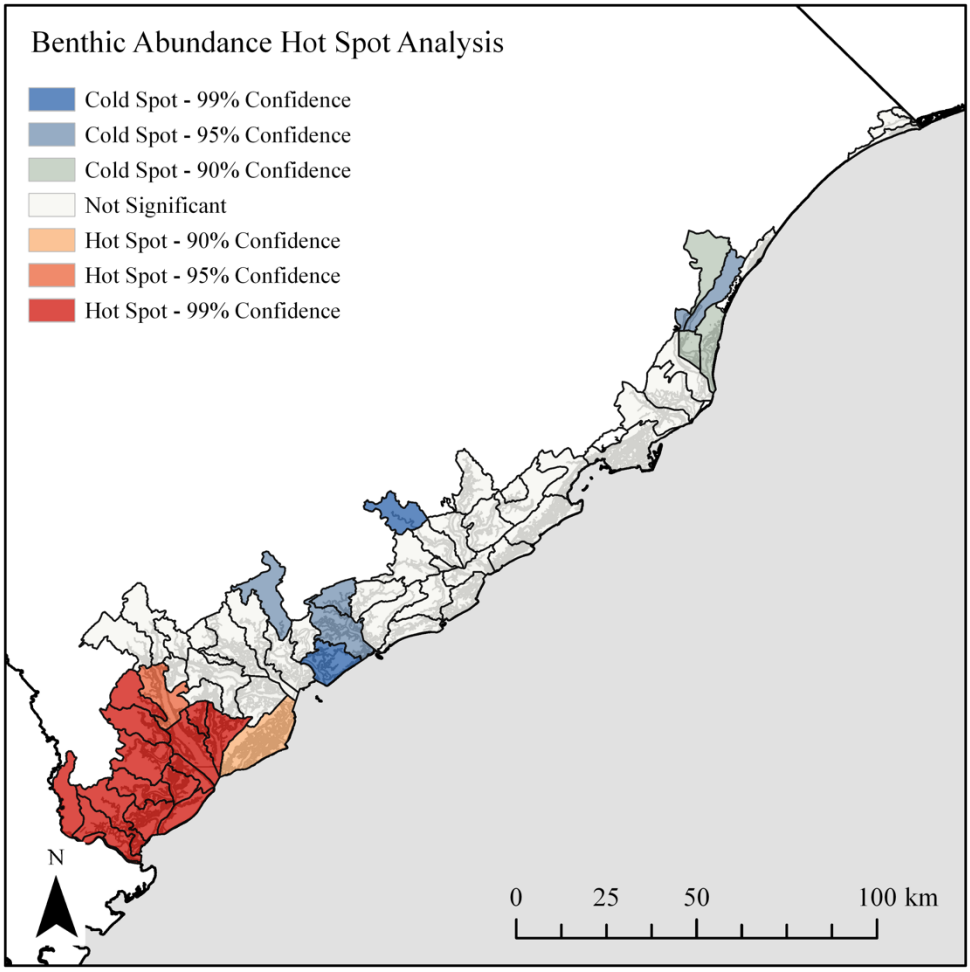

Figure 50. Map of benthic abundance hot spots in coastal South Carolina by 14-digit HUC watershed

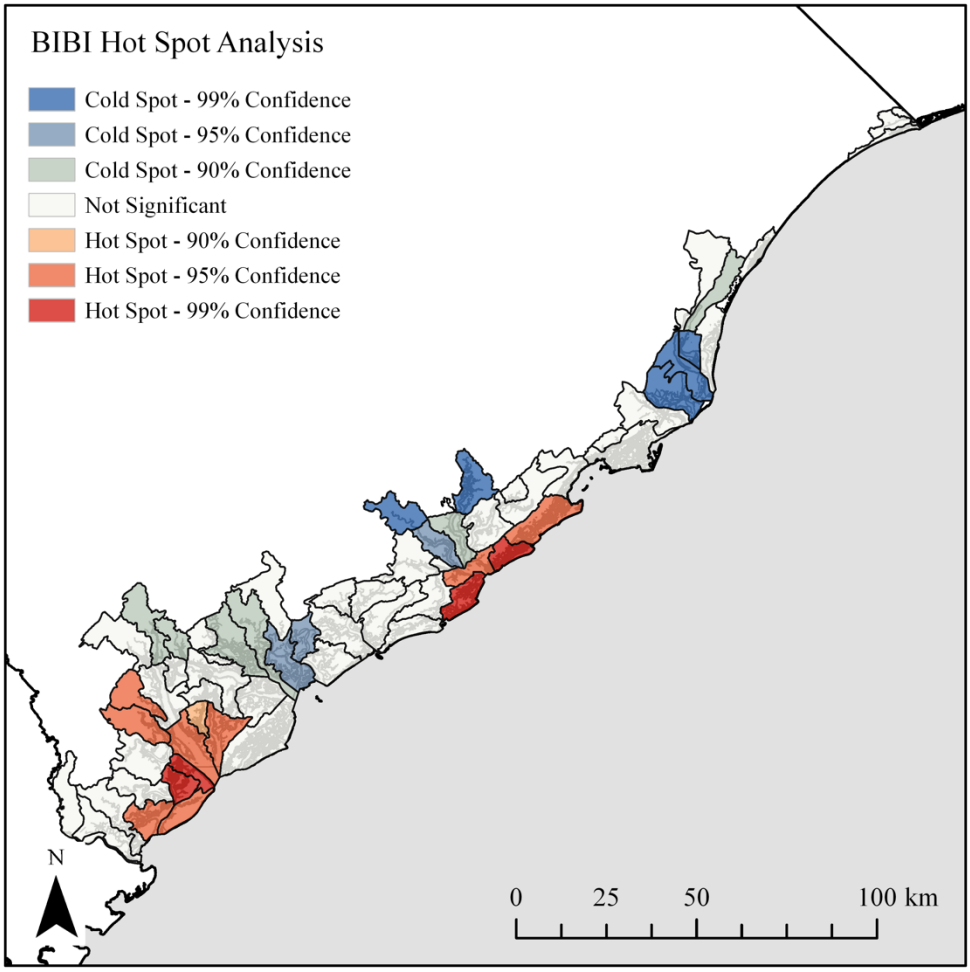

Figure 51. Map of BIBI hot spots in coastal South Carolina by 14-digit HUC watershed

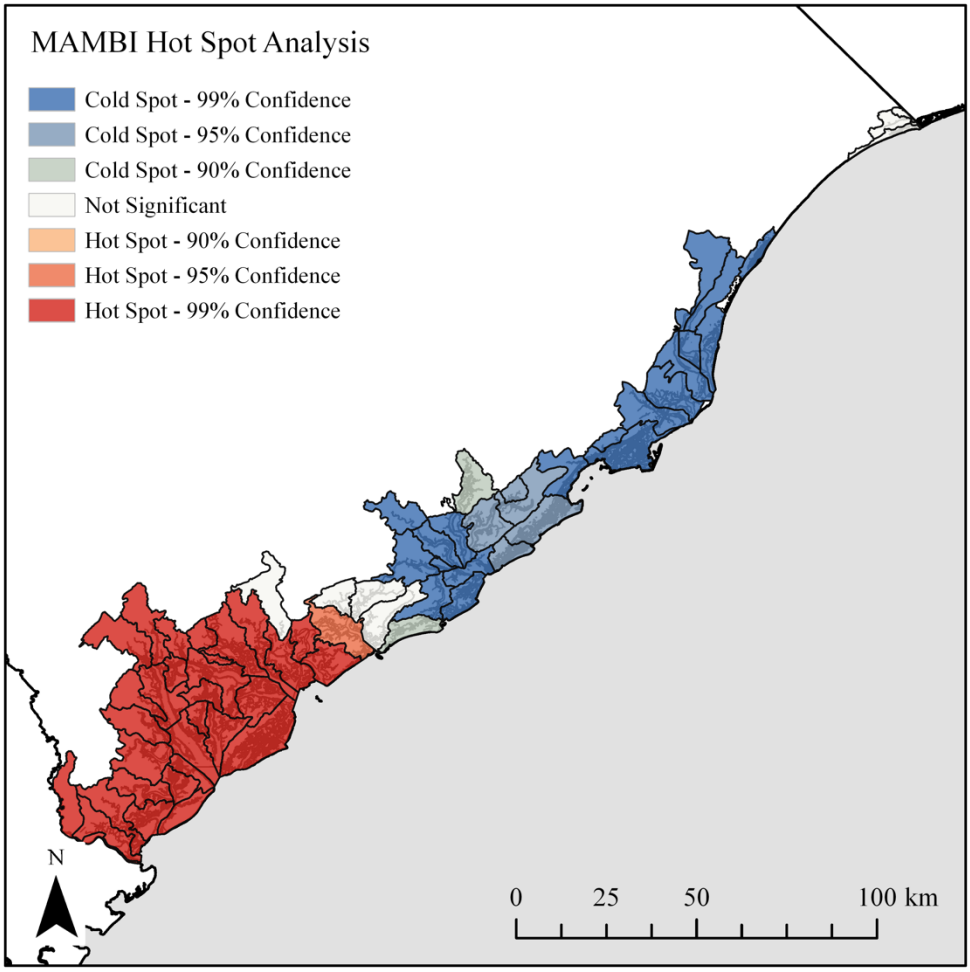

Figure 52. Map of MAMBI hot spots in coastal South Carolina by 14-digit HUC watershed

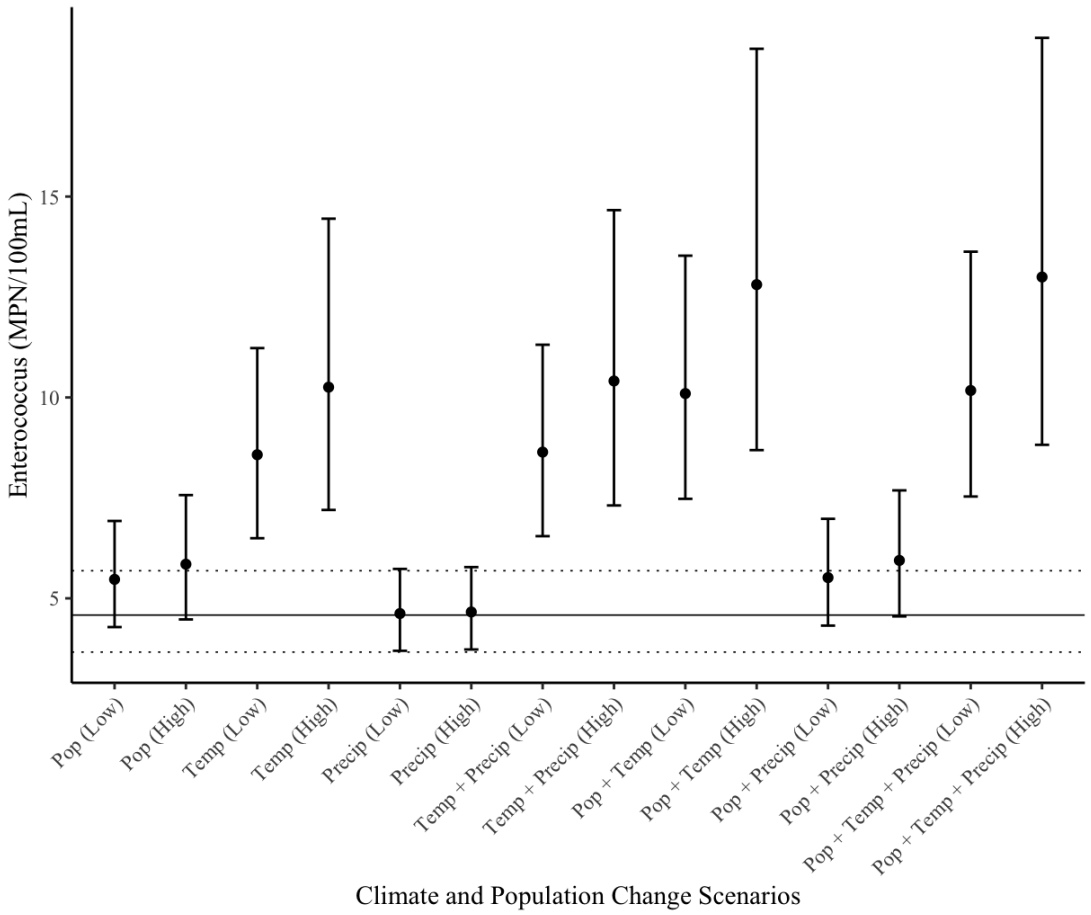

Figure 53. Predicted enterococci levels in South Carolina's estuaries under 14 climate and population change scenarios. Error bars represent 95th percentile upper and lower confidence intervals. Baseline conditions represented by solid horizontal line (dotted horizontal lines indicate baseline upper and lower 95th confidence intervals). These data represent all SCECAP habitats (open water and tidal creek). For supplementary results, see Table 27.

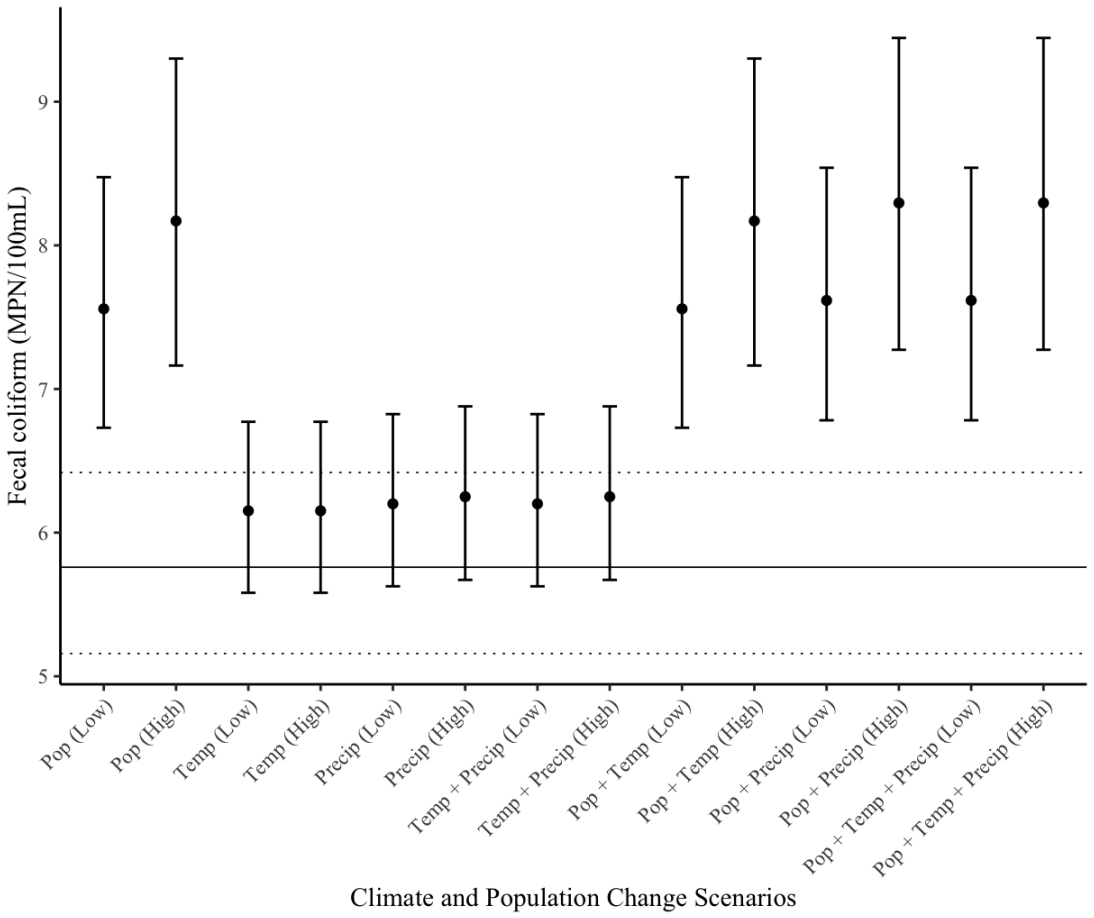

Figure 54. Predicted fecal coliform levels in South Carolina's estuaries under 14 climate and population change scenarios. Error bars represent 95th percentile upper and lower confidence intervals. Baseline conditions represented by solid horizontal line (dotted horizontal lines indicate baseline upper and lower 95th confidence intervals). These data represent all SCECAP habitats (open water and tidal creek). For supplementary results, see Table 28.

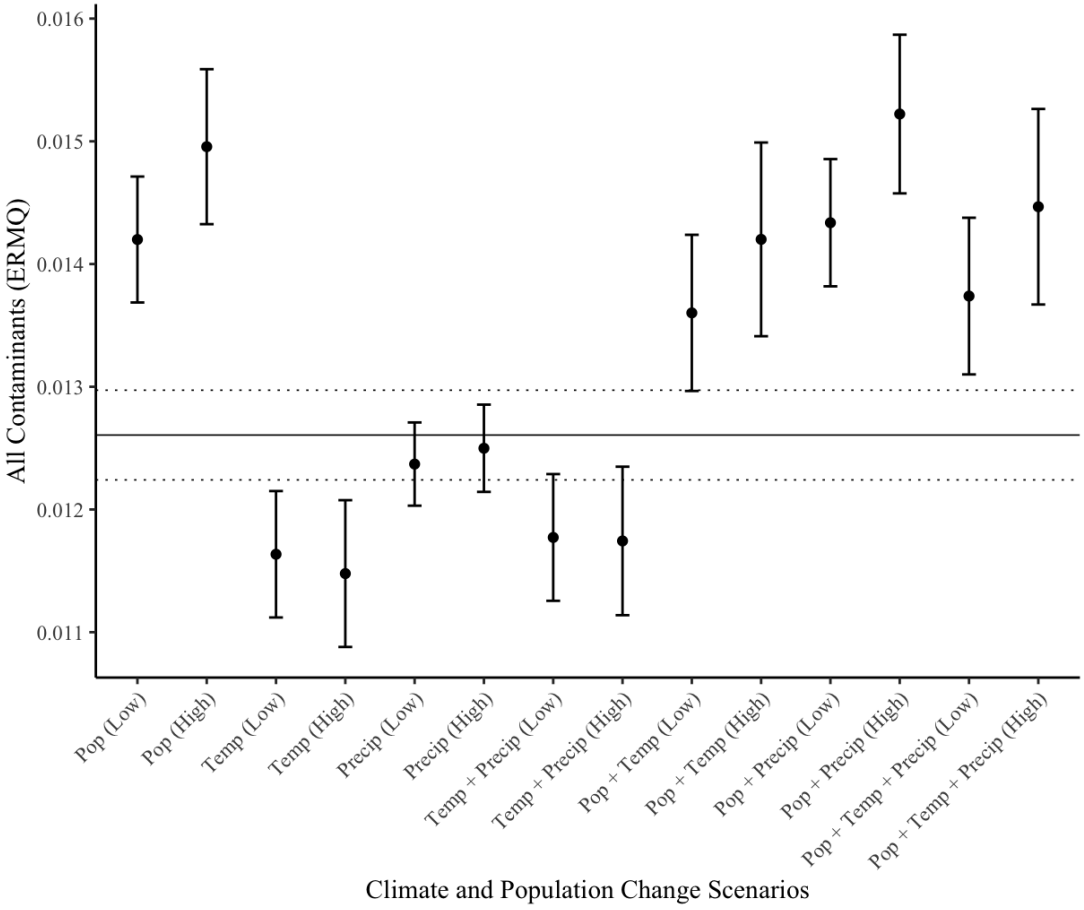

Figure 55. Predicted ERMQs (all contaminants) in South Carolina's estuarine sediments under 14 climate and population change scenarios. Error bars represent 95th percentile upper and lower confidence intervals. Baseline conditions represented by solid horizontal line (dotted horizontal lines indicate baseline upper and lower 95th confidence intervals). These data represent all SCECAP habitats (open water and tidal creek). For supplementary results, see Table 29.

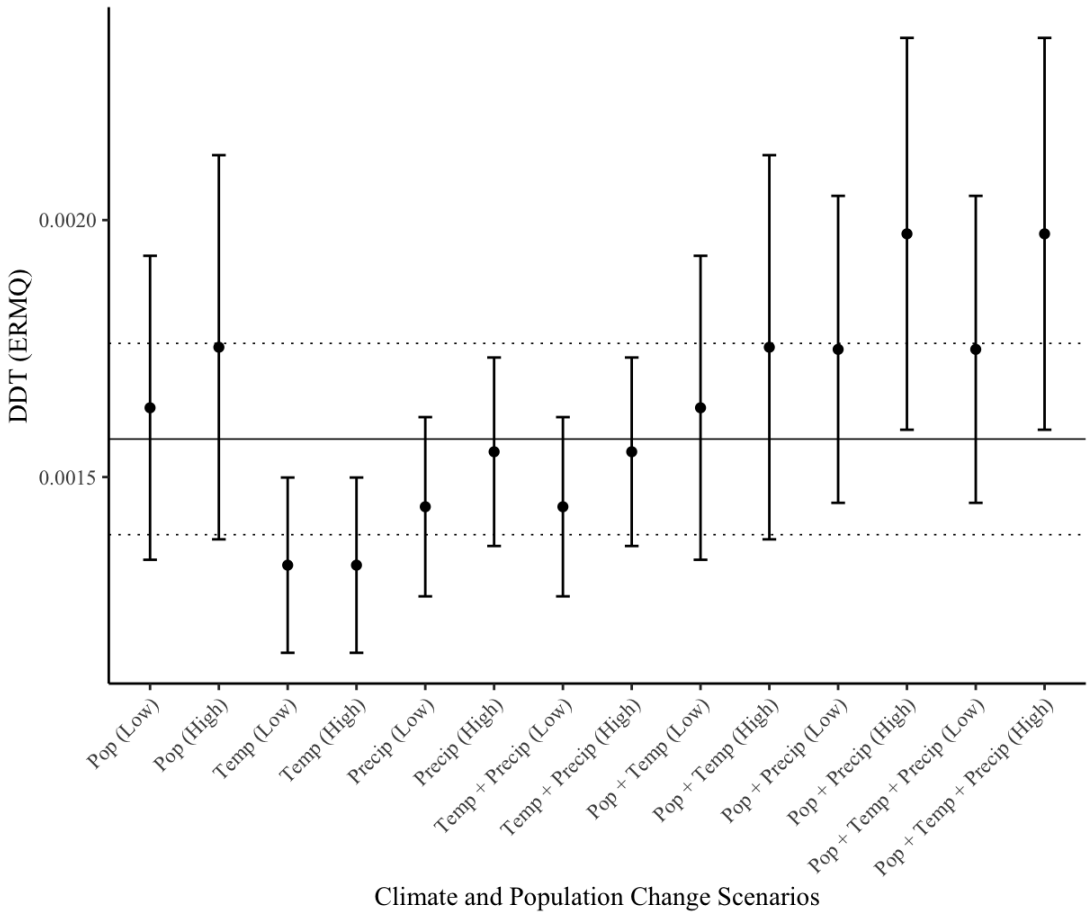

Figure 56. Predicted ERMQs (DDT) in South Carolina's estuarine sediments under 14 climate and population change scenarios. Error bars represent 95th percentile upper and lower confidence intervals. Baseline conditions represented by solid horizontal line (dotted horizontal lines indicate baseline upper and lower 95th confidence intervals). These data represent all SCECAP habitats (open water and tidal creek). For supplementary results, see Table 30.

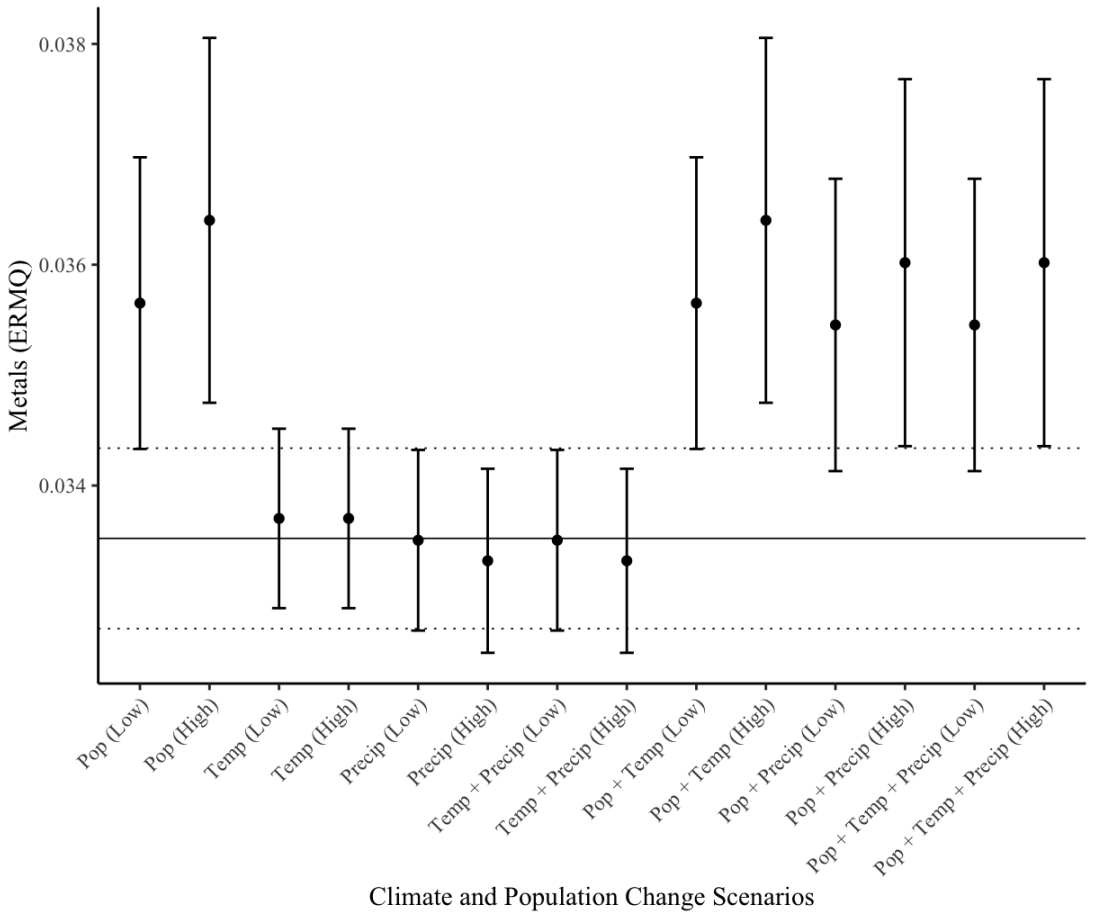

Figure 57. Predicted ERMQs (metals) in South Carolina's estuarine sediments under 14 climate and population change scenarios. Error bars represent 95th percentile upper and lower confidence intervals. Baseline conditions represented by solid horizontal line (dotted horizontal lines indicate baseline upper and lower 95th confidence intervals). These data represent all SCECAP habitats (open water and tidal creek). For supplementary results, see Table 31.

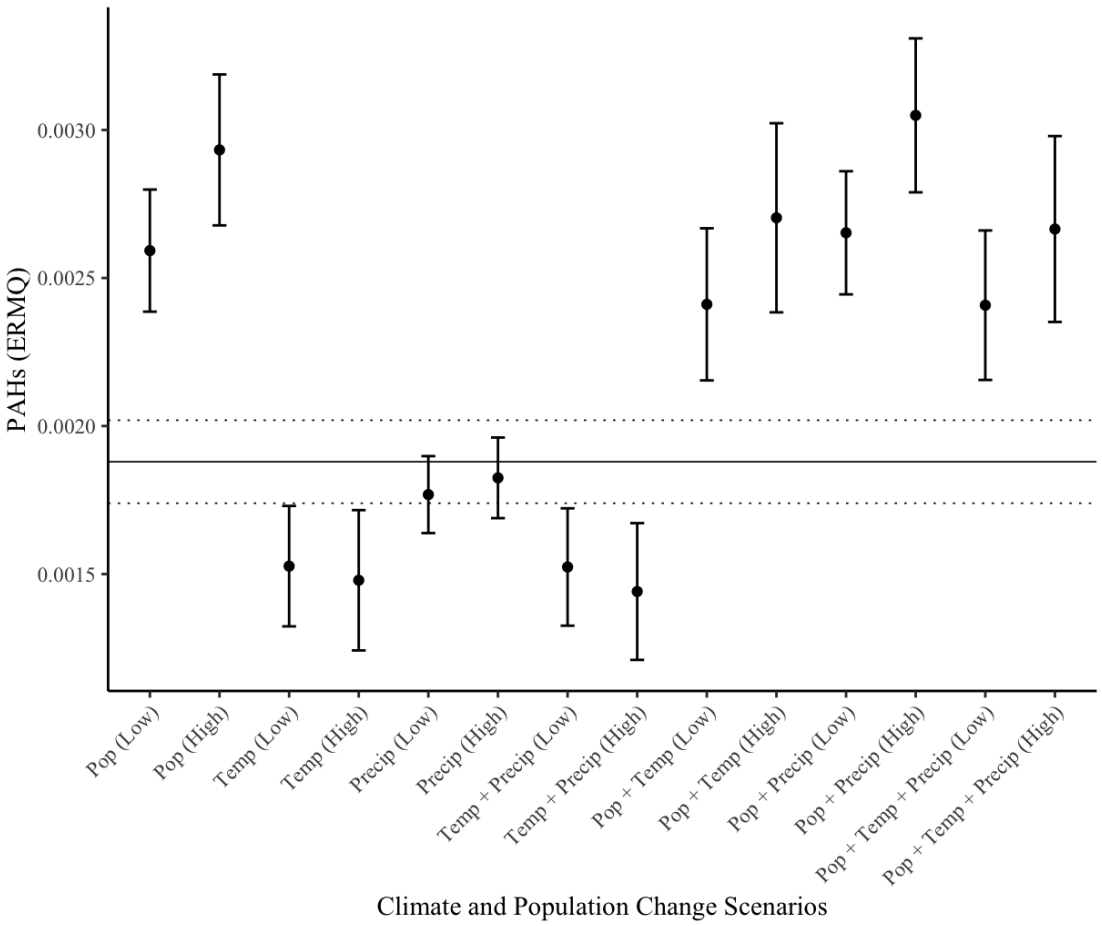

Figure 58. Predicted ERMQs (PAHs) in South Carolina's estuarine sediments under 14 climate and population change scenarios. Error bars represent 95th percentile upper and lower confidence intervals. Baseline conditions represented by solid horizontal line (dotted horizontal lines indicate baseline upper and lower 95th confidence intervals). These data represent all SCECAP habitats (open water and tidal creek). For supplementary results, see Table 32.

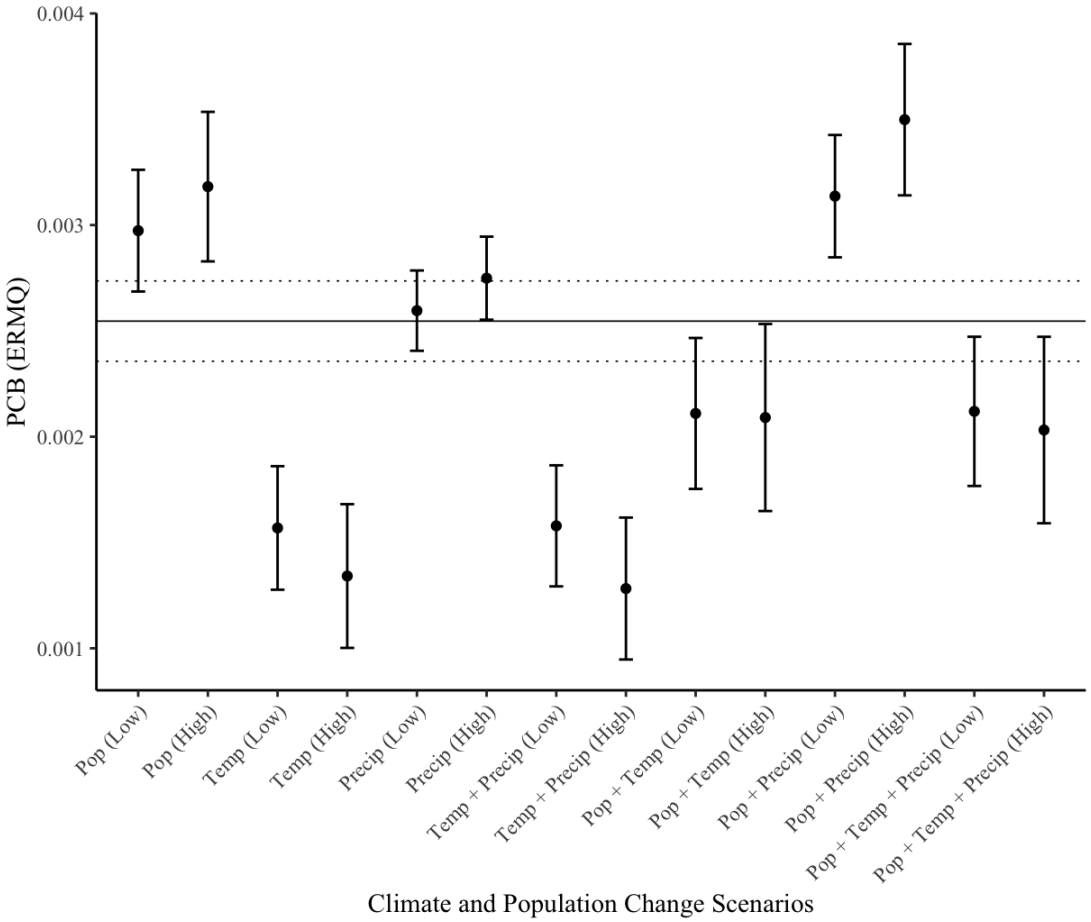

Figure 59. Predicted ERMQs (PCBs) in South Carolina's estuarine sediments under 14 climate and population change scenarios. Error bars represent 95th percentile upper and lower confidence intervals. Baseline conditions represented by solid horizontal line (dotted horizontal lines indicate baseline upper and lower 95th confidence intervals). These data represent all SCECAP habitats (open water and tidal creek). For supplementary results, see Table 33.

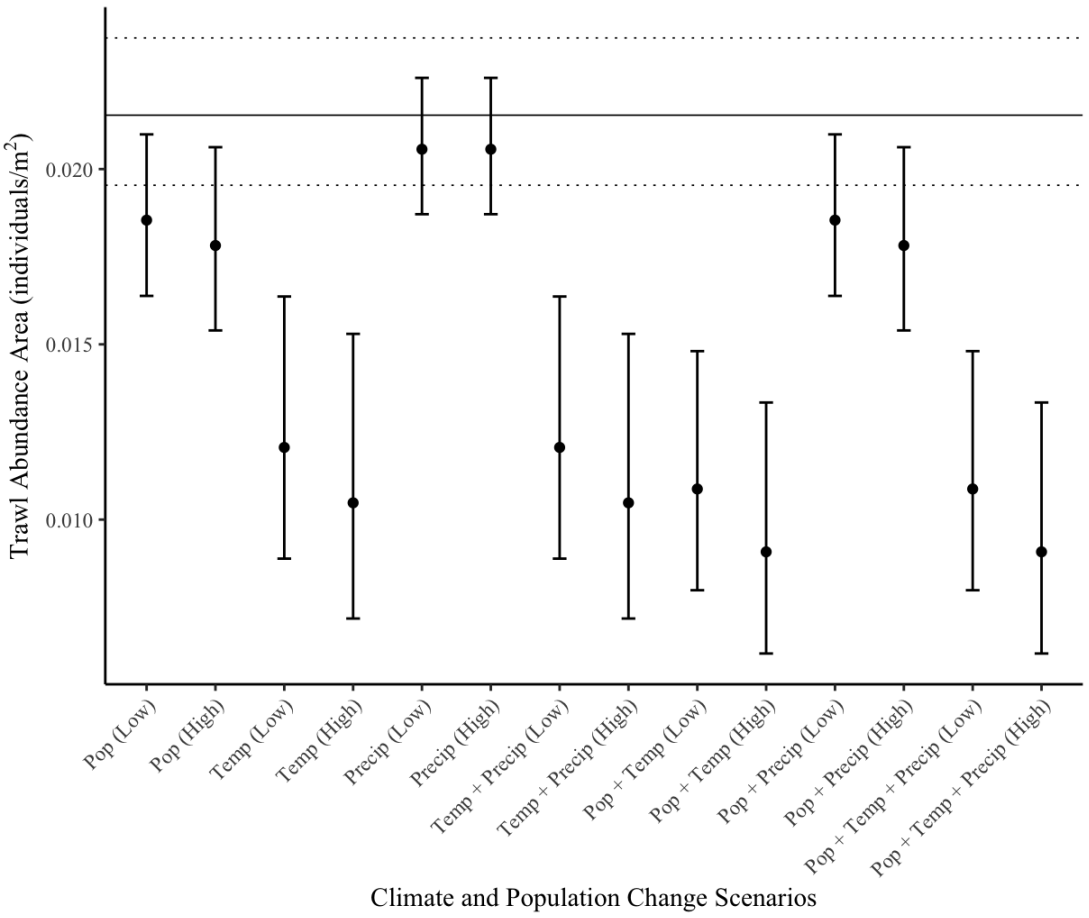

Figure 60. Predicted nekton abundance per area in South Carolina's estuaries under 14 climate and population change scenarios. Error bars represent 95th percentile upper and lower confidence intervals. Baseline conditions represented by solid horizontal line (dotted horizontal lines indicate baseline upper and lower 95th confidence intervals). These data represent all SCECAP habitats (open water and tidal creek). For supplementary results, see Table 34.

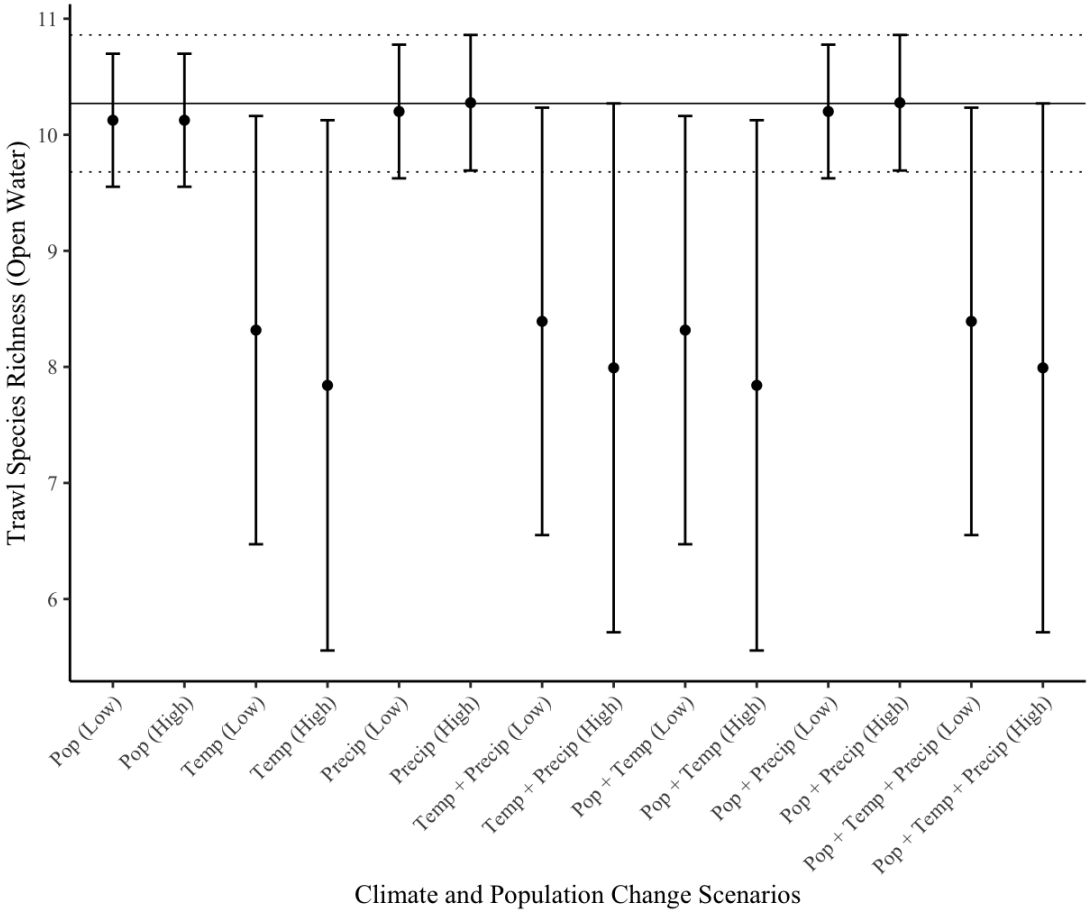

Figure 61. Predicted nekton species richness in South Carolina's open water estuarine habitats under 14 climate and population change scenario. Error bars represent 95th percentile upper and lower confidence intervals. Baseline conditions represented by solid horizontal line (dotted horizontal lines indicate baseline upper and lower confidence intervals). For supplemental results, see Table 35.

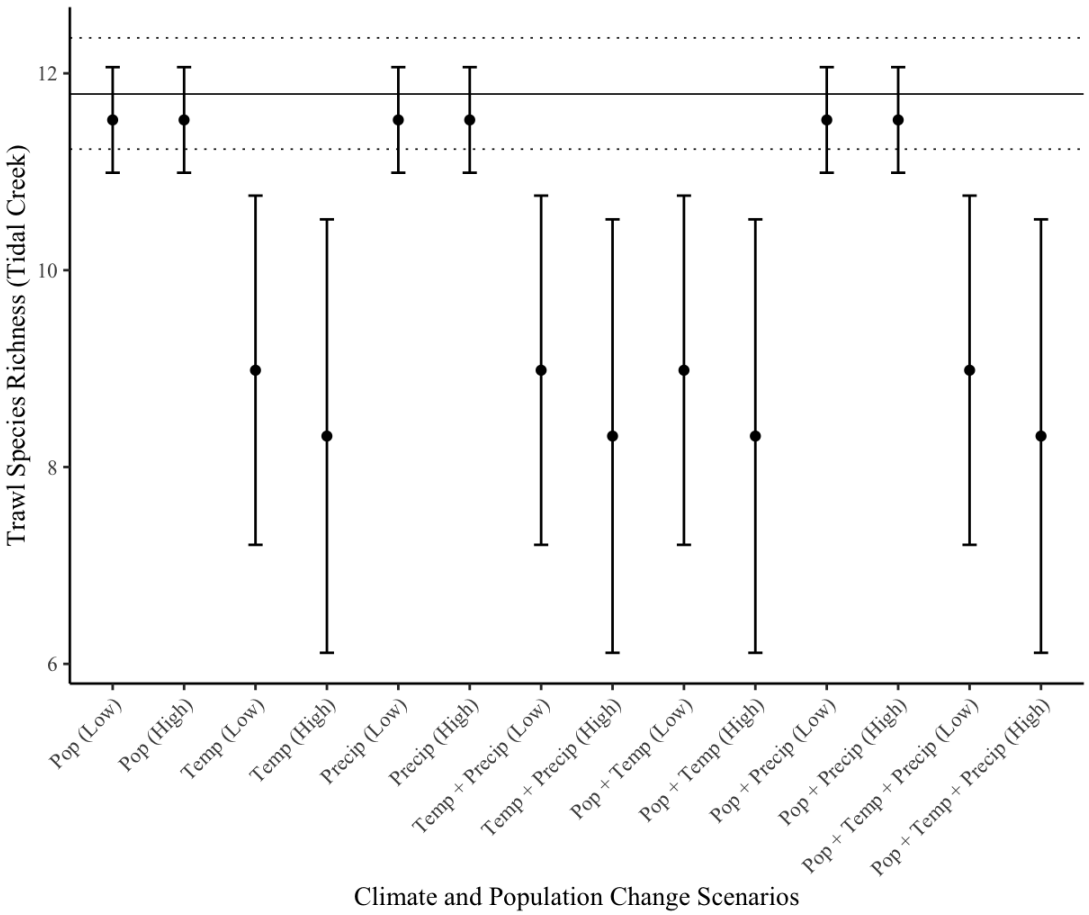

Figure 62. Predicted nekton species richness in South Carolina's tidal creek estuarine habitats under 14 climate and population change scenario. Error bars represent 95th percentile upper and lower confidence intervals. Baseline conditions represented by solid horizontal line (dotted horizontal lines indicate baseline upper and lower confidence intervals). For supplemental results, see Table 35.

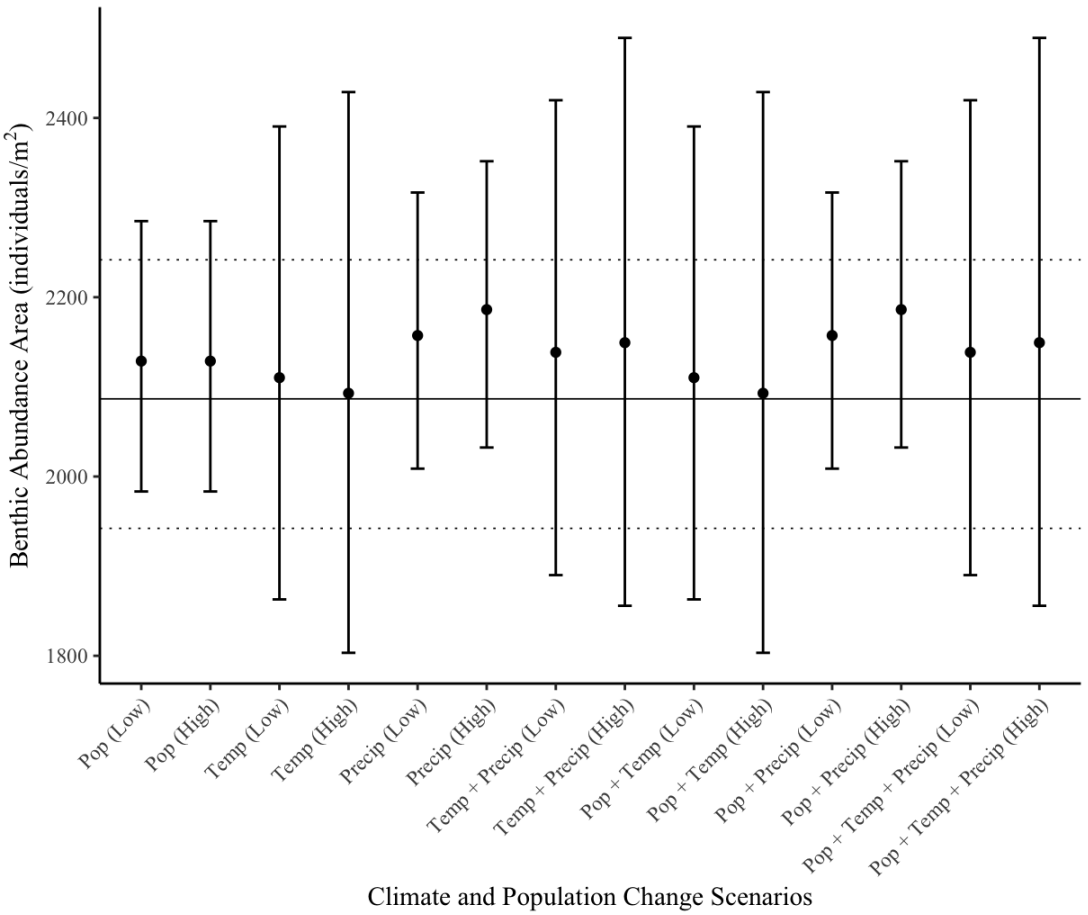

Figure 63. Predicted benthic abundance per area in South Carolina's estuaries under 14 climate and population change scenario. Error bars represent 95th percentile upper and lower confidence intervals. Baseline conditions represented by solid horizontal line (dotted horizontal lines indicate baseline upper and lower 95th confidence intervals). These data represent all SCECAP habitats (open water and tidal creek). For supplementary results, see Table 36.

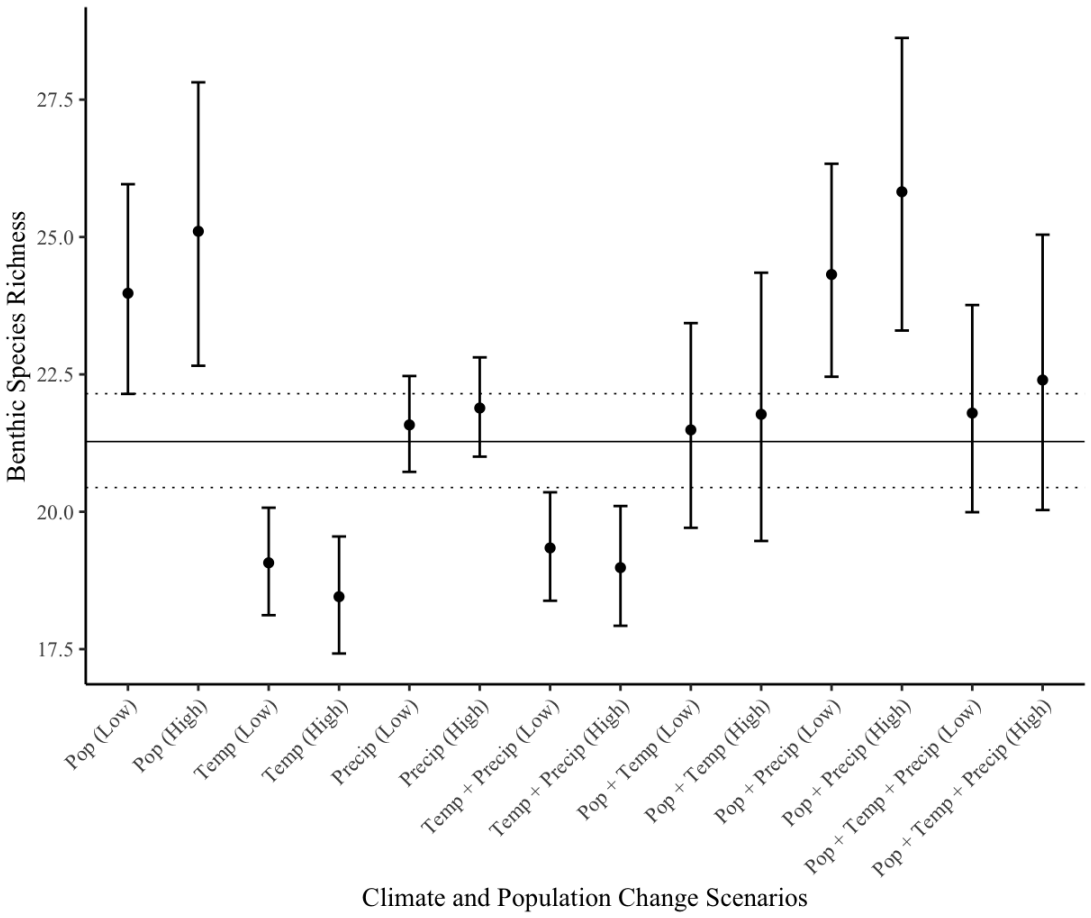

Figure 64. Predicted benthic species richness in South Carolina's estuaries under 14 climate and population change scenario. Error bars represent 95th percentile upper and lower confidence intervals. Baseline conditions represented by solid horizontal line (dotted horizontal lines indicate baseline upper and lower 95th confidence intervals). These data represent all SCECAP habitats (open water and tidal creek). For supplementary results, see Table 37.

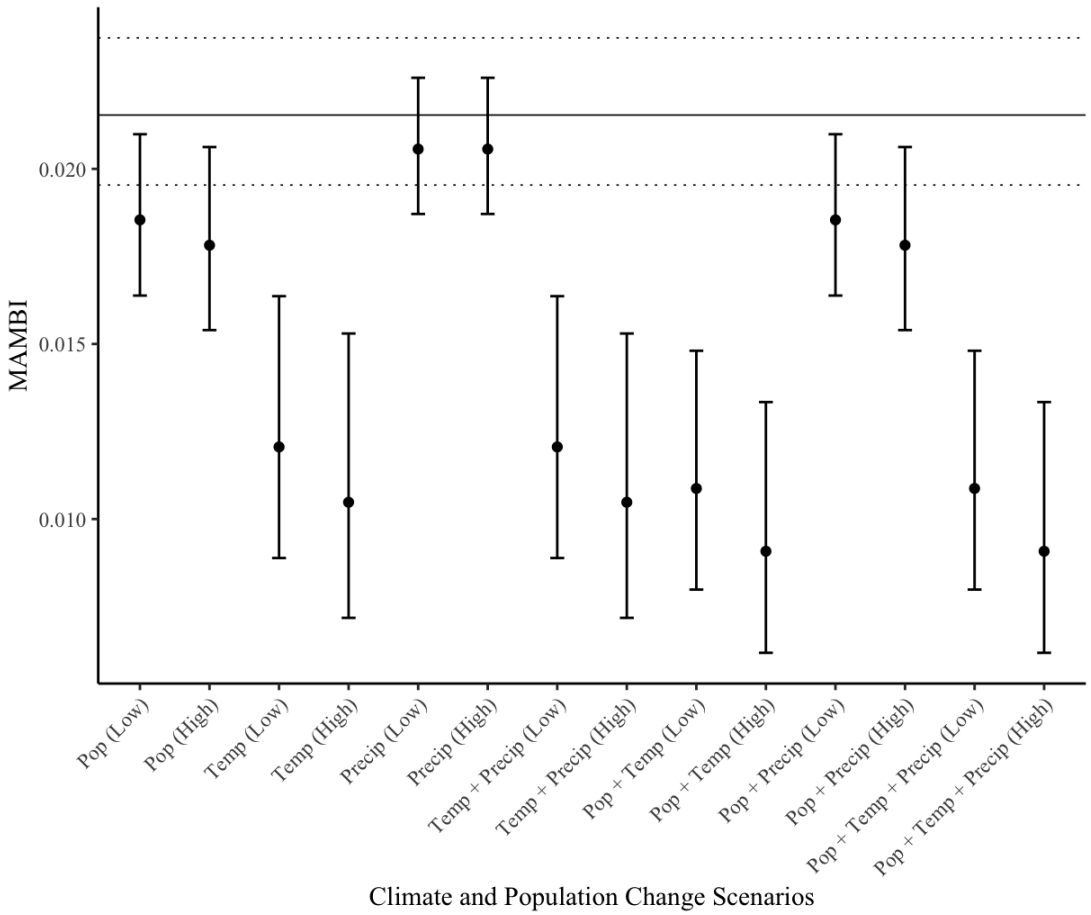

Figure 65. Predicted MAMBI values in South Carolina's estuaries under 14 climate and population change scenario. Error bars represent 95th percentile upper and lower confidence intervals. Baseline conditions represented by solid horizontal line (dotted horizontal lines indicate baseline upper and lower 95th confidence intervals). These data represent all SCECAP habitats (open water and tidal creek). For supplementary results, see Table 38.

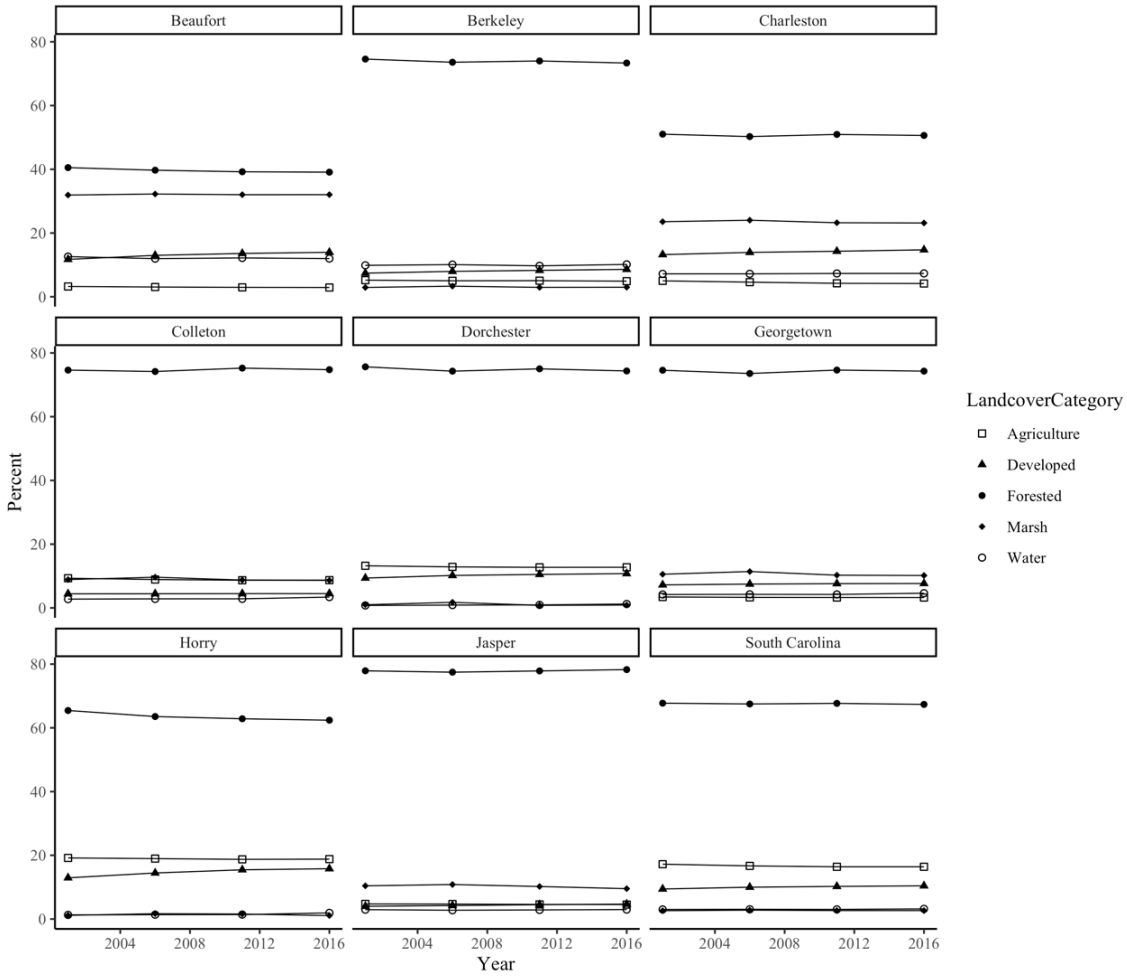

Figure 66. Change in landcover in coastal South Carolina counties from 2001 to 2016

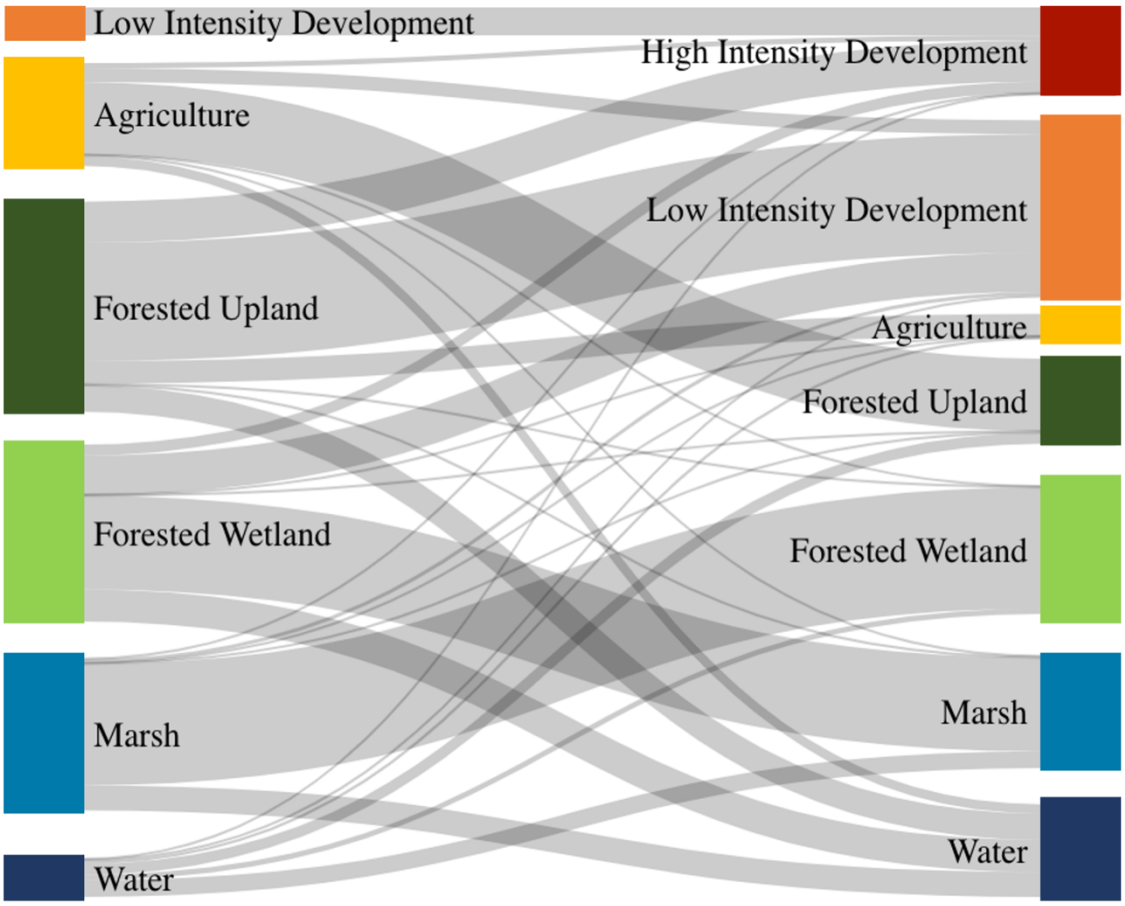

Figure 67. Sankey diagram showing transitions in landcover types by hectare in coastal South Carolina from 2001 (left) to 2016 (right). Total area represented in Sankey diagram equals 72,148 ha – 4% of coastal South Carolina's total area (1,844,407 ha). Figure created using 'networkD3' R package (https://CRAN.R-project.org/package=networkD3).

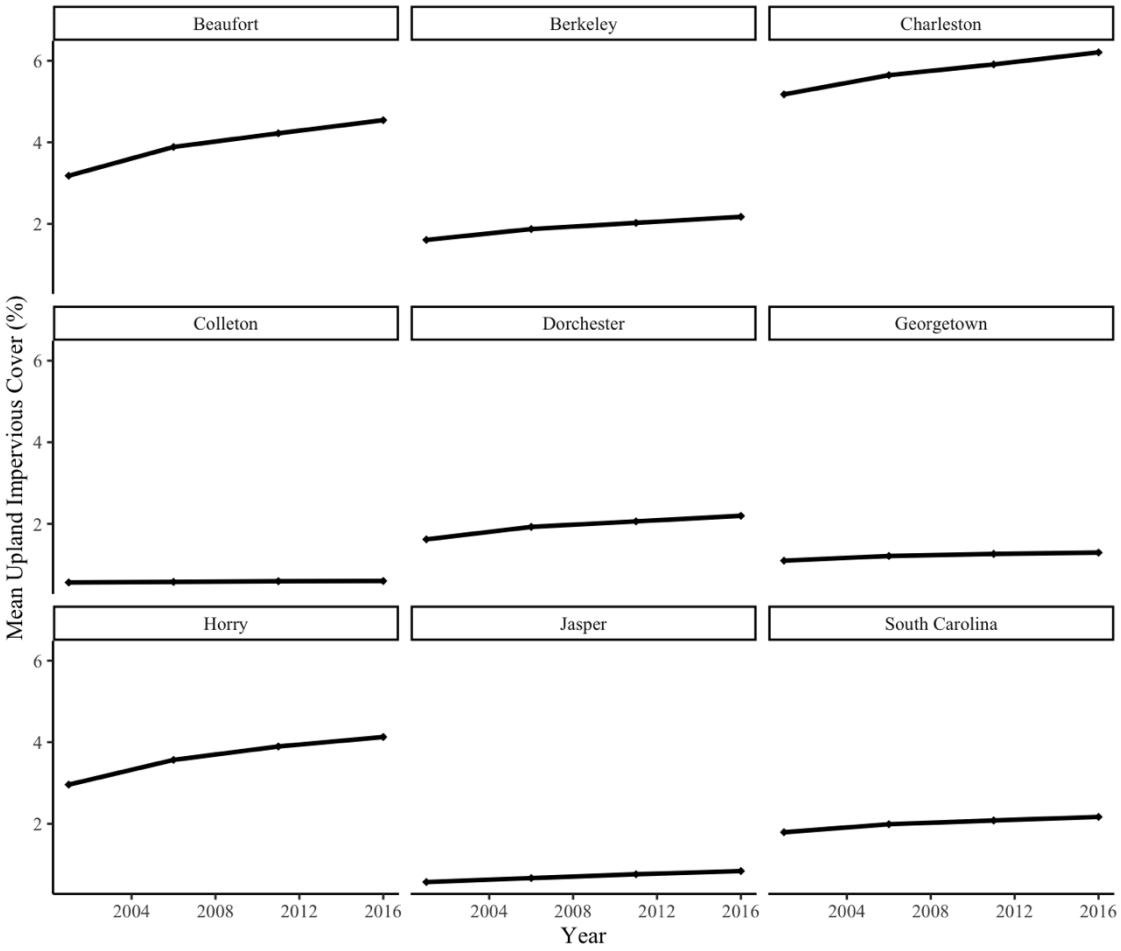

Figure 68. Change in impervious cover in coastal South Carolina counties from 2001 to 2016

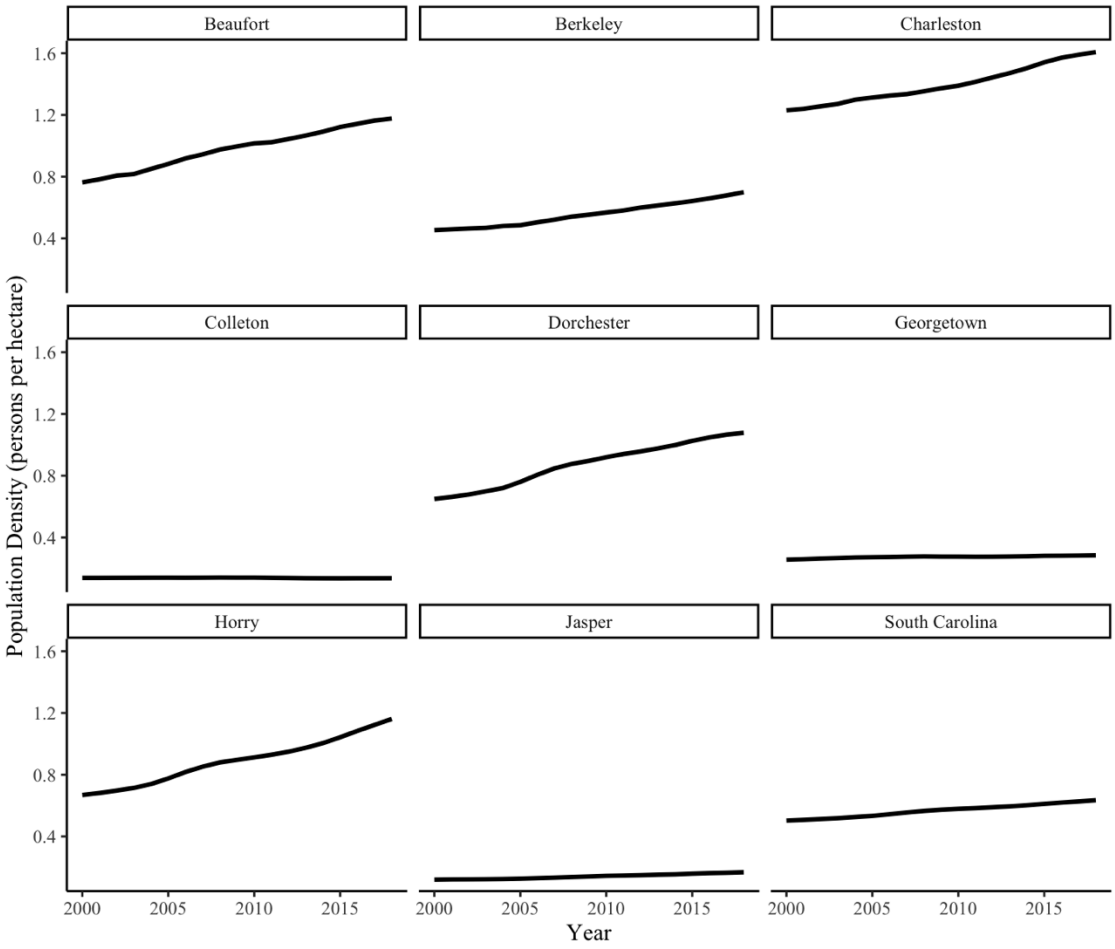

Figure 69. Change in population density in coastal South Carolina counties from 2000 to 2018

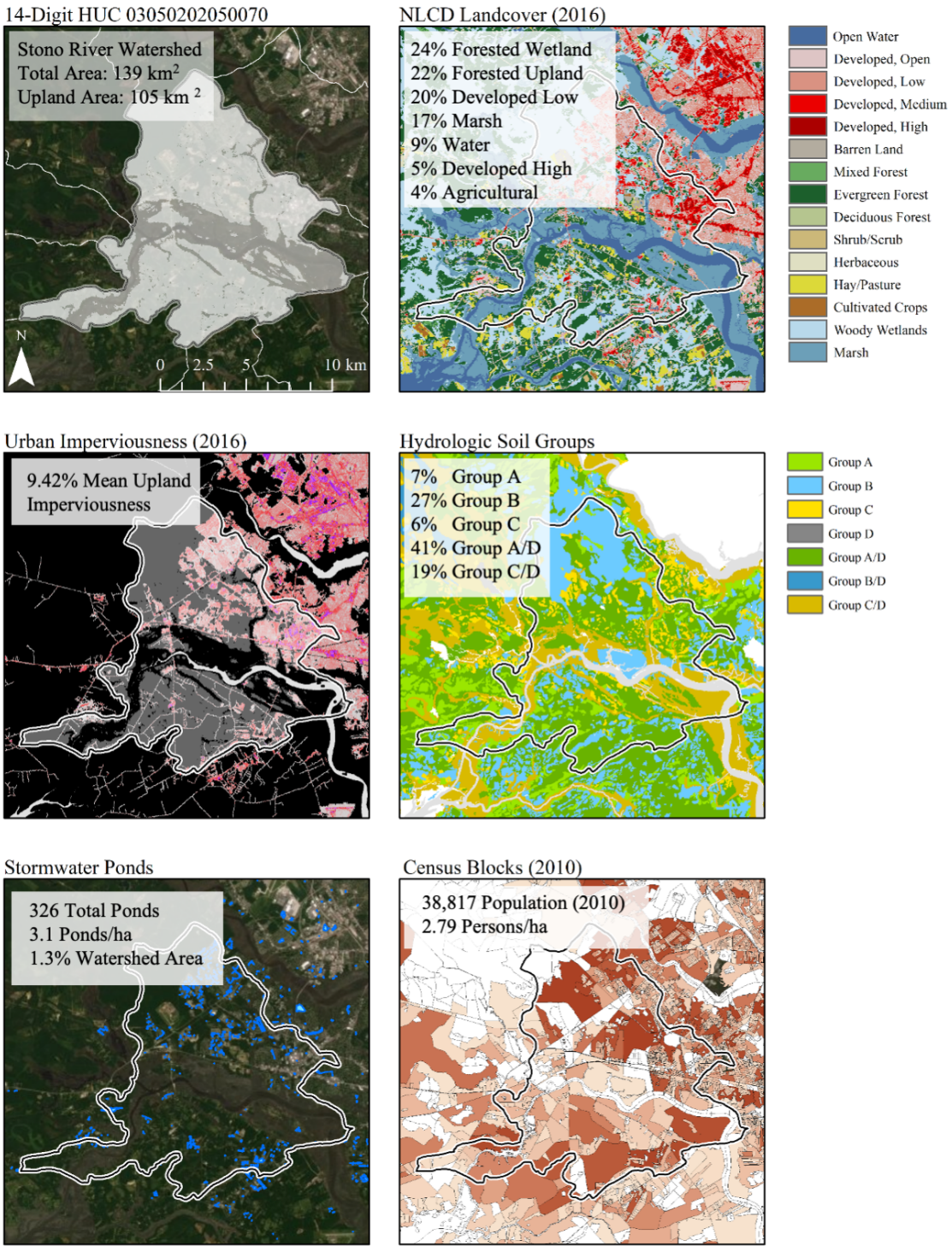

Figure 70. Watershed summary sheet for a 14-digit HUC in Charleston County, SC

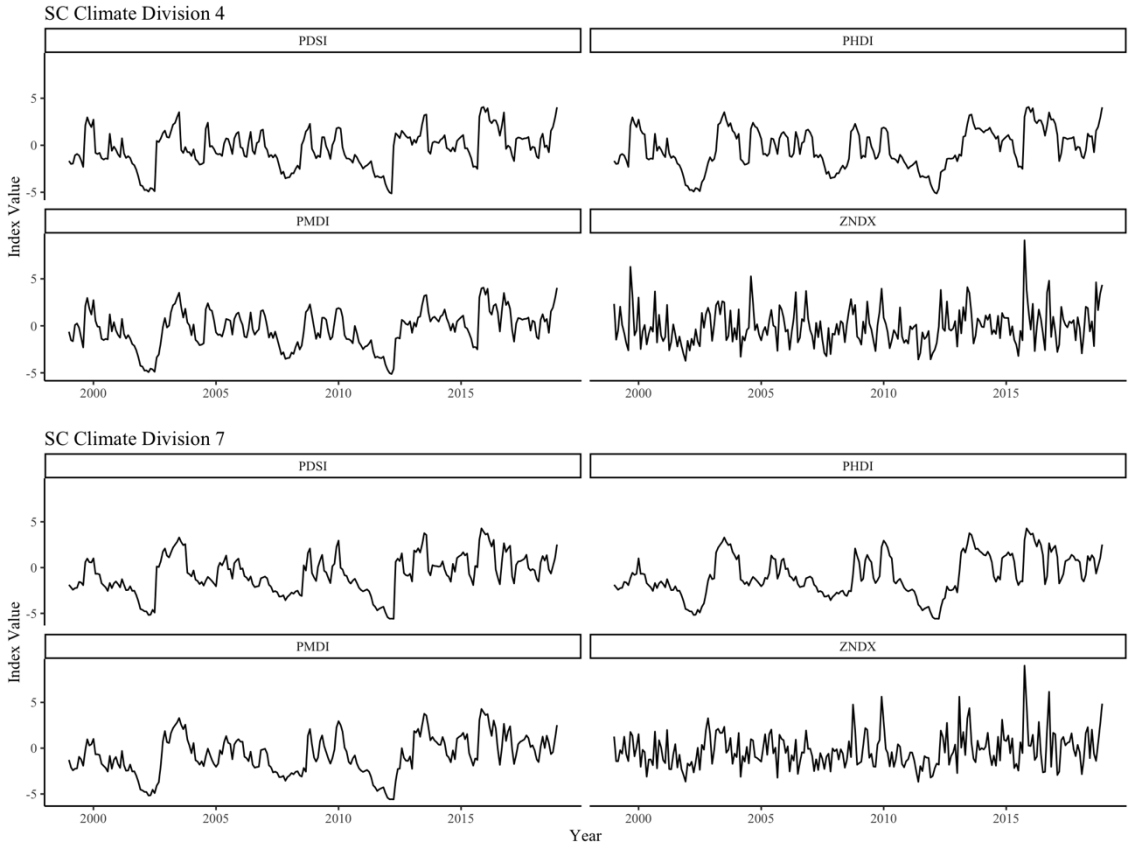

Figure 71. Observed monthly drought index values during 1999-2018 study period by coastal South Carolina climate divisions

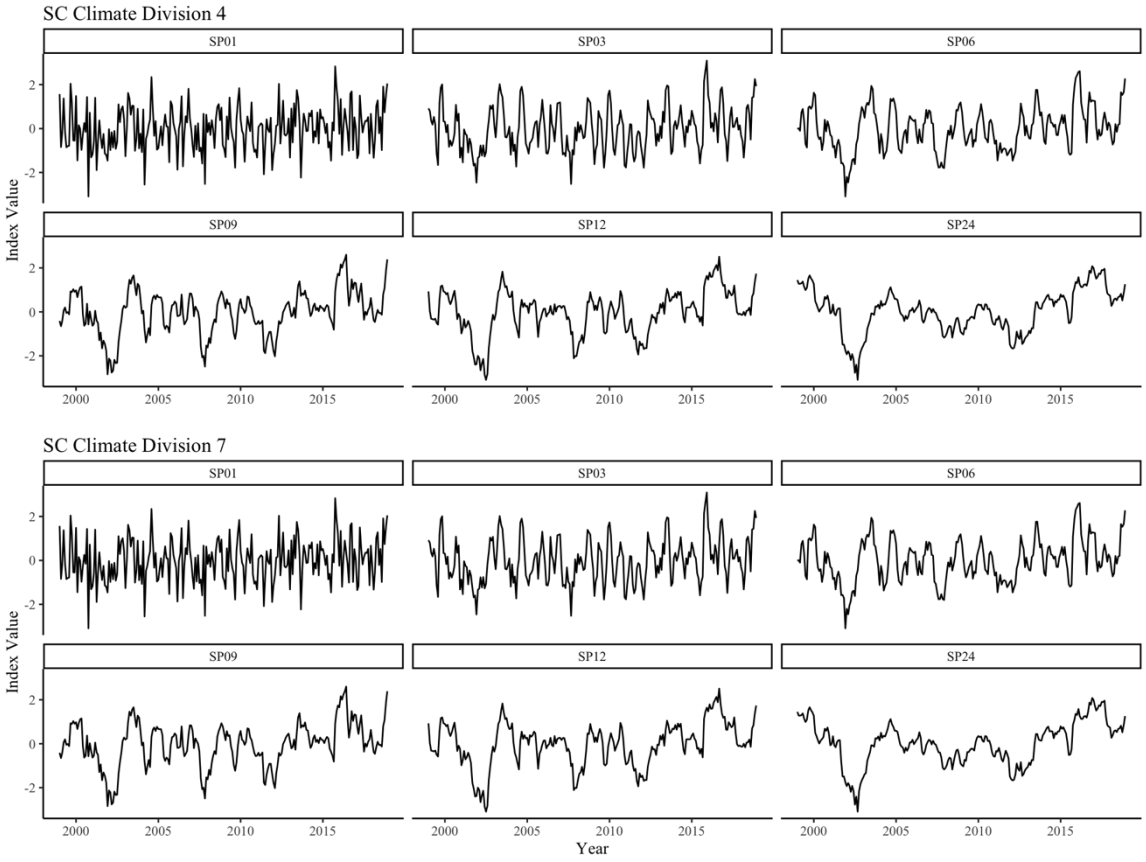

Figure 72. Observed monthly standard precipitation index values during 1999-2018 study period by coastal South Carolina climate divisions

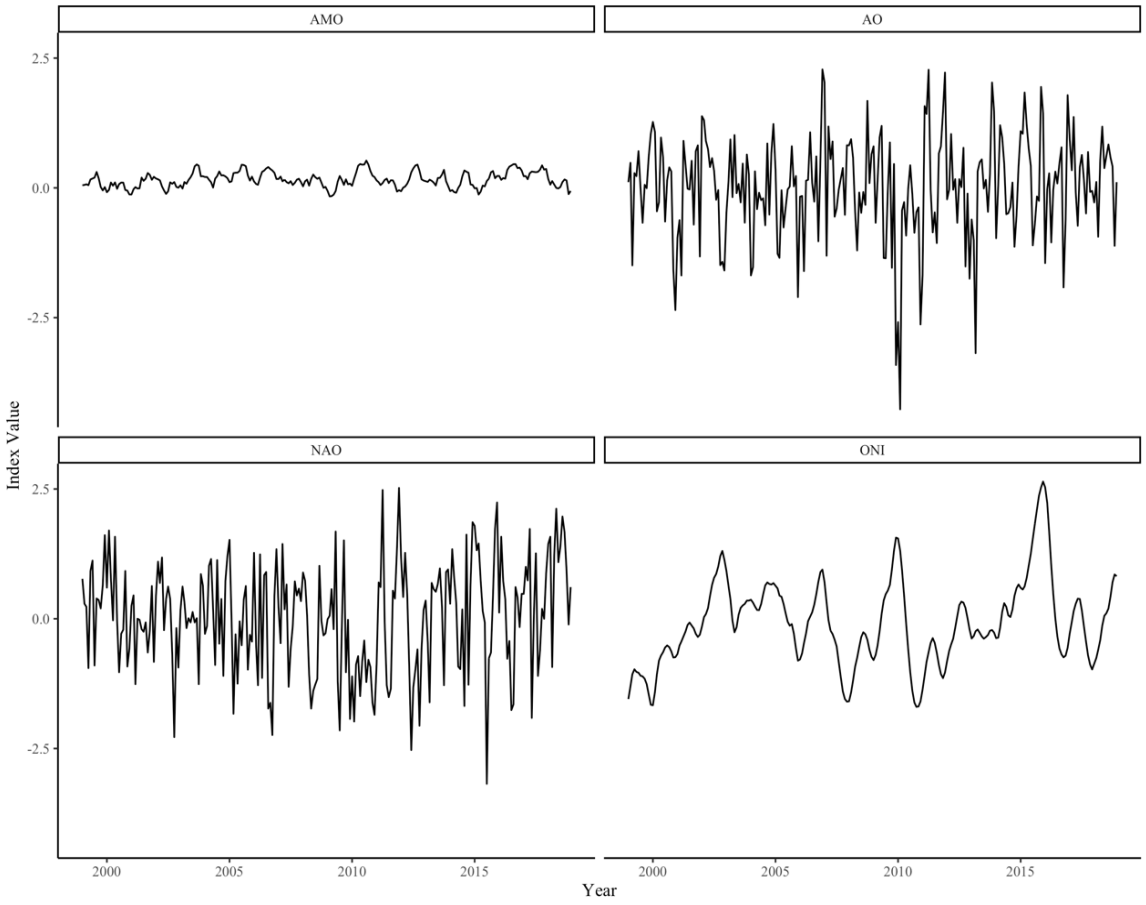

Figure 73. Observed monthly climate teleconnection index values during 1999-2018 study period

TABLES

Table 1. NLCD landcover data summarized for the state of South Carolina and its coastal counties. Percent state area represents the proportion of area each landcover class contributes to the total area of South Carolina. Percent coastal area represents the proportion of area each landcover class contributes to the total area of South Carolina's eight coastal counties (Figure 2).

Original NLCD Landcover Class Percent coastal area (percent state area)	**Condensed Landcover Subcategory** Percent coastal area (percent state area)	**Condensed Landcover Category** Percent coastal area (percent state area)
Open Water 5.54 (3.18)	**Water** 5.54 (3.18)	**Water** 5.54 (3.18)
Emergent Herbaceous Wetlands 10.12 (2.65)	**Marsh** 10.12 (2.65)	**Marsh** 10.12 (2.65)
Deciduous Forest 1.34 (9.15)	**Forested Upland** 32.03 (47.32)	**Forest** 66.36 (67.36)
Evergreen Forest 26.34 (24.67)		
Mixed Forest 0.71 (5.97)		
Shrub and Scrub 1.89 (3.40)		
Herbaceous 1.75 (4.13)		
Woody Wetlands 34.33 (20.04)	**Forested Wetland** 34.33 (20.04)	
Barren Land 0.32 (0.23)	**Agriculture** 7.84 (16.40)	**Agriculture** 7.84 (16.40)
Hay and Pasture 1.64 (6.81)		
Cultivated Crops 5.88 (9.36)		
Developed, Open 5.54 (3.18)	**Low Intensity Development** 8.33 (5.97)	**Development** 10.14 (10.42)
Developed, Low Intensity 2.79 (2.79)		
Developed, Medium Intensity 1.08 (0.95)	**High Intensity Development** 1.41 (1.30)	
Developed, High Intensity 0.33 (0.35)		

Notes: Data from 2016 NLCD (Yang et al., 2018).

Table 2. Climate normals and extreme weather summary data for three weather stations representing coastal South Carolina

Variable	Season	Brookgreen Gardens	Charleston Int'l Airport	Savannah Int'l Airport	Average of All 3
Temperature (°C)					
	Annual	18.85	18.85	19.30	19.00
	Winter	10.00	10.15	10.75	10.30
	Spring	18.40	18.50	19.00	18.63
	Summer	27.30	27.10	27.50	27.30
	Fall	19.80	19.55	20.00	19.78
Precipitation (cm)					
	Annual	137.62	129.62	121.82	129.69
	Winter	29.29	24.84	23.95	24.49
	Spring	27.38	24.49	24.84	25.57
	Summer	43.54	49.10	46.00	46.21
	Fall	37.41	31.19	27.03	31.88
Extreme Temperature (°C)					
		33.3	34.3	35.0	34.4
Extreme Precipitation (cm)					
		2.34	2.26	2.11	2.24

Notes: Temperature and precipitation from 30-year (1980-2010) climate normals (NOAA NCEI). Seasons broken down as follows: Winter (Dec., Jan., Feb.), Spring (Mar., Apr., May), Summer (Jun., Jul., Aug.), and Fall (Sep., Oct., Nov.). Extreme weather data represent the 95th percentiles of daily temperature maximums and 24-hour precipitation totals from project's 1999-2018 weather dataset.

Table 3. *t*-test results comparing SCECAP environmental data by habitat type. Values indicate averages.

Parameter	Open Water (*n*=408)	Tidal Creek (*n*=403)	*p*-value
Water Quality			
Water Temperature (°C)	**29.49**	**29.83**	**<0.001**
Dissolved Oxygen (mg/L)	**5.14**	**4.41**	**<0.001**
Salinity (ppt)	27.51	28.45	0.112
pH	**7.60**	**7.42**	**<0.001**
Fecal Coliform (log MPN 100/mL)	**0.64**	**0.98**	**<0.001**
***Enterococcus* spp. (log MPN/100mL)**	**0.66**	**0.94**	**<0.001**
Sediment Quality			
Metals (ug/g)	**63.44**	**78.32**	**0.001**
Metals (ERMQ)	**0.0348**	**0.0428**	**<0.001**
PAHs (ng/g)	84.94	56.52	0.218
PAHs (ERMQ)	0.0037	0.0028	0.308
PCBs (ng/g)	0.61	0.64	0.719
PCBs (ERMQ)	0.0034	0.0036	0.719
DDT (ng/g)	**0.08**	**0.19**	**0.001**
DDT (ERMQ)	**0.0018**	**0.0041**	**0.001**
PBDEs (ng/g)	0.05	0.04	0.399
All Contaminants (ERMQ)	**0.0141**	**0.0162**	**0.044**
Biological Quality			
Nekton Species Richness	**10.17**	**11.52**	**0.002**
Nekton Abundance (abundance/m^2)	**0.03**	**0.08**	**<0.001**
Benthic Species Richness	**29.17**	**24.88**	**0.001**
Benthic Abundance (abundance/m^2)	**4500.76**	**3429.29**	**0.001**
BIBI	**3.63**	**3.33**	**<0.001**
MAMBI	**0.47**	**0.42**	**<0.001**

Notes: Rows in **bold** represent *t*-test results with *p*-values≤0.05.

Table 4. *t*-test results comparing SCECAP environmental data by time period (all sites). Values indicate averages.

Parameter	1999 to 2008 (*n*=511)	2009 to 2018 (*n*=300)	*p*-value
Water Quality			
Water Temperature (°C)	**29.54**	**29.86**	**0.001**
Dissolved Oxygen (mg/L)	4.78	4.76	0.789
Salinity (ppt)	28.14	27.71	0.474
pH	**7.53**	**7.49**	**0.036**
Fecal Coliform (log MPN 100/mL)	0.83	0.78	0.388
***Enterococcus* spp. (log MPN/100mL)**	**0.52**	**0.84**	**0.013**
Sediment Quality			
Metals (ug/g)	73.48	66.33	0.081
Metals (ERMQ)	0.0401	0.0366	0.096
PAHs (ng/g)	68.49	74.74	0.802
PAHs (ERMQ)	0.0030	0.0036	0.526
PCBs (ng/g)	0.61	0.65	0.637
PCBs (ERMQ)	0.0034	0.0036	0.638
DDT (ng/g)	**0.10**	**0.20**	**0.005**
DDT (ERMQ)	**0.0021**	**0.0044**	**0.005**
PBDEs (ng/g)	**0.01**	**0.07**	**<0.001**
All Contaminants (ERMQ)	0.0153	0.0149	0.764
Biological Quality			
Nekton Species Richness	**11.78**	**9.23**	**<0.001**
Nekton Abundance (abundance/m^2)	**0.06**	**0.03**	**<0.001**
Benthic Species Richness	**29.00**	**23.68**	**<0.001**
Benthic Abundance (abundance/m^2)	**4266.19**	**3459.71**	**0.024**
BIBI	**3.53**	**3.40**	**0.044**
MAMBI	**0.45**	**0.42**	**0.034**

Notes: Rows in **bold** represent *t*-test results with *p*-values≤0.05.

Table 5. *t*-test results comparing SCECAP environmental data by time period (open water sites). Values indicate averages.

Parameter	1999 to 2008 (*n*=259)	2009 to 2018 (*n*=149)	*p*-value
Water Quality			
Water Temperature (°C)	29.41	29.63	0.136
Dissolved Oxygen (mg/L)	5.13	5.17	0.649
Salinity (ppt)	27.74	27.11	0.449
pH	7.62	7.57	0.072
Fecal Coliform (log MPN 100/mL)	0.67	0.60	0.374
Enterococcus spp. (log MPN/100mL)	0.59	0.67	0.625
Sediment Quality			
Metals (ug/g)	65.32	60.15	0.395
Metals (ERMQ)	0.0359	0.0329	0.305
PAHs (ng/g)	93.88	69.29	0.520
PAHs (ERMQ)	0.0039	0.0033	0.693
PCBs (ng/g)	0.58	0.66	0.489
PCBs (ERMQ)	0.0032	0.0037	0.489
DDT (ng/g)	**0.05**	**0.14**	**0.006**
DDT (ERMQ)	**0.0012**	**0.0030**	**0.006**
PBDEs (ng/g)	**0.02**	**0.08**	**0.003**
All Contaminants (ERMQ)	0.0143	0.0136	0.678
Biological Quality			
Nekton Species Richness	**11.16**	**8.47**	**<0.001**
Nekton Abundance (abundance/m^2)	**0.037**	**0.021**	**0.001**
Benthic Species Richness	**31.55**	**25.01**	**0.001**
Benthic Abundance (abundance/m^2)	**4971.81**	**3679.60**	**0.024**
BIBI	3.69	3.52	0.065
MAMBI	**0.43**	**0.39**	**0.010**

Notes: Rows in **bold** represent *t*-test results with *p*-values≤0.05.

Table 6. *t*-test results comparing SCECAP environmental data by time period (tidal creek sites). Values indicate averages.

Parameter	1999 to 2008 (*n*=252)	2009 to 2018 (*n*=151)	*p*-value
Water Quality			
Water Temperature (°C)	**29.68**	**30.08**	**0.001**
Dissolved Oxygen (mg/L)	4.43	4.38	0.642
Salinity (ppt)	28.55	28.29	0.771
pH	7.44	7.40	0.256
Fecal Coliform (log MPN 100/mL)	0.99	0.96	0.644
***Enterococcus* spp. (log MPN/100mL)**	**0.44**	**1.01**	**0.006**
Sediment Quality			
Metals (ug/g)	81.89	72.38	0.079
Metals (ERMQ)	0.0444	0.0403	0.156
PAHs (ng/g)	42.40	80.08	0.231
PAHs (ERMQ)	0.0022	0.0039	0.157
PCBs (ng/g)	0.64	0.64	0.983
PCBs (ERMQ)	0.0036	0.0035	0.982
DDT (ng/g)	0.14	0.27	0.071
DDT (ERMQ)	0.0031	0.0058	0.071
PBDEs (ng/g)	**0.01**	**0.06**	**0.016**
All Contaminants (ERMQ)	0.0162	0.0162	0.997
Biological Quality			
Nekton Species Richness	**12.42**	**9.99**	**<0.001**
Nekton Abundance (abundance/m^2)	**0.09**	**0.05**	**0.001**
Benthic Species Richness	**26.39**	**22.35**	**0.009**
Benthic Abundance (abundance/m^2)	3540.88	3241.31	0.404
BIBI	3.37	3.27	0.330
MAMBI	**0.43**	**0.39**	**0.010**

Notes: Rows in **bold** represent *t*-test results with *p*-values≤0.05.

Table 7. *t*-test results comparing SCECAP environmental data by level of watershed development (all sites). Values indicate averages.

Parameter	Developed (*n*=49)	Undeveloped (*n*=752)	*p*-value
Water Quality			
Water Temperature (°C)	**29.25**	**29.68**	**0.013**
Dissolved Oxygen (mg/L)	**5.14**	**4.75**	**0.004**
Salinity (ppt)	27.37	28.02	0.503
pH	**7.70**	**7.50**	**<0.001**
Fecal Coliform (log MPN 100/mL)	**1.19**	**0.79**	**<0.001**
Enterococcus spp. (log MPN/100mL)	0.99	0.79	0.271
Sediment Quality			
Metals (ug/g)	**101.73**	**68.89**	**0.023**
Metals (ERMQ)	**0.0531**	**0.0379**	**0.041**
PAHs (ng/g)	**499.87**	**43.77**	**0.003**
PAHs (ERMQ)	**0.0178**	**0.0023**	**0.003**
PCBs (ng/g)	**1.60**	**0.56**	**0.008**
PCBs (ERMQ)	**0.0089**	**0.0031**	**0.008**
DDT (ng/g)	**0.35**	**0.12**	**0.044**
DDT (ERMQ)	**0.0076**	**0.0027**	**0.045**
PBDEs (ng/g)	**0.01**	**0.04**	**<0.001**
All Contaminants (ERMQ)	**0.0318**	**0.0141**	**<0.001**
Biological Quality			
Nekton Species Richness	10.82	10.84	0.983
Nekton Abundance (abundance/m^2)	**0.02**	**0.06**	**<0.001**
Benthic Species Richness	31.29	26.77	0.163
Benthic Abundance (abundance/m^2)	4145.41	3957.60	0.780
BIBI	3.55	3.48	0.618
MAMBI	0.44	0.44	0.941

Notes: Rows in **bold** represent *t*-test results with *p*-values≤0.05. Developed sites defined as 14-digit HUC watersheds with >18.9% upland impervious cover.

Table 8. *t*-test results comparing SCECAP environmental data by level of watershed development (open water sites). Values indicate averages.

Parameter	Developed (*n*=30)	Undeveloped (*n*=378)	*p*-value
Water Quality			
Water Temperature (°C)	**29.02**	**29.53**	**0.029**
Dissolved Oxygen (mg/L)	5.33	5.13	0.217
Salinity (ppt)	26.83	27.57	0.471
pH	**7.75**	**7.59**	**<0.001**
Fecal Coliform (log MPN 100/mL)	**1.26**	**0.59**	**<0.001**
Enterococcus spp. (log MPN/100mL)	0.97	0.63	0.184
Sediment Quality			
Metals (ug/g)	**109.06**	**59.94**	**0.024**
Metals (ERMQ)	**0.0561**	**0.0332**	**0.038**
PAHs (ng/g)	**668.93**	**40.14**	**0.011**
PAHs (ERMQ)	**0.0238**	**0.0021**	**0.011**
PCBs (ng/g)	**1.59**	**0.53**	**0.026**
PCBs (ERMQ)	**0.0088**	**0.0030**	**0.026**
DDT (ng/g)	**0.26**	**0.07**	**0.036**
DDT (ERMQ)	**0.0056**	**0.0015**	**0.036**
PBDEs (ng/g)	**0.01**	**0.05**	**0.010**
All Contaminants (ERMQ)	**0.0368**	**0.0123**	**0.008**
Biological Quality			
Nekton Species Richness	11.36	10.07	0.319
Nekton Abundance (abundance/m^2)	**0.02**	**0.03**	**<0.001**
Benthic Species Richness	32.23	28.92	0.412
Benthic Abundance (abundance/m^2)	4119.70	4531.16	0.647
BIBI	3.70	3.62	0.669
MAMBI	0.48	0.47	0.920

Notes: Rows in **bold** represent *t*-test results with *p*-values≤0.05. Developed sites defined as 14-digit HUC watersheds with >18.9% upland impervious cover.

Table 9. *t*-test results comparing SCECAP environmental data by level of watershed development (tidal creek sites). Values indicate averages.

Parameter	Developed (*n*=19)	Undeveloped (*n*=384)	*p*-value
Water Quality			
Water Temperature (°C)	29.62	29.84	0.377
Dissolved Oxygen (mg/L)	**4.85**	**4.39**	**0.034**
Salinity (ppt)	28.23	28.46	0.903
pH	**7.62**	**7.42**	**0.005**
Fecal Coliform (log MPN 100/mL)	1.07	0.98	0.571
Enterococcus spp. (log MPN/100mL)	1.04	0.93	0.698
Sediment Quality			
Metals (ug/g)	90.55	77.71	0.446
Metals (ERMQ)	0.0486	0.0426	0.508
PAHs (ng/g)	**241.84**	**47.35**	**0.027**
PAHs (ERMQ)	**0.0086**	**0.0025**	**0.046**
PCBs (ng/g)	1.63	0.59	0.141
PCBs (ERMQ)	0.0090	0.0033	0.141
DDT (ng/g)	0.50	0.17	0.209
DDT (ERMQ)	0.0108	0.0037	0.209
PBDEs (ng/g)	0.01	0.04	0.065
All Contaminants (ERMQ)	0.0242	0.0158	0.129
Biological Quality			
Nekton Species Richness	9.88	11.60	0.208
Nekton Abundance (abundance/m^2)	**0.03**	**0.08**	**<0.001**
Benthic Species Richness	29.79	24.64	0.357
Benthic Abundance (abundance/m^2)	4186.01	3391.55	0.460
BIBI	3.32	3.33	0.951
MAMBI	0.39	0.42	0.457

Notes: Rows in **bold** represent *t*-test results with *p*-values≤0.05. Developed sites defined as 14-digit HUC watersheds with >18.9% upland impervious cover.

Table 10. Generalized least squares time-series regression results: water quality (1999-2018). Values indicate μ ± *SE* with positive values indicating increasing trend over time.

	Temperature (°C)	**DO (mg/L)**	**Salinity (ppt)**	**pH**	**Fecal coliform (MPN/100mL)†**	**Enterococci (MPN/100mL)†**
All Sites						
Year	0.007 (±0.034)	0.007 (±0.011)	-0.099 (±0.149)	-0.004 (±0.003)	-0.001 (±0.006)	0.014 (±0.075)
Intercept	16.415 (±67.719)	-8.714 (±21.825)	227.588 (±300.060)	15.670** * (±5.174)	2.727 (±12.992)	-26.922 (±163.442)
Observations	20	20	20	20	20	12
Log Likelihood	-19.480	-3.878	-52.939	16.647	3.646	-1.528
AIC	46.960	15.757	113.877	-25.294	0.708	11.057
BIC	50.522	19.318	117.439	-21.732	4.270	12.267
Open Water Sites						
Year	0.003 (±0.033)	0.008 (±0.015)	-0.065 (±0.133)	-0.003 (±0.003)	-0.004 (±0.005)	-0.006 (±0.035)
Intercept	23.240 (±66.265)	-10.113 (±30.726)	158.325 (±267.456)	14.199** (±5.798)	9.616 (±10.879)	13.087 (±69.465)
Observations	20	20	20	20	20	12
Log Likelihood	-22.806	0.194	-52.124	13.526	1.205	0.841
AIC	53.612	7.611	112.248	-19.052	5.589	6.318
BIC	57.173	11.173	115.810	-15.490	9.151	7.528
Tidal Creek Sites						
Year	0.007 (±0.040)	0.008 (±0.015)	-0.141 (±0.180)	-0.005 (±0.003)	0.002 (±0.009)	0.037 (±0.031)
Intercept	15.092 (±80.694)	-12.269 (±29.868)	312.575 (±361.905)	16.611** (±6.952)	-3.684 (±17.902)	-72.817 (±63.305)
Observations	20	20	20	20	20	12
Log Likelihood	-16.631	-11.482	-55.220	14.652	-0.796	-6.108
AIC	41.262	30.965	118.441	-21.305	9.591	20.216
BIC	44.824	34.526	122.002	-17.743	13.153	21.426

Notes: ***$p \leq 0.01$, **$p \leq 0.05$, *$p \leq 0.10$

†Log transformed variable.

Table 11. Generalized least squares time-series regression results: sediment quality (1999-2018). Values indicate μ ± *SE* with positive values indicating increasing trend over time.

	Metals (ug/g)	**PAHs (ng/g)**	**PCBs (ng/g)**	**DDT (ng/g)**	**PBDEs (ng/g)**
All Sites					
Year	-0.854 (±1.112)	-0.923 (±3.506)	-0.016 (±0.026)	0.006 (±0.005)	-0.001 (±0.009)
Intercept	1,785.08 (±2,234.15)	1,921.94 (±7,041.13)	32.97 (±53.19)	-12.01 (±9.21)	2.10 (±17.94)
Observations	20	20	20	20	16
Log Likelihood	-82.470	-104.227	-21.105	5.760	2.410
AIC	172.940	216.453	50.211	-3.520	3.180
BIC	176.501	220.015	53.772	0.042	5.736
Open Water Sites					
Year	-0.849 (±1.391)	-3.343 (±2.666)	-0.016 (±0.030)	0.005 (±0.004)	-0.002 (±0.010)
Intercept	1,766.82 (±2,792.95)	6,793.42 (±5,353.86)	32.35 (±60.50)	-9.81 (±8.92)	3.50 (±20.95)
Observations	20	20	20	20	16
Log Likelihood	-84.997	-107.287	-22.300	11.333	0.608
AIC	177.994	222.573	52.600	-14.666	6.784
BIC	181.556	226.135	56.162	-11.104	9.340
Tidal Creek Sites					
Year	-0.801 (±0.769)	0.809 (±4.705)	-0.017 (±0.023)	0.007 (±0.007)	-0.0004 (±0.007)
Intercept	1,686.80 (±1,545.21)	-1,565.67 (±9,449.94)	34.46 (±46.48)	-13.74 (±14.01)	0.75 (±14.96)
Observations	20	20	20	20	16
Log Likelihood	-82.952	-105.475	-21.075	-2.704	4.444
AIC	173.905	218.950	50.149	13.408	-0.887
BIC	177.466	222.512	53.711	16.969	1.669

Notes: $^{***}p \leq 0.01$, $^{**}p \leq 0.05$, $^{*}p \leq 0.10$

Table 12. Generalized least squares time-series regression results: ERMQ sediment quality (1999-2018). Values indicate μ ± *SE* with positive values indicating increasing trend over time.

	Metals (ERMQ)	**PAHs (ERMQ)**	**PCBs (ERMQ)**	**DDT (ERMQ)**	**All (ERMQ)**
All Habitats					
Year	-0.0004 (±0.0004)	-0.00000 (±0.0001)	-0.0001 (±0.0001)	0.0001 (±0.0001)	-0.0002 (±0.0002)
Intercept	0.798 (±0.716)	0.009 (±0.244)	0.183 (±0.296)	-0.261 (±0.200)	0.328 (±0.407)
Observations	20	20	20	20	20
Log Likelihood	56.818	79.551	72.368	74.719	74.407
AIC	-105.636	-151.102	-136.736	-141.439	-140.814
BIC	-102.075	-147.540	-133.174	-137.877	-137.253
Open Water					
Year	-0.0005 (±0.001)	-0.0001 (±0.0001)	-0.0001 (±0.0002)	0.0001 (±0.0001)	-0.0002 (±0.0002)
Intercept	0.997 (±1.025)	0.196 (±0.191)	0.180 (±0.336)	-0.213 (±0.193)	0.445 (±0.489)
Observations	20	20	20	20	20
Log Likelihood	56.132	76.935	71.173	80.288	73.368
AIC	-104.263	-145.869	-134.346	-152.576	-138.735
BIC	-100.702	-142.308	-130.785	-149.015	-135.174
Tidal Creek					
Year	-0.0003 (±0.0003)	0.0001 (±0.0002)	-0.0001 (±0.0001)	0.0002 (±0.0002)	-0.0001 (±0.0001)
Intercept	0.712 (±0.538)	-0.140 (±0.315)	0.192 (±0.258)	-0.299 (±0.304)	0.141 (±0.261)
Observations	20	20	20	20	20
Log Likelihood	54.641	77.722	72.399	66.256	69.587
AIC	-101.282	-147.444	-136.797	-124.512	-131.174
BIC	-97.721	-143.882	-133.236	-120.950	-127.613

Notes: $^{***}p \leq 0.01$, $^{**}p \leq 0.05$, $^{*}p \leq 0.10$

Table 13. Generalized least squares time-series regression results: biological quality (1999-2018). Values indicate μ ± *SE* with positive values indicating increasing trend over time.

	Nekton Sp. Richness	Nekton Abundance	Benthic Sp. Richness	Benthic Abundance	BIBI	MAMBI
All Habitats						
Year	-0.22*** (±0.08)	-0.002*** (±0.001)	-0.38*** (±0.14)	-22.4 (±54.1)	-0.007 (±0.010)	-0.003*** (±0.001)
Intercept	459.85*** (±154.71)	4.860*** (±1.422)	785.11*** (±279.85)	48,832 (±108,609)	17.759 (±19.483)	5.571*** (±1.635)
Observations	20	20	20	20	20	20
Log Likelihood	-34.789	40.973	-54.076	-157.729	-0.921	38.686
AIC	77.578	-73.947	116.152	323.458	9.843	-69.372
BIC	81.139	-70.385	119.713	327.019	13.404	-65.811
Open Water						
Year	-0.208** (±0.091)	-0.001 (±0.001)	-0.503*** (±0.113)	-60.471 (±59.356)	-0.012* (±0.007)	-0.001 (±0.001)
Intercept	428.093** (±181.853)	1.150 (±1.898)	1,038.109*** (±227.213)	125,879 (±119,217)	28.152** (±14.169)	3.152 (±1.996)
Observations	20	20	20	20	20	20
Log Likelihood	-38.884	49.408	-55.291	-162.737	-2.879	30.260
AIC	85.767	-90.815	118.582	333.474	13.758	-52.521
BIC	89.329	-87.254	122.143	337.036	17.320	-48.959
Tidal Creek						
Year	-0.247*** (±0.076)	-0.004*** (±0.001)	-0.258 (±0.178)	1.993 (±46.309)	-0.004 (±0.012)	-0.003*** (±0.001)
Intercept	507.562*** (±151.972)	7.398*** (±2.116)	542.962 (±356.845)	-577.4 (±93,012)	10.597 (±23.855)	7.167*** (±2.179)
Observations	20	20	20	20	20	20
Log Likelihood	-35.791	32.265	-62.308	-160.854	-10.458	30.380
AIC	79.582	-56.530	132.615	329.708	28.915	-52.759
BIC	83.143	-52.969	136.177	333.270	32.477	-49.198

Notes: $^{***}p \leq 0.01$, $^{**}p \leq 0.05$, $^{*}p \leq 0.10$

Table 14. Generalized least squares time-series regression results: temperature (1999-2018). Values indicate μ ± *SE* with positive values indicating increasing trend over time.

	Annual Temp. (°C)	Winter Temp. (°C)	Spring Temp. (°C)	Summer Temp. (°C)	Fall Temp. (°C)	Extreme Temp. (days/year)
All Stations						
Year	0.051***	0.070	0.025	0.042	0.043	0.278
	(0.018)	(0.076)	(0.032)	(0.028)	(0.039)	(0.409)
Intercept	-82.484**	-130.128	-31.682	-57.627	-66.574	-537.726
	(36.575)	(151.827)	(64.976)	(55.364)	(79.251)	(821.603)
Observations	20	20	20	20	20	20
Log Likelihood	-13.551	-37.960	-28.069	-18.937	-24.360	-71.043
AIC	35.102	83.921	64.139	45.874	56.719	150.085
BIC	38.663	87.482	67.700	49.435	60.281	153.647
Brookgreen Gardens, SC						
Year	-0.006	0.008	-0.046	0.004	0.016	-0.329
	(0.041)	(0.080)	(0.037)	(0.064)	(0.082)	(0.338)
Intercept	29.937	-6.704	109.343	18.243	-12.919	678.817
	(81.817)	(159.881)	(74.149)	(129.376)	(164.414)	(678.352)
Observations	19	20	20	18	17	19
Log Likelihood	-21.502	-39.622	-29.863	-20.925	-22.373	-66.392
AIC	51.004	87.244	67.726	49.851	52.747	140.784
BIC	54.337	90.805	71.288	52.941	55.579	144.116
Charleston Int'l Airport, SC						
Year	0.068***	0.080	0.048	0.066***	0.062*	0.595
	(0.017)	(0.080)	(0.031)	(0.020)	(0.034)	(0.381)
Intercept	-117.328***	-148.877	-77.900	-105.247***	-105.451	-1,174.225
	(34.207)	(160.767)	(63.012)	(40.750)	(67.685)	(764.664)
Observations	20	20	20	20	20	20
Log Likelihood	-10.155	-38.097	-27.258	-19.038	-25.497	-72.985
AIC	28.310	84.193	62.515	46.075	58.994	153.969
BIC	31.871	87.755	66.077	49.637	62.556	157.531
Savannah Int'l Airport, SC						
Year	0.087***	0.119	0.071*	0.069***	0.077**	0.532
	(0.019)	(0.075)	(0.040)	(0.025)	(0.036)	(0.652)
Intercept	-155.173***	-227.883	-123.344	-111.678**	-134.238*	-1,047.063
	(37.883)	(150.317)	(79.986)	(49.478)	(72.398)	(1,309.834)
Observations	20	20	20	20	20	20
Log Likelihood	-12.552	-36.941	-29.717	-18.769	-23.432	-75.055
AIC	33.105	81.883	67.434	45.537	54.865	158.111
BIC	36.666	85.444	70.996	49.099	58.426	161.672

Notes: $^{***}p \leq 0.01$, $^{**}p \leq 0.05$, $^{*}p \leq 0.10$

Table 15. Generalized least squares time-series regression results: precipitation (1999-2018). Values indicate μ ± *SE* with positive values indicating increasing trend over time.

	Annual Precip. (cm)	**Winter Precip. (cm)**	**Spring Precip. (cm)**	**Summer Precip. (cm)**	**Fall Precip. (cm)**	**Extreme Precip. (days/year)**
All Stations						
Year	0.965	0.356	0.530	0.163	-0.222	0.251**
	(1.091)	(0.232)	(0.339)	(0.259)	(0.731)	(0.109)
Intercept	-1,812.542	-692.204	-1,037.201	-281.016	475.459	-487.072**
	(2,191.76)	(465.75)	(680.475)	(520.885)	(1,467.665)	(218.117)
Observations	20	20	20	20	20	20
Log Likelihood	-79.612	-68.383	-70.735	-66.350	-74.920	-50.025
AIC	167.225	144.765	149.471	140.699	157.839	108.049
BIC	170.786	148.327	153.032	144.261	161.401	111.611
Brookgreen Gardens, SC						
Year	0.388	0.154	0.340	0.466	-0.807	0.212
	(1.699)	(0.321)	(0.362)	(0.649)	(0.907)	(0.184)
Intercept	-645.164	-283.907	-652.944	-892.575	1,657.012	-407.919
	(3,412.72)	(644.125)	(727.961)	(1,304.26)	(1,822.703)	(369.426)
Observations	20	20	20	19	18	20
Log Likelihood	-87.743	-68.612	-72.409	-72.292	-73.332	-54.596
AIC	183.486	145.224	152.819	152.584	154.664	117.192
BIC	187.047	148.785	156.380	155.916	157.754	120.753
Charleston Int'l Airport, SC						
Year	1.851**	0.277	0.553	0.340	0.127	0.358***
	(0.917)	(0.241)	(0.391)	(0.395)	(1.000)	(0.115)
Intercept	-3,588.61*	-533.155	-1,085.92	-633.728	-223.994	-700.260***
	(1,841.46)	(483.442)	(785.86)	(792.653)	(2,007.924)	(231.203)
Observations	20	20	20	20	20	20
Log Likelihood	-84.930	-69.267	-70.430	-75.297	-79.540	-55.195
AIC	177.859	146.534	148.861	158.594	167.080	118.389
BIC	181.421	150.095	152.422	162.155	170.641	121.951
Savannah Int'l Airport, SC						
Year	1.200	0.601**	0.723*	-0.192	-0.012	0.126
	(0.778)	(0.254)	(0.430)	(0.458)	(0.399)	(0.211)
Intercept	-2,294.74	-1,185.34**	-1,427.17*	428.249	48.402	-236.317
	(1,563.10)	(509.23)	(864.010)	(920.510)	(801.966)	(423.056)
Observations	20	20	20	20	20	20
Log Likelihood	-83.858	-71.305	-75.759	-73.461	-70.551	-56.477
AIC	175.715	150.609	159.518	154.921	149.102	120.955
BIC	179.277	154.171	163.080	158.483	152.664	124.516

Notes: ***$p \leq 0.01$, **$p \leq 0.05$, *$p \leq 0.10$

Table 16. Linear models meta-analysis summaries: mean adjusted R^2 by spatial grouping and response category

Spatial Unit	Mean Area (ha)	Water Quality	Sediment Quality	Biological Quality	All Models
Buffer					
1	314	0.3537	0.3611	0.2095	**0.3045**
2	1,257	0.3596	0.3695	0.2091	**0.3091**
3	2,827	0.3497	0.3752	0.2162	**0.3193**
All	*1,466*	*0.3543*	*0.3686*	*0.2116*	***0.3093***
Grid					
25	2,500	0.3401	0.2891	0.2137	**0.2667**
100	10,000	0.3309	0.3120	0.2144	**0.2780**
400	40,000	0.3134	0.3187	0.2213	**0.2823**
1600	160,000	0.3055	0.3265	0.2148	**0.2831**
All	*53,125*	*0.3267*	*0.3116*	*0.2161*	***0.2775***
HUC					
08	262,213	0.3239	0.3894	0.2256	**0.3222**
10	51,632	0.3268	0.4013	0.2292	**0.3301**
12	9,581	0.3472	0.3850	0.2294	**0.3237**
14	8,937	0.3089	0.3923	0.2271	**0.3227**
All	*83,091*	*0.3267*	*0.3920*	*0.2278*	***0.3247***
Total	**45,894**	**0.3327**	**0.3564**	**0.2191**	**0.3033**

Table 17. Linear model meta-analysis parameter summaries: water quality models (*N*=22). Mean coefficient estimate represents positive (+) or negative (-) correlation between independent and dependent variable (bacteria concentration).

Independent Variable	Frequency (%)	Mean Coefficient Estimate (±)
Physical Habitat		
Channel Width	100	-
Salinity	100	-
Station Depth	9	-
Landcover and Land Use		
Impervious Cover	64	+
Marsh	41	-
Population Density	23	+
Forested †	14	+
Mixed Forest	14	+
Well Drained Soils †	5	-
All Ponds	5	-
Weather and Climate		
Precipitation 2-day Total	95	+
Temperature 30-day Average	50	+
Precipitation 14-day Total	36	-
SP02	36	-
PDSI	14	-

Notes: Full list of independent variables available in Appendices B. F, and G.
† Condensed landcover categories (Appendix F)

Table 18. Linear model meta-analysis parameter summaries: sediment quality models (*N*=110). Mean coefficient estimate represents positive (+) or negative (-) correlation between independent and dependent variable (sediment contamination).

Independent Variable	Frequency (%)	Mean Coefficient Estimate (±)
Physical Habitat		
Silt-Clay Content	75	+
Salinity	20	-
TOC Sediment	10	+
Channel Width	8	+
Landcover and Land Use		
Impervious Cover	47	+
Population Density	37	+
Marsh	17	-
Agricultural †	11	+
Cultivated Crops	9	+
Open Water	7	-
Group C Soils	5	+
Poorly Drained Soils †	5	+
All Ponds Density	5	-
Group D Soils	5	-
Developed High †	4	+
High Intensity Developed	4	+
Mixed Forest	4	-
Group A Soils	4	-
Forested †	1	-
Group B Soils	1	-
Well Drained Soils †	1	-
Weather and Climate		
Winter Precipitation	60	+
Winter Temperature	40	-
Preceding Fall Precipitation	30	-
Spring Temperature	23	+
Spring Precipitation	20	+
SP02	20	+
AMO	10	+
Summer Temperature	7	+

Notes: Full list of independent variables available in Appendices B. F, and G.
† Condensed landcover categories (Appendix F)

Table 19. Linear model meta-analysis parameter summaries: biological quality models (*N*=77). Mean coefficient estimate represents positive (+) or negative (-) correlation between independent and dependent variable (biological condition).

Independent Variable	Frequency (%)	Mean Coefficient Estimate (±)
Physical Habitat		
Salinity	86	+
Channel Width	82	-
Silt-Clay Content	57	-
Station Depth	14	+
Landcover and Land Use		
Marsh	39	+
Impervious Cover	19	-
Developed Low †	16	+
Agricultural †	10	+
Open Spaces Developed	9	+
Population Density	9	-
Developed High †	5	-
Group B Soils	5	+
Cultivated Crops	3	-
Forested †	3	+
Mixed Forest	3	+
Medium Intensity Developed	1	-
Open Water	1	+
Group C Soils	1	-
Group D Soils	1	-
All Ponds	1	+
Weather and Climate		
Temperature 90-day Average	57	-
Precipitation 45-day Total	57	+
Annual Temperature	29	-
NAO	29	+
Winter Temperature	14	+
Precipitation 30-day Total	14	+
SP02	14	+
Preceding Annual Temperature	10	-

Notes: Full list of independent variables available in Appendices B. F, and G.
† Condensed landcover categories (Appendix F)

Table 20. Linear model meta-analysis parameter summaries: all models (*N*=209). Mean coefficient estimate represents positive (+) or negative (-) correlation between independent and dependent variables.

Independent Variable	Frequency (%)	Mean Coefficient Estimate (±)
Physical Habitat		
Silt-Clay Content	61	-
Salinity	53	+
Channel Width	45	-
Station Depth	6	+
TOC Sediment	5	+
Landcover and Land Use		
Impervious Cover	39	-
Marsh	28	+
Population Density	25	+
Agricultural †	10	+
Cultivated Crops	6	-
Developed Low †	6	+
Mixed Forest	4	+
Open Water	4	-
Developed High †	4	-
Open Spaces Developed	3	+
Group C Soils	3	+
Forested †	3	+
Group D Soils	3	-
Poorly Drained Soils †	3	+
All Ponds Density	3	-
Group B Soils	2	+
High Intensity Developed	2	+
Group A Soils	2	-
Well Drained Soils †	1	-
All Ponds	1	+
Medium Intensity Developed	<1	-
Weather and Climate		
Winter Precipitation	32	+
Winter Temperature	26	+
Temperature 90-day Average	21	-
Precipitation 45-day Total	21	+
SP02	20	+
Preceding Fall Precipitation	16	-
Spring Temperature	12	+
Annual Temperature	11	-
Spring Precipitation	11	+
NAO	11	+
Precipitation 2-day Total	10	+
Temperature 30-day Average	5	+
Precipitation 30-day Total	5	+
AMO	5	+
Preceding Annual Temperature	4	-
Summer Temperature	4	+
Precipitation 14-day Total	4	-
PDSI	1	-

Notes: Full list of independent variables available in Appendices B. F, and G.
† Condensed landcover categories (Appendix F)

Table 21. Linear model output summaries: sediment ERMQ scores

	Dependent Variables:				
	All	**DDT**	**Metals**	**PAHs**	**PCBs**
Observations	788	780	801	773	773
Adjusted R^2	0.74	0.17	0.82	0.45	0.32
Residual Std. Error	0.004752	0.002420	0.011716	0.001796	0.002628
F Statistic	452.47*** (df=5; 782)	33.60*** (df=5; 774)	740.39*** (df=5; 795)	91.12*** (df=7; 765)	74.27*** (df=5; 767)
Intercept	0.005197*** (±0.000485)	0.001223*** (±0.000251)	0.000756 (±0.002031)	-0.000668** (±0.000283)	0.001269*** (±0.000154)
Physical Habitat					
Channel Width (m)†				0.000147*** (±0.000044)	
Silt-Clay Content (%)	0.000306*** (±0.000007)		0.000967*** (± 0.000016)	0.000057*** (±0.000003)	0.000035*** (±0.000004)
TOC Sediment (mg/L)		0.000511*** (±0.000060)			
Landcover and Land Use					
Agricultural (%)		0.000073*** (±0.000018)			
Mixed Forest (%)				-0.000140*** (±0.000029)	
Open Water (%)		-0.000031*** (±0.000005)			
Upland Impervious Cover (%)		0.000068** (±0.000027)	0.000430*** (±0.000116)		
Population Density (persons per ha)	0.002139*** (±0.000210)			0.000961*** (±0.000084)	0.000588*** (±0.000117)
Group A Soils (%)	-0.000062*** (±0.000013)				
Poorly Drained Soils (%)			0.000118*** (±0.000029)		
Weather and Climate					
Spring Precipitation (cm)					0.000108*** (±0.000009)
Winter Precipitation (cm)	0.000081*** (±0.000019)	0.000067*** (±0.000010)		0.000040*** (±0.000007)	
Winter Temperature (°C)	-0.000315*** (±0.000106)			-0.000167*** (±0.000041)	-0.000455*** (±0.000060)
Fall Precipitation (cm)			-0.000116*** (±0.000029)		
SP02			0.002703*** (±0.000500)		
Winter Precipitation x Winter Temperature				-0.000020*** (±0.000004)	
Spring Precipitation x Winter Temperature					-0.000047*** (±0.000006)

Notes: All models were analyzed at the 10-digit HUC scale. Values in column represent coefficient estimate with error term (±) in parentheses.
***$p \leq 0.01$, **$p \leq 0.05$, *$p \leq 0.10$; †Log transformed variable

Table 22. Linear model output summaries: bacteria contamination

	Dependent Variables:	
	***Enterococcus* spp. (MPN/100mL)†**	**Fecal coliform (MPN/100mL)†**
Observations	337	798
Adjusted R^2	0.24	0.46
Residual Std. Error	0.6172	0.5195
F Statistic	22.60^{***} (df=5; 331)	98.18^{***} (df=7; 790)
Intercept	-2.4323^{*} (±1.2589)	3.2847^{***} (±0.1314)
Physical Habitat		
Channel Width (m)†	-0.1160^{***} (±0.0216)	-0.1999^{***} (±0.0141)
Salinity (ppt)	-0.0350^{***} (±0.0044)	-0.04290^{***} (±0.0023)
Landcover and Land Use		
Marsh (%)		-0.0082^{***} (±0.0012)
Mixed Forest (%)		0.0174^{***} (±0.0053)
Upland Impervious Cover (%)	0.0112^{***} (±0.0040)	0.01440^{***} (±0.0024)
Weather and Climate		
2-day Precipitation Total (in)	0.1734^{***} (±0.0449)	0.1733^{***} (±0.0281)
30-day Temperature Average (°C)	0.1693^{***} (±0.0459)	
PDSI		-0.0248^{***} (±0.0094)

Notes: All models were analyzed at the 2 km buffer scale. Values in column represent coefficient estimate with error term (±) in parentheses.
$^{***}p \leq 0.01$, $^{**}p \leq 0.05$, $^{*}p \leq 0.10$
†Log transformed variable

Table 23. Linear model output summaries: trawl data

	Dependent Variables:		
	Nekton Abundance (individuals/m²)†	**Tidal Creek Nekton Species Richness**	**Open Water Nekton Species Richness**
Observations	740	374	365
Adjusted R^2	0.18	0.15	0.17
Residual Std. Error	1.3079	5.6331	5.1978
F Statistic	42.59*** (df=4; 735)	12.03*** (df=6; 367)	15.70*** (df=5; 359)
Intercept	-1.7683*** (±0.1788)	11.6192*** (±2.3627)	9.2077*** (±2.0823)
Physical Habitat			
Channel Width (m) †	-0.3538*** (±0.0312)	-1.3080*** (±0.2631)	-0.8155* (±0.4387)
Salinity (ppt)		0.1493*** (±0.0375)	0.1552*** (±0.0337)
Landcover and Land Use			
Agricultural (%)			0.1956*** (±0.0396)
Marsh (%)		0.0775*** (±0.0269)	
Upland Impervious Cover (%)	-0.0167** (±0.0067)		
Weather and Climate			
30-day Precipitation Total (cm)		0.1031*** (±0.0396)	
Annual Temperature (°C)	-0.2809*** (±0.0775)		-1.338*** (±0.4521)
Preceding Annual Temperature (°C)		-0.9517** (±0.4656)	
SP02			0.9435*** (±0.3613)
NAO	0.1537*** (±0.0474)	1.0911*** (±0.2943)	

Notes: All models were analyzed at the 12-digit HUC scale. Values in column represent coefficient estimate with error term (±) in parentheses.
***$p \leq 0.01$, **$p \leq 0.05$, *$p \leq 0.10$
†Log transformed variable

Table 24. Linear model output summaries: benthic data

	Dependent variable:		
	Benthic Abundance (individuals/m^2)†	**Benthic Species Richness†**	**MAMBI**
Observations	795	806	571
Adjusted R^2	0.19	0.42	0.47
Residual Std. Error	1.0162	0.5593	0.09203
F Statistic	32.02*** (df=6; 788)	85.47*** (df=7; 798)	71.65*** (df=7; 563)
Intercept	9.1743*** (±0.5894)	3.181088*** (±0.3354)	0.46393*** (±0.06505)
Physical Habitat			
Channel Width (m)†		0.0358*** (±0.01335)	0.01721*** (±0.00271)
Salinity (ppt)	0.0476*** (±0.0046)	0.0514*** (±0.0026)	0.00595*** (±0.00050)
Silt-Clay Content (%)	-0.0064*** (±0.0015)	-0.0042*** (±0.0008)	-0.00060*** (±0.00015)
Landcover and Land Use			
Marsh (%)	0.0092*** (±0.0030)	0.0052*** (±0.0018)	
Developed Open Spaces (%)			0.00601*** (±0.00077)
Low Intensity Developed (%)		0.0050*** (±0.0014)	
High Intensity Developed (%)			-0.00482*** (±0.00091)
Weather and Climate			
45-day Precipitation Total (cm)	0.0125*** (±0.0042)	0.0133*** (±0.0023)	0.00100** (±0.00047)
90-day Temperature Average (°C)	-0.1279*** (±0.0234)	-0.0862*** (±0.0127)	-0.01400*** (±0.00245)
Winter Temperature (°C)	0.08090*** (±0.0227)		

Notes: All models were analyzed at the 12-digit HUC scale with the exception of MAMBI which was analyzed at the 400 km^2 scale. Values in column represent coefficient estimate with error term (±) in parentheses.

$^{***}p \leq 0.01$, $^{**}p \leq 0.05$, $^{*}p \leq 0.10$

†Log transformed variable

Table 25. Summary of population growth and climate change projections for coastal South Carolina

Parameter	Year	Projection	Percent Change	Prediction
Population	2010	Baseline	-	1,224,717 (0.66 persons/ha)
	2065	Low	+130%	2,808,625 (1.52)
	2065	High	+180%	3,421,083 (1.86)
Impervious Cover	2011	Baseline	-	2.59%
	2065	Low	+130%	5.96
	2065	High	+180%	7.26
Developed Landcover	2011	Baseline	-	9.89%
	2065	Low	+130%	22.75
	2065	High	+180%	27.69
Annual Precipitation	1980-2010	Baseline	-	129.7 cm
	2065	Low	+5%	136.4
	2065	High	+10%	142.8
Annual Temperature	1980-2010	Baseline	-	19.0 °C
	2065	Low	+5%	20.9
	2065	High	+6.5%	21.4

Notes: Population, impervious cover, and developed landcover calculated for eight coastal South Carolina counties. Baseline conditions determined from 2010 census data and 2011 NLCD data (US Census Bureau, 2018; Yang et al., 2018). Population growth predictions from Hauer dataset (2019). Precipitation and temperature data from 30-year climate normal data averaged from three weather stations (Brookgreen Gardens, Charleston Int'l Airport, Savannah Int'l Airport) (NOAA NCEI). Percent change precipitation and percent change temperature values taken from Fourth National Climate Assessment's Climate Science Special Report (Easterling et al., 2017, Vose et al., 2017).

Table 26. Scenarios of population growth and climate change for coastal South Carolina

Scenario	Change	Projection	Population Growth [1]	Temperature Change [2]	Precipitation Change [3]
0	No Change (Baseline)	–	–	–	–
1	Population Only	Low	+130%	–	–
2	Temperature Only	Low	–	+5%	--
3	Precipitation Only	Low	–	–	+5%
4	Temperature and Precipitation	Low	–	+5%	+5%
5	Population and Temperature	Low	+130%	+5%	–
6	Population and Precipitation	Low	+130%	–	+5%
7	Population, Temperature, and Precipitation	Low	+130%	+5%	+5%
8	Population Only	High	+180%	–	–
9	Temperature Only	High	–	+6.5%	–
10	Precipitation Only	High	–	–	+10%
11	Temperature and Precipitation	High	–	+6.5%	+10%
12	Population and Temperature	High	+180%	+6.5%	–
13	Population and Precipitation	High	+180%	–	+10%
14	Population, Temperature, and Precipitation	High	+180%	+6.5%	+10%

Notes: [1] Hauer, 2019
[2] Vose *et al*., 2017
[3] Easterling *et al.*, 2017

Table 27. Scenario prediction model outputs: *Enterococcus* spp. (MPN/100mL)

	Open Water Sites		Tidal Creek Sites		All Sites	
Scenario	**Prediction**	**Percent Change**	**Prediction**	**Percent Change**	**Prediction**	**Percent Change**
0	3.18 (±1.03)	-	6.49 (±1.81)	-	4.58 (±1.10)	-
1	3.94 (±1.36)	24.12	7.50 (±2.21)	15.57	5.47 (±1.45)	19.38
2	6.16 (±2.18)	93.97	11.85 (±4.18)	82.50	8.57 (±2.65)	87.07
3	3.20 (±1.03)	0.85	6.55 (±1.82)	0.83	4.62 (±1.11)	0.83
4	6.20 (±2.19)	95.42	11.94 (±4.21)	83.93	8.64 (±2.67)	88.50
5	7.47 (±2.89)	135.32	13.59 (±5.08)	109.21	10.10 (±3.43)	120.30
6	3.97 (±1.37)	25.12	7.57 (±2.22)	16.52	5.52 (±1.46)	20.34
7	7.53 (±2.91)	137.04	13.69 (±5.12)	110.83	10.17 (±3.45)	121.96
8	4.27 (±1.61)	34.54	7.93 (±2.48)	22.11	5.85 (±1.72)	27.63
9	7.42 (±3.30)	133.55	14.11 (±6.29)	117.26	10.26 (±4.19)	123.75
10	3.23 (±1.04)	1.70	6.60 (±1.83)	1.67	4.66 (±1.12)	1.67
11	7.52 (±3.34)	136.98	14.33 (±6.38)	120.64	10.41 (±4.25)	127.12
12	9.63 (±4.83)	203.16	17.00 (±8.20)	161.83	12.81 (±5.87)	179.45
13	4.34 (±1.63)	36.68	8.06 (±2.52)	24.10	5.94 (±1.74)	29.68
14	9.76 (±4.90)	207.49	17.26 (±8.32)	165.85	13.00 (±5.95)	183.58

Notes: For detailed description of scenarios, see Table 26.

Table 28. Scenario prediction model outputs: fecal coliform (MPN/100mL)

	Open Water Sites		Tidal Creek Sites		All Sites	
Scenario	**Prediction**	**Percent Change**	**Prediction**	**Percent Change**	**Prediction**	**Percent Change**
0	3.54 (±0.55)	-	9.12 (±1.24)	-	5.76 (±0.66)	-
1	4.92 (±0.81)	39.20	11.42 (±1.54)	25.22	7.56 (±0.92)	31.23
2	3.80 (±0.54)	7.50	9.71 (±1.21)	6.40	6.15 (±0.62)	6.81
3	3.83 (±0.55)	8.37	9.78 (±1.22)	7.25	6.20 (±0.62)	7.66
4	3.83 (±0.55)	8.37	9.78 (±1.22)	7.25	6.20 (±0.62)	7.66
5	4.92 (±0.81)	39.20	11.42 (±1.54)	25.22	7.56 (±0.92)	31.23
6	4.96 (±0.82)	40.28	11.51 (±1.55)	26.21	7.62 (±0.92)	32.24
7	4.96 (±0.82)	40.28	11.51 (±1.55)	26.21	7.62 (±0.92)	32.24
8	5.42 (±1.00)	53.28	12.16 (±1.75)	33.24	8.17 (±1.13)	41.85
9	3.80 (±0.54)	7.50	9.71 (±1.21)	6.40	6.15 (±0.62)	6.81
10	3.86 (±0.55)	9.25	9.86 (±1.23)	8.10	6.25 (±0.63)	8.52
11	3.86 (±0.55)	9.25	9.86 (±1.23)	8.10	6.25 (±0.63)	8.52
12	5.42 (±1.00)	53.28	12.16 (±1.75)	33.24	8.17 (±1.13)	41.85
13	5.50 (±1.01)	55.62	12.35 (±1.78)	35.33	8.30 (±1.15)	44.03
14	5.50 (±1.01)	55.62	12.35 (±1.78)	35.33	8.30 (±1.15)	44.03

Notes: For detailed description of scenarios, see Table 26.

Table 29. Scenario prediction model outputs: combined ERMQ for all contaminants

	Open Water Sites		Tidal Creek Sites		All Sites	
Scenario	**Prediction**	**Percent Change**	**Prediction**	**Percent Change**	**Prediction**	**Percent Change**
0	0.0109 (±0.0004)	-	0.0143 (±0.0004)	-	0.0126 (±0.0004)	-
1	0.0126 (±0.0005)	15.05	0.0158 (±0.0005)	10.78	0.0142 (±0.0005)	12.64
2	0.0100 (±0.0005)	-8.86	0.0133 (±0.0005)	-6.81	0.0116 (±0.0005)	-7.71
3	0.0107 (±0.0003)	-2.14	0.0141 (±0.0004)	-1.67	0.0124 (±0.0003)	-1.88
4	0.0101 (±0.0005)	-7.61	0.0135 (±0.0005)	-5.85	0.0118 (±0.0005)	-6.62
5	0.0120 (±0.0006)	9.57	0.0153 (±0.0006)	6.60	0.0136 (±0.0006)	7.90
6	0.0127 (±0.0005)	16.3	0.0160 (±0.0005)	11.73	0.0143 (±0.0005)	13.73
7	0.0121 (±0.0006)	10.83	0.0154 (±0.0006)	7.55	0.0137 (±0.0006)	8.98
8	0.0133 (±0.0006)	22.14	0.0166 (±0.0006)	15.93	0.0150 (±0.0006)	18.64
9	0.0098 (±0.0006)	-10.31	0.0132 (±0.0006)	-7.91	0.0115 (±0.0006)	-8.95
10	0.0108 (±0.0004)	-0.96	0.0142 (±0.0004)	-0.77	0.0125 (±0.0004)	-0.85
11	0.0101 (±0.0006)	-7.87	0.0134 (±0.0006)	-6.05	0.0117 (±0.0006)	-6.84
12	0.0126 (±0.0008)	15.23	0.0158 (±0.0008)	10.65	0.0142 (±0.0008)	12.65
13	0.0136 (±0.0007)	24.57	0.0169 (±0.0006)	17.79	0.0152 (±0.0006)	20.75
14	0.0129 (±0.0008)	17.66	0.0161 (±0.0008)	12.51	0.0145 (±0.0008)	14.76

Notes: For detailed description of scenarios, see Table 26.

Table 30. Scenario prediction model outputs: ERMQ DDT

	Open Water Sites		Tidal Creek Sites		All Sites	
Scenario	**Prediction**	**Percent Change**	**Prediction**	**Percent Change**	**Prediction**	**Percent Change**
0	0.0014 (±0.0002)	-	0.0017 (±0.0002)	-	0.0016 (±0.0002)	-
1	0.0015 (±0.0003)	3.16	0.0018 (±0.0003)	4.47	0.0016 (±0.0003)	3.87
2	0.0012 (±0.0002)	-17.59	0.0015 (±0.0002)	-13.88	0.0013 (±0.0002)	-15.59
3	0.0013 (±0.0002)	-9.71	0.0016 (±0.0002)	-7.22	0.0014 (±0.0002)	-8.37
4	0.0013 (±0.0002)	-9.71	0.0016 (±0.0002)	-7.22	0.0014 (±0.0002)	-8.37
5	0.0015 (±0.0003)	3.16	0.0018 (±0.0003)	4.47	0.0016 (±0.0003)	3.87
6	0.0016 (±0.0003)	11.03	0.0019 (±0.0003)	11.14	0.0017 (±0.0003)	11.09
7	0.0016 (±0.0003)	11.03	0.0019 (±0.0003)	11.14	0.0017 (±0.0003)	11.09
8	0.0016 (±0.0004)	11.14	0.0019 (±0.0004)	11.53	0.0018 (±0.0004)	11.35
9	0.0012 (±0.0002)	-17.59	0.0015 (±0.0002)	-13.88	0.0013 (±0.0002)	-15.59
10	0.0014 (±0.0002)	-2.30	0.0017 (±0.0002)	-0.94	0.0015 (±0.0002)	-1.57
11	0.0014 (±0.0002)	-2.30	0.0017 (±0.0002)	-0.94	0.0015 (±0.0002)	-1.57
12	0.0016 (±0.0004)	11.14	0.0019 (±0.0004)	11.53	0.0018 (±0.0004)	11.35
13	0.0018 (±0.0004)	26.42	0.0021 (±0.0004)	24.47	0.0020 (±0.0004)	25.37
14	0.0018 (±0.0004)	26.42	0.0021 (±0.0004)	24.47	0.0020 (±0.0004)	25.37

Notes: For detailed description of scenarios, see Table 26.

Table 31. Scenario prediction model outputs: ERMQ metals

	Open Water Sites		Tidal Creek Sites		All Sites	
Scenario	**Prediction**	**Percent Change**	**Prediction**	**Percent Change**	**Prediction**	**Percent Change**
0	0.0282 (±0.0008)	-	0.0389 (±0.0008)	-	0.0335 (±0.0008)	-
1	0.0303 (±0.0013)	7.48	0.0411 (±0.0014)	5.53	0.0357 (±0.0013)	6.36
2	0.0284 (±0.0008)	0.71	0.0391 (±0.0008)	0.41	0.0337 (±0.0008)	0.54
3	0.0282 (±0.0008)	0.01	0.0389 (±0.0008)	-0.09	0.0335 (±0.0008)	-0.05
4	0.0282 (±0.0008)	0.01	0.0389 (±0.0008)	-0.09	0.0335 (±0.0008)	-0.05
5	0.0303 (±0.0013)	7.48	0.0411 (±0.0014)	5.53	0.0357 (±0.0013)	6.36
6	0.0301 (±0.0013)	6.78	0.0409 (±0.0014)	5.03	0.0355 (±0.0013)	5.77
7	0.0301 (±0.0013)	6.78	0.0409 (±0.0014)	5.03	0.0355 (±0.0013)	5.77
8	0.0310 (±0.0016)	10.08	0.0419 (±0.0017)	7.50	0.0364 (±0.0017)	8.59
9	0.0284 (±0.0008)	0.71	0.0391 (±0.0008)	0.41	0.0337 (±0.0008)	0.54
10	0.0280 (±0.0009)	-0.65	0.0387 (±0.0009)	-0.57	0.0333 (±0.0008)	-0.60
11	0.0280 (±0.0009)	-0.65	0.0387 (±0.0009)	-0.57	0.0333 (±0.0008)	-0.60
12	0.0310 (±0.0016)	10.08	0.0419 (±0.0017)	7.50	0.0364 (±0.0017)	8.59
13	0.0306 (±0.0016)	8.72	0.0415 (±0.0017)	6.52	0.0360 (±0.0017)	7.45
14	0.0306 (±0.0016)	8.72	0.0415 (±0.0017)	6.52	0.0360 (±0.0017)	7.45

Notes: For detailed description of scenarios, see Table 26.

Table 32. Scenario prediction model outputs: ERMQ PAHs

	Open Water Sites		Tidal Creek Sites		All Sites	
Scenario	**Prediction**	**Percent Change**	**Prediction**	**Percent Change**	**Prediction**	**Percent Change**
0	0.0017 (±0.0002)	-	0.0020 (±0.0002)	-	0.0019 (±0.0001)	-
1	0.0025 (±0.0002)	42.48	0.0027 (±0.0002)	34.03	0.0026 (±0.0002)	37.94
2	0.0014 (±0.0002)	-20.17	0.0017 (±0.0002)	-17.56	0.0015 (±0.0002)	-18.76
3	0.0016 (±0.0002)	-6.38	0.0019 (±0.0002)	-5.51	0.0018 (±0.0001)	-5.91
4	0.0014 (±0.0002)	-20.26	0.0017 (±0.0002)	-17.78	0.0015 (±0.0002)	-18.92
5	0.0023 (±0.0003)	32.25	0.0025 (±0.0003)	24.86	0.0024 (±0.0003)	28.29
6	0.0025 (±0.0002)	46.04	0.0028 (±0.0002)	36.92	0.0027 (±0.0002)	41.14
7	0.0023 (±0.0003)	32.16	0.0025 (±0.0003)	24.65	0.0024 (±0.0003)	28.13
8	0.0028 (±0.0003)	62.64	0.0031 (±0.0003)	50.34	0.0029 (±0.0003)	56.04
9	0.0013 (±0.0003)	-22.86	0.0016 (±0.0003)	-19.97	0.0015 (±0.0002)	-21.30
10	0.0017 (±0.0002)	-3.03	0.0020 (±0.0002)	-2.79	0.0018 (±0.0001)	-2.89
11	0.0013 (±0.0003)	-24.91	0.0016 (±0.0003)	-21.98	0.0014 (±0.0002)	-23.33
12	0.0026 (±0.0003)	49.72	0.0028 (±0.0003)	38.77	0.0027 (±0.0003)	43.84
13	0.0029 (±0.0003)	69.55	0.0032 (±0.0003)	55.95	0.0030 (±0.0003)	62.25
14	0.0026 (±0.0003)	47.67	0.0028 (±0.0003)	36.77	0.0027 (±0.0003)	41.82

Notes: For detailed description of scenarios, see Table 26.

Table 33. Scenario prediction model outputs: ERMQ PCBs

	Open Water Sites		Tidal Creek Sites		All Sites	
Scenario	**Prediction**	**Percent Change**	**Prediction**	**Percent Change**	**Prediction**	**Percent Change**
0	0.0024 (±0.0002)	-	0.0027 (±0.0002)	-	0.0025 (±0.0002)	-
1	0.0028 (±0.0003)	18.57	0.0032 (±0.0003)	15.19	0.0030 (±0.0003)	16.79
2	0.0014 (±0.0003)	-40.69	0.0017 (±0.0003)	-36.40	0.0016 (±0.0003)	-38.39
3	0.0024 (±0.0002)	2.14	0.0028 (±0.0002)	1.74	0.0026 (±0.0002)	1.94
4	0.0014 (±0.0003)	-40.13	0.0017 (±0.0003)	-36.17	0.0016 (±0.0003)	-38.00
5	0.0020 (±0.0004)	-17.21	0.0023 (±0.0004)	-17.11	0.0021 (±0.0004)	-17.14
6	0.0030 (±0.0003)	25.62	0.0033 (±0.0003)	21.03	0.0031 (±0.0003)	23.19
7	0.0020 (±0.0004)	-16.65	0.0023 (±0.0004)	-16.88	0.0021 (±0.0004)	-16.75
8	0.0030 (±0.0004)	27.60	0.0034 (±0.0003)	22.61	0.0032 (±0.0004)	24.96
9	0.0012 (±0.0003)	-50.11	0.0015 (±0.0003)	-44.90	0.0013 (±0.0003)	-47.31
10	0.0026 (±0.0002)	8.77	0.0029 (±0.0002)	7.23	0.0027 (±0.0002)	7.97
11	0.0011 (±0.0003)	-52.34	0.0014 (±0.0003)	-47.31	0.0013 (±0.0003)	-49.63
12	0.0019 (±0.0004)	-17.59	0.0022 (±0.0004)	-18.20	0.0021 (±0.0004)	-17.89
13	0.0033 (±0.0004)	41.29	0.0037 (±0.0004)	33.94	0.0035 (±0.0004)	37.39
14	0.0019 (±0.0004)	-19.82	0.0022 (±0.0004)	-20.60	0.0020 (±0.0004)	-20.21

Notes: For detailed description of scenarios, see Table 26.

Table 34. Scenario prediction model outputs: nekton abundance per area (individuals/m^2)

	Open Water Sites		Tidal Creek Sites		All Sites	
Scenario	**Prediction**	**Percent Change**	**Prediction**	**Percent Change**	**Prediction**	**Percent Change**
0	0.014 (±0.002)	-	0.034 (±0.005)	-	0.022 (±0.002)	-
1	0.012 (±0.002)	-13.49	0.029 (±0.005)	-14.32	0.019 (±0.002)	-13.90
2	0.008 (±0.003)	-43.47	0.019 (±0.007)	-44.55	0.012 (±0.004)	-44.01
3	0.013 (±0.002)	-3.85	0.032 (±0.004)	-5.67	0.021 (±0.002)	-4.76
4	0.008 (±0.003)	-43.62	0.019 (±0.007)	-44.69	0.012 (±0.004)	-44.15
5	0.007 (±0.003)	-49.27	0.017 (±0.006)	-49.76	0.011 (±0.004)	-49.51
6	0.012 (±0.002)	-13.71	0.029 (±0.005)	-14.54	0.018 (±0.002)	-14.12
7	0.007 (±0.003)	-49.40	0.017 (±0.006)	-49.89	0.011 (±0.004)	-49.64
8	0.011 (±0.002)	-17.01	0.028 (±0.005)	-17.51	0.018 (±0.003)	-17.26
9	0.007 (±0.003)	-50.88	0.016 (±0.008)	-51.82	0.010 (±0.005)	-51.35
10	0.013 (±0.002)	-4.10	0.032 (±0.004)	-5.91	0.020 (±0.002)	-5.00
11	0.007 (±0.003)	-51.14	0.016 (±0.008)	-52.06	0.010 (±0.005)	-51.60
12	0.006 (±0.003)	-57.72	0.014 (±0.007)	-57.97	0.009 (±0.004)	-57.84
13	0.011 (±0.002)	-17.45	0.028 (±0.005)	-17.93	0.018 (±0.003)	-17.69
14	0.006 (±0.003)	-57.94	0.014 (±0.007)	-58.18	0.009 (±0.004)	-58.06

Notes: For detailed description of scenarios, see Table 26.

Table 35. Scenario prediction model outputs: nekton species richness

	Open Water Sites		Tidal Creek Sites	
Scenario	**Prediction**	**Percent Change**	**Prediction**	**Percent Change**
0	10.27 (±0.59)	0	11.79 (±0.56)	0
1	10.13 (±0.57)	-1.42	11.53 (±0.54)	-2.26
2	8.32 (±1.84)	-19.03	8.98 (±1.77)	-23.82
3	10.18 (±0.58)	-0.87	11.53 (±0.54)	-2.26
4	8.37 (±1.84)	-18.48	8.98 (±1.77)	-23.82
5	8.32 (±1.84)	-19.03	8.98 (±1.77)	-23.82
6	10.18 (±0.58)	-0.87	11.53 (±0.54)	-2.26
7	8.37 (±1.84)	-18.48	8.98 (±1.77)	-23.82
8	10.13 (±0.57)	-1.42	11.53 (±0.54)	-2.26
9	7.84 (±2.28)	-23.66	8.31 (±2.2)	-29.49
10	10.24 (±0.58)	-0.32	11.53 (±0.54)	-2.26
11	7.95 (±2.28)	-22.56	8.31 (±2.2)	-29.49
12	7.84 (±2.28)	-23.66	8.31 (±2.2)	-29.49
13	10.24 (±0.58)	-0.32	11.53 (±0.54)	-2.26
14	7.95 (±2.28)	-22.56	8.31 (±2.2)	-29.49

Notes: For detailed description of scenarios, see Table 26. Separate nekton species richness models were run for tidal creek and open water sites due to differing sampling protocols; therefore, data were not summarized by all habitat types.

Table 36. Scenario prediction model outputs: benthic abundance per area (individuals/m^2)

	Open Water Sites		Tidal Creek Sites		All Sites	
Scenario	**Prediction**	**Percent Change**	**Prediction**	**Percent Change**	**Prediction**	**Percent Change**
0	2090.0 (±160.4)	-	2083.2 (±160.3)	-	2086.6 (±155.2)	-
1	2125.1 (±161.3)	1.68	2132.5 (±161.6)	2.37	2128.8 (±156.1)	2.02
2	2106.9 (±280.8)	0.81	2113.7 (±286.1)	1.47	2110.3 (±280.2)	1.13
3	2153.7 (±164.4)	3.04	2161.0 (±165.4)	3.74	2157.3 (±159.5)	3.39
4	2135.2 (±281.6)	2.16	2142.0 (±287.4)	2.82	2138.6 (±281.2)	2.49
5	2106.9 (±280.8)	0.81	2113.7 (±286.1)	1.47	2110.3 (±280.2)	1.13
6	2153.7 (±164.4)	3.04	2161.0 (±165.4)	3.74	2157.3 (±159.5)	3.39
7	2135.2 (±281.6)	2.16	2142.0 (±287.4)	2.82	2138.6 (±281.2)	2.49
8	2125.1 (±161.3)	1.68	2132.5 (±161.6)	2.37	2128.8 (±156.1)	2.02
9	2089.6 (±335.8)	-0.02	2096.2 (±341.7)	0.63	2092.9 (±336.0)	0.30
10	2182.6 (±170.0)	4.43	2189.8 (±171.7)	5.12	2186.2 (±165.5)	4.77
11	2146.2 (±339.4)	2.69	2152.6 (±346.2)	3.33	2149.3 (±340.0)	3.01
12	2089.6 (±335.8)	-0.02	2096.2 (±341.7)	0.63	2092.9 (±336.0)	0.30
13	2182.6 (±170.0)	4.43	2189.8 (±171.7)	5.12	2186.2 (±165.5)	4.77
14	2146.2 (±339.4)	2.69	2152.6 (±346.2)	3.33	2149.3 (±340.0)	3.01

Notes: For detailed description of scenarios, see Table 26.

Table 37. Scenario prediction model outputs: benthic species richness

	Open Water Sites		Tidal Creek Sites		All Sites	
Scenario	**Prediction**	**Percent Change**	**Prediction**	**Percent Change**	**Prediction**	**Percent Change**
0	22.14 (±1.12)	-	20.36 (±1.04)	-	21.24 (±0.84)	-
1	25.01 (±2.21)	12.97	22.78 (±1.91)	11.91	23.88 (±1.90)	12.44
2	19.85 (±1.20)	-10.36	18.24 (±1.12)	-10.38	19.03 (±0.98)	-10.37
3	22.46 (±1.14)	1.43	20.65 (±1.06)	1.42	21.54 (±0.86)	1.42
4	20.13 (±1.21)	-9.08	18.50 (±1.13)	-9.11	19.30 (±0.99)	-9.10
5	22.42 (±2.14)	1.26	20.42 (±1.87)	0.30	21.4 (±1.87)	0.78
6	25.37 (±2.24)	14.58	23.11 (±1.94)	13.50	24.22 (±1.92)	14.04
7	22.74 (±2.17)	2.71	20.71 (±1.89)	1.72	21.71 (±1.89)	2.22
8	26.21 (±2.96)	18.40	23.79 (±2.52)	16.87	24.98 (±2.60)	17.63
9	19.20 (±1.28)	-13.26	17.65 (±1.19)	-13.28	18.42 (±1.07)	-13.27
10	22.78 (±1.18)	2.87	20.94 (±1.09)	2.85	21.84 (±0.89)	2.86
11	19.76 (±1.31)	-10.76	18.16 (±1.22)	-10.80	18.95 (±1.10)	-10.78
12	22.74 (±2.80)	2.70	20.63 (±2.40)	1.35	21.67 (±2.49)	2.03
13	26.97 (±3.06)	21.80	24.47 (±2.60)	20.20	25.70 (±2.69)	21.00
14	23.39 (±2.87)	5.65	21.22 (±2.47)	4.24	22.29 (±2.55)	4.95

Notes: For detailed description of scenarios, see Table 26.

Table 38. Scenario prediction model outputs: MAMBI

	Open Water Sites		Tidal Creek Sites		All Sites	
Scenario	**Prediction**	**Percent Change**	**Prediction**	**Percent Change**	**Prediction**	**Percent Change**
0	0.471 (±0.011)	-	0.418 (±0.009)	-	0.445 (±0.008)	-
1	0.566 (±0.028)	20.20	0.502 (±0.024)	20.26	0.535 (±0.026)	20.23
2	0.453 (±0.013)	-3.77	0.400 (±0.011)	-4.26	0.427 (±0.010)	-4.00
3	0.472 (±0.011)	0.23	0.419 (±0.009)	0.25	0.446 (±0.008)	0.24
4	0.455 (±0.013)	-3.54	0.401 (±0.011)	-4.01	0.428 (±0.010)	-3.76
5	0.549 (±0.029)	16.43	0.485 (±0.025)	16.00	0.517 (±0.027)	16.23
6	0.567 (±0.028)	20.42	0.503 (±0.024)	20.51	0.536 (±0.026)	20.47
7	0.550 (±0.029)	16.65	0.486 (±0.025)	16.25	0.518 (±0.026)	16.47
8	0.603 (±0.038)	27.97	0.535 (±0.033)	28.05	0.569 (±0.035)	28.01
9	0.448 (±0.014)	-4.90	0.395 (±0.012)	-5.54	0.422 (±0.011)	-5.20
10	0.473 (±0.011)	0.45	0.420 (±0.010)	0.51	0.447 (±0.008)	0.48
11	0.450 (±0.014)	-4.45	0.397 (±0.012)	-5.03	0.424 (±0.011)	-4.72
12	0.580 (±0.039)	23.07	0.512 (±0.034)	22.52	0.546 (±0.036)	22.81
13	0.605 (±0.038)	28.42	0.537 (±0.033)	28.56	0.571 (±0.035)	28.48
14	0.582 (±0.039)	23.52	0.514 (±0.034)	23.02	0.548 (±0.036)	23.29

Notes: For detailed description of scenarios, see Table 26.

Table 39. Population estimates for coastal South Carolina counties

County	Population (2000)	Population (2018)	Percent Change (%)
Beaufort	122,306	188,715	+54.30
Berkeley	143,410	221,091	+54.17
Charleston	310,749	405,905	+30.62
Colleton	38,304	37,660	-1.68
Dorchester	96,757	160,647	+66.03
Georgetown	56,080	62,249	+11.00
Horry	198,019	344,147	+73.80
Jasper	20,721	28,971	+39.82
All Coastal Counties	*986,346*	*1,449,385*	*+46.94*
South Carolina Total	*4,024,223*	*5,084,127*	*+26.34*

Notes: Population data from US Census Bureau (2018).

Table 40. HUC watershed summary

HUC Digits	Count	Mean Area (min. - max.) (ha)
8	19	262,213 (41,224-533,412)
10	60	51,632 (16,321-122,611)
12	264	9,581 (1,614-50,912)
14	205	8,937 (217-22,003)
All	*548*	*83,091 (217-533,412)*

APPENDICES

Appendix A. Hydrologic soil group descriptions

Hydrologic Soil Group	Description
Group A	deep, well drained sands or gravelly sands with high infiltration and low runoff rates
Group B	deep well drained soils with a moderately fine to moderately coarse texture and a moderate rate of infiltration and runoff
Group C	soils with a layer that impedes the downward movement of water or fine textured soils and a slow rate of infiltration
Group D	soils with a very slow infiltration rate and high runoff potential. This group is composed of clays that have a high shrink-swell potential, soils with a high water table, soils that have a clay pan or clay layer at or near the surface, and soils that are shallow over nearly impervious material
Group A/D	soils naturally have a very slow infiltration rate due to a high water table but will have high infiltration and low runoff rates if drained
Group B/D	soils naturally have a very slow infiltration rate due to a high water table but will have a moderate rate of infiltration and runoff if drained
Group C/D	soils naturally have a very slow infiltration rate due to a high water table but will have a slow rate of infiltration if drained

Notes: Table adapted from NRCS soils layer downloaded from ArcGIS Online (NRCS, 2019).

Appendix B. List of independent variables: weather and climate

Weather Station Data [1]

Precipitation (1-7-day totals) (in)
Days since rain
Temperature (1-7-day averages) (°F)

DAYMET [2]

Precipitation (10, 14, 30, 45, 60, 90-day totals) (cm)
Temperature (10, 14, 30, 45, 60, 90-day averages) (°C)

Seasonal Weather Data [3]

Fall Precipitation (cm) [SON]
Winter Precipitation (cm) [DJF]
Spring Precipitation (cm) [MAM]
Summer Precipitation (cm) [JJA]
Fall Temperature (cm) [SON]
Winter Temperature (°C) [DJF]
Spring Temperature (°C) [MAM]
Summer Temperature (°C) [JJA]
Annual Precipitation (cm)
Preceding Annual Precipitation (cm)
Annual Temperature (°C)
Preceding Annual Temperature (°C)

Seasonal Monthly Breakdown
[SON] Sep., Oct., Nov. (all from preceding year)
[DJF] Dec. (of preceding year), Jan., Feb.
[MAM] Mar., Apr., May
[JJA] Jun., Jul., Aug.

Drought Indices [4]

PDSI (Palmer Drought Severity Index)
PHDI (Palmer Hydrologic Drought Index)
PMDI (Palmer Modified Drought Index)
ZNDX (Palmer Z-Index)
SPI (1, 2, 3, 6, 9, 12, or 24-month Standard Precipitation Index)

Climate Teleconnections [5]

AMO (Atlantic Multidecadal Oscillation)
AO (Arctic Oscillation)
NAO (North Atlantic Oscillation)
ONI (Oceanic Nino Index)

Notes: [1] Data from nearest weather station from NOAA's climate data online tool (NOAA NCEI)
[2] Data extracted from DAYMET gridded dataset (Thornton et al., 2018)
[3] Data summarized at Brookgreen Gardens, Charleston Int'l Airport, or Savannah Int'l Airport weather stations and compared to corresponding 30-year climate normals (1980-2010) to calculate difference from normal value (NOAA NCEI)
[4] NOAA NCDC
[5] Albers, 2019

Appendix C. Drought indices descriptions

Drought Index	Description
Palmer Drought Severity Index (PDSI)	The PDSI is calculated using monthly precipitation, temperature and soil storage. The PDSI was developed in the 1960's for agricultural purposes and is the oldest index in use today.
Palmer Modified Drought Index (PMDI)	A modified version of the PDSI to better capture transitions between wet and dry periods.
Palmer Hydrologic Drought Index (PHDI)	Based upon the PDSI with a focus on longer-term drought conditions that may impact water storage and groundwater.
Palmer Z-Index (ZNDX)	Derivative of the PDSI with a focus on short-term drought conditions.
Standard Precipitation Index (SP01, SP02, SP03 [1],…)	Derived from long-term precipitation data and is available for multiple timescales (1 to 24-months)

Notes: For all index values, positive numbers indicate wet conditions and negative numbers indicate drought conditions. Descriptions from the Handbook of Drought Indicators and Indices (WMO and GWP, 2016).

[1] Number following SP-- represents number of preceding months used in its calculation

Appendix D. Climate teleconnection descriptions

Climate Teleconnection	Description
El Niño-Southern Oscillation (ONI)	El Niño years (ONI≥0.5) correlate with wet and cool winters in the Southeast and reduced Atlantic tropical cyclone activity. La Niña years (ONI≤-0.5) correlate with warm and dry winters in the South Carolina and increased Atlantic tropical cyclone activity (Mizzell and Simmons, 2015).
Atlantic Multidecadal Oscillation (AMO)	The AMO represents long-term (20-40 year) trends in sea surface temperature in the northern Atlantic Ocean. The AMO has been in the positive (warming) phase since the 1990's. Positive AMO phases are often associated with more frequent and severe droughts for the continental US; however, coastal South Carolina may experience greater rainfall due to increased hurricane activity during positive AMO phases (Curtis, 2007).
North Atlantic Oscillation (NAO)	The NAO represents fluctuations in atmospheric pressure in the northern Atlantic Ocean. The NAO is more often associated with weather impacts in western Europe; however, positive NAO phases have been associated with warmer and wetter winters and negative NAO phases with cooler and drier winters in the southeastern US (NCSU NCCO).
Arctic Oscillation (AO)	The AO is closely related to the NAO and influences the trajectory of the jet stream across the Arctic. The effects of the AO are similar to the NAO. Positive AO phases are associated with warmer winters and negative AO phases with cooler winters in the southeastern US (NCSU NCCO).

Appendix E. List of dependent variables: SCECAP [1]

Water Quality
Enterococcus spp. (MPN/100mL) [2]
Fecal coliform (MPN/100mL)
Sediment Quality
DDT (ng/L) [3]
Metals (ug/L)
PAHs (ng/L)
PBDEs (ng/L) [4]
PCBs (ng/L)
All Contaminants (ERMQ) [5]
DDT (ERMQ) [3]
Metals (ERMQ)
PAHs (ERMQ)
PCBs (ERMQ)
Biological Quality
Nekton Abundance (individuals/m^2)
Nekton Species Richness [6]
Benthic Abundance (individuals/m^2)
BIBI [7]
MAMBI [8]

Notes: [1] South Carolina Estuarine and Coastal Assessment Program (Sanger et al., 2016)
[2] Data availability beginning in 2007
[3] Total DDT, including its metabolites (*e.g.*, DDD and DDE)
[4] Data availability beginning in 2003
[5] Effects Range Median Quotient (Long et al., 1995)
[6] Data separated by habitat type due to differing trawl sampling protocols between tidal creek and open water sites (Sanger et al., 2016)
[7] Benthic Index of Biotic Integrity (Van Dolah, 1999)
[8] Multivariate AZTI's Marine Biotic Index (Muxika, 2007)

Appendix F. List of independent variables: landcover and land use

NLCD [1, HGB]	
Barren Land (%†) [A]	*Condensed Landcover Categories*
Cultivated Crops (%†) [A]	[A] Agricultural
Deciduous Forest (%†) [F]	[D] Developed All
Developed Open Spaces (%†) [D,DL]	[DL] Developed Low
Emergent Herbaceous Wetlands (%) [M]	[DH] Developed High
Evergreen Forest (%†) [F]	[F] Forest
Hay-Pasture (%†) [A]	[M] Marsh
Herbaceous (%†) [F]	[W] Water
High Intensity Developed (%†) [D,DH]	
Low Intensity Developed (%†) [D,DL]	
Medium Intensity Developed (%†) [D,DH]	
Mixed Forest (%†) [F]	
Open Water (%) [W]	
Shrub-Scrub (%†) [F]	
Woody Wetlands (%†) [F]	

NLCD Urban Imperviousness [2, HGB]
Upland Impervious Cover (%†)

US Census [3, HG]
Population
Population Density (persons per ha)

USDA Hydrologic Soil Groups [4, HG]	
Group A (%†) [WD]	*Condensed Soil Categories*
Group B (%†) [WD]	[WD] Well Drained
Group C (%†) [PD]	[PD] Poorly Drained
Group D (%†) [PD]	
Group A/D (%†) [PD]	
Group B/D (%†) [PD]	
Group C/D (%†) [PD]	

SCDNR Stormwater Pond Dataset [5, H]
All Ponds (#/ha, %)
Commercial Ponds (#/ha, %)
Golf Ponds (#/ha, %)
Mixed Ponds (#/ha, %)
Residential Ponds (#/ha, %)

Notes: [H] Analyzed by HUC watershed; [HG] analyzed by HUC watershed and grid cell; [HGB] analyzed by HUC watershed, grid cell, and buffer

† Calculated as percentage of upland area (*i.e.*, non-water and non-marsh landcover)

[1] National Land Cover Dataset (Yang et al., 2018). Data available for years 2001,2003, 2006, 2008, 2011, 2013, 2016

[2] National Landcover Dataset's urban imperviousness data (Yang et al., 2018). Data available for years 2001, 2006, 2011, 2016

[3] 2010 US Census Blocks' population data (source)

[4] NRCS 2019

[5] Cotti-Rausch *et al*., 2018

Appendix G. List of independent variables: physical habitat [1]

Structure
Habitat Type (open water or tidal creek)
Channel Depth (m)
Channel Width (m) [2]
Chemistry
Dissolved Oxygen (mg/L)
pH
Salinity (ppt)
Water Temperature (°C)
Sediment Composition
Silt-Clay Content (%)
Total Organic Carbon Sediment (mg/L)

Notes: [1] Data collected at each SCECAP station (Sanger et al., 2016)
[2] Estimated via satellite imagery

Appendix H. Area of coastal South Carolina that experienced a change in NLCD [1] landcover type between 2001 and 2016. Percent of total county area in parentheses.

County	Change in Landcover (2001-2016)	No Change in Landcover (2001-2016)	Total Area
Beaufort	7,410 ha (4.6%)	152,920 ha (95.4%)	160,330 ha
Berkeley	9,074 ha (2.9%)	307,101 ha (97.1%)	316,175 ha
Charleston	10,254 ha (4.1%)	242,377 ha (96.0%)	252,631 ha
Colleton	9,545 ha (3.4%)	268,583 ha (96.6%)	278,128 ha
Dorchester	5,160 ha (3.5%)	143,863 ha (96.5%)	149,023 ha
Georgetown	6,388 ha (2.9%)	212,775 ha (97.1%)	219,163 ha
Horry	16,988 ha (5.7%)	279,301 ha (94.3%)	296,289 ha
Jasper	7,329 ha (4.2%)	165,339 ha (95.8%)	172,668 ha
Total	*72,148 ha (3.9%)*	*1,772,259 ha (96.1%)*	*1,844,407 ha*

Notes: [1] National Land Cover Dataset (Yang et al., 2018)

Appendix I. NLCD [1] landcover changes observed in coastal South Carolina counties between 2001 and 2016. Data shown as area gained, area lost, and net change for each landcover category [2].

	Beaufort	Berkeley	Charleston	Colleton	Dorchester	Georgetown	Horry	Jasper	All Coastal Counties
High Intensity Developed (ha)									
Gain	987	1,469	1,929	98	752	331	2,923	361	8,850
Loss	0	0	0	0	0	0	0	0	0
Net	*987*	*1,469*	*1,929*	*98*	*752*	*331*	*2,923*	*361*	*8,850*
Low Intensity Developed (ha)									
Gain	2,812	2,607	2,686	134	1,517	803	6,620	867	18,046
Loss	-227	-326	-823	-40	-182	-170	-1,059	-25	-2,852
Net	*2,585*	*2,281*	*1,863*	*94*	*1,335*	*633*	*5,561*	*842*	*15,194*
Agriculture (ha)									
Gain	214	261	126	372	280	113	724	504	2,594
Loss	-727	-1,289	-2,230	-2,036	-981	-509	-1,832	-868	-10,472
Net	*-513*	*-1,028*	*-2,104*	*-1,664*	*-701*	*-396*	*-1,108*	*-364*	*-7,878*
Forested Upland (ha)									
Gain	1,157	681	1,947	1,976	713	439	948	816	8,677
Loss	-3,211	-3,272	-2,649	-664	-1,869	-1,034	-7,080	-1,647	-21,426
Net	*-2,054*	*-2,591*	*-702*	*1,312*	*-1,156*	*-595*	*-6,132*	*-831*	*-12,749*
Forested Wetland (ha)									
Gain	737	1,058	1,599	2,347	619	1,993	1,850	2,832	13,035
Loss	-969	-2,379	-1,914	-3,272	-1,400	-2,003	-4,741	-1,349	-18,027
Net	*-232*	*-1,321*	*-315*	*-925*	*-781*	*-10*	*-2,891*	*1,483*	*-4,992*
Marsh (ha)									
Gain	1,016	1,664	1,094	2,551	558	1,474	1,779	1,366	9,444
Loss	-809	-1,413	-2,096	-3,237	-684	-2,340	-2,009	-2,901	-3,882
Net	*207*	*251*	*-1,002*	*-686*	*-126*	*-866*	*-230*	*-1,535*	*5,562*
Water (ha)									
Gain	487	1,334	873	2,067	721	1,235	2,144	583	11,502
Loss	-1,467	-395	-542	-296	-44	-332	-267	-539	-15,489
Net	*-980*	*939*	*331*	*1,771*	*677*	*903*	*1,877*	*44*	*-3,987*

Notes: [1] National Land Cover Dataset (Yang et al., 2018)
[2] Condensed landcover categories (Appendix F)

Appendix J. Link to author's GitHub profile. The processed data and R scripts used in this project's analyses and data visualization are available in the 'thesis' project folder on the author's GitHub profile.

https://github.com/WhateverLloyd/thesis